Programa de doctorado en Biotecnología

Characterizing BCL-2 family protein domains in membranes: Insertion, interaction and apoptotic modulation roles

Vicente Andreu Fernández

Doctoral thesis, Valencia 2015

Thesis supervisors

Dr. Enrique Pérez Payá

Dra. Mar Orzáez Calatayud

Dr. Ismael Mingarro Muñoz

PRINCIPE FELIPE
CENTRO DE INVESTIGACION

Programa de doctorado en Biotecnología

Characterizing BCL-2 family protein domains in membranes: Insertion, interaction and apoptotic modulation roles

Vicente Andreu Fernández

Doctoral thesis, Valencia 2015

Thesis supervisors

Dr. Enrique Pérez Payá

Dra. Mar Orzáez Calatayud

Dr. Ismael Mingarro Muñoz

PRINCIPE FELIPE
CENTRO DE INVESTIGACION

Mar Orzáez Calatayud, Doctora en Ciencias Biológicas, Investigadora del Centro de Investigación Príncipe Felipe, e Ismael Mingarro Muñoz, Doctor en Ciencias Biológicas, Catedrático de la Universidad de Valencia:

CERTIFICAN, que el presente trabajo titulado "Characterizing BCL-2 family protein domains in membranes: Insertion, interaction and apoptotic modulation roles" ha sido realizado por Vicente Andreu Fernández, bajo su dirección, en el Centro de Investigación Príncipe Felipe, como proyecto de tesis doctoral, para optar al grado de Doctor por la Universidad de Valencia.

Dra. Mar Orzáez Calatayud Dr.Ismael Mingarro Muñoz

To my family and specially, to Q,

AGRADECIMIENTOS

Resulta difícil comprimir en unas líneas el apoyo y la ayuda de todas y cada una de las personas que han hecho posible la consecución de este largo, y a menudo difícil camino que tuve la suerte de emprender allá por el año 2010.

Mi familia siempre ha estado a mi lado, pero quería agradecerles especialmente su apoyo durante los momentos más duros, ya que han sido el bastión que me ha mantenido en pie y me ha dado fuerzas para finalizar esta etapa de mi vida. Aquí me gustaría destacar a mi madre, Amparo, a la que se lo debo absolutamente todo; a mis tios Mari Carmen y Paco, a mis abuelos, y como no a mi chica, Elisabet, que ha sido siempre mi ejemplo a seguir y ha sabido darme el cariño, la comprensión y la paz que necesito. Muchas gracias a todos, de corazón.

Se dice que es en los momentos difíciles cuando se conoce realmente a las personas, y tras la muerte de Quique pensé que si una tesis era un proyecto complicado, sin tu referente y tu guía sería casi imposible. Sin embargo, me equivoqué radicalmente. Tanto Mar como Ismael me han demostrado no sólo lo grandes que son científicamente, lo que ya sabía de sobra, sino lo grandes que son como personas. A ambos quiero agradecerles su tiempo, su dedicación y su ayuda, ya que sin ellos nunca hubiese podido completar mi trabajo. Eso es algo que recordaré siempre. Mar ha tomado las riendas del laboratorio de una manera brillante, y le auguro un gran futuro como jefa de grupo, es realmente buena. A Isma quería agradecerle el saber que siempre he podido contar con él, así como sus consejos, aunque nunca alcanzaré su ojo quirurjico con Illustrator. A los dos sólo tengo una cosa mas que decirles, Quique estará muy orgulloso de vosotros.

Por supuesto, quiero agradecer a todos los miembros del I-12 durante estos años su ayuda en el día a día del lab. Ainhoa, con la que empecé en este proyecto y que me ayudó a introducirme en el mundo de las Bcl's. Ally, un técnico top y una gran amiga. Moni, que me ha prestado su ayuda en incontables ocasiones para hacer posible muchos de los ensayos que aparecen en esta tesis. Maria Jesús, cuya colaboración desde el lab de Ismael ha sido imprescindible. Guille, Fede, Andy (mae Junior) y Yubeli Tatiana, que han sido mis compañeros de aventuras y desventuras a lo largo de estos años, y que se han convertido en amigos para toda la vida. Y al resto de la gran familia que ha sido el I-12, Eliana, Rebe, Anna, Yadira, Ana, Inmaculada, Rosa, Cris, Alba, y Pablo.

También quería dar las gracias al Dr. Frank Edlich por permitirme realizar una estancia en su laboratorio y hacerme sentir totalmente integrado en su grupo. Su estrecha colaboración aún después de haber finalizado mi estancia ha sido muy importante para la elaboración de los artículos. De este lab me llevo a buenos amigos como Silvie, Zaynep y Jo a los q les deseo toda la suerte del mundo.

Pero quiero reservar este último espacio para él, para Q. Una de las espinas que no podré quitarme y que me acompañaran toda la vida es no haberle dado las gracias por darme la oportunidad de trabajar con él. Quería haberlo hecho cuando acabase la tesis, cuando ya no me vinculase nada a él, pero no he llegado a tiempo. Quique ha sido un ejemplo tanto profesional como personal, ha sido el modelo a seguir. Es muy difícil encontrarte una persona tan positiva como él, alguien que cuando te veía atascado en lugar de presionarte te animaba a seguir trabajando, porque trabjando al final se obtenían resultados. Creía que lo que hacíamos todos y cada uno de los miembros del laboratorio era importante, y nos lo transmitía haciendo que todos estuviésemos siempre motivados. Quiero agradecerle de todo corazón que confiase en mí, que siempre estuviese dispuesto a dar una nueva idea, un nuevo enfoque, que siempre estuviese ahí, que siempre tuviese en cuenta las ideas de un becario recién llegado. Quiero agradecerle haberme demostrado que no todos los tópicos en ciencia son reales, que puedes tener la suerte de encontrarte con alguíen que te enseña que lo importante son las personas, no los experimentos. Sólo lo conocí durante dos años, pero no lo olvidaré, ahora es el espejo en el que mirarme. Espero no defraudarlo.

Muchas Gracias Q. Un abrazo. Esta tesis va por ti.

INDEX

COMMON ABBREVIATIONS AND SYMBOLS

λ	Wavelength
θ	Molar Ellipticity
Δψm	Mitochondrial potential
ΔG	Gibbs Free energy
ΔG_{app}	Apparent free energy difference
Δn_f	Birefringence
3MA	3-methyladenine
ACD	Accidental cell death
AIDS	Acquired immune deficiency síndrome
AML	Acute myeloid leukemia
ANT	Adenine nucleotide translocator
APAF-1	Apoptosis protease activating factor-1
ApoG2	Apogossypolone
ASOs	Antisense oligonucleotides
ATAP	Amphipathic tail anchoring peptide
ATGs	Autophagy-related genes
Bad	BCL-2 antagonist of cell death
Bak	BCL-2 Associated Killer protein
Bax	BCL-2 Associated X protein
BCA	Bicinchoninic acid
BC groove	BCL-2 family BH3 C-terminus-binding groove
Bcl-2	B-cell lymphoma 2
Bcl-xL	B-cell lymphoma-extra large
Bcl-w	Bcl-2-like protein 2
Bfl-1 (A1)	Bcl-2-related protein A1
BH3	BCL-2 homology domain 3
Bid	BH3-interacting domain death agonist
BiFC	Bimolecular fluorescent complementation
Bik	BCL-2-interacting killer
Bim	BCL2-interacting mediator of cell death
BL-193	Gossypol
Bmf	BCL.2-modifying factor
Bok	BCL2-related ovarian killer
C. elegans	*Caenorhabditis elegans*
CD	Circular Dichroism
CDDP	Cisplatin
CerS	Ceramide synthase
CL	Cardiolipin
CS	Mitochondrial contact sites
CT20p	C-terminal alpha-9 helix of Bax derived peptide
CypD	Cyclophilin D
Cyt-*c*	Cytochrome-c
DAPI	4'-6-diamidino-2-phenylindole

Diva	Bcl-b, BCL2-like 10
DLS	Dynamic light scattering
DMEM	Dulbecco's Modified Eagle's Medium
DPI	Dual Polarization Interferometry
E.coli	Escherichia coli
EBV	Epstein-Barr virus
EGFR	Epidermal growth factor receptor
ER	Endoplasmic reticulum
FBS	Fetal bovine serum
FITC	Fluorescein isothiocyanate
FKBP38	FK506-binding protein 38
FL	Full-length
G-3139	Oblimersen
GAPDH	Glyceraldehyde 3-phosphate dehydrogenase
GpA	Glycophorin A
Grp78	Glucose-regulated protein 78
GX-015-070	Obatoclax
HCT 116	Human colorectal carcinoma
HeLa	Human cervix adenocarcinoma
HDAC	Histone deacetylase
HKI and HKII	Hexokinase I and II
Hrk	Activator of apoptosis Harakiri
IAPs	Inhibitors of apoptosis proteins
IL3	Interleukin 3
IMS	Intermembrane space
KO	Knockout
LC3	Light chain 3, a mammalian ortholog of yeast Atg8
LDH	Lactate dehydrogenase
Lep	Protein leader peptidase
MAC	Mitochondrial apoptosis- induced channel
MAM	ER-mitochondria associated membranes
MBP	Maltose binding protein
Mcl-1	Myeloid cell Leukemia-1
MEFs	Mouse embryonic fibroblasts
MIM	Mitochondrial inner membrane
MM	Multiple myeloma
MM39	*malE*-deficient *E. coli* MM39 (DE3) cells
MOMP	Mitochondrial outer membrane permeabilization
MPT	Mitochondrial permeability transition
MTT	3-(4,5-dimethylthiazol-2-yl)-2,5-dipheny ltetrazoliumbromide
NAD^+	Nicotinamide adenine dinucleotide
NCCD	Nomenclature committee on cell death
Nec	Necrostatin-1
NMDA	N-metil-D- aspartate
Noxa	Phorbol-12-myristate-13-acetate-induced protein(PMAIP1)
NSCLC	Non small cell lung cancer
OD	Optical density

PARP-1	Poly [ADP-ribose] polymerase 1
PC	Phosphatidylcholine
PCD	Programmed cell death
PE	Phosphatidylethanolamine
P_i	Probability of insertion
PI	Phosphatidylinositol
PI	Propidium Iodide
PI3K	Phosphoinositide 3-kinase
PK	Proteinase K
PNK	Polinucleotide kinase
PO	1-palmitoyl-2-oleoyl
PS	Phosphatidylserine
PTP	Permeability transition pore
Puma	p53 up-regulated modulator of apoptosis
QM31	Apoptosome inhibitor compound
Rambo	BCL2-like 13
RCD	Regulated cell death
RFP	Red fluorescent protein
RIP1	Receptor-interacting protein 1
RIPK1	Receptor-interacting protein kinase 1
ROS	Reactive oxygen species
SCLC	Small cell lung cancer
SDS	Sodium dodecyl sulfate
SMase	Sphingomyelinase
SMIs	Small molecule inhibitors
SNP	Single nucleotide polymorphisms
STS	Staurosporine
SUV	Small unilamellar vesicles
tBid	Truncate form of Bid
TFE	Trifluoroethanol
TIM	Transporter inner membrane
TLR	Toll-like receptors
TNF	Tumor necrosis factor
TMRM	Tetramethylrhodamine methyl ester perchlorate
TOM	Transporter outer membrane
ToxR	Cholera toxin transcriptional activator
TRAIL	TNF-Related apoptosis-inducing ligand
VDAC1	Voltage-dependent anion channel 1
VDAC2	Voltage-dependent anion channel 2
VFP	Venus fluorescent protein
YFP	Yellow fluorescent protein
zVAD-fmk	Carbobenzoxy-valyl-alanyl-aspartyl-[O-methyl]-fluoromethylketone

INTRODUCTION

1.1 CONCEPT OF CELL DEATH.

In an organism cell death occurs in essentially two different ways: accidental cell death (ACD) or regulated cell death (RCD). ACD is consequence of severe damages and caused by mechanical damages, hypoxia, complement-mediated cell lysis or highly toxic agents. Uncontrolled cell swelling is showed at the end of this process. In RCD, cells die in response to a specific stimulus and genetically encoded machinery initiates cell death. The course of some 'regulated cell death' (RCD) variants can be influenced, at least to some extent, by specific pharmacologic or genetic interventions. The term 'programmed cell death' (PCD) is used to indicate RCD instances that occur as part of a developmental program or to preserve physiologic adult tissue homeostasis. In 1842, Carl Vogt was the first investigator who reported the appearance of physiological cell death during development of the midwife toad. Then, histologists started to recognize cell death as a natural process and different morphologies of cell death were described. Much of the work in the 19th century relied on the histological characterization of dying cells with limited recognition of its importance and regulation (1).

In 1965, Lockshin and Williams used for the first time the concept of programmed cell death (PCD) to define the loss of cells observed in insect metamorphosis following a sequence of controlled steps towards their own destruction (2).

Apoptosis was first decribed by Kerr and collaborators in 1972 (3), who established the morphological differences with necrotic cell death. Since 1970, several types of cell death have been characterized such as autophagy, necroptosis or pyroptosis, each one characterized by their own morphological and biochemical features (4). The increasing number of cell death types has led to the creation of the Nomenclature Committee on cell death (NCCD) to normalize the classification of different cell death processes. The actual classification of cell death is not based on morphological features but on quantifiable biochemical parameters (5). In the following sections the differential characteristics of the main cell death forms will be described.

1.1.1 Apoptosis.

Once the apoptotic process was characterized by Kerr *et al.* in 1972, research focused to determine the proteins involved in this process. However, our understanding of mechanisms involved in apoptosis of mammalian cells experienced the biggest progress in the 1990s when the genome of the nematode *Caenorhabditis elegans* (*C. elegans*) was sequenced. On one hand, some results demonstrated that a fixed number of cells were committed to die during development, and that this process was both, positively and negatively, regulated by specific genes (6). On the other hand, the discovery of the

linkage between the *Bcl-2* gene (B-cell lymphoma 2) and some leukemia processes demonstrated that Bcl-2 protein was able to produce tumoral processes by suppressing cell death instead of promoting cell proliferation as usually happens with traditional oncogenes. The studies on *C. elegans* programmed cell death led to the identification of most of the intracellular proteins that mediate and regulate apoptosis (7). Subsequent studies demonstrated that related proteins operate in similar ways in many other metazoans, including humans (8).

A large set of proteins and cellular components are used as biochemical markers of apoptosis. There is a family of cysteine proteases (named caspases) that execute cell death by the cleavage of several intracellular substrates. Apoptosis is also regulated by a group of proteins known as BCL-2 family proteins, which activate or inhibit the cell death program. There are other relevant partners in the mammalian apoptotic process such as IAPs (Inhibitors of Apoptosis Proteins), APAF-1 (Apoptosis Protease Activating Factor-1), mitochondrial apoptogenic factors such as cytochrome-c (Cyt-*c*), members of the TNF (Tumor Necrosis Factor) family and TNF receptors.

The apoptotic program shows a well-characterized serie of morphological changes in cells that are committed to die. In the early state of apoptosis cells round-up and undergo shrinkage and pyknosis, reducing their size (3). Pyknosis, the most characteristic feature of apoptosis, is generated by chromatin condensation. The process continues with the plasma membrane blebbing followed by nuclear fragmentation (karyorrhexis) and separation of cell fragments into apoptotic bodies. The organelle integrity is still maintained and plasma membrane remains intact. These bodies are phagocytosed by macrophages and finally removed within phagolysosomes. There is essentially no inflammatory reaction associated neither with apoptosis nor with the elimination of apoptotic cells due to these cells do not release their cellular content into the surrounding tissue; they are quickly phagocytosed by surrounding cells, avoiding secondary necrosis; and the inflammatory response of engulfing cells is not activated. Hence, the term apoptosis should be used exclusively in those cases of cell death wherein many of the above described biochemical and morphological features are observed (9, 10).

Importantly, apoptosis is a homeostatic mechanism to maintain cell populations in tissues and normally associated to development, aging (11) and defense mechanisms in immune reactions or following cell damaged by disease or toxic agents (12). Although there is a wide variety of stimuli and conditions, both physiological and pathological, that can trigger apoptosis, not all cells will necessarily die in response to the same stimulus.

Alterations in the regulation mechanisms of cell death can generate a large variety of diseases such as cancer (13), ischemia, neurodegenerative diseases (for example, Parkinson, Alzheimer, and Huntington's disease), Amyotrophic Lateral Sclerosis,

autoimmune lymphoproliferative syndrome, and AIDS (14, 15). Some of them correlate with insufficient apoptosis whereas others are due to excessive apoptosis. For example, insufficient apoptosis correlates with the development of cancer and autoimmunity, while excessive apoptosis is linked to neurological diseases, heart failure and stroke (16, 17). For that reason, the study of the apoptotic mechanisms and the control of this cell death program has been intensively studied in the last decades with therapeutic purposes.

1.1.2. Necrosis and necroptosis.

Morphologically necrosis refers to a gain in cell volume (oncosis), swelling of organelles and plasma membrane permeabilization that produces cell rupture and subsequent loss of intracellular content. Unlike apoptotic cells, the nuclei of necrotic cells remain largely intact. Different organelles and cellular processes take part in necrotic cell death but the relationships among them are still unclear. The cellular changes include mitochondrial alterations (e.g., production of reactive oxygen species (ROS), and mitochondrial outer membrane permeabilization (MOMP)), lysosomal (lysosomal membrane permeabilization) and nuclear (hyperactivation of poly (ADP-ribose) polymerase-1) changes, lipid degradation in plasma membrane and an increase of cytosolic calcium (Ca^{2+}) concentration that produce activation of non- caspase proteases like calpains and cathepsins (18, 19). The necrotic pathways can activate inflammatory response by the release of cytosolic molecules to the intercellular space through the damaged plasma membrane; in apoptosis these products are isolated inside macrophages. Alterations of the fine equilibrium between necrosis and apoptosis may be a key element in development of some diseases (20).

Historically, necrosis has been considered an accidental or uncontrolled form of cell death, but recent studies have postulated that necrotic cell death is a regulated process, introducing terms ‘‘programmed necrosis’’ or ‘‘necroptosis’’ (18). Necroptosis is defined as a type of cell death that can be avoided by inhibiting RIP1 kinase. Several components have been implicated in necroptotic cell death, including death domain receptors (e.g., TNFR1, Fas/CD95 and TRAIL-R) and Toll-like receptors (e.g., TLR3 and TLR4). Interestingly, certain BCL-2 family members have been recently implicated in necroptosis regulation (21).

1.1.3. Autophagic cell death.

Autophagy is morphologically defined as a type of cell death that occurs in the absence of chromatin condensation but accompanied by massive autophagic vacuolization of the

cytoplasm. It is considered a highly conserved degradation pathway for bulk cellular components and is also generally agreed that autophagy is an important housekeeping process for degrading and recycling damaged organelles, long-lived proteins and cellular aggregates..

There are three different autophagy subclasses: macroautophagy, microautophagy and chaperone-mediated autophagy. The most studied is macroautophagy, morphologically known as the formation of double membrane autophagosomes, which take control of damaged organelles or unwanted cellular components and deliver them to lysosomes for degradation and recycling (22). The main difference with apoptotic cells is the absence of phagocytosis.

Autophagy predominantly serves as a cell survival mechanism, via its suppressive role in necrotic cell death, such as necroptosis and poly ADP-ribose polymerase-1 (PARP-1)-mediated cell death. More importantly, the anti-necrosis function of autophagy has relevant biological functions in various pathological processes and diseases, including cancer and neurodegenerative diseases and metabolic disorders (23). Nonetheless, there is a intense discussion around the dual role of autophagy in cell death and cell survival (24). When analyzing relationships between autophagy and cancer, a common challenge is to determine whether autophagy protects cell survival or contributes to cell death. Autophagy is well known to be crucial for cell survival under extreme conditions, and degradation of intracellular macromolecules provides energy required for minimal cell functioning when nutrients are scarce (25). Consequently, autophagic activation can play a protective role in early stages of cancer progression (26). On the other hand, autophagy behaves as a tumour suppressor by activating pro-autophagic genes and blocking anti-autophagic genes in oncogenesis. However, autophagy can also play the reverse part (a pro-tumour role in carcinogenesis, named ‘Janus-faced’ effect) by regulating a number of pathways involving Beclin-1, Class III and I PI3K, mTORC1/C2 and p53 (26).

Recent studies have also related some BCL-2 proteins with autophagic cell death regulation (27). The most studied example is the autophagy-related Beclin-1 protein, which contains a BH3-like region and has been found to interact with the anti-apoptotic Bcl-2, Bcl-xL and Mcl-1 proteins. Several BH3-only proteins or BH3 mimetics can elicit autophagy by displacing Beclin-1 from Bcl-2/Bcl-xL/Mcl-1 proteins at the level of the endoplasmic reticulum (ER) (28).

1.1.4. Other types of programmed cell death.

In addition to the pathways previously described, other programmed cell death mechanisms have been uncovered (Table 1.I), including cornification (produced by the

death and transformation of keratinocytes into corneocytes, providing structural stability, mechanic resistance, elasticity to the skin); anoikis (caused by cellular detachment of cells from the extracellular matrix or from other cells of surrounding tissue); pyroptosis (that generates caspase-1 activation when macrophages are infected by specific pathogens); paraptosis (characterized by increased mitochondrial size and the presence of vacuoles in cytoplasm. This pathway is triggered by expression of the insulin-like growth factor receptor 1); and mitotic catastrophe (characterized by micronucleation and multinucleation and consequence of unproductive mitosis). The majority of these novel cell death pathways are cell-type specific and still remain poorly characterized (4) (Table 1.I).

1.1.5. Interrelationships between different Programmed cell death pathways.

Apoptosis, autophagy and necrosis are different physiological processes with distinct morphological characteristics. However, there still exist intricate interrelationships between them. Under some circumstances, apoptosis and autophagy can exert synergistic effects, whereas in other situations autophagy can be triggered only when apoptosis is suppressed (29). Programmed necrosis is always triggered as a backup mechanism for apoptosis when caspases are inactivated (for example, by a pharmacological treatment with (zVAD-fmk) (30). However, shikonin-induced necroptosis can revert to apoptosis in the presence of necrostatin-1 (Nec-1), a specific necroptosis inhibitor. This death mode switch is partially due to conversion from mitochondrial inner membrane permeability to mitochondrial outer membrane permeability (MOMP) (31). Under certain conditions, apoptosis and programmed necrosis are induced simultaneously and deficiency of both apoptosis and necrosis can be found in some cancer cells (32). Moreover, programmed necrosis is accompanied by autophagy, but the specific relationship between them remains an enigma (19).

The mode of cell death is influenced by many factors. One of them is the intensity of death stimulus. For example, low doses of cisplatin (CDDP) induce apoptosis, but higher doses trigger necrosis in mouse renal epithelial cells (33). In a similar way, a continued and weak signal of p53 usually promotes senescence; however, an intense p53 activation promotes apoptosis (34). Another factor is the energy requirement of the cell. When a cell is dying, bioenergetics consumption promotes necroptosis, since the apoptotic pathway requires a high energy consume (ATP) for the apoptosome formation and caspase cascade activation (35).

Table 1.I. Functional classification of regulated cell death modes. Adapted from **(4).**

Type of cell death	Biochemical features	Caspase dependence	Inhibitory Mechanism
Anoikis	Downregulation of EGFR Inhibition of ERK1 signaling Lack of b1-integrin engagement Overexpression of Bim Caspase-3 (-6,-7) activation	YES	Bcl-2 overexpression Z-VAD-fmk administration
Autophagic cell death	MAP1LC3 lipidation SQSTM1 degradation	NO	VPS34 inhibitors AMBRA1, ATG5, ATG7, ATG12 or BCN1 genetic inhibition
Caspase-dependent intrinsic apoptosis	MOMP Irreversible Dc_m dissipation	YES	Bcl-2 overexpression Z-VAD-fmk administration
Caspase-independent intrinsic apoptosis	Release of IMS proteins Respiratory chain inhibition	NO	Bcl-2 overexpression
Cornification Entosis	Activation of transglutaminases Caspase-14 activation	YES	Genetic inhibition of TG1, TG3 or TG5 Genetic inhibition of caspase-14
Entosis	RHO activation ROCK1 activation	NO	Genetic inhibition of metallothionein 2A Lysosomal inhibitors
Extrinsic apoptosis by death receptors	Death receptor signaling Caspase-8 (-10) activation BID cleavage and MOMP (in type II cells) Caspase-3 (-6,-7) activation	YES	CrmA expression Genetic inhibition of caspases (8 and 3) Z-VAD-fmk administration
Extrinsic apoptosis by dependence receptors	Dependence receptor signaling PP2A activation DAPK1 activation Caspase-9 activation Caspase-3 (-6,-7) activation	YES	Genetic inhibition of caspases (9 and 3) Genetic inhibition of PP2A Z-VAD-fmk administration
Mitotic catastrophe	Caspase-2 activation (in some instances) TP53 or TP73 activation (in some instances) Mitotic arrest	NO	Genetic inhibition of TP53 (in some instances) Pharmacological or genetic inhibition of caspase-2 (in some instances)
Necroptosis	Death receptor signaling Caspase inhibition RIP1 and/or RIP3 activation	NO	Administration of necrostatin(s) Genetic inhibition of RIP1/RIP3
Netosis	Caspase inhibition NADPH oxidase activation NET release (in some instances)	NO	Autophagy inhibition NADPH oxidase inhibition Genetic inhibition of PAD4
Parthanatos	PARP1-mediated PAR accumulation Irreversible $\Delta\psi_m$ dissipation ATP and NADH depletion PAR binding to AIF and AIF nuclear translocation	NO	Genetic inhibition of AIF Pharmacological or genetic inhibition of PARP1
Pyroptosis	Caspase-1 activation Caspase-7 activation Secretion of IL-1b and IL-18	YES	Administration of Z-YVAD-fmk Genetic inhibition of caspase-1

Abbreviations; BCN1, beclin 1; Dcm, mitochondrial transmembrane potential; CrmA, cytokine response modifier A; DAPK1, death-associated protein kinase 1; EGFR, epidermal growth factor receptor; ERK1, extracellular-regulated kinase 1; IL, interleukin; MAP1LC3, microtubule-associated protein 1 light chain 3; MOMP, mitochondrial outer membrane permeabilization; NET, neutrophil extracellular trap; PAD4, peptidylarginine deiminase 4; PAR, poly(ADP-ribose); PARP1, poly(ADP-ribose) polymerase 1; PP2A, protein phosphatase 2A; ROCK1, RHO-associated, coiled-coil containing protein kinase 1; SQSTM1, sequestosome 1; TG, transglutaminase; Z-VAD-fmk, N-benzyloxycarbonyl-Val-Ala-Asp-fluoromethylketone; Z-YVAD-fmk, N-benzyloxycarbonyl-Tyr-Val-Ala-DL- Asp-fluoromethylketone. A.

1.2. MAIN APOPTOTIC PATHWAYS.

The mechanisms of apoptosis are highly complex and sophisticated, involving an energy-dependent cascade of molecular events (Figure 1.1). There are two main apoptotic pathways: the extrinsic or death receptor pathway and the intrinsic or mitochondrial pathway. However, although the initial death signals are heterogeneous there is now evidence that both pathways are linked and that molecules from one pathway can influence the other (36). There is an additional pathway called perforin/granzyme that induces apoptosis via granzyme A or B and involves T-cell mediated cytotoxicity. All These pathways converge with the cleavage and activation of the executioner caspases-3/7 that results in DNA fragmentation, degradation of cytoskeletal and nuclear proteins, formation of apoptotic bodies and finally elimination by phagocytic cells (14, 37).

1.2.1. Extrinsic apoptotic pathway.

This pathway is initiated by the interaction of specific ligands (FasL, TNF-α or TRAILR) to the cysteine-rich extracellular domains of specific death receptors (FasR, TNFR1 or TRAIL). Following this binding, the cytoplasmic domain of death receptors (called the "death domain") (38, 39) transmit the death signal from the surface to the inner of the cell and then the cytoplasmic adapter proteins are recruited. FasL/FasR interaction recruits the adapter protein FADD and TNF-α/TNFR1 recruits TRADD, FADD and RIP (40). Finally, "death-inducing signaling complex" (DISC) is formed by the interaction between FADD and procaspase-8 when death effector domains dimerize. Caspase-8 and/or -10 are then activated generating the activation of executioner caspases-3/7 (41, 42).

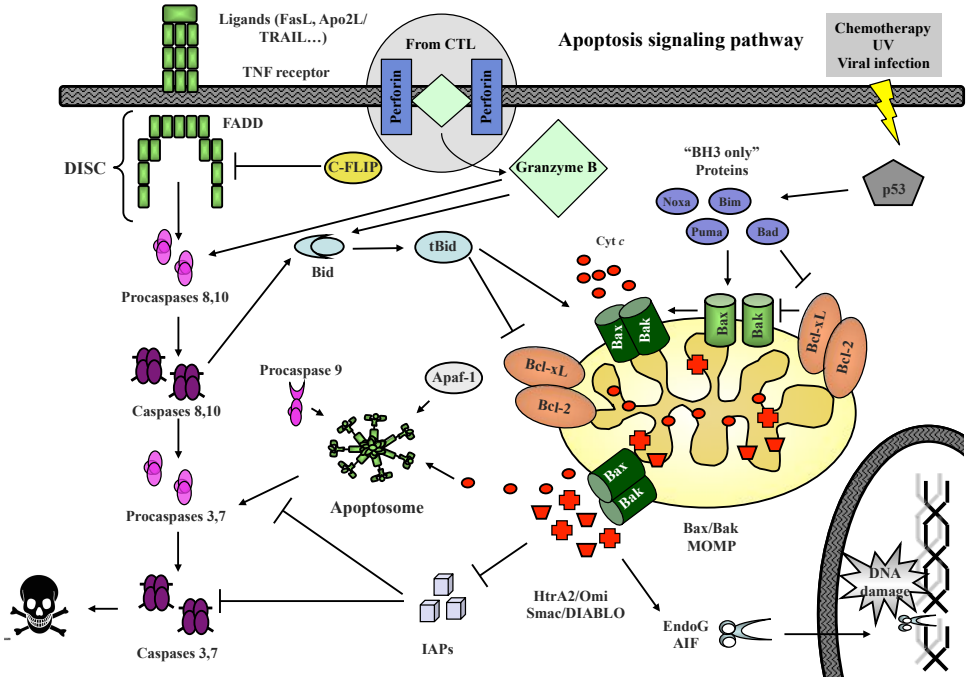

Figure 1.1. **Extrinsic and intrinsic apoptotic pathways**. In the extrinsic pathway, binding of the ligands to the corresponding death receptor triggers the recruitment of death domain (DD)-containing adaptor proteins (represented by FADD), procaspase-8 and -10 forming the supracomplex named DISC. Then caspase-8 (or-10) activates and promotes subsequent activation of executioner caspases-3 and -7, inducing apoptosis. The cleavage of the BH3-only protein Bid to generate tBid can also activate caspase-8, which is related to the intrinsic signaling pathway. In the mitochondrial pathway, mitochondrial outer membrane permeabilization (MOMP) produces the release of cytochrome *c* and other apoptogenic factors from mitochondria. In the cytosol the apoptosome is formed, triggering a caspase cascade by caspase-9 activation. The balance between anti-apoptotic BCL-2 proteins (represented by Bcl-2 and Bcl-xL) and pro-apoptotic BH3-only proteins (represented by tBid, Noxa, Puma, Bim and Bad) regulate the Bax/Bak activation and then the MOMP process. Inspired by (43)

1.2.2. Intrinsic apoptotic pathway.

The large variety of stimuli that initiate the signaling pathways of intrinsic apoptosis can behave in either a positive or negative manner. Negative signals correlate with the absence of hormones, cytokines and some growth factors that produce a failure of death programs suppression, thereby triggering apoptosis. Other stimuli generate apoptotic activation such as radiation (UV and gamma), DNA-damage, toxins, hypoxia, hyperthermia, viral infections, and free radicals (oxidative stress) (44).

All of these stimuli act directly on targets within the cell that promote changes in the inner mitochondrial membrane, the loss of the mitochondrial transmembrane potential

($\Delta\psi m$) (45), alterations in mitochondrial structure and function (46) and the opening of the mitochondrial permeability transition (MPT) pore, finally triggering mitochondrial outer membrane (MOM) permeabilization (MOMP). In vertebrates, this is usually considered "the point of no return" of the apoptotic cascade (44). MOMP produces the release of two pro-apoptotic groups of proteins (normally located in the intermembrane space (IMS)) to the cytosol (47). The first group consists of cytochrome-*c* (Cyt-*c*, 12 kDa), Smac/DIABLO (25kDa), and the serine protease HtrA2/Omi (37kDa) (48). These proteins activate the caspase-dependent mitochondrial pathway. Cyt-*c* is loosely associated to the mitochondrial lipid cardiolipin (CL) in the mitochondrial inner membrane (MIM). When CL is oxidated upon MOMP, Cyt-*c* can diffuse to the cytosol, wherein it promotes the assembly of the apoptosome platform that includes Cyt-*c*, apoptosis protease activating factor (APAF-1), pro-caspase- 9 and ATP/dATP. This multiprotein complex activates caspase-9 producing caspase cascade activation (48-50). Smac/DIABLO and HtrA2/Omi are reported to promote apoptosis by inhibiting IAP (inhibitors of apoptosis proteins) activity (51, 52), thus favoring caspase activation.

The second group of pro-apoptotic proteins, AIF (62 kDa) and endonuclease G (23 kDa) are released from the mitochondria during apoptosis, but this is a late event that occurs after the cell has committed to die. Once released to the cytosol, both proteins translocate to the nucleus and mediate chromatin condensation and DNA fragmentation (53, 54). AIF and endonuclease G both function in a caspase-independent manner.

The control and regulation of the apoptotic mitochondrial events, especially MOMP, is accomplished by the members of the Bcl-2 family of proteins (55). They govern mitochondrial membrane permeability and can be either pro-apoptotic or anti-apoptotic, establishing a complex interaction network within themselves and with other cellular factors to determinate whether cells dye by apoptosis or abort the process (56, 57). The main mechanism of action of the Bcl-2 family of proteins is regulation of Cyt-*c* release from the mitochondria via alteration of mitochondrial membrane permeability.

1.3. THE BCL-2 PROTEIN FAMILY.

1.3.1. General classification.

There are approximately 20 proteins in the BCL-2 family, defined by their α-helical composition of up to 4 BCL-2 homology domains (BH). Based on the cellular function this protein family is divided into 3 different groups: the anti-apoptotic BCL-2 proteins Bcl-2, Bcl-xL, Bcl-w, Mcl-1 A1 and Bcl-b (Diva), the pro-apoptotic BCL-2 effectors Bax, Bak and Bok and the pro-apoptotic BH3-only proteins Bid, Bik, Bim, Bmf, Noxa, Puma,

Rambo, Bad and Hrk (56, 57)(Figure 1.2A). The presence of a BH3 motif defines all Bcl-2 proteins (58). The BH3 domain is defined as a sequence that could form a four-turn amphipathic alpha helix containing the sequence motif A-X-X-X-A-X-X-A-B-C-X-A, wherein A represents a hydrophobic residue (one of these residues is an almost invariant leucine), B represents a small residual, typically glycine, and C is Asp or Glu (59).

A

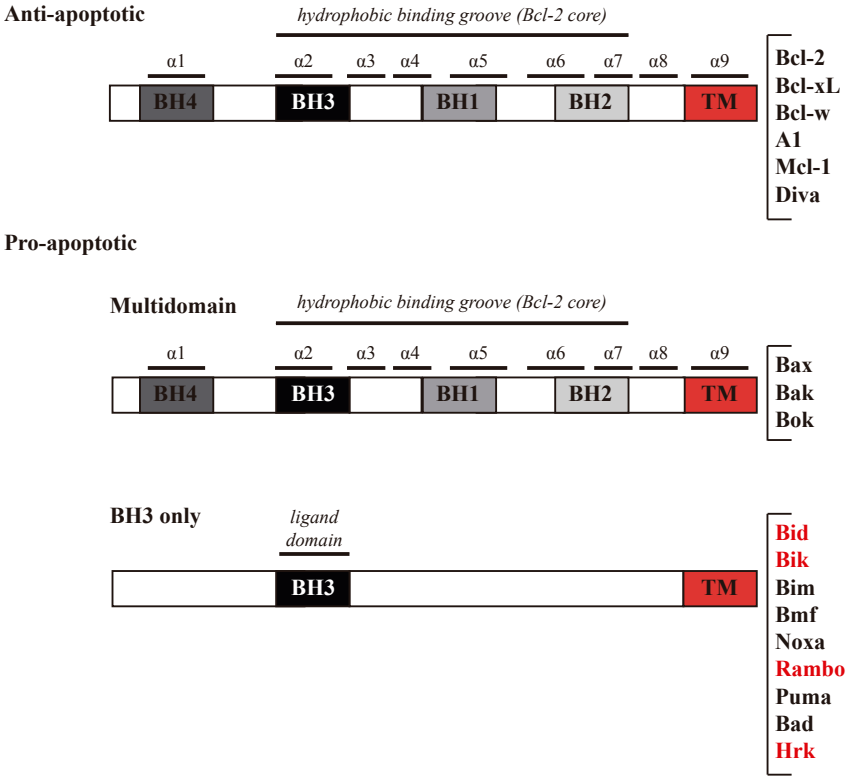

B

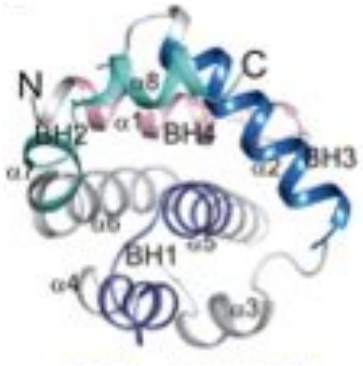

Figure 1.2. BCL-2 structural and functional organization. (A) Three subfamilies of BCL-2 proteins. BCL-2 homology domains 1 to 3 constitute the BCL-2 structural core that forms the BCL-2 hydrophobic groove (the binding site of the BH3 domains of BCL-2 pro-apoptotic proteins). The family is divided into anti- and pro-apoptotic members. The anti-apoptotic members share homology in all 4 BCL-2 homology (BH) domains (BH1-4) and include A1, Bcl- 2, Bcl-xL, Bcl-w, Mcl-1 and Diva. The pro-apoptotic members are subdivided into "multidomain" proteins and "BH3-only" proteins. The multidomain proteins share homology domains 1 to 4, whereas the BH3-only proteins contain only one BH domain, the BH3, which binds the anti-apoptotic proteins. Many BCL-2 proteins also contain a hydrophobic transmembrane domain (TMD). In the BH3-only group, the TMD is confirmed for Bid, Bik, Rambo and Hrk (marked as red). (B) The Bcl-2 core of Bcl-xL (PDB:1MAZ) and the respective locations of the four BH regions.

1.3.2. Structure of BCL-2 proteins.

The X-ray and NMR structures of BCL-2 members revealed that the multidomain anti-apoptotic and effector BCL-2 proteins are globular proteins that share a conserved ''BCL-2 core'' (Figure 1.2B). This core is also preserved in BH3-only proteins Bid and Bik, even though they have the least structural homology to the folded members (60). The BCL-2 core is structured by eight amphipathic alpha (α) helices that hide and bury a central hydrophobic helix α5 (Figure 1.2B). In this structure, the hydrophobic groove (BC groove) is the result of BH1 (α4– α5), BH2 (α7– α8), BH3 (α2) and α3 coalescence, showing BC groove at the ''front'' of the BCL-2 core.

Most of the structural studies used truncated forms that do not include the C-terminal hydrophobic domain of the Bcl-2 proteins (61, 62). The elimination of the hydrophobic C-terminal domain improves the solubility of these proteins, so they can be easily produced in the high quantities required for structural studies, whereas full-length proteins are difficult to produce. Only in the case of Bax and Bcl-w the structure of the full-lengh protein has been determined by NMR (63, 64). In both cases the C-terminal domain occupies the hydrophobic pocket responsible of the interactions with other BCL-2 proteins.

The three dimensional structure of Bcl-xL lacking the C-terminal segment (ΔC) (65), showed that BH domains 1 to 3 are close in order to form the hydrophobic groove wherein the BH3 domains of pro-apoptotic effectors (Bax, Bak and Bok) and BH3-only family members are able to bind (65). Unusual features of Bcl-xL are the splicing forms Bcl-xS and Bcl-xAK (66, 67) with pro-apoptotic functions when the BH3 domain is absent. Moreover, the unstructured loop between $\alpha 1$ and $\alpha 2$ helices of Bcl-xL can be cleaved by caspases triggering its conversion again into a Bax-like pro-apoptotic protein (68). Bcl-2, Bcl-xL, A1, and Mcl-1 show structural differences and similarities in the BCL-2 cores structures, depending on the free and BH3 peptide-bound states. The BH3-binding groove of Mcl-1 is flanked by regions of high positive electrostatic potential and

helix 3 and 4 are not as closely packed as seen in Bcl-xL (69). Moreover, the N-terminal PEST region of Mcl-1 negatively modulates BH3 peptide access to the groove (70). In the case of A1, the BH3 domain-binding groove has an acidic patch (71). For Bcl-2, the exposed BH3-binding groove presents topological and electrostatic potential differences respect to Bcl-xL hydrophobic groove (72).

All together, the BC groove and α1/α6 structural components compose the BCL-2 core and, in Bcl-w, Bcl-xL and Bax, the C-terminal helix binds and block this BC groove. Such an arrangement of alpha helices is similar to that of the membrane translocation domain of bacterial toxins, in particular diphtheria toxin and the colicins, and suggests that the Bcl-2 family proteins may be capable of forming pores. Indeed, Bcl-xL, Bcl-2, Bax, and Bid have been shown to possess ion channel activities *in vitro* in lipid bilayers or liposomes. This activity should be related with the mitochondrial permeability regulating function of these molecules (65) (73). The major differences between anti-apoptotic and effector proteins are structural features of the individual BCL-2 cores, wherein the C-terminal TM tail modulate interactions with the BH3-only proteins. In addition, many BCL-2 family members use the C-terminal hydrophobic regions to target and/or anchor them to intracellular membranes.

From an evolutionary point of view, differences in the structure as well as sequence of the various BH3-only proteins suggest a diverse origin and evolution of these molecules. This indicates that the BCL-2 family may be further divided into the core group (Bcl-2, Bcl-xL, Bcl-w, Mcl-1, A1, Bax, Bak, Bok, Bik and Bid) that shares both the sequence and structure homology (common and ancient origin) and the group that differs in structure and sequence, including Bim, Puma, Rambo, Diva, Bad, Bmf Hrk and Noxa. This may further imply that non-conserved functions may be expected among these molecules (56, 74).

1.3.3. Anti-apoptotic BCL-2 proteins.

The main function of anti-apoptotic BCL-2 proteins is the blockade of pro-apoptotic BCL-2 effectors (Bax and Bak) and BH3-only proteins to ensure MOM integrity. For that reason, they are mainly located in MOM, but can also be found in endoplasmic reticulum (ER) membrane and cytosol (75). All the members of this subfamily share the BH domains 1 to 4 and the "BCL-2 core". This subfamily include A1 (Bcl-2-related gene A1), Bcl-2, Bcl-xL (Bcl-2-related gene, long isoform), Bcl-w, and Mcl-1 (myeloid cell leukemia 1).

Although these proteins are classified into one category the differences observed in the solution structures of the anti-apoptotic proteins generate differences in the patterns of

binding to BH3-only or BAX-like proteins in solution. For that reason, it is possible to separate the anti-apoptotic members in two subgroups: one includes Bcl-xL, Bcl-2 and Bcl-w and the other is formed by Mcl-1 and A1 (59, 69).

Several studies, based on the genetic knockouts have revealed specific physiologic roles for the different anti-apoptotic proteins. The *Bcl-2 KO* mouse shows a normal development, but the adult mouse displays several dysfunctions in thymus, spleen and kidney due to increased apoptosis (76). *Bcl-xL KO* mouse dies during embryonic development due to massive apoptosis of hematopoietic and neuronal cells (77), while the *Bcl-w KO* mouse has demonstrated its relevance in spermatogenesis (78). Loss of Mcl-1 blocked embryo implantation and is lethal in early embryonic stages (79). Moreover, Mcl-1 deletion in the adult mouse revealed the requirement of this protein for hematopoietic stem cell survival (80).

1.3.4. Pro-apoptotic BCL-2 effectors.

The pro-apoptotic BCL-2 effector subfamily includes: BCL2-related ovarian killer (Bok, Matador) BCL-2 antagonist killer 1 (Bak) and BCL-2-associated X protein (Bax). They are the responsible to permeabilize the MOM following apoptotic stimuli, therefore are found in MOM, although Bax is also located in cytosol in absence of apoptotic signalling (in normal healthy cells) and Bok and a fraction of Bak can be found in ER (81). BCL-2 effectors are composed by BH3 domains 1 to 3 (82) and contain "BCL-2 core" structure, sharing sequence, domain, and structural homology (64, 65, 83) with anti-apoptotic members. Bak (in MOM) and Bax (in cytosol) are monomeric in absence of apoptotic stimuli. During apoptosis, both proteins undergo conformational changes at the MOM to activate and promote homo- and hetero-oligomerizations between them to triger MOMP. This fact has been largely corroborated in several studies using *Bax/Bak KO* mice, wherein the experimental data showed the absence of MOMP upon apoptotic activation (84). The majority of *Bak /Bax DKO* mice are embryonic lethal and the few mice that survive to birth (<10%) display a variety of apoptosis-related phenotypes, including interdigital webbing, splenomegaly, and lymphadenopathy. However, *Bak KO* and *Bax KO* mice display less aggressive phenotypes compared to the combined *DKO* mice. While the *Bak KO* (85) mice do not present any homeostatic or developmental defects, the *Bax KO* (86) mice show reproductive abnormalities and T and B cell hyperplasia.

1.3.5. Pro-apoptotic BH3-only proteins.

The BH3-only proteins promote MOMP (triggered by appropriate stimuli) when they bind to and sequester anti-apoptotic BCL-2 family members, avoiding their association with the multi-domain effectors (Bax and Bak) or when they bind directly to these apoptotic effectors, activating them. They include Bid (BH3 interacting domain death agonist, Bim (BCL-2-interacting mediator of cell death), Puma (p53 up-regulated modulator of apoptosis), Bad (BCL-2 antagonist of cell death), Bik (BCL-2-interacting killer), Bmf (BCL.2-modifying factor), PMAIP1 (Phorbol-12-myristate-13-acetate-induced protein) commonly known as Noxa, Hrk (Activator of apoptosis harakiri), Rambo (BCL2-like 13) and Diva (Bcl-b, BCL2-like 10). All members of this this subclass share the BH3 domain.

BH3-only proteins have been mainly classified as intrinsically unstructured proteins due to their structures have been solved (e.g. Bim, Bmf, Puma and Bad) without their C-terminal regions, and only after interation to multidomain BCL-2 member, BH3-only proteins acquire a structured conformation. This correlates with the fact that synthetic peptides representing BH3 domains of almost all BH3-only proteins have been crystallized bound to anti-apoptotic members (60, 87). However, Bid protein is a globular protein that contains the BCL-2 core structural motif with one central hydrophobic helix (α 6) surrounded by the remaining seven amphiphathic helices (88). Bid also contains a consensus sequence for caspase-8 cleavage localized between helices α 2 and α 3 that results crucial for Bid localization and interaction with Bax/Bak to promote MOMP (89).

The different BH3-only *KO* mice showed tissue- and/or stimulus-specific effects in development and tissue homeostasis. *Bid KO* mice are developmentally normal and only show resistance to induced liver injury (90). *Bim KO* mice have lymphoid and myeloid cell hyperplasia (91). *Hrk KO* mice have defects in nerve growth factor withdrawal, generating apoptosis in sensory neurons (92). However, *Puma KO* mice display a broader role in ER stress, ischemia/reperfusion, bacterial/viral/ fungal infections, MOMP and apoptosis (93), showing resistance against several stimuli like irradiation, cytokine withdrawal and glucocorticoids.

Bad KO generates diffuse lymphomas in large B cell (94). The lymphocytes of *Bmf KO* animals are resistent to apoptosis induced by glucocorticoids or histone deacetylase inhibitors (95). *Bik KO* does not show any significant effect and only in combination with *Bim KO* generate male infertility (96). *Noxa KO* shows mild resistance to etoposide in MEFs and thymocytes (97). All these studies highlight the existence of different models regarding the regulatory function of the BH3-only proteins.

BH3-only proteins can interact to anti-apoptotic proteins to block their pro-survival function and/or can bind and activate Bax/Bak effectors directly. For that reason they are

divided in two groups: sensitizers/de-repressors and direct activators. Direct activators includes Bid, Bim, and Puma which are responsible (by direct interaction) for promoting the active form of Bax and Bak by conformational changes to induce MOMP (98, 99). This group of BH3-only proteins can also bind and inhibit the anti-apoptotic proteins. Furthermore, triple-knockout mice for Bid, Bim, and Puma (100) showed a similar phenotype compared to *Bax/Bak KO* mice, indicating their crucial role in BCL-2 effectors activity and MOMP. Of note, the role of Puma as activator is controversial (100), and Bid/Bim double-knockout generates a minor apoptotic phenotype,.

The sensitizers/de-repressors subclass of BH3-only proteins is composed by Bad, Bmf, Hrk, and Noxa and their functions are associated to the blockade of anti-apoptotic BCL-2 members (by binding hydrophobic groove of these) to induce MOMP (101-105). However, the precise mechanism(s) of interaction between BH3-only proteins and the anti-apoptotic BCL-2 network to promote Bax/Bak activation and MOMP remains to be elucidated.

Finally, some BH3-only proteins such as Bik, Rambo or Diva have different behavior in comparison to the rest of the proteins present in this subgroup. Bik shares the BH3 domain and the C-terminal domain with other BCL-2 family proteins. It is predominantly localized in the ER, interacts with Bcl-2, Bcl-xL, Bcl-w, A1 and Diva, and induces apoptosis through the mitochondrial pathway by selective activation of Bax, mobilizing calcium from the ER to the mitochondria and remodeling the mitochondrial cristae. Bik also induces non-apoptotic cell death in certain cell types by an unknown mechanism and appears to be a critical effector in apoptosis induced by toxins, cytokines and virus infection (106). Rambo shows high structural homology with the anti-apoptotic BCL-2 members containing the four conserved BH motifs and a c-terminal membrane anchor region. Rambo does not interact with either anti-apoptotic (Bcl-2, Bcl-xL, Bcl-w, A1, Mcl-1) or pro-apoptotic (Bax, Bak, Bik, Bid, Bim, and Bad) members of the Bcl-2 family. In mammalian cells, Rambo is localized in mitochondria, and its over-expression induces apoptosis that is specifically blocked by the caspase inhibitors, IAPs. Surprisingly, the cell death activity promoted by Rambo is induced by its membrane-anchored C-terminal domain and not by the BCL-2 homology region (107). Diva/Bcl-B is considered an anti-apoptotic member of the BCL-2 family and interacts with Bim and Bik BH3-only proteins, blocking apoptosis induced by Bax. However, Diva also acts as pro-apoptotic inducing apoptosis independently of the BH3 region through direct binding to APAF-1, thus preventing Bcl-xL from binding to the caspase-9 regulator APAF-1. For that reason, Diva apparently can both promote and inhibit apoptosis depending on the cellular context. In conclusion, the Figure 1.3 shows the interactions/relationships established between the different members of the BCL-2 family. In this highly orchestrated context, the relevance

of the cytosolic domain in the interaction network has been extensively studied. However, the contribution of the TMD to this interaction network has been poorly investigated.

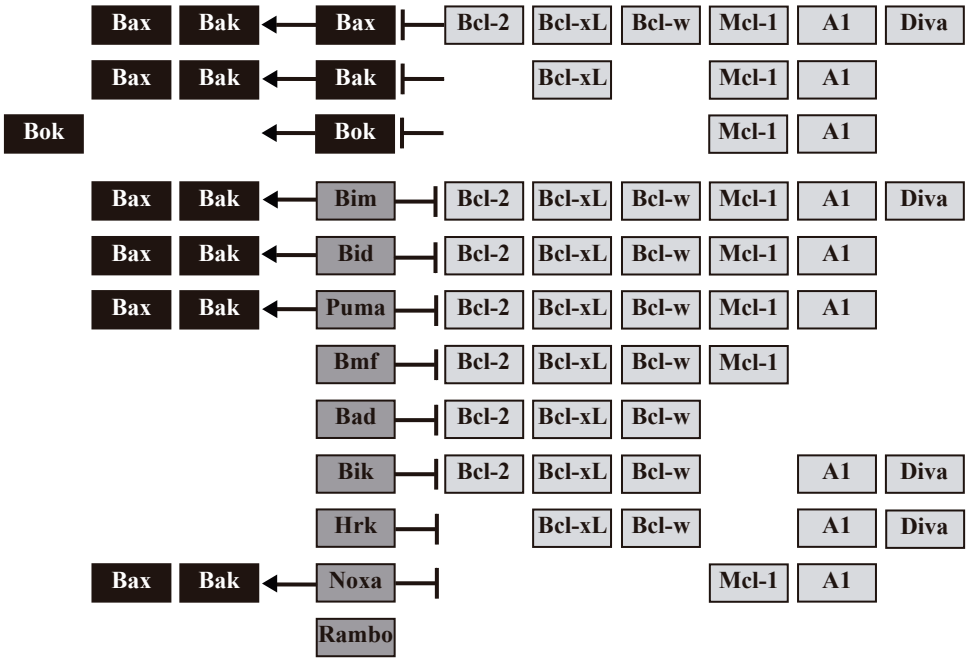

Figure 1.3. Schematic representation of BCL-2 family interactions. Black and dark grey squares represent pro-apoptotic effectors and BH3-only proteins, respectively. Light grey squares represent the anti-apoptotic proteins. The arrows indicate an inducing effect, whilst the bars indicate an inhibitor/repressor effect.

1.4. BCL-2 FAMILY: MODELS OF MECHANISM OF ACTION.

All the models proposed for the apoptotic regulation of the BCL-2 family share some well established points such as:

- BCL-2 anti-apoptotic proteins block the activation of the effectors Bax and Bak.
- Bax and Bak are inactive in healthy cells, and their activation triggers MOMP and the release of the apoptogenic factors.
- BH3-only proteins activate Bax and Bak and avoid the action of the anti-apoptotic members.

However, the mechanism of action for the different partners and the interaction network among them is still controversial. During the last decades, several studies have been developed to study the interaction networks between the different pro- and anti-apoptotic members of the BCL-2 family, concluding that different models of MOMP

regulation mediated by the BCL-2 proteins are possible. The different models propose different binding partners and functions for both the BH3 and the anti-apoptotic family members. All these models accumulate positive evidence from a variety of assays to indicate that specific aspects of each model are correct, including co-immunoprecipitation assays in transfected cells, binding of peptides to truncated proteins *in vitro*, and gene knockout experiments in mice. In addition, the MOM itself also plays an important role in BCL-2 family member interactions and functions. Thus, four non-mutually exclusive models coexist to explain how interactions among the BCL-2 family proteins regulate MOMP and apoptosis (Figure 1.4).

1.4.1. Initial models: rheostat, direct activation and de-repression.

The first model of Bcl-2 regulation called "Rheostat" was hypothesized when Bax protein was discovered in 1993. This model is based on the ratio between anti-apoptotic members and pro-apoptotic proteins like Bcl-2 and Bax, respectively (105, 108). When an excess of Bax is generated compared to Bcl-2, apoptosis is triggered. Some years latter, when other BCL-2 proteins were identified, two classical models were elicited: the "direct activation" and "de-repression" models.

1.4.1.1. De-repression model.

This model (also called indirect activation model) postulates that Bax and Bak are constitutively and structurally active in non-apoptotic conditions. Therefore, they need continuous binding to anti-apoptotic proteins to repress their activity. In this situation, the BH3-only proteins displace the anti-apoptotic proteins from Bax and Bak interaction to let MOMP (Figure 1.4). Specific combinations of different BH3-only proteins, activated by specific apoptotic signals, interact with different anti-apoptotic proteins and allow Bax/Bak activation by highly regulated mechanisms (59). For example, Bid, Bim and Puma show more pro-apoptotic effect than the rest of BH3 only proteins due to their direct interaction with the anti-apoptotic members; Furthermore, Noxa interacts with Mcl-1 and A1 specifically while Bad only binds to Bcl-2, Bcl-xL, and Bcl-w (Figure 1.3). Only when Noxa and Bad are combinated cell death is induced (59). Of note, Bak is inhibited not only by Mcl-1 and Bcl-xL but also by VDAC2 (109, 110).

However, the de-repression model does not explain that only a small fraction of Bax/Bak can be co-immunoprecipitated with anti-apoptotic proteins *in vivo*, in contrast to experimental data that suggest that all Bax/Bak needs to be neutralized for survival (111).

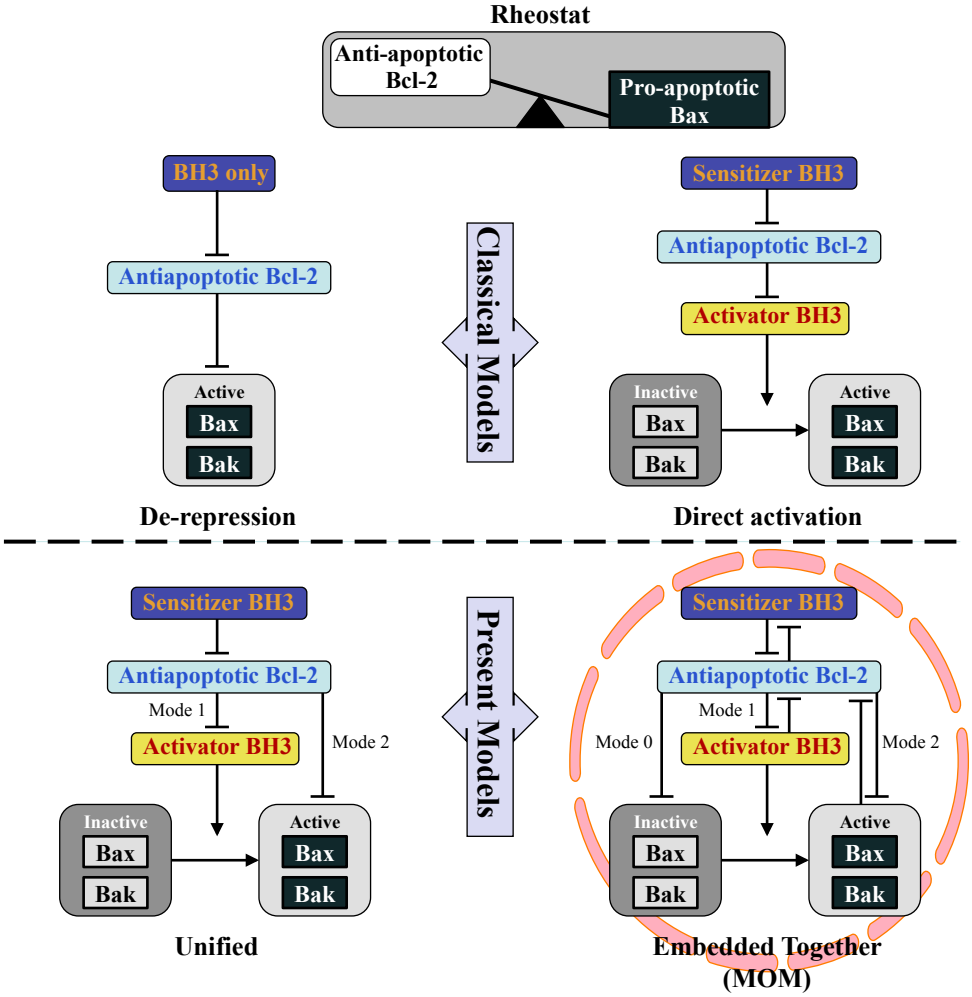

Figure 1.4. Models of apoptotic regulation by the BCL-2 family. (Upper panel) **In** the "Rheostat" model, the equilibrium between pro- and anti- apoptotic BCL-2 proteins is crucial to cell fate. De-repression (left) and Direct Activation models (right) highlight the role of BH3-only proteins and anti-apoptotic proteins. (Bottom panel) The Embedded Together model (right) and the Unified model (left) propose that BH3 proteins have to activate Bax/Bak and the inhibition of MOMP by the BCL-2 anti-apoptotic proteins is produced by their interaction with BH3 only proteins and/or Bax/Bak efectors.. The Embedded Together highlights the active role of MOM in the interactions between BCL-2 family proteins. Adapted from (112).

1.4.1.2. Direct activation model.

The direct activation model postulates that Bax/Bak need to be activated to oligomerize and promote MOMP. In this scenario, BH3 proteins behave as: activators, such as Bim, Puma and tBid, binding of Bax/Bak directly (113); or sensitizers (Bad,Noxa, Bmf, Hrk),

whose function is to block the anti-apoptotic proteins, releasing the BH3 activators from the anti-apoptotic proteins to Bax and Bak to generate MOMP (99, 113). In this context, several groups showed that tBID (BH3 activator) promotes MOMP by Bax/Bak activation (98, 114).

The problem of this model is consequence of BCL-2 anti-apoptotic ability to bind and inhibit directly the activation of Bax/Bak (115). In addition, another problem is the difficulty to detect interactions between the BH3-only proteins and Bax/Bak. Moreover, de-repression model and the direct activation model postulate that all these interactions are unidirectional. The solution for these limitations was to propose a "hit-and-run" mechanism for Bax/Bak activation by BH3-only proteins based on transient interaction between BH3-only "ligands" and Bax/Bak "receptors" (99, 116).

1.4.2. The embedded together model: role of membranes in apoptotic regulation.

In the models previously described, the active role of membranes in the functions of Bcl-2 family members is not considered. However, the BCL-2 proteins are mainly membrane-inserted proteins via their C-terminal domain and the interactions between different Bcl-2 members take place generally in the MOM. Moreover, these BCL-2 proteins generally have a different conformation when inserted in the mitochondrial membrane.

The membrane-Embedded Model highlights the role of the MOM in the BCL-2 family protein interactions during apoptosis, mediating in these interactions rather than being only the place where this interaction network occurs. The model suggests that the association/insertion of BCL-2 proteins to the MOM promotes conformational changes in these molecules that affect their binding interactions (117, 118). For example, Bax undergoes conformation changes during activation when it translocates from a cytoplasmic location to a protein with helices 5, 6 and 9 integrated in the membrane. This conformational change is necessary to oligomerize with other Bax monomers to form a pore in the MOM, and this event only take place when Bax is inserted in MOM (119). Other example is Bid: Following caspase-8 cleavage, tBid targets MOM, undergoing conformational changes that allows tBid to activate Bax and the recruitment of cytoplasmic Bcl-xL (120). These tBid membrane interactions can be modulated by membrane lipid composition and, interestingly, the membrane interaction between tBid and Bax can promote redistribution of membrane lipids (121).

This model exposes that the activation of Bax/Bak at the membrane is the rate-limiting step in MOMP. The BH3-only activators such as Bim, tBid and Puma can bind to MOM spontaneously where they recruit Bax (and some antiapototic members as Bcl-xL),

generating several conformational changes in Bax to induce oligomerization. Bak is constitutively located to the membrane, so this first step is not necessary. Anti-apoptotic proteins located in MOM bind to activator BH3 proteins (Bid, Puma and Bim) inhibiting their pro-apoptotic function. However, in this context the activator proteins behave as sensitizers because they also inhibit anti-apoptotic proteins. For that reason, this kind of inhibition was called mutual sequestration (122).

Based on the idea of the mutual sequestration, the difference between activator and inhibitor is more quantitative than qualitative and then the amount of anti-apoptotic and BH3-only proteins in MOM determinates these equilibria.

Finally, this model introduces the concept of dominant negative of Bax/Bak that refers to the inhibition of Bax/Bak activation and oligomerization induced by the binding of BCL-2 antiapoptotic in the MOM context.

1.4.3. Unified model.

This model also takes into account the different modes of apoptotic inhibition and the role of mitochondrial dynamics in apoptosis regulation (123). In MODE 1 the anti-apoptotic proteins inhibit BH3-only activators (similar to mutual sequestration). MODE 2 represents the inhibition of Bax/Bak by anti-apoptotic proteins (equivalent to dominant negative function of the anti-apoptotic proteins). Both mechanisms could inhibit MOMP, but binding to Bax/Bak is considered more effective than binding BH3-only activators, (123), due to once activated by a BH3-only protein, Bax and Bak can activate other Bax/Bak molecules (124).

Thus, unlike the Unified model, the Embedded Together model proposes that the dominance of MODE 1 *vs* MODE 2 depends on the membrane bound dynamics refers to the amount of protein and post-translational modifications of the BCL-2 proteins. .

Finally, the lipid composition of the MOM determines the binding interactions and functions of BCL-2 family proteins so “Lipid-Centric Model” has been also proposed (125, 126), wherein apoptosis-related lipids modulate the activation and action of BCL-2 family members at the MOM level, either through a direct and stereoselective interaction (125), or via a bilayer-mediated effect (126).

1.5 MITOCHONDRIAL PORES: RELEVANCE OF MITOCHONDRIAL OUTER MEMBRANE (MOM) COMPOSITION IN ITS PERMEABILIZATION.

Upon apoptotic stimuli, the release of Cyt-*c* and other pro-apoptotic proteins from mitochondria to cytosol involves different mechanisms represented in different models. Some of them propose that the presence of Cyt-*c* and other mitochondrial proteins in cytosol is produced by the loss of MOM integrity, whereas other models suggest that the formation of different types of channels produces an increase in MOM permeability, generating the release of these mitochondrial proteins. However, none of the MOMP models is able to integrate all the experimental data.

1.5.1. Bax/Bak activation and oligomerization to form mitochondrial pores.

The activation of Bax and Bak is ultimately regulated through complex protein-protein interactions between the direct activator BH3-only proteins and Bax/Bak at the MOM. However, the understanding of mechanisms leading to Bax/Bak activation is still controversial. Bax and Bak could be activated by the exposure to MOM components, like certain lipids (125) and by various physical factors as changes in pH and heat. However, the most studied mode of Bax/Bak activation is through activator BH3-only proteins binding (98, 116, 127). This interaction between BH3-only proteins and Bax/Bak is a transient interaction (99) described as a “hit and run” mechanism. After binding to activator BH3-only proteins, Bax/Bak undergo major conformational changes generating several structural changes of the N-terminal region that contains the BH3 domain, and helices 5, 6 and 9 (helix 9 only change its conformation in Bax) (Figure 1.5) (119, 127). As a result of these structural arrangements, the affinity between Bax/Bak and BH3-only proteins decreases, confirming the hypothesis of a ‘hit-and-run’ mechanism.

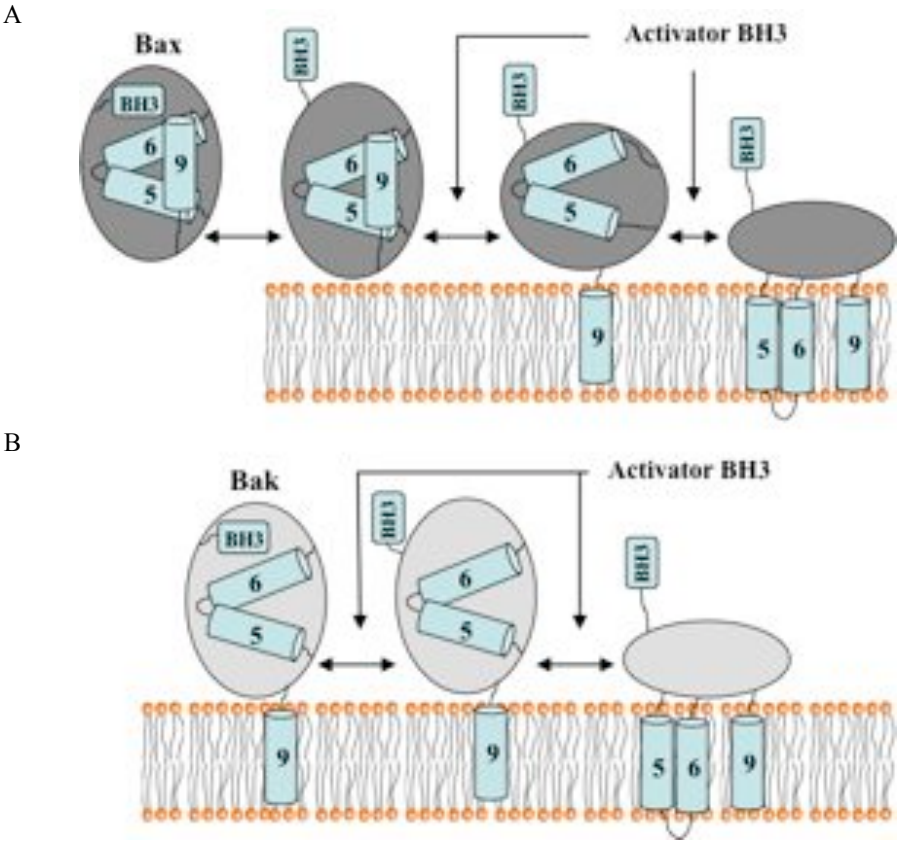

Figure 1.5. Bax and Bak undergo a step-wise activation mechanism. (A) In healthy cells, Bax is mainly in cytoplasmic conformation when apoptotic stimuli is absent. After apoptotic activation, Bax undergoes conformational changes triggering the insertion of helices 5, 6 and 9 into the membrane. The activated form of Bax generates the recruitment of more cytoplasmic Bax that oligomerizes promoting the MOMP. (B) Bak helix 9 is constitutively inserted in the MOM. Upon apoptotic signaling, BH3 activators bind to Bak to generate conformational changes that trigger the insertion of helices 5, 6 into the membrane. Inspired by (112).

Bak is constitutively present in MOM through insertion of its helix 9 (TM). The high affinity of Bak for membrane insertion may be due to the increased hydrophobicity of the Bak TM region (ΔG= -0.735) compared to that of Bax (ΔG= 0.510), which facilitates its binding to membranes rather than to the hydrophobic groove (128). Following activation by BH3-only binding, conformational changes produced, the rearrangement of the N-terminus, exposing Bak BH3 domain and inserting helix 5 and 6 into the MOM (129) (Figure 1.5A). The exposure of the BH3 domain promotes the dimerization Bak, forming

a "groove-to-groove" dimer, that can multimerize with other Bak dimers through an α6-α6 interaction (130).

In contrast, the inactive form of Bax monomer is in continuous movement between the cytoplasm and mitochondria in healthy cells (131). In this inactive conformation, the hydrophobic helix 9 (TMD) is buried in the hydrophobic groove (132) to increase the solubility of Bax in cytosol. Recent studies, have been demonstrated that Bcl-xL is the responsible of Bax retro-translocation back from the MOM to the cytoplasm to avoid apoptotic activation (133). This mechanism maintains low Bax levels in MOM. When a BH3-only binds to Bax, the resulting arrangements produce the release of α9 from the hydrophobic groove (119), increasing Bax affinity to MOM and promoting its membrane insertion. This process triggers the permeabilization of the MOM. In addition It is thought that not only Bax α9 inserts into the MOM but also α5, α6, and (Figure 1.5B) and that activation of a single molecule of Bax can propagate the activation of other Bax molecules via the exposed BH3 domain, which manages Bax oligomerization (Figure 1.6 (124)). Moreover, crystal structure of Bax, binded to Bid BH3 peptide showed that this interaction mediated by the hydrophobic groove of Bax generates a relevant position change of Bax helix 2 (134). Interestingly, this displacement debilitate the contacts between Bid BH3 peptide and Bax and facilitate Bax/Bak oligomerization (134). Then, it is thought that can be a credible explanation of "hit and run mechanism".

1.5.2. MOMP: Bax/Bak pore formation in the MOM.

Although the fact that Bax and Bak are the executioners of MOMP is extensively accepted, the way in which these proteins generate the pore to produce the permeabilization process is still unclear. Several models have been proposed describing the composition of the Bax/Bak pore (Figure 1.6). These models can be divided in two groups: On the one hand, Indirect Activation Models postulate that the Bax and Bak function is to modify the existing mitochondrial proteinaceous channels (see below) permeabilizing MOM via a physical interaction with the components of the mPTP (mitochondrial Permeability Transition Pore) found at mitochondrial contact sites (CS) (135). For example, Bax may increase the permeability of the MOM by regulating VDAC1 channels (Figure 1.7) (136).

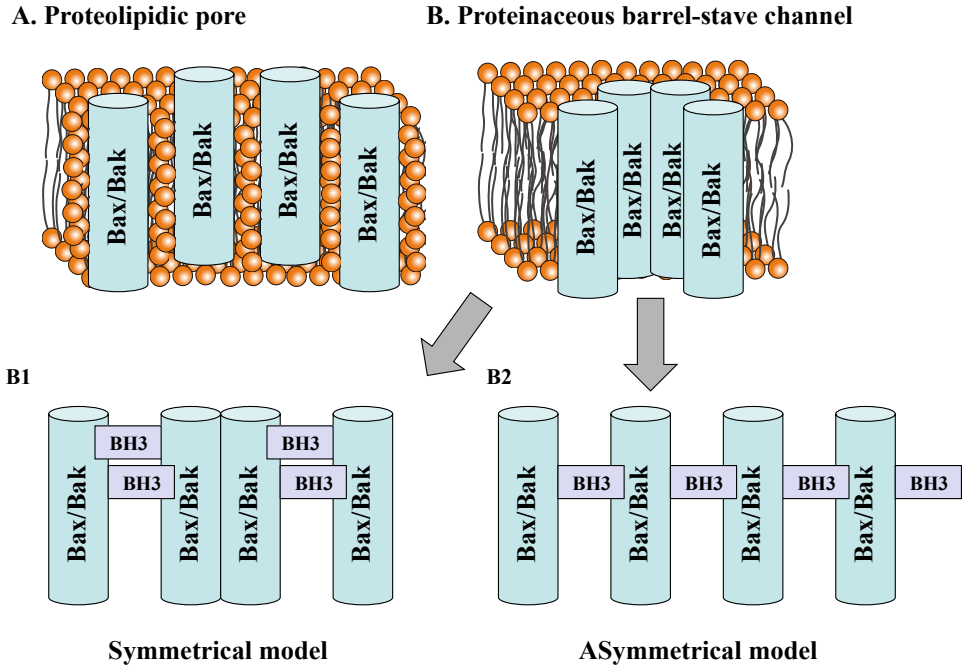

Figure 1.6. Mechanisms of Bax/Bak MOMP. (A) The protein–lipidic pore mechanism involves the interactions of some lipids with Bax/Bak, regulating the pore formation. (B) In the Proteinaceus barrel-stave channel, only the Bax/Bak oligomers are considered as components of the pore. (B1) In The symmetrical model Bax/Bak oligomers are formed by the interaction of the BH3 domains into the canonical groove and α6 helix interactions are the responsible of higher order oligomers. (B2) The asymmetrical model is based on the interaction of Bax BH3 domain with another Bax molecule by the non canonical groove. Inspired by (112).

On the other hand, the Direct Activation Models postulate that the only partners contributing to pore formation are Bax and Bak. The structure of these channels could be a proteolipidic pore (Figure 1.6A) or a proteinaceous barrel-stave channel (Figure 1.6B). These models are based on the structural similarities found between BCL-2 proteins and bacterial pore-forming toxins (73) as well as the capability of activated Bax and Bak to permeabilize lipid membranes in the absence of other mitochondrial components (137, 138).

1.5.3. MOMP: Other mitochondrial channels with capacity to release apoptogenic proteins.

There are other mitochondrial channels different to Bax/Bak pore complex that promote

different mechanism of release for Cyt-*c* and other pro-apoptotic molecules (Figure 1.6; (139)). Some models suggest that MOM permeability is caused by proteins large enough to form channels that cross the MOM to allow the permeabilization and the release of proteins. However, other models consider that the efflux of the apoptogenic proteins is due to disruption of MOM integrity. Some of the alternative channels proposed as responsible of MOMP are described in this section.

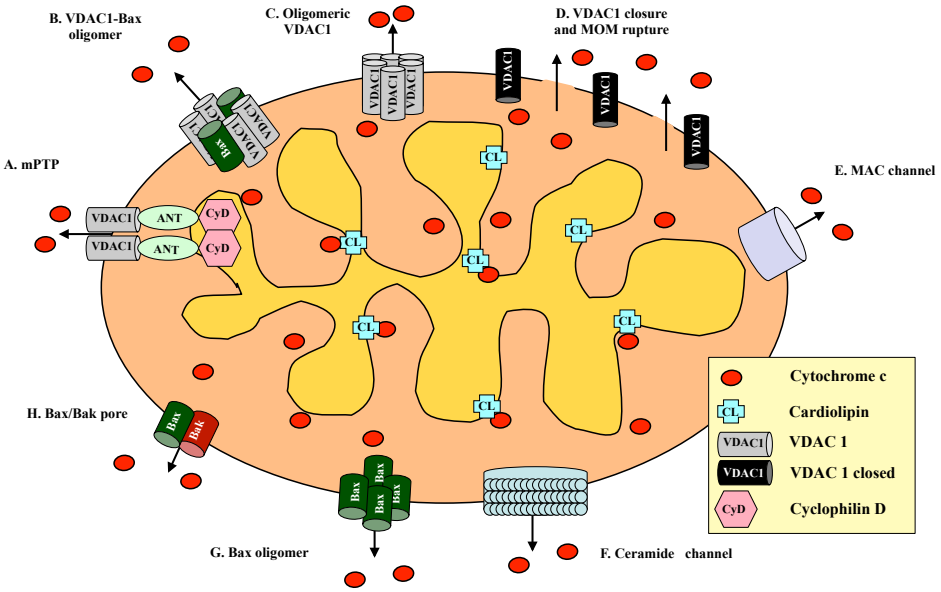

Figure 1.7. Release Models for the apoptogenic proteins from MIM space during apoptosis. (A) Permeability transition pore (PTP) is formed by VDAC (MOM), ANT (MIM) and CypD (matrix). (B) Bax-VDAC hetero-oligomers. (C) VDAC1 homo-oligomer (regulated by oxidative stress and Ca^{2+}) can also produce the release of apoptogenic proteins. (D) MOM rupture produced by VDAC closure promotes a non-specific release of apoptogenic proteins. (E) The mitochondrial apoptosis-induced channel (MAC) formation is controlled by the apoptotic maquinery (BCL-2 proteins). (F) A lipid channel formed by the lipid ceramide. (G)(H) Upon apoptosis induction, Bax and/or Bak activation and oligomerization promotes MOMP. Adapted from (140).

The permeability transition pore. . The mPTP (permeability transition pore. Model A, Figure 1.7) is a multi-protein complex present at mitochondrial contact sites (CS)(135) composed by the adenine-nucleotide translocator (ANT, located in the MIM), the voltage-dependent anion channel (VDAC, located in the MOM) and the cyclophilin-D (CyP-D, located into the matrix surface of the MIM) (141-143). PTP opening produces an increase of (Ca^{2+}) ions and water in the mitochondrial matrix, generating mitochondrial swelling,

loss of membrane potential, and finally the loss of MOM integrity. PTP-induced cell death is generally considered to be necrotic rather than apoptotic (144). CypD was found to be essential for MOMP mediated by Ca^{2+} overload and this CypD-dependent MOMP regulates some forms of necrotic cell death but not apoptotic death (145).

Of note, the mechanisms responsible for PTP opening and its physiological function are still unclear. Mitochondria isolated from animals models with *ANT* or *VDAC KO* genes show PTP opening produced by oxidative stress (ROS) and an increase of Ca^{2+} in the mitochondrial matrix, suggesting that more components of the PTP complex have to be uncovered (144, 146).

VDAC1-Bax Hetero-oligomeric channel. Hetero-oligomers of VDAC1 and Bax form a high conductance channel also proposed as a mechanism for Cyt-*c* release (Model B, Figure 1.7; (147, 148)). Studies in VDAC1-depleted cells, wherein cisplatin-induced activation of Bax was inhibited (149), demonstrate that VDAC1 is involved in Bax-mediated apoptosis. Furthermore, some proteins of the BCL-2 family, such as Bid, Bim, Bcl-2, and specially Bcl-xL interact with VDAC1, modulating the efflux mechanism of apoptotic proteins through this channel (150). Bcl-2 and Bcl-xL interact with VDAC1 reducing channel conductance and apoptosis. However, mutated forms of VDAC1 avoid these interactions (151). It has been proposed that the interaction of Bax-Bim complex with VDAC produces Cyt-*c* release, and Bcl-xL prevents this release (152).

Finally, other studies propose that Bax is the regulatory protein of oligomeric VDAC channel, promoting Cyt-*c* release through this pore (153).

VDAC1 oligomerization. The single molecule VDAC1 pore diameter (2.5–3.0 nm) avoids the efflux of folded proteins like Cyt-*c*. However, homo-oligomers of VDAC1 can form a large protein-conducting channel following apoptosis stimuli to promote the release of the apoptogenic proteins (Model C, Figure 1.7; (155)). However, the molecular mechanism that trigger VDAC1 oligomerization upon apoptosis induction remains unknown.

Osmotic matrix swelling and MOM rupture leading to non-specific release from inter-membrane proteins to the cytosol. The dysregulation of ATP/ADP exchange produced by VDAC1 closure (Model D, Figure 1.7; (157)) generates a sudden increase in MIM permeability, mitochondria swelling, rupture of the MOM and finally the release of IMS proteins, such as Cyt-*c*, to the cytosol (158).

Mitochondrial apoptosis-induced channel. Mitochondrial apoptosis-induced channel (MAC), a supramolecular high-conductance channel in the MOM, can be assembled during early apoptosis and serve as the Cyt-*c* release channel regulated by BCL-2 family

members (160, 161) Model E, Figure 1.7)). The complete molecular identity of MAC is unknown but recently it has been proposed that Bax is an essential constituent of this channel since depletion of Bax significantly diminishes MAC activity (162).

Ceramides and the release of cytochrome c. Ceramides, a family of waxy lipid molecules, were postulated to form a pore in the MOM with a diameter large enough to accommodate Cyt-*c* (163). For that reason, this model suggests that a self-assembled ceramide-based lipid channel is formed in the MOM to release Cyt-*c* (Model F, Figure 1.7; (163)). Ceramides can also promote the release of Cyt-*c c* by altering MIM lipid microdomains (164). In addition, ceramides in combination with low cholesterol concentrations could generate mitochondrial membrane microenvironments to facilitate Bax activation (165, 166). Finally, Bak (but not Bax) could activate ceramide synthesis. The increase in ceramide levels would result in synergistic channel formation at the MOM by ceramide and Bax/Bak, showing a different function of Bax and Bak in apoptosis (167).

Depending on the cell death stimulus and the cell type the mechanisms and models of Cyt-*c* release proposed could co-exist within a single model of cell death (168).

1.5.4. Role of mitochondrial membrane lipids in MOMP regulation.

The involvement of lipids in MOMP has been suggested recently (169) since the lipid composition of the MOM changes during apoptosis. Current theories support that mitochondrial lipids are not only structural elements of the MOM but also display a functional role. The function of these lipids would be either to produce changes in the physical properties of the MOM and/or to interact specifically with some mitochondrial proteins (170, 171).

The mitochondrial lipid composition is conserved among different cell types. This underscores the potential role of lipid composition changes as an additional regulation mechanism to control general processes as apoptosis. The lipid composition of the mitochondrial membrane in healthy conditions is: 40% phosphatidylcholine (PC), 30% phosphatidylethanolamine (PE), 5-10% Cardiolipin (CL), 15% phosphatidylinositol (PI), whereas phosphatidic acid (PA) and phosphatydilserine (PS) comprise approximately 5% (172).

The relevance of membrane composition in Bcl-2 family regulation started with the importance of CL in liposome permeabilization process mediated by tBid-Bax interaction (173) and the blockage of pores formation in MOM-like liposomes when this lipid was absent (121). CL is a four-alkyl groups mitochondria-specific membrane lipid with potentially two negative charges, localized predominantly to the inner mitochondrial

membrane. Only a minor fraction of CL is located in the MOM (173). However, it was observed that local CL concentrations at specific MOM domains known as the mitochondrial membrane contact sites (CS) can be as high as ≈25% (174). Different studies indicate that during apoptosis the total content of CL at the MOM increases. Several reports have related CL and CS with Bid, indicating that CL can recruit Bid to MOM and mitochondrial CS specifically (175). CL also promotes caspase-8 translocation to mitochondrial localization, promoting then the activation of Bid (176). Of note, it has also been described that other phospholipids such as PC, PG and PE (177) allow membrane translocation of tBid. CL can also interact through its negatively charges with the lipid-binding region of Bad BH3-only protein (178). However, the role of CL in the apoptotic pathways is still controversial.

Despite of mitochondria contains only 5% of the total cellular cholesterol, this lipid can also be relevant in apoptosis due to it regulates the fluidity of membranes in mammalian cells (179). An increase of cholesterol concentration produces a decrease of membrane fluidity that correlates to inhibition Bax-mediated MOMP (180) and resistance to chemotherapy in cancer cells, whereas low levels of cholesterol are related to Bax activation via p53 (181, 182). However, role of cholesterol in apoptotic control is not fully characterized yet .

Inside the sphingolipid group, the ceramide has been largely analyzed by its relevance in the MOMP and apoptosis (183). Increased amounts of ceramide at the mitochondria in response to apoptotic stimuli (TNF-α, FAS ligand or DNA damage) promote Bax translocation to the MOM, MOMP and apoptosis (183, 184). Nevertheless the molecular mechanism by which ceramide promotes apoptosis is still controversial. In addition, hexadecenal (a downstream metabolite of ceramide) induces Bax activation and pore formation in liposomes where CL is not present (125).

Future studies will be needed to shed light on the role of lipids in MOMP and in the mitochondrial membrane regulation during apoptosis**.**

1.6. BCL-2 TRANSMEMBRANE DOMAINS (TMDs): SUBCELLULAR TARGETING AND ROLE IN THE APOPTOTIC PATHWAY.

Most of Bcl-2 proteins are defined as tail-anchored proteins that have a single, highly hydrophobic and helical C-terminal segment (known as transmembrane domain, TMD). The TM segments of the tail-anchored proteins range from 15 to 22 amino acids in length and are typically flanked by one to three positively charged residues. Protein folding in

the cytoplasm of eukaryotic cells tends to occur co-translationally (Figure 1.8) (186) and a number of ribosome-associated chaperones are available to mediate co-translational folding. Hence, the N-terminal domains of tail-anchored proteins can fold, sequentially, before the hydrophobic tail emerges from the ribosome to be inserted into the membrane. This would prevent any unfavourable folding reactions that might otherwise occur between the cytosolic domain and either the hydrophobic tail or the membrane surface. Not surprisingly, since the N-terminus of the protein folds before the emergence of the membrane anchor from the ribosome, the membrane-insertion of tail-anchored proteins should occur post-translational. The length and the hydrophobicity of the TMD are important for the post-insertional sorting to the correct membrane within the secretory pathway and some works have postulated a relevant role of the flanking regions in defining the membrane-specificity of the tail-anchored proteins (187).

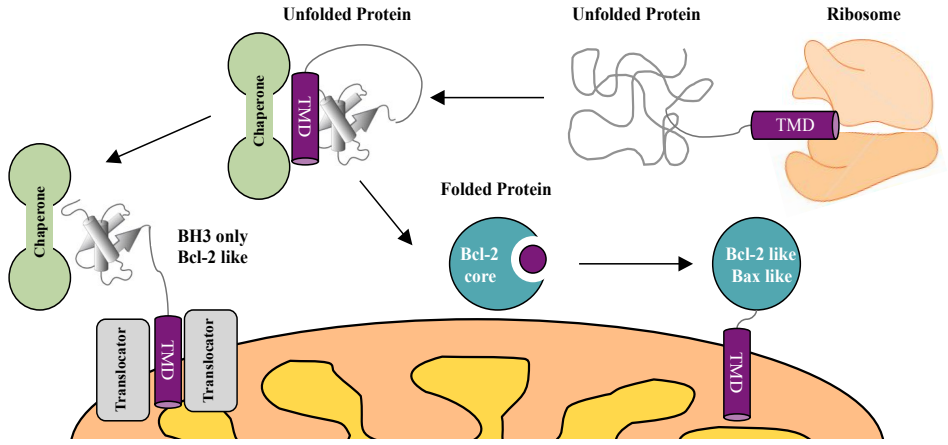

Figure 1.8. Stages of targeting tail-anchored proteins to mitochondria. Tail-anchored proteins can fold in the cytoplasm co-translationally. The hydrophobic tail-segments interact with some proteins such as chaperones like HSP70 (green) to keep the proteins soluble in the cytosol. (Left side) Tail-anchored proteins can also interact with some subunits of the TOM complex (grey) to target to mitochondria. (Right side) Some Bcl-2 proteins can fold themselves and target to mitochondria. Inspired by (188).

The BCL-2 family proteins are usually found not only in the mitochondria but also in the cytosol, the endoplasmic reticulum (ER) and the nucleus (189) (Figure 1.9). Although some Bcl-2 family members are targeted directly to the membrane on which they execute their function via specific targeting sequences, others require a secondary level of regulation allowing them to translocate to MOM in response to an apoptotic stimulus. Moreover, BCL-2 members that are not targeted to MOM seem to regulate MOMP from

the ER (190). This secondary level of regulation may act as a 'safety switch' preventing premature activation or inactivation of these proteins. Several groups have studied the mechanism used by the BCl-2 proteins target to mitochondria (191, 192) and they propose: 1) Direct anchorage post-translation of the BCL-2 TMD into the MOM. 2) Targeting mediated by the interaction with other BCL-2 members. 3) Interaction with non-BCL-2 family proteins, such as TOM/TIM complexes (193). 4) Interacting with mitochondrial lipids.

Among the BCL-2 family, some members have a well-defined TMD with all the properties observed in the canonical tail-anchor sequences. These are the cases of the pro-apoptotic proteins Bax and Bak, and the anti-apoptotic Bcl-2, Bcl-xL, Bcl-w and Mcl-1. For other BCL-2 proteins, such as Bok, A1, and some of the BH3-only proteins hydrophobic sequences can be detected, but these regions do not accomplish all the criteria established for the canonical TMDs. Furthermore, the targeting signals and mechanisms by which BCL-2 proteins reach their final destination are still controversial.

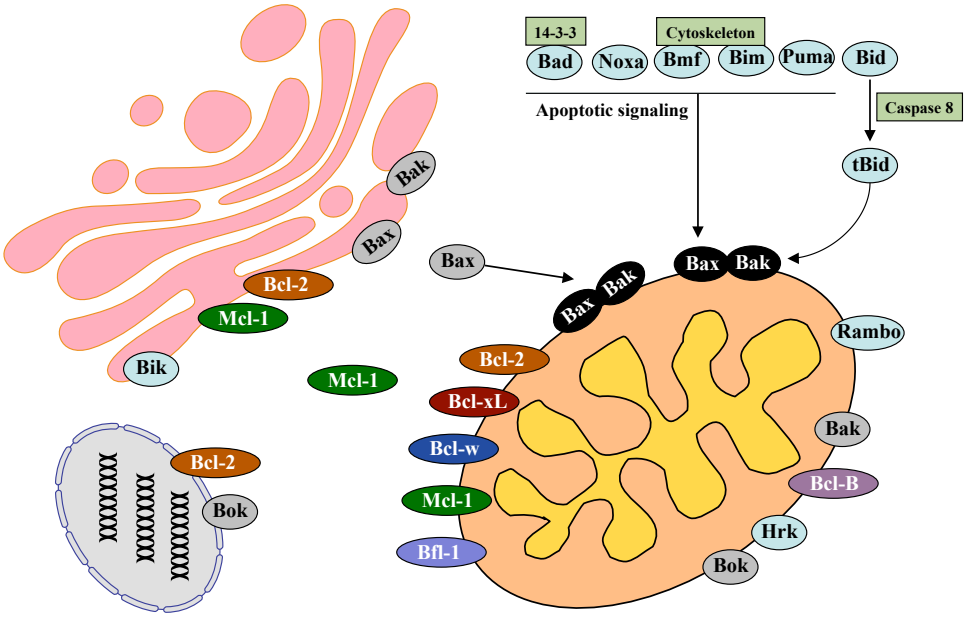

Figure 1.9. Localization of Bcl-2 family proteins. BCL-2 proteins are present in the cytoplasm, ER and on the MOM in healthy cells. Bak is constitutively found on the MOM. Bax inactive form is found in the cytoplasm and translocates to MOM after apoptotic activation. Bcl-2 and Bcl-xL are mainly inserted into the MOM interacting with Bax and Bak to inhibit apoptosis. Bcl-w and Mcl-1 can be present in cytosol or integrated into the membrane. BH3-only proteins Rambo, Hrk are always present in MOM. The expression of Bim, Puma and Noxa is up-regulated following apoptotic signals, whereas Bad, Bim and Bid BH3-only proteins target to MOM following post-translationally modifications. Inspired by (194).

1.6.1. Subcellular distribution and targeting of BCL-2 anti-apoptotic proteins.

In healthy cells, the majority of endogenous Bcl-2 is located in the ER membrane and associated with the nuclear envelope, and the remaining fraction (30%) is located on the MOM (195, 196). Bcl-xL and Bcl-w are both found in cytosolic form as membrane inserted (63, 197, 198). During apoptosis, they translocate from the cytosol to mitochondria. In the case of Bcl-w, its anchoring to the MOM is only triggered when a BH3-only protein binds to its hydrophobic groove (199). When comparing the TMDs of Bcl-2 and Bcl-xL, no great differences in length or in mean hydrophobicity were detected. However, MOM-targeted proteins such as Bcl-xL show an increased hydrophobicity in the C-terminal half of their TMD. On the other hand, proteins that are also targeted to the ER/nuclear envelope, such as Bcl-2, are more hydrophobic in the N-terminal half of their TMDs. In addition, the number of positive flanking residues of the TMD seems to play an important role in the mitochondrial membrane specific targeting of Bcl-2 anti-apoptotic proteins. High basicity surrounding the TMD usually leads to a more MOM-specific targeting, whereas TMDs surrounded by fewer basic residues have a higher tendency to be targeted to the ER membrane. In this sense, Bcl-xL can be specifically targeted to the MOM by increasing the net positive charge at the very terminus of the protein. Furthermore, a decrease in the number of basic residues at this region in Bcl-2 protein causes a decrease in MOM-specificity, leading to an accumulation of this protein on the ER/nuclear outer membrane.

It has also been proposed that cytosolic binding proteins or putative membrane receptors can target the anti-apoptotic BCL-2 family members. For instance, it has been shown that the mitochondrial FK506-binding protein 38 (FKBP38) interacts with both Bcl-2 and Bcl-xL, probably by associating with members of the TOM machinery (200).

Finally, the subcellular localization of Mcl-1 depends on the physiological cellular status and cell-type, Mcl-1 has been localized to the mitochondria, ER, the cytoplasm and the nucleus (201).

1.6.2. Subcellular distribution and targeting of BCL-2 pro-apoptotic proteins.

Bax, Bak and Bok were initially described to be targeted to the MOM wherein they are thought to exert their function. Recently, ER localization and, in consequence, ER specific functions have been reported for these proteins (189) (202). In addition to its membrane attached form, Bax is found up to 60% as a soluble protein in the cytosol in healthy cells and it is proposed to translocate to and insert into the MOM during apoptosis (132) . In contrast to Bax, Bak is inserted constitutively into the MOM and to a lesser

extent into the ER membrane (203). Moreover, the higher hydrophobicity of the C-terminal hydrophobic region of Bak in comparison with Bax may account for the stable anchorage of the former but not the latter protein to the MOM.

Bok is described as either having a nuclear or mitochondrial distribution. The C-terminus of Bok does not fit the consensus for a functional tail-anchored, as it contains lysine and arginine residues within what should be the hydrophobic TMD. Whether or not Bok has a functional TMD remains controversial (204).

1.6.3. Subcellular distribution and targeting of BH3-only proteins.

BH3-only proteins are located in the cytoplasm of healthy cells, but during apoptosis they are targeted to the MOM, either alone or in association with the multidomain BCL-2 family members.

Following apoptotic stimuli, BH3-only proteins Noxa, Puma, Bim, and Hrk are transcriptionally induced. In the cases of Bim, Bik, Bmf and Bad, are posttranslationally modified and/or proteolytically processed in response to apoptotic stimuli (191, 205). These modifications increase the affinity of BH3-only proteins for multidomain Bcl-2 family members, directing some BH3-only proteins to the MOM and ER membrane (206). Alternatively, other BH3-only proteins seem to contain their own C-terminal TMD regions, such as Bik (constitutively localized to the ER), Hrk, Rambo, (both in MOM) and Bid targeting to MOM or ER directly or by protein-lipid interactions (207). In the case of Bim, Puma, Noxa and Bmf the presence of a TMD region is still controversial. A recent study postulates that the C-ternimal region of Noxa could be responsible of its mitochondrial targeting (207). Bim and Bmf seem to be bound to cytoskeletal structures under healthy conditions. During apoptosis, they are released from the cytoskeleton to allow their translocation to the MOM and modulation of MOM-localized multidomain BCL-2 proteins (104, 208, 209) Recent studies propose that Bim spontaneously inserts into the MOM via its putative tail-anchor, and that binding to the MOM is crucial for activating Bax. However, it is unlikely because the putative tail-anchor sequence of Bim contains charged residues, which are normally incompatible with tail-anchored mediated insertion into the membrane. Bid is located in the cytosol in an inactive form in healthy cells. In response to apoptotic stimuli, Bid is cleaved by caspase-8 to form truncated Bid (tBid), translocating from cytosol to MOM to interact with the BCL-2 family proteins located in mitochondria. This targeting could be mediated by the interaction with the CL-binding domains as in the case of Bad (210). In absence of apoptotic stimuli, phosphorylated Bad is sequestered in the cytosol by its interaction with 14-3-3 scaffold proteins and only after dephosphorylation is targeted to MOM (208).

Table 1.II. The TMD of the BCL-2 family.

BCL-2	TMD	Predicted sequence	Target	Role
Bcl-2	Yes	$_{212}$FSWLSLKTLLSLALVGACITLGAYLGHK$_{239}$	ER,MOM,Nucleus	Not clear
Bcl-xL	Yes	$_{203}$SRKGQERFNRWFLTGMTVAGVVLLGSLFSRK$_{233}$	MOM	Apoptotic isoform, Form pores
Bcl-w	Yes	$_{163}$REGNWASVRTVLTGAVAL GALVTVGAFFASK$_{193}$	MOM	Not clear
Mcl1	Yes	$_{328}$IRNVLLAFAGVAGVGAGLAYLIR$_{350}$	MOM,ER	Apoptotic isoform
Bfl-1	Yes	$_{151}$KSGWMTFLEV TGKICEMLSL LKQYC$_{175}$	MOM	Form pores
Bcl-B	Yes	$_{168}$FWRKQLVQAFLSCLLTTAFIYLWTRLL$_{194}$	MOM	NM23-H2 interaction
Bax	Yes	$_{169}$TWQTVTIFVAGVLTASLTIWKKMG$_{192}$	MOM	Form Pores
Bak	Yes	$_{188}$ILNVLVVLGVVLLGQFVVRRFFKS$_{211}$	MOM	VDAC2 interaction
Bok	Yes	$_{186}$RSHWLVAALCSFGRFLKAAFFVLLPER$_{212}$	ER,Golgi,Nucleus	Not clear
Bid	Yes	$_{144}$KEKTMLVLALLLAKKVA$_{160}$	MOM	Destabilize MOM, Form pores
Bim	N.C	$_{179}$PRMVILRLLRYIVRLVWRMH$_{198}$	MOM??	Not clear
Bmf	N.C	$_{157}$NRVWWQILLFLHNLALNGEENRNG$_{180}$	MOM??	Not clear
Puma	N.C	$_{162}$RHRPSPWRVLYNLIMGLLPLPRGHRAPEMEPN$_{193}$	MOM??	Not clear
Noxa	N.C	$_{35}$KLNFRQKLLNLISKLFCSGT$_{54}$	MOM??	Not clear
Bad	Yes	$_{137}$TATQMRQSSSWTRVFQSWWDRNLGRGSSAPSQ$_{168}$	MOM??	Not clear
Bik	Yes	$_{136}$VLLALLLLLALLLPLLSGGLHLLLK$_{160}$	ER	Not clear
Hrk	Yes	$_{61}$APGALPTYWPWLCAAAQVAALAAWLLGRRNL$_{91}$	MOM	Form pores
Rambo	Yes	$_{457}$GKSILLFGGAAAVAILAVAIGVALRKK$_{485}$	MOM	Not clear

Underlined residues represent the flanking regions of the transmembrane domain, which are important in the subcellular targeting. The predicted sequences have been calculated using ΔG. Not confirmed (N.C).

1.7. ROLE OF BCL-2 TMDs IN THE CONTEXT OF FULL-LENGTH PROTEINS AND RELEVANCE IN MOMP DURING APOPTOSIS.

1.7.1. Anti-apoptotic BCL-2 proteins.

Bcl-2

The Bcl-2 C-terminal tail improves the anti-apoptotic effects of the protein, including cell survival after IL-3 deprivation (211) and suppression of apoptosis caused by E1B-defective adenovirus (212). Some authors have postulated that helices 5 and 6 of Bcl-2 are able to form pores in lipid membranes (213, 214). Bcl-2 protein exhibited pore-forming activity with properties similar to those of the bacterial toxins, diphtheria toxin, and colicins, showing a dependence on low pH and acidic lipid membranes. In planar lipid bilayers, Bcl-2 formed two types of channels: discrete ion-conducting, cation-selective channels, with a four-helix bundle structure arising from Bcl-2 dimers and a larger

channel detected with progressively lower occurrence, implying the step-wise formation of larger oligomers of Bcl-2 in membranes. The role of the Bcl-2 C-terminus TMD in these pores is still unclear (213, 214).

Bcl-w

Bcl-w C-terminus-deleted mutants lose their anti-apoptotic function, although they are still able to bind BH3-only proteins, such as Bim and Bad, suggesting that C-terminal residues modulate pro-survival activity by regulating the ligand access to the hydrophobic groove by the BH3-only proteins (63). However, further studies have to be designed focusing in the TMD specifically to evaluate the relevance of this TMD in apoptotic regulation and interaction with other Bcl-2 proteins.

Bcl-xL

Bcl-xL undergoes a conformational change from a cytosolic to a membrane bound state promoted by its TMD (215). When the Bcl-xL TMD is removed, a decrease in membrane insertion is observed. It has been demonstrated that Bcl-xL interacts with a Bak BH3 domain peptide in the presence of membranes. Under these conditions, the TMD of the protein unfolds from the hydrophobic groove and inserts into the membrane (216).

Some localization studies for Bcl-xL TMD have fused the TMD of Bcl-xL or the complete Bcl-xL to the yellow fluorescent protein (YFP) in order to investigate the relevance of the TMD in the targeting of the protein. Both YFP-Bcl-xL and YFP-Bcl-xL-TMD localized to the mitochondria. However, cells expressing YFP-Bcl-xL-TMD showed increased autophagy and moderate cell death resistance in response to staurosporine (a classical apoptotic inductor), suggesting the existence of a secondary function of Bcl-xL mediated by the TMD (217). In contrast, YFP-Bcl-xL was diffusely distributed in the cells, and its expression did not alter the mitochondrial morphology compared with control cells. Recent studies have postulated that some isoforms of Bcl-xL that contain the TMD are pro-apoptotic (66, 67, 218). This is the case for Bcl-xS that contains BH4, BH3 and TMD domains (218). In constrast, Bcl-AK is constituted by BH4, BH2 and the TMD domain and does not interact with other Bcl-2 antiapototic proteins (66, 219). However, both isoforms promote different ways of caspase-dependent and caspase-independent apoptosis. Interestingly, Bcl-xS can also disrupt the interaction between VDAC2 and the TMD of Bak, producing the caspase-dependent apoptosis (67).

Furthermore, it has been postulated that Bcl-xL homodimerizes by the TMD, which could be related to its role in mitochondrial morphology alteration and apoptosis inhibition (220). As described previosly, this Bcl-xL TMD is also important to mediate

retrotranslocation of Bax from the mitochondria to the cytosol (221). Unexpectedly, substitution of the Bcl-xL TMD by the corresponding Bax segment reverses the Bax retrotranslocation activity of Bcl-xL, while Bcl-xL shuttling is independent of interactions with Bax or Bcl-xL (221). Therefore, it is not clear how the retrotranslocation of Bcl-xL to the cytosol is induced.

Bfl-1

The C-terminal domain of Bfl-1 (A1) significantly differs from Bcl-2, Bcl-xL, and Bcl-w TM sequences (222), and targets Bfl-1 specifically to mitochondria (see Table 1.II). Bfl-1 may co-exist in two distinct conformational states: one with its C-terminal helix inserted in the hydrophobic groove and another with its C terminus bound to the MOM (223). The helix 9 of Bfl-1, and therefore the binding of Bfl-1 to mitochondria, is not essential for the anti-apoptotic activity of Bfl-1.

A synthetic peptide called ATAP (amphipathic tail-anchoring peptide) derived from the C-terminal domain of Bfl-1 produces the release of fluorescent molecules of the size of Cyt-c from liposomes (224). In addition, although the pro-apoptotic activities of BH3 peptides are largely inhibited by over-expression of anti-apoptotic proteins (Bcl-2 or Bcl-xL) or the depletion of pro-apoptotic Bax and Bak in cells, the pro-apoptotic function of ATAP is not affected by these cellular factors (223).

Mcl-1

It has been established that the C-terminal domain of Mcl-1 becomes pro-apoptotic as a result of caspase-3 cleavage, and its physical interaction and cooperation with tBid, Bak, and VDAC1 promoted mitochondrial apoptosis. However, in these studies, the C-terminal domain included not only the putative TM segment but also by domain BH2 (225). For that reason, the specific role played by the TM segment in these observations is not clear.

Bcl-B

Bcl-B is also known as Bcl-2L10 or Diva in the mouse. Bcl-B has anti-apoptotic function in MOM, but interestingly it does not have BH3 motif (226). The deletion of the TMD in Bcl-B decreases its anti-apoptotic function and its association with intracellular organelles (227). Interestingly, it has been postulated that Bcl-B interacts with NM23-H2, a regulator of the Bcl-B activity, via its TMD (228).

1.7.2. Pro-apoptotic BCL-2 members.

Bax

Bax lacking the C-terminal domain is not functional and the insertion in MOM is blocked (229) (230). There are three critical residues in the Bax TMD and its flanking regions: G179, S184 and P168. G179E mutant abrogates the Bax activation mediated by ABT-199 antitumoral drug due to this mutation avoid its anchoring to the MOM (230). The mutation of S184K led to the diffuse cytoplasmic localization of Bax after the cells had received an apoptotic signal and the deletion of this residue produces a Bax mutant constitutively localized in the mitochondria and more active than wild type Bax. P168 mutants lack pro-apoptotic activity.

Interestingly, the substitution of the C-terminus of Bax by that of Bcl-xL does not affect its subcellular localization but abrogates its pro-apoptotic properties (231). In addition, mutations in the C-terminal part of the Bax protein impaired the inhibitory effect that anti-apoptotic Bcl-xL has on Bax insertion, suggesting that the conformation of the TMD plays a significant role in the Bax/Bcl-xL interaction (232).

As previously described, the pore complex proposed by helices 5 and 6 of Bax can be proteolipidic (134) but no conclusive evidences about the participation of the C-terminal domain in this type of pores have been observed. In presence of phosphatidylglycerol in model membranes, the C-terminal domain of Bax formed complexes with these lipids (233). Moreover, a recent work suggests that the TMD of Bax could contribute to oligomerization process in the MOM, by direct TMD interaction between different molecules of Bax (234). In the same line, other studies have suggested that Bax TMD could contribute the pore complex constitution. It was observed that Bax channels reconstituted *in vitro* showed voltage gating. Then, two different Bax channels have been proposed: Type A, which is homogeneous, small and voltage-gated; and Type B, which is large and voltage-independent (235). It has been suggested that the TMD of Bax may be involved in the formation of both. During apoptosis, changes in the lipid composition of the MOM can influence orientation and exposition of the C-terminal of Bax within these channels, modifying their organization.

Several studies using vesicles with encapsulated carboxyfluorescein have been developed to determinate the role of the BCL-2 C-terminal domains in permeabilization of membranes. Some synthetic peptides of anti-apoptotic (Bcl-2) and pro-apoptotic (Bax and Bak) TMDs were used (236). The results highlighted that addition of both peptides to large unilamellar vesicles destabilized the vesicles and released encapsulated carboxyfluorescein (CF) at different degrees. Moreover, it was observed that fluidity and

the increase in negative curvature promoted this release. In general, Bcl-2 and Bax TMD peptides produced the highest content release, with Bak TMD peptide close to these levels of release. In comparison to pure phosphatidylcholine vesicles, the addition of diacylglycerol produced an increase in the percentage of CF released in the case of Bak TMD peptide. However, the addition of cholesterol reduced the membrane fluidity and the TMD insertion (237, 238), reducing the capacity of the peptides to induce CF release.

Recent works have proposed a model for pores (radius of at least 13 Å) based on the Bax TMD peptide (^{173}VTIFVAGVLTASLTIWKKMG^{192}) wherein eight peptide molecules form an "α/β-ring" structure within the membrane. This peculiar pore allowed the suggestion of a new mechanism through which Bax C-terminus can efficiently perforate cell membranes, a mechanism that differs from that accepted until now for other domains of Bax (239, 240). When this peptide is expressed intracellularly, it is translocated to the mitochondria and kills cancer cells, so the Bax TMD peptide represent a firm candidate for acting as molecular drug (241).

Bak

The hydrophobic C-terminal domain of Bak acts as a membrane anchor (242), promoting the localization of Bak as an integral MOM protein (Figure 1.9). Several works when replaced the C-terminal domain of Bak with Bax TMD (Bak/BaxCS), the chimeric protein rescues the stability and the function of Bak, but resulted in a semicytosolic protein with its hydrophobic TMD blocking its hydrophobic surface groove. Upon apoptotic signaling, Bak/BaxCS translocated to the MOM where inserted its TMD (128).

On the other hand, some studies have found that the C-terminal domain of Bak interacts with model phospholipid membranes, altering their physical properties and making them leaky to carboxyfluorescein (243). The peptide is folded to adopt a secondary structure in which α-helix is predominant. These results suggest that this domain may help to create a pore through the MOM.

It has been postulated that Bak interacts by the TMD (helix 9) with VDAC2 protein in the MOM. This interaction between TMD of Bak and VDAC2 suppresses the activation of Bak in healthy cells. During apoptosis, the arrival of the BH3-only protein tBid to MOM results in the release of Bak from VDAC2 (110).

Bok

Bok can also be classified as a tail-anchored protein (244). In fact, its C-terminal domain has been described as a "tail anchor" specific for targeting the Golgi and the ER, wherein

it develops its major pro-apoptotic functions (204). Interestingly, a splicing variant of Bok called Bok-S, which contains only the BH1, BH2 and the TMD, does not dimerize with anti-apoptotic proteins and forms mitochondrial channels to regulate apoptosis (245). Because Bok-S does not interact with anti-apoptotic proteins, apoptosis mediated through Bok-S may be important in situations when unwanted cells need to be eliminated quickly despite the presence of anti-apoptotic proteins in the same cell. In the ovary and uterus known to express high levels of Bok transcripts, Bok-S expression could provide a short circuit to promote cell demise in hormone-dependent cell populations that express abundant anti-apoptotic proteins (such as Mcl-1) but have to be removed swiftly because of cyclic cell turnover during reproductive cycles (245).

1.7.3. BH3-only proteins.

Bid. In the case of Bid, it is postulated that helix 6 and helix 7 have the ability to insert into the mitochondrial membrane (246). However, the capability of these regions to destabilize the mitochondrial membrane and to form channels is still controversial. Schendel *et al.* (247) described the channel forming activity of caspase-8 cleaved Bid or Bid lacking 55 N-terminal residues in planar lipid bilayers at acidic and neutral pH. Moreover, Kudla *et al* (248) reported that p15 Bid (a truncated form of Bid from residue Gly^{60} to the end of the protein) permeabilizes liposomes at physiological pH. In addition, recent studies postulate that CS interact with these helices and this interaction promotes the remodeling of the inner membrane and the cristae structures of the mitochondria in a Bax/Bak-independent manner (246). However, topology studies indicate that helices 6 to 8 do not span the lipid bilayer (249). Helices 3 to 5 are amphipathic, and none of them are long enough to span the bilayer. These findings point to the existence of a mediator that would relay the signal from the outer membrane where Bid is targeted to the inner membrane. Furthermore, Terrones *et al.* (121) reported that tBid alone does not form pores in the membrane, but it activates Bax to form large lipic pores permeable to dextran molecules of 10–70 kDa.

All these contradictory data expose that it is uncertain how the helices 6 to 8 might be involved in channel formation or membrane destabilization, so further studies are necessary to understand these phenomena.

Bad. Bad presents a C-terminal region with the capacity to bind to MOM, although this tail is not homologous to the rest of the BCL-2 TMDs. As previously mentioned, Bad is regulated by phosphorylation, association with 14-3-3 proteins, binding to membrane

lipids and pore formation (178) (see section 1.6.3). Polzien *et al*. (250) demonstrated that the C-terminal region of Bad presents a well-ordered structure and stable conformation in aqueous solution, although the helical conformation increases in a lipid context. The interaction of the C-terminal region of Bad with its isolated BH3 domain promotes the formation of permanently open pores, although it is necessary the phosphorylation of serine 118 within the BH3 domain for effective pore formation. In contrast, the phosphorylation of serine 99 in combination with 14-3-3 association suppresses channel formation (250).

Hrk. Hrk is inserted to the MOM through its TMD (251). Interestingly, the C-terminal region of Hrk adopts a predominantly α -helical structure with a clear insertion perpendicular to the plane of the membrane. These properties give Hrk C-terminal domain the capability to form pores in the mitochondrial membrane. The percentage of helix and its potential to destabilize membranes are modulated by phospholipid composition (252).

Rambo. The TMD of Rambo is responsible of the mitochondrial targeting of this protein. It has also been demonstrated that Rambo causes apoptotic cell death independent of the Bax-Bak pore complex and that the TMD of this protein is crucial for its pro-apoptotic activity (107, 253). As described in Figure 1.3 Rambo does not interact with other BCL-2 members (107). A recent work proposed that Rambo interacts with ANT protein (253), which is one of the components of the PTP in the mitochondrial membrane to generate non-mediated Bax/Bak apoptosis. However, the role of the TMD in the apoptotic activation is still controversial.

Bik. Bik presents a well-defined TMD that targets mainly to ER (106, 254), but more studies need to be done to determinate the role of its TM region in the context of the full lengh protein Bik.

Other BH3-only proteins

The presence of a TM region in the BH3-only proteins Puma, Noxa, Bim and Bmf is currently under study. Some authors have recently concluded that these BH3-only proteins present a TMD region to target mitochondria (207, 255, 256). However, the presence of several polar residues inside their C-terminal sequence and the low hydrophobicity of these regions generate controversy about this issue.

1.8. APOPTOSIS AND DISEASE.

As well as a pivotal role during development, apoptosis and BCL-2 proteins regulation are essential for homeostasis in mature tissues. For this reason, defects or abnormalities in cell death regulation contribute to a range of pathologies: in some cases by insufficient apoptosis, such as cancer and autoimmune lymphoproliferative syndrome (ALPS), whereas in another situations by excessive apoptosis such as ischemia or neurodegenerative diseases including Parkinson's disease, Alzheimer's disease, Huntington's disease, and Amyotrophic Lateral Sclerosis.

1.8.1. Importance of BCL-2 family proteins in cancer.

The balance between cell survival and cell death is a fine tuned process wherein slight imbalances are responsible of several diseases. In fact, defective cell death mechanisms are now recognized as one of the six hallmarks of cancer (257). The BCL-2 proteins, as crucial modulators of the apoptotic process, have been implicated in the development of several types of tumors. In general, dysregulation of the BCL-2 proteins could contribute to cancer development and progression at different levels (258). They could be directly implicated in the generation of the disease (drivers) but also could be involved in the acquired resistance to antitumoral treatments. For that reason, apoptosis, cancer development, and cancer therapy are closely associated. Impaired apoptosis is critical for tumor development. Specifically, BCL-2 proteins play a crucial role as regulators in the mitochondrial permeabilization process. Depending on Bcl-2 subfamily affected, cancer cells have can be classified in: Class A cell death blockade is associated to loss of BH3-only activator function. Class B is related to inactivation of Bax and Bak effectors, and class C is the result of upregulation of Bcl-xL/Bcl-2/Mcl-1.

It is important to note that although alterations in BH3-only and Bax/Bak proteins expression have been reported in several cancers, such as colon and lung cancer, this is not a common phenotype. In contrast, the regulation of anti-apoptotic members is more widely demonstrated in many cancer types. This may be a mechanism selected for tumor cells to block the activity of several BH3-only proteins and Bax/Bak, along with additional metabolic and survival advantages conferred by increased anti-apoptotic BCL-2 protein expression.

1.8.1.1. Dysregulation of anti-apoptotic proteins.

Overexpression of the BCL-2 pro-survival proteins by itself has not demonstrated to be related to highly tumorigenic profiles; however, in combination with additional alterations

as mutations that enhance tumor growth generates a severe increase of malignancy (259)..

Bcl-2. High levels of *BCL2* gene expression correlate with malignancy of human tumors (260, 261). Bcl-2 upregulation correlates with poor prognosis and/or clinical response in several cancers (262-264), and resistance to chemotherapy and radiation (260, 261). Moreover, some tumor-associated viruses (for example, Epstein-Barr virus (EBV) and Kaposi's sarcoma-associated herpes virus (90)) encode homologue proteins of Bcl-2, developing similar anti-apoptotic functions (265).

Bcl-xL. Bcl-xL also produces resistance to several apoptosis pathways (266). An increase of Bcl-xL expression is associated to multiple myeloma (MM) (267), pancreatic cancers in combination with c-myc overexpression (267, 268), prostate cancers associated to Bcl-2 upregulation (269) and apoptotic resistance produced by constitutive activation of epidermal growth factor receptor (EGFR)(270)..

Mcl-1. Mcl-1 overexpression was observed in leukemia, ovarian cancer and human cervical neoplasms patients (271, 272).

1.8.1.2. Inactivation of pro-apoptotic proteins.

In addition to upregulation of pro-survival genes, tumors also develop apoptosis resistance by loss of function or downregulation of pro-apoptotic proteins Bax and Bak**,** which are common in hematologic malignancies (273). Knockout or interference studies of Bax and Bak proteins, in particular in human colorectal carcinoma cells (274), demonstrated the role of these proteins in the apoptosis blockade of tumor cells. Bak downregulation has been observed in skin and pancreatic cancer (275, 276) and it is required for the transformation of intestinal epithelial cells to malignant cells, promoted by the ras oncogene (277)..

In the case of Bax, it was observed during the tumor clonal evolution of gastric and colon cancer cells that the clones with Bax inactivated and/or mutated showed a clear advantage in comparison to the clones with normal expression of Bax (278). The work of Manoochehri et al. concluded that Bax down-regulation could contribute as an important factor during both colorectal carcinogenesis and cell resistance to antitumoral agent 5-Flourouracil (279). Furthermore, the contribution of Bax downregulation to drug responsiveness in cancer cells was also demonstrated when the resistance of no tumoral cells, with normal expression levels of Bax and also Bid, was compared to cancer colon cells with low or no expression of Bax and Bid (280). Of note, it was observed that a single nucleotide polymorphisms (SNPs) of Bax, rs4645878, showed a significantly

increased recurrence risk in gastric cancer correlated with a decrease of Bax expression and functionality (281).

1.8.1.3. Mutations of BH3-only proteins.

Noxa and Puma. Since BH3-only proteins Noxa and Puma are transcriptional targets of p53, loss of p53 by itself suppresses apoptosis induced by these proteins (102, 282). Frameshift mutations causing loss of expression and mutation of BH domains of pro-apoptotic proteins that lead to loss of their function are also common in colon cancers and result in apoptosis resistance (273).

Puma and Noxa can also be activated independently of p53 and thus play a role in p53-independent apoptosis. Puma can be transcriptionally upregulated by FoxO3a CHOP, and E2F1 (283) in response to ER stress. This protein can also be negatively regulated through phosphorylation; therefore several chemotherapeutic strategies are focused to promote its proteasomal degradation (284). Interestingly, *Puma KO* mice and *Noxa KO* mice have a normal phenotype during development and adult mice (93)(285).

Bim. Bim activity is transcriptionally (Foxo3a, CHOP transcription factors) and posttranscriptionally (Phosphorylation via JNK and MAPK) regulated. Some of these regulatory mechanisms are used as targets of chemotherapeutic drugs. Low levels of Bim protein are associated with colon cancer and B cell lymphoma a (286). *Bim KO* mice present a normal development with an excess of myeloid and lymphoid cells (287).

Bid. Caspase-2 produces Bid cleavage in response to ER stress (288). Furthermore, Bid cleavage can be regulated posttranslationally by phosphorylation in response to apoptosis DNA damage-induced (289). *Bid KO* mice show myeloproliferative and leukemic disorders with age (291).

Bad. Some breast and prostate cancers can be iniciated by dysregulation of Bad phosphorylation in PI3K/AKT pathway (293). If PTEN (an inhibitor of the pathway) is blocked, S136 is constitutively phosphorylated and Bad remains inactive. *Bad KO* mice experiments (94) demonstrated that this BH3-only protein acts as tumor suppressor in the lymphocyte lineage.

Bmf. The role of Bmf in tumorigenesis still remains to be fully elucidated, but there have been several reports suggesting that this protein plays a role in suppressing tumor development. In *Bmf KO* mice, lymphocytes are protected against apoptosis induced by glucocorticoids or histone deacetylase inhibition (95). It is important to note that in

hematopoietic tumors the disruption of normal cell adhesion is due to the lack of Bmf binding to some cytoskeletal components. Bmf upregulation promotes apoptosis in mammary epithelial morphogenesis and anoikis (295). Moreover, histone deacetylase inhibitors (HDAC), used as chemotherapeutic agents in tumoral cells, upregulates Bmf expression due to the presence of CpG islands at its promoter.

1.8.2. Antitumoral treatments based on BCL-2 proteins.

The complex network between pro-apoptotic and anti-apoptotic members of the BCL-2 family plays a crucial role in cellular fate determination. From a therapeutical standpoint, the process of apoptosis is intricately balanced, and then the recovery of this equilibrium after the dysregulation promoted by a tumoral process should be the goal of cancer therapy. Bcl-2 interfering strategies have been accepted as a potential approach to induce apoptosis in cancer cells. There are three classical strategies to overcome the cytoprotective effects of Bcl-2, Bcl-xL and Mcl-1 in cancer: inhibiting gene transcription, promoting mRNA degradation with antisense oligonucleotides, and directly blocking the function of these proteins with small-molecule drugs or peptides (Table 1.III).

Recently, several studies focus on a new concept, the *mitochondrial priming* of a cell that could be used in cancer therapeutics (see 1.8.2.2)

1.8.2.1. Pharmacological inhibition of bcl-2 proteins.

Antisense oligonucleotides (ASOs) and antibodies

This methodology is based on the introduction of a mRNA strand complementary to the target sequence in Bcl-2, generating a DNA heteroduplex that can be degraded by RNAse H and then silencing the target mRNA (296). One of the first drugs developed for inhibiting the BCL-2 family was Oblimersen (G-3139), an antisense complementary to the *BCL2* gene. The problem of Oblimersen correlates to its limited effect over BCL-2 network, observed in several clinical studies (297), because is targeted only against Bcl-2. Downregulation of *Bcl-2* gene may generate upregulation of other anti-apoptotic BCL-2 proteins, reducing the effect of this antisense (298).

A similar strategy was used for Bcl-xL ASOs (299). Bcl-xL ASOs alone also have similar problems as Oblimersen. However, combinated treatments of ASOs and Oblimersen increase each other their anti-tumoral effect (300). Finally, Mcl-1 antisense strategy showed interesting results *in vitro* in hepatocellular carcinomas (HCC) in combination with cisplatin treatment (301).

Other strategies based on the use of antibodies or ribozimes against Bcl-2 have been tested, showing a significant effect in cotreatments with other chemotherapeutic agents in breast and other cancers (302). The main problem of this methodology is the low stability of antisense mRNA, limiting their use as therapeutic agents.

Peptide and peptidomimetics

Due to limitations of strategies based on anti-apoptotic BCL-2 downregulation, a new methodogy was developed focusing on the control of anti-apoptotic BCL-2 function. For example, Bax-BH3 peptide was designed to inhibit Bcl-xL protein specifically (304), binding to its hydrophobic groove. The success of this study opened the field to the design of short peptides based on the BH3 domain of several BH3-only proteins against the hydrophobic groove of the different anti-apoptotic proteins.

BCL-2 C-terminal domain-derived peptides have also been designed as therapeutic agents. One example is CT20p peptide derived from the C-terminal, alpha-9 helix of Bax (241). CT20p contains hydrophobic and cationic residues (typically present in TM domains) to associate with lipid membranes. Mitochondrial localization as well as the capability to release calcein from mitochondrial-like lipid vesicles without disrupting vesicle integrity were demonstrated (241). Moreover, CT20p amphipathic nature has let to combine with nanoparticles (pharmaceutical vehicle). CT20p has been tested in colon and breast cancer cells *in vitro* and *in vivo*, demonstrating its efficiency as tumoral cells killer (241).

The pro-apoptotic activity of Bfl-1 peptide, based on its C-terminal domain, showed a clear independency of BCL-2 proteins. For that reason, it has been used as an anti-cancer drug in apoptosis-resistant tumors (224). .

Small molecule inhibitors (SMIs) targeting BCL-2 proteins

BH3 mimetics are organic molecules of low molecular weigths whose function is based on the blockade of the hydrophobic groove of anti-apoptotic BCL-2 proteins, imitating the mechanism of action used by BH3-only proteins to promote apoptosis. Some of these SMIs are in clinical and preclinical phases (Table 1.III):

One of the most succesfull BH3 mimetics is ABT-737, developed by Abbott Laboratories. ABT-737 binds selectively to Bcl-2 (higher affinity), Bcl-xL and Bcl-w and is based on the BH3 domain of Bad. However, this molecule was not effective promoting apoptosis in *Bax/Bak KO* cells (305). Experimental data demonstrates that ABT-737 results effective against several types of lung cancer *in vitro* and *in vivo* (306), follicular lymphoma and leukemia. However, tumoral cells with Mcl-1 upregulated showed

resistance to ABT-737 treatment (308). ABT-263 is an oral derivative with longer half-life than ABT-737 that also inhibits Bcl-2, Bcl-xL and Bcl-w. This molecule has been tested in clinical trials for small cell lung carcinomas (SCLCs) and leukemia (309).

Gossypol (BL-193) binds to the hydrophobic groove of Bcl-2 and Bcl-xL (310) and is a polyphenol derived from cottonseeds (311). This SMI has been modified several times in different isoforms such as (−)-BL-193 (312), TW37 and Apogossypolone (ApoG2) to increase its effectiveness against tumoral cells. Its mechanism of action is related to induction of DNA breaks in the presence of metal ions (copper) (311). It is currently in clinical trials as a single agent and in combinated therapies (Table 1.III). TW-37 has higher affinity to Bcl-2, Bcl-xL in comparison to other BH3 mimetics.. ApoG2 can also bind to Mcl-1, results less toxic and then more specific than others BH3 mimmetics and it has been tested in different types of lymphomas (315). (-)AT-101 is the negative enantiomer of gossypol and has also been used in lymphomas (316). This molecule interacts with Bcl-2, Bcl-xL and Mcl-1, with a low IC50 (1-10 μ M). Finally, One of the last gossypol derivative is Sabutoclax that inhibits Bcl-xL (with low binding affinity) Bcl-2, Mcl-1 and Bfl-1 (317). Interestingly, this molecule did not generate toxicity in KO *Bax/Bak KO* MEFs and it had shown promising results in some types of lymphoma resistant to ABT-737 (318).

Obatoclax is a synthetic molecule developed by Gemin X (GX015-070) that can inhibit Bcl-2, Bcl-xL, Bcl-w and also Mcl-1 although the affinity values to Bcl-2 family are lower than ABT-737 (319). However, some of the mechanisms involved in Obatoclax function to promote cell death are not directly related to Bax/Bak effector proteins (321). For example, low concentrations of Obatoclax are able to block cell-cycle in S/G2 phase and can also trigger autophagy by Beclin-1 release from Mcl-1, or Atg7 dependent (322). However, its high toxicity restrict the use of this BH3 mimetic in humans.

Table 1.III. Bcl-2-family targeting drugs. Adapted from (323).

Class	Name	Target	CSA	Combination	Tumor type	CSC
ASO	Oblimersen sodium	Bcl-2	Phase III	Dacarbazene	Melanoma	Phase III
				Doxorubicin	Hepatocellular	Phase I/II
				Docetaxel	HR-Prostate cancer	Phase II
	Bcl-xL antisense	Bcl-xL	Preclinical			
	Mcl-1 antisense	Mcl-1	Preclinical			
BH3 peptides	Bim BH3	Bcl-2, Bcl-xL, Bcl-w, Mcl-1	Preclinical	Cisplatin, Staurosporin, Doxoribicin, Etoposide	Several, depending on the BH3 profile	
	Puma BH3	Bcl-2, Bcl-xL, Bcl-w, Mcl-1				
	Noxa BH3	Mcl-1				
	Bad BH3	Bcl-2				
TMD peptides	CT20p	MOM destabilization	Preclinical		murine breast cancer tumor model	
	Bfl-1 C-terminal	MOM destabilization	Preclinical			
BH3 mimetics	Gossypol (AT-101)	Bcl-2, Bcl-xL	Phase II	Paclitaxel, Carboplatin	Lymphoma	Phase I
				Cisplatin, Etoposide	SCLC	Phase I/II
				Docetaxel, Prednisone	HR-Prostate cáncer	Phase I
	TW-37	Bcl-2, Bcl-xL, Mcl-1, Bfl-1	Preclinical		Lymphoma	
	Apogossypol (ApoG2)	Bcl-2, Bcl-xL, Mcl-1	Preclinical		Lymphoma	
	(-) AT-101	Bcl-2, Bcl-xL, Mcl-1	Phase II		B-cell lymphomas	

Sabutoclax (BI-97C1)	Bcl-2, Bcl-xL, Mcl-1, Bfl-1	Preclinical		B-cell lymphomas	
ABT-737	Bcl-2, Bcl-xL, Bc-w	Phase II/III	Platinum	Ovarian cáncer and leukemia	Phase II/III
ABT-263	Bcl-2, Bcl-xL, Bc-w	Phase II/III		(SCLCs) and leukemia	
Obatoclax (GX-15-070)	Bcl-2, Bcl-xL, Bc-w, Mcl-1	Phase II	Etoposide Bortezomib Docetaxel Rituximab	Extensive stage-SCLC MCL, Hodgkin's or Non Hodgkins lymphoma, MM NSCLC Lymphoma	Phase II Phase II Phase II Phase II
HA-14	Bcl-2, Bcl-xL	Preclinical	Cisplatin	MDA-MB-231 breast cancer cells	
BI-97D6	Bcl-2, Bcl-xL, Mcl-1, Bfl-1	Preclinical		Prostate, lung cancer and lymphoma cell lines	
BH-3 M6	Bcl-2, Bcl-xL, Mcl-1	Preclinicla l		Lung adenocarcinoma cell line A549	

Clinical state combinated (CSC); Clinical state alone (CSA)

1.8.2.2. Mitochondrial priming.

To determine the threshold of apoptosis, regulation of the balance between pro- and anti-apoptotic proteins is critical and depends on many factors. Cells express sufficient anti-apoptotic proteins to bind and inactivate pro-apoptotic members and other pro-death signals that are present under physiological conditions (324). However, the amount of prosurvival proteins that a cell may dispose varies depending on the type of cell. Some cells in the hematopoietic and immune systems maintain relatively small buffers of anti-apoptotic proteins (324) to activate their elimination quickly when the situation is required (325). However, highly specialized and fully differentiated cells with a longer lifespan display high expression levels of anti-apoptotic proteins to survive against stochastic fluctuations in cellular stress (324). These differences in the levels of anti-apoptotic proteins can affect the outcome of chemotherapy treatments. These cells that have a small reserve of unbound anti-apoptotic proteins are 'primed' for apoptosis whereas cells with large reserves are 'unprimed' (Figure 1.10). When these two types of cells are treated with equal doses of chemotherapy, the primed cell will be more sensitive to apoptosis than the unprimed cell. The priming state of the mitochondria is important because cells within tumors that have undergone treatment and then recurred are

frequently less primed, making them less sensitive to subsequent rounds of chemotherapy (324, 326). The selective pressure of chemotherapy likely culls primed cancer cells, leaving only unprimed cells to repopulate the tumor (324, 326). These unprimed relapsed tumors are frequently intractable.

To analyze the mitochondrial priming state of a cell line, a functional assay called "BH3 profiling" has been developed to measure the apoptotic threshold in cancerous and normal cells (113). The idea is to expose mitochondria to peptides and/or SMI derived from the BH3 domains of pro-death BH3-only proteins and measure the concentration necessary to induce MOMP (327). As an example, sensitivity of mitochondria to Bad BH3 or Noxa BH3 peptides indicates a selective dependence on Bcl-2 or Mcl-1, respectively (328, 329). In the case of Bim BH3 or Puma BH3 peptides, more promiscuous to bind to anti-apoptotic proteins, sensitivity indicates a highly primed state, with a low reserve of unbound anti-apoptotic proteins (324, 326, 329). Detection of MOMP (Figure 1.9) is measured by mitochondrial potential, which occurs when the anti-apoptotic reserve cannot avoid the Bax and/or Bak activation in response to a fixed titration of pro-death BH3 peptides: the faster a cell is depolarized, or the lower concentration of peptide required for MOMP, the more primed it is. As the activities of the BCL-2 family proteins are regulated by several posttranslational modifications and interactions with other proteins (330), the treatment with fixed doses of pro-apoptotic peptides let to measure the integrated functional output of the BCL-2 family efficiently (324).

It has been shown that increasing mitochondrial priming by treating cells with a drug, which binds to anti-apoptotic factors, increases the response of a myeloid leukaemia cell line to various cytotoxic agents (331). These studies raise the possibility that increasing mitochondrial priming may be a useful adjunctive treatment to increase response to cytotoxic therapies in human cancer treatments. Therefore, Bcl-2 inhibition strategies also represent a form of 'synthetic lethality' that selectively kills cancer cells addicted to Bcl-2 expression for survival.

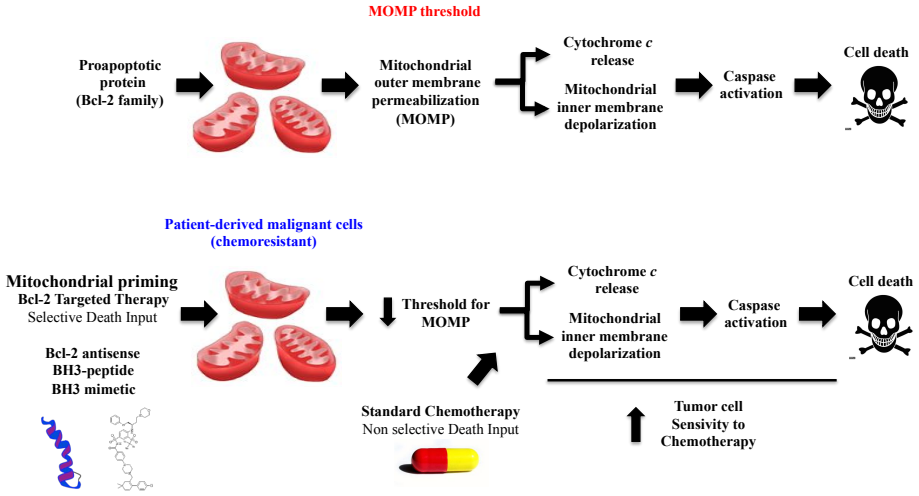

Figure 1.10. Model of mitochondrial priming. (upper image) Unprimed cells have their, pro-apoptotic BH3 only proteins sequestered by anti-apoptotic proteins. In primed cells (down), the anti-apoptotic proteins are blocked by treatments against their BH3 domain, releasing the pro-apoptotic proteins to decrease the MOMP threshold when Chemotherapy is applied. For this reason, a cell primed for apoptosis is more likely to undergo cell death in response to chemotherapy than an unprimed cell. Inspired by (324).

OBJECTIVES

Apoptosis is a common type of programmed cell death. This cellular process is centrally regulated by the BCL-2 family proteins. Members of this family are found in the cytoplasm, ER and MOM in healthy cells. However, during apoptotis most of the interactions between these proteins occur at the membranes of intracellular organelles. The general aim of this Thesis is to expand the knowledge of the mechanism of action of the BCL-2 family proteins in the presence and absence of membranes. This aim was approached with the following specific objectives:

- Despite the fact most BCL-2 proteins exert their functions in the mitochondrial membrane, the role of the TMDs in protein-protein interactions and apoptotic modulation has been poorly understood. The first objective of this project has been *to determine the involvement of the BCL-2 TMDs in the interaction network of the BCL-2 protein family*. The importance of BCL-2 TMDs interactions in the context of Bcl-2 full length proteins has also been studied, along with the functional relevance of BCL-2 TMDs in the apoptotic pathways.

- The capacity of BH3-only proteins to insert into the mitochondrial membrane is controversial. Then, the second objective has been *to clarify the ability of predicted BH3-only TMDs to insert into different biological membranes*.

- The role of BCL-2 cytosolic domains such as MOMP sensitizers in chemotherapy has been extensively studied. However, little is known about the contribution of BCL-2 TMDs to this process. The third objective of this thesis has been *to investigate the contribution of BCL-2 TMDs-derived peptides to mitochondrial outer membrane permeabilization (MOMP) process*.

- This project also addresses the study of the different cell death pathways activated in response to proapoptotic drugs, depending on the apoptotic machinery available in the cell.

According to accomplish these objectives, the project has been divided in four chapters as follow:
CHAPTER I. Interactions between BCL-2 family members via their transmembrane domain (TMD): Relevance in apoptotic control.

CHAPTER II. Insertion of BH3-only C-terminal domains into biological membranes.

CHAPTER III. Peptides derived from the transmembrane domain of BCL-2 proteins as potential mitochondrial priming tools.

CHAPTER IV. BH3-mimetics and cisplatin-induced cell death proceeds through different pathways depending on the availability of death-related cellular components.

MATERIAL AND METHODS

3.1 CHAPTER I.

3.1.1. Design and cloning of ToxRed BCL-2 TMD constructs.

Maltose-complementation assay was performed as described (332, 333) in order to determine the correct orientation and insertion in the inner membrane of constructs containing TM domains and to study transmembrane helix-helix associations in a natural membrane environment. ToxR original plasmids were kindly provided from Prof. William De Grado (UCSF School of Pharmacy). In this system, a putative transmembrane (TM) sequence is cloned between a sequence encoding the transcription activator domain of *Vibrio cholerae* ToxR and a sequence encoding the periplasmic domain of the E. coli MBP (see Figure 4.1). To determine whether the putative transmembrane sequence mediates transmembrane oligomerization, the ToxR-TM-MBP fusion proteins are expressed in *E. coli MM39*. Membrane localization of the fusion protein is detected based on complementation of a non-polar *malE* mutant *E. coli MM39* strain. Insertion of the ToxR-TM-MBP fusion protein into the inner membrane, such that the MBP domain localizes to the periplasmic space, is detected by determining whether the bacteria are able to transport maltose and thus grow on maltose-minimal medium. Dimerization of the fusion protein is determined based on expression of the *RFP* gene, which is under the control of the *ctx* promoter. Recognition of the promoter sequence only occurs when ToxR dimerize, and this dimerization is only possible if BCL-2 TMDs interact and bring closer the ToxR monomers to dimerize. The inactivating ToxR mutation R96K (ToxR*) was chosen as a system control (334) by its capability to dimerize but not to recognize the promoter sequence. GpA TMD was used as positive control of interaction, and the point mutant GpA G83I was used as negative control.

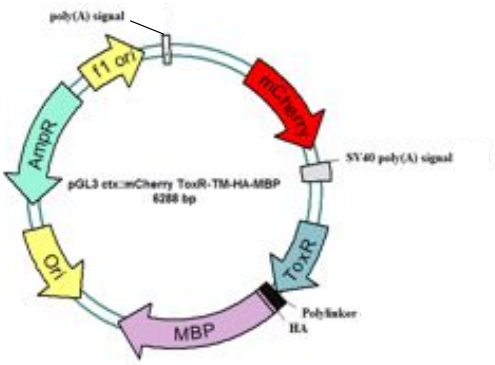

Figure 3.1. pGL3 plasmid adapted to ToxR system.

To generate ToxR quimeric constructs, DNA oligonucleotides from BCL-2 TMD were designed and cloned in pGL3 ToxR-HA-MBP plasmid. This plasmid contains a sequence for ampicillin resistance and a polilinker site (Figure 3.1). Reverse and forward BCL-2 TMDs primers (100 μM) were annealed with annealing buffer (20 mM Tris-HCl, 20 mM $MgCl_2$, 500 mM NaCl), using Eppendorf 5331 Gradiant Master Cycler with a multistep temperature protocol (95ºC 10 min, 90°C 10 min and over night at 60°C). HindIII/XhoI restriction sites were introduced in primers flanking the TMD sequence. Annealed primers were treated 4 h with polynucleotide kinase (PNK, Roche) and ligated overnight with T4 DNA ligase (Promega) at 16ºC, using HindIII/XhoI restriction enzymes (Roche) to digest the ToxR plasmids for 2 h. Alkaline Phosphatase (Roche) was used 2 h to remove the 5' phosphate in the ToxR vector.

All the constructs were transformed by heat shock (90 sec at 42ºC) in *E.coli DH5α* competent cells and incubated in Lysogeny Broth (LB) for 30 minutes at 37°C, pelleted at 3000×g and plated directly onto LB agar petri dish containing ampicillin. After 24 h, positive colonies were isolated and cultured on LB medium with ampicillin for 24 h at 37°C. Plasmid DNA was isolated with QIAprep Spin MiniPrep Kit (Qiagen) for sequencing analysis.

Primers for mutagenesis were designed with GeneRuler software. All transmembrane sequences were codon-optimized for *E. coli.* TMD mutants were cloned using standard site directed mutagenesis with commercially available Stratagene Quikchange II kit (Agilent, CA, USA). All molecular biology techniques were performed according to standard procedures.

3.1.2. Expression of ToxR chimera.

ToxR-TMD-MBP constructs (200 ng) were transformed using of 200 μL *MM39* competent cells with heat shock at 42°C for 90 sec and incubation on ice for two minutes, followed by addition of 800 μL LB medium and incubation with shaking at 37°C for one hour. The transformation mixture was pellet and plated in minimal-agar media in the presence of ampicillin 100 μg/ml. After 48 h, *MM39* cells containing ToxR-TM-MBP plasmids were grown into LB with ampicilin for 6 h in triplicate. Then, cultures were pelleted and incubated with shaking in 24-well plates (Thermo scientific) at 37°C for 36 h into minimal media to grow to OD_{600} 0.8. RFP emission spectra were collected by Wallac 1420 Workstation with an excitation wavelength of 570 nm and emission wavelengths of 620 nm. All the results obtained for each ToxR-TMD-MBP were normalized according to ToxR*-TMD-MBP basal fluoresecence signal and cell growth.

3.1.3. Immunoblotting experiments of ToxR-TMD chimera.

MM39 cells were pelleted by centrifugation for 5 min at 3000×g, the supernatant was removed and cell pellets were resuspended in 10× initial volume of FastBreak cell lysis reagent (Promega). Then the cells were transfered to 1.5-mL Eppendorf tubes and the mixture was incubated at room temperature with gentle agitation for 30 min. Samples were centrifuged for 10 min and the spheroplasmic and periplasmic fractions were separated and quantified by the BCA protein assay kit (Thermo Scientific). 50 µg of protein from spheroplasmic fraction was dissolved in protein loading buffer (Tris-HCl pH 6.8, 10% w/v SDS, 250 mM DTT, 0.03% w/v bromophenol blue, and 50% v/v glycerol), boiled 5 min at 95ºC and resolved by SDS-PAGE (acrylamide 12%). Then samples were transferred to nitrocellulose membranes, blocked with 5% non fat milk, washed three times with TBS-Tween 20 0.1% and incubated overnight at 4ºC with a specific primary antibody (MBP from New England Biolabs (#E8038S); HA C29F4 (#3724S) and c-myc 9B11 (#2276S, from Cell Signaling). Membranes were washed with TBS-Tween 20 0.1% and probed with the appropriate secondary antibody α-mouse (1:3000, A4937, Sigma) or α-rabbit (1:3000,A0545, Sigma) conjugated to horseradish peroxidase for enhanced chemiluminescence detection (Amersham Pharmacia Biotech).

3.1.4. Cell culture, treatments, transfections and chemicals.

ABT-263 and staurosporine (STS) were from Abbott Laboratories and Deltaclone, respectively. The human cervix adenocarcinoma HeLa cell line was purchased from ATCC and Human colorectal carcinoma HCT 116 *Wt, KO Bax/Bak, KO Bax, and KO Bak* were kindly provided by Prof. Richard Youle and by Prof Bert Vogelstein. HeLa cell line was grown in Dulbecco's Modified Eagle's Medium (DMEM) and HCT 116 cells were grown in McCoy's 5A medium, both supplemented with 10% fetal bovine serum (FBS). Cultures were maintained at 37°C in a 5% CO_2 atmosphere. Cell media and FBS were purchased from GIBCO BRL Life Technologies. When indicated, cells were treated with 0.1-1 µM of staurosporine and 5-15 µM of ABT-263. When required, 5 µM zVAD was administered 30 min after treatment addition, and cells were maintained in culture for 24 h. All cell lines were transfected using LipofectamineTM 2000 (Invitrogen) or Turbofect Transfection Reagent (Thermo scientific) following the manufacturer's protocol.

3.1.5. BiFC-TMDs assays.

BiFC (bimolecular fluorescence complementation) analyses were performed as previously described (335-337). Venus protein (a green variant of the yellow fluorescent portein,

YFP) can be separated in two fragments: BiFC-VN (1-155, with the point mutation I152L that decreases the signal noise and reduces false positive results) and BiFC-VC (155-238, A206K). The BiFC system is based on the capability of these fragments to reconstitute Venus protein when they are closer to each other. The transmembrane region of the different BCL-2 proteins were fused to both VN/VC with a linker sequence between the BCL-2 TMDs and the Venus fragments (see Figure 4.5A). When BCL-2 TMDs interact, Venus protein will be restored and green fluorescence emission will be measured. The nuclear proteins b-Jun and b-fos were used as positive control of interaction, as well as the truncated form d-Δfos that not interacts with d-jun to establish a negative control.

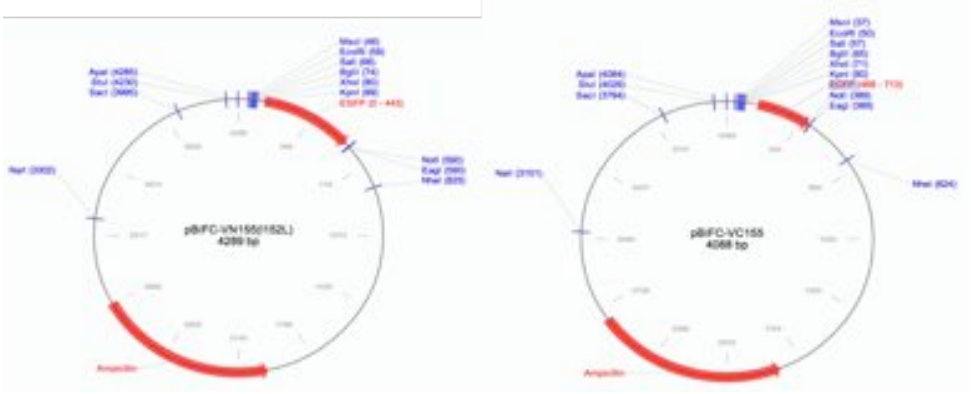

Figure 3.2. Plasmids encoding for N- and C- terminal Venus protein (https://www.addgene.com).

BiFC plasmids were adquired in Addgene (Figure 3.2, 27097 and 22011) and were modified with a linker and restriction site sequences behind Venus fragments, in order to clone the BCL-2 TMDs in the adequate topology. BCL-2 TMDs primers were then designed flanked with NotI restriction site to insert the TMDs in the C-terminal of each fragment of Venus. Reverse and forward BCL-2 TMDs primers (100 μM) were annealed in the presence of annealing buffer (20 mM Tris-HCl, 20 mM $MgCl_2$, 500 mM NaCl), using Eppendorf 5331 Gradiant Master Cycler with a multistep temperature protocol (95ºC 10 min, 90°C 10 min and over night at 60°C). Annealed primers were treated 4 h with polynucleotide kinase (PNK, Roche) and ligated overnight with T4 DNA ligase (Promega) at 16ºC, using NotI restriction enzymes (Roche) to digest the ToxR plasmids for 2 h. Alkaline Phosphatase (Roche) was used 2 h to remove the 5' phosphate in the ToxR vector.

All the constructs were transformed by heat shock (90 sec at 42ºC) in *E.coli DH5α* competent cells and incubated in Lysogeny Broth (LB) for 30 minutes at 37°C, pelleted at 3000×g and plated directly onto LB agar petri dish containing ampicillin. After 24 h, positive colonies were isolated and cultured on LB medium with ampicillin for 24 h at

37°C. Plasmid DNA was isolated with QIAprep Spin MiniPrep Kit (Qiagen) for sequencing analysis.

BiFC-TMD point mutant constructs were obtained using standard site directed mutagenesis with Stratagene Quikchange II kit (Agilent, CA, USA). Finally, constructs were verified by sequencing.

HeLa and HCT 116 cells were maintained under conditions recommended by the American Type Culture Collection. Cells were grown in six-well plates to 60% confluence and transfected with 0.25 to 1 μg of the plasmids expressing the proteins indicated in each experiment. Transfected cells were incubated at 37°C for 24 h and then Venus fluorescence emission was measured in a Wallac 1420 Workstation at 535 nm (using 500 nm as excitation wavelength).

3.1.6. Immunoblotting of BiFC-TMD chimera.

All cell extracts were prepared from 2×10^5 cells seeded in 6-well plates. After 24 h, cells were treated and/or transfected as indicated. Cells were scraped, washed with PBS and collected by centrifugation at 500×g 24 h later. Whole cell extracts were obtained by lysing cells in a buffer containing 25 mM Tris-HCl pH 7.4, 1 mM EDTA, 1 mM EGTA, 1% SDS, plus protease and phosphatase inhibitors. Protein concentration was determined by BCA protein assay kit (Thermo Scientific). Cell lysates were dissolved in protein loading buffer (Tris-HCl pH 6.8, 10% w/v SDS, 250 mM DTT, 0.03% w/v bromophenol blue, and 50% v/v glycerol), boiled 5 min at 95ºC and resolved by SDS-PAGE (acrylamide 12%). Then samples were transferred to nitrocellulose membranes, blocked with 5% non fat milk, washed three times with TBS-Tween 20 0.1% and incubated overnight at 4ºC with a specific primary antibody. Membranes were washed again with TBS-Tween 20 0.1% and probed with the appropriate secondary antibody conjugated to horseradish peroxidase for enhanced chemiluminescence detection (Amersham Pharmacia Biotech). Antibodies against HA C29F4 (1:1000, #3724S), c-myc 9B11 (1:1000, #2276S), Caspase-3 (1:1000, #9662S) and Bax (1:1000, #2772) came from Cell Signaling. α-tubulin antibody (#T8203) was from Sigma-Aldrich. Secondary antibodies α-mouse (1:3000, A4937) and α-rabbit (1:3000, A0545) were provided by Sigma.

3.1.7. Determination of caspase activity upon transfection with BiFC-BCL-2 TMD construts in HCT 116 cells.

The purpose of this assay was to determine the activity of the apoptotic executioner caspase-3 in cells treated with BCL-2 TMDs and/or pro-apoptotic treatments. All cell

extracts were prepared from 2×10^5 cells seeded in 6-well plates. After 24 h, cells were treated and/or transfected as indicated above. 24 h later, cells were then scraped, washed with PBS and collected by centrifugation at 500×g. Pellets were resuspended in caspase assay buffer (PBS 10% glycerol, 0.1 mM EDTA, 2 mM DTT) supplemented with protease inhibitor cocktail (Sigma) and kept on ice for 5 min. Once pellets were frozen and thawed three times in liquid nitrogen, cell lysates were centrifuged at 14000 rpm for 5 min and supernatants were collected. Quantification of total protein concentration was performed using the BCA protein assay kit (Thermo Scientific). Total protein (50 µg) was mixed with 200 µL of caspase assay buffer (PBS, 10% glycerol, 0.1 mM EDTA, 2 mM DTT) containing 20 µM of the Ac-DEVD-afc (Figure 3.3) (Enzo Life Sciences) caspase-3 specific substrate. Caspase activity was continuously monitored following the release of fluorescent afc at 37°C using a Wallac 1420 Workstation (λexc 400 nm; λem 508 nm). Caspase-3 activity was expressed as the increase of relative fluorescence units per min (A.U.).

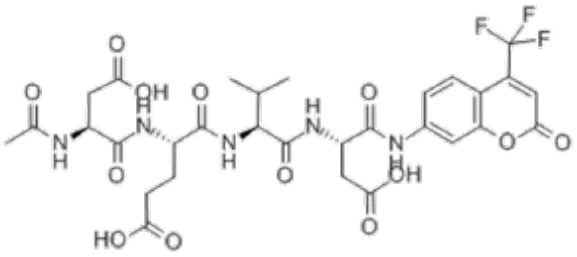

Figure 3.3. AC-DEVD-AFC Structure.

3.1.8. Flow cytometry of BCL-2 TMDs in HCT 116 Wt and Bax/Bak KO.

After treatment and/or transfection, the cell culture medium was collected to retain floating cells and attached cells were dislodged using 0.5% Trypsin-EDTA (GIBCO). Floating and attached cells were combined and harvested by centrifugation at 400×g 10 min. Cell pellets were suspended in 100 µl binding buffer (10 mM HEPES pH 7.4, 140 mM NaCl, 2.5 mM $CaCl_2$) and incubated with 10 µl FITC Annexin V (BD Biosciences) and 10 µl of Propidium Iodide (PI, 6 µM; BD Biosciences) for 10 min at 37°C. Staining for Annexin V and PI was assessed by flow cytometry on a FC500 cytometer (Beckman Coulter) followed by data analysis using FlowJo software (Tree Star Inc).

3.1.9. Immunofluorescence of BCL-2 TMD BiFC constructs in mitochondria.

For confocal microscopy, 2×10^5 cells were seeded on glass cover slips to reach 50%

confluence next day. Cells were transfected as indicated in 3.1. To analyze the mitochondrial localization of the BCL-2 TMDs, HCT 116 cells were incubated (37ºC) with Mitotracker dye 500 nM (Invitrogen) 30 min. Microscopic images of living cells were taken 24 hours after transfection and colocalization was defined as completely overlapping or partially overlapping signals.

For cytochrome *c* release assay, after cell attachment, spreading, and transfection with the BiFC-TMD constructs, HeLa and HCT 116 cells were fixed with 4% paraformaldehyde 20 min, following the treatment indicated in the corresponding figure. After three washes with PBS, cells were permeabilized with 0.1% Triton X-100 10 min and blocked in 2% gelatin PBS 30 min. Cells were then labeled with antibodies against Cyt-c (1:200; SC13561; Santa Cruz) in 2% gelatin PBS followed by an anti-mouse IgG-Alexa 555 (1:400) secondary antibody also in 2% gelatin PBS (Invitrogen). Cover slips were mounted on glass slides with 5 µL of Mowiol/Dapi (nuclear marker, 5 µg/ml) (Sigma). Images were obtained using confocal microscopy (LSM 510) with a 63x objective. Two hundred cells were counted and classified according to the localization of Cyt-c in mitochondria (tubular morphology) or cytosol (diffuse pattern). Fluorescence images were analyzed with ImageJ 1.46i "JACoP plugin" according to the provider's instructions. All background fluorescence was eliminated to avoid false-positives. All experiments were repeated three times. At least 30 images of each sample were analysed.

3.1.10. Subcellular fractionation in HCT 116 cells.

To obtain mitochondrial and cytosolic fractions, cells were harvested and centrifuged at 1200×g for 5 min at 4ºC. Cell pellet were re-suspended in SEM buffer (10 mM HEPES, 250 mM sucrose, pH 7.2) supplemented with protease inhibitors and homogenized with 30 strokes in tight douncer. Then, samples were centrifuged at 500×g for 3 min at 4ºC to remove nuclear fractions. The supernatant was transferred to a new tube and subsequently subjected to a centrifugation step at 13 000×g for 30 min at 4ºC. The supernatant of this step, the cytosolic fraction, was ultracentrifuged at 100 000×g for 1 h at 4ºC, followed by an ultrafiltration step. Finally, cellular fractions were dissolved in protein Loading Buffer (Tris-HCl pH 6.8, 10% w/v SDS, 250 mM DTT, 0.03% w/v bromophenol blue, and 50% v/v glycerol), boiled 5 min at 95ºC, separated by SDS-PAGE (12%) and subjected to western blot analysis (see 3.1.6). Sedimented mitochondria were washed two times and then analyzed by SDS- PAGE and subsequent western blotting. Tom 20 FL-145 (1:1000, sc-11415, Santa Cruz) and GAPDH FL-335 (1:1000, sc-25778, Santa Cruz) were used as mitochondrial and cytosolic markers, respectively. C-myc 9B11 (1:1000, #2276S), antibody came from Cell Signalling. Secondary antibodies α-mouse (1:3000, A4937) and

α-rabbit (1:3000, A0545) were provided by Sigma.

3.1.11. Cell toxicity assays LDH activity in HCT 116 cells.

Lactate dehydrogenase (LDH) release is commonly used as a marker for necrotic/oncotic cell death. In this assay, release of the cytosolic enzyme lactate dehydrogenase from cells with a damaged plasma membrane (indicating necrotic cell death) to the culture medium is evaluated. Cytotox-ONE Homogeneous Membrane Integrity Assay Kit (Promega) was used for evaluation of cellular integrity of the cell cultures, measuring the enzymatic conversion of resazurin compound to resorufin fluorescent compound. The amount of resorufin formed is directly proportional to the amount of LDH released into the medium (Figure 3.4).

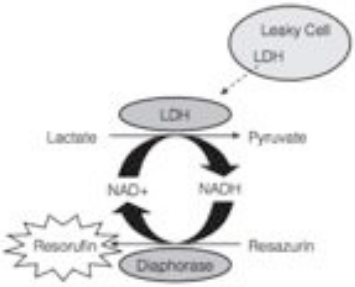

Figure 3.4. Lactate dehydrogenase (LDH) release. The amount of fluorescent resorufin is directly proportional to the amount of LDH released from a leaky cell (https://www.lifetechnologies.com).

Briefly, cell cultures were plated and treated as described in section 3.1.4. After 24 h of transfection and/or treatment, cultures were centrifuged at 1500 rpm for 5 min and supernatants were recovered. 50 µL of the supernatant were mixed with 50 µL of commercial substrate in black 96-well plates and incubated in darkness at room temperature for 30min. Fluorescence was measured at a λexc 560 nm and λem 590 nm on the Wallac Victor 1420 spectrofluorimeter. Each sample was analyzed in triplicate and results were expressed as the percent of lactate dehydrogenase release for each sample compared to the positive control (100% release) 0.1% Triton X-100 treatment.

3.1.12. Bioinformatic analysis of the BCL-2 sequences hydrophobicity.

Prediction of TMDs was done using three of the most common methods available online: Dense Alignment Surface method in DAS server (http://www.sbc.su.se/~miklos/DAS/); TransMembrane Hidden Markov Model at the TMHMM Server v. 2.0

(http://www.cbs.dtu.dk/services/TMHMM/); while prediction of Gibbs Free Energy (ΔG) was obtained with ΔG prediction server v1.0 (http://dgpred.cbr.su.se/) using standard parameters in all cases. The entire protein sequences were obtained from UniProt (http://www.uniprot.org).

3.1.13. Statistical analysis.

Bars represent the mean ± s.d. of at least three independent experiments. Statistical significance was determined by Dunnett's Multiple Comparison Test (95%CI) using the Graph Pad software. $p<0.05$ was designated as statistically significant.

3.2 CHAPTER II

3.2.1. Enzymes and chemicals.

The plasmid pGEM1, the TnT coupled transcription/translation system, the RiboMAX SP6 RNA polymerase system and rabbit reticulocyte lysate were from Promega (Madison, WI). Dog pancreas microsomes were purchased from tRNA Probes (College Station, TX),. GFP Plasmid was provided by addgene (#17999). [^{35}S] Met and ^{14}C-labeled methylated markers were from Perkin-Elmer. All the restriction enzymes were from Roche Molecular Biochemicals. Proteinase K (PK) was from Sigma-Aldrich (St. Louis, MO). The DNA plasmid, RNA clean-up, and PCR purification kits were from Qiagen (Hilden, Germany). The oligonucleotides were from Thermo (Ulm, Germany).

3.2.2. Computer-assisted analyses of the BH3-only TMD sequences.

Prediction of TM helices was performed using some of the most common methods available online described in 3.1.12.

3.2.3. DNA manipulations.

The BH3-only putative TMDs were introduced into the modified Lep sequence (Lep', see Figure 5.1A) from the pGEM1 plasmid (338, 339) between the *Spe*I and *Kpn*I sites by PCR amplification (Taq polymerase Pwo, dNTPs and PCR Buffer provided by Roche) of the different TMD sequences containing appropriate restriction sites. For GFP-TMDs cloning sites were *Bgl*II and *EcoR*I. After PCR amplification, PCR products were purified, digested, and ligated to the corresponding Lep or GFP vector digested with the

appropriate enzymes using standard molecular biology protocols. All new constructs were confirmed by DNA sequencing. The Lep' construct carried one glycosylation acceptor site in positions 3–5 of an extended sequence of 24 residues previously described (340).

3.2.4. *In vitro* transcription and translation of BH3-only TMDs in Lep' constructs.

Full-length Lep constructs were transcribed and translated in the presence of reticulocyte lysate (TnT Quick system (Promega)). 1 µg DNA template, 1 µL ^{35}S-Met/Cys (5 µCi) and 1 µL dog pancreas microsomes (341) (tRNA Probes) were added at the start of the reaction, and samples were incubated for 90' at 30°C.

After translation, membranes were collected by ultra-centrifugation at 10,000×*g* 4°C for 10 min using a TLA-45 rotor. Samples (pellets and supernatants) were dissolved in protein loading buffer (Tris-HCl pH 6.8, 10% w/v SDS, 250 mM DTT, 0.03% w/v bromophenol blue, and 50% v/v glycerol), boiled 5 min at 95ºC and analyzed by sodium-dodecylsulfate-polyacrylamide gel electrophoresis (SDS-PAGE, acrylamide 12%). Fuji FLA3000 phosphorimager and ImageGauge software was used to visualize BH3-only TMD insertion. For proteinase K protection assay, the translation mixture was supplemented with 1 µL of 50 mM $CaCl_2$ and 1 µL of proteinase K (4 mg/mL) and then digested 40 min on ice. The reaction was stopped by adding 1 mM phenylmethanesulfonylfluoride before SDS-PAGE analysis. Negative control experiments were developed in absence of microsomes. Lep native TMD (fragment H2) was used as positive control of insertion. All the experiments were repated at least three times.

3.2.5. Design and cloning of ToxRed BH3-only TMD constructs.

Maltose-complementation assay was performed as described in 3.1.1. (332, 333) in order to determine the correct insertion/orientation of BH3-only TMD constructs in the *E. coli* MM39 strain inner membrane.

3.2.6. Expression of ToxRed chimera.

ToxR-TMD-MBP constructs (200 ng) were transformed into 200 µL MM39 competent cells with heat shock at 42 °C for 90 sec and incubation on ice for two minutes, followed by addition of 800 µL LB medium and incubation with shaking at 37 °C for one hour. The transformation mixture was pelleted and plated in minimal-agar media in the presence of ampicillin (100 µg/ml) for two days to analyze the efficiency of the BH3-only TMD insertion.

3.2.7. Cell Lines and Cultures.

The human cervix adenocarcinoma HeLa cells were obtained from the ATCC. Cells were grown in Dulbecco's modified Eagle's medium plus 10% FBS. GFP protein was fused at the N-terminus of the putative TM regions of the different BH3-only proteins as described in 3.2.3. GFP-TMD constructs were transfected into mammalian cells with LipofectamineTM 2000 (Invitrogen) as indicated in 3.1.4.

3.2.8. Immunofluorescence of GFP BH3-only TMD constructs in HeLa cells.

Immunolocalization assays were performed following the protocol described in 3.1.9. HeLa cells were labeled in the different assays with antibodies against Cyt-*c* (1:200; SC13561; Santa Cruz) and Grp78 (1:400; ab21685; Abcam) followed by an anti-mouse IgG-Alexa 555 secondary antibody (1:400; Invitrogen). Cover slips were mounted on glass slides with Mowiol/Dapi (Sigma). Images were obtained using confocal microscopy (LSM 510) with a 63x objective. Colocalization assays of the GFP-TMD constructs and Mitotracker dye (500 nM, 20 min, 37ºC, Invitrogen) was also developed *ex vivo*. Microscopic images of living cells were taken 24 hours after transfection (green channel, λ_{exc} 488 nm, λ_{emi} 488 nm; Red channel, λ_{exc} 561 nm, λ_{emi} 598 nm). The experiments were reproduced three times. At least 30 images of each sample were analyzed.

3.2.9. Immunoblotting and determination of caspase activity for BH3-only TMD construts in HeLa cells.

After 24 h of GFP-TMD transfections, cells were treated as indicated in sections 3.1.6. and 3.1.7., GFP (1:1000, ab13970, Abcam) and α-tubulin (1:1000, #T8203, Sigma-Aldrich) antibodies were used for immunoblotting. Caspase-3 activity was expressed as the increase of relative fluorescence units per min (A.U.). All assays were repeated at least three times.

3.2.10. Statistical analyses.

Statistical analyses were performed as described above (3.1.13).

3.3 CHAPTER III

3.3.1. Bioinformatic analyses of BCL-2 TMD-pepts.

The prediction of BCL-2 TMDs was performed as described in section 3.1.12.

3.3.2 BCL-2 TMD Peptides Synthesis.

Peptides were prepared by Fmoc (N-(9-fluorenyl) methoxycarbonyl)-based solid phase synthesis in a 433A Applied Biosystems peptide synthesizer with a Rink Amide Resin as reported previously (342, 343). Fmoc is a base-label protecting group for amines: incoming amino acids require protection of their amino group in order to obtain coupling to free amino attached to the resin. Elimination of Fmoc group was performed via base-induced β-elimination. Then, dibenzofulvene and carbon dioxide are split off. Secondary bases such as piperidine add to the former molecule whereas bases such as DBU do not react with the dibenzofulvene, which has to be removed rapidly from the peptide resin or scavenged by a secondary amine (piperidine) to avoid irreversible attachment to the liberated amino group.

Peptides were synthesized with 2 or 3 lysines on both the N- and C-termini of the selected sequences in order to improve solubility (see Table 6.I). Peptides were cleaved from the resin by treatment with trifluoroacetic acid (TFA, 70%) and purified by preparative/analitical RP-HPLC (Lichrospher1 100 C18, 10 mm) system up to 95% of peptide purity using different acetonitrile gradients in aqueous 0.1 % TFA. Identity was confirmed by MALDI-TOF mass spectroscopy. Stock solutions of the peptides were prepared in Milli-Q water and the concentrations were determined by spectrophotometry in NanoDrop 1000 (Thermo Scientific).

3.3.3. Circular Dichroism (CD) Measurements.

CD is a powerful tool for the analysis of secondary structure in proteins and peptides. This methodology is based on light absorption spectroscopy that measures the difference in absorbance of right- and left-circularly polarized light by a substance (Figure 3.5A). In proteins, the chromophores of interest include the peptide bond (absorption below 240 nm), aromatic amino acid side chains (absorption in the range 260 to 320 nm) and disulphide bonds (weak broad absorption bands centered around 260 nm). For all of that, CD studies give information about secondary structure configuration (alpha helix, parallel and antiparallel beta sheet and turn) of the peptide/protein analyzed (Figure 3.5B).

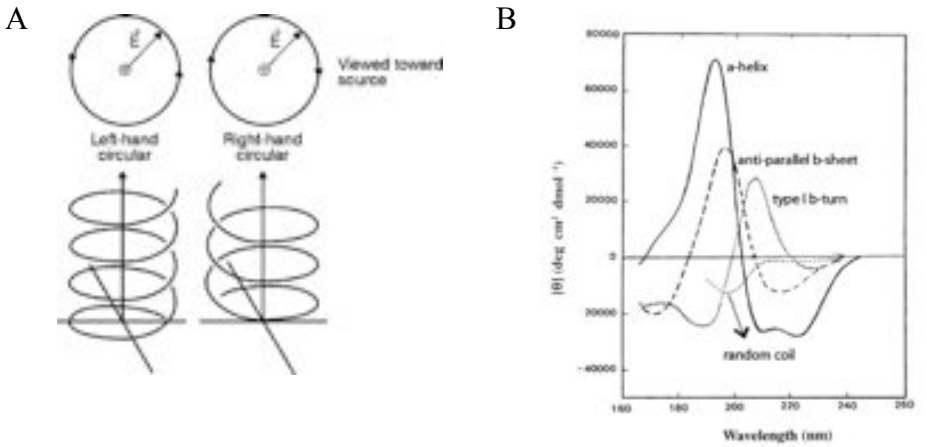

Figure 3.5. Circular dichroism. (A) Scheme of circularly polarized light. (B) CD spectra of secondary structures. (http://chemistry.rutgers.edu/grad/chem585/lecture1.html).

CD spectra were recorded between 190 and 250 nm at 25°C on a Jasco J-810 spectropolarimeter in quartz cells of 0.1-cm path length. Peptides were dissolved at 10 μM in phosphate buffer (50 mM, pH 7.0), and their ability to adopt a secondary conformation was analyzed in pure 2,2,2-trifluoro-ethanol (TFE), 1% sodium dodecyl sulfate (SDS), and methanol (MeOH, 50 and 100%), respectively. Each CD spectrum was the average of 20 scans performed at 1 nm intervals. CD spectra were interpreted with the K2D software provided by Dichroweb (available on the World Wide Web). Results are expressed as mean molar residue ellipticities (degrees x cm^2 x $dmol^{-1}$). For measurements with liposomes, 1 mM of extruded liposome solution (POPC:PE:PS:PI or POPC only) prepared in 10 mM Sodium Phosphate 137 mM NaCl pH7.4 buffer was added to the cuvette where peptide stocks (10mM HEPES 150 mM NaCl pH 7.4) were titrated in to incrementally increase the peptide-liposome ratio. The ratios 1:201, 1:101, 1:51 and 1:31 were analysed to determine the effect of peptide concentration on structure. Calculation of Molar Ellipticity (θ) of the peptides and spectra smoothing was achieved using Jasco instrument software.

3.3.4. Dynamic Light Scattering.

Malvern instruments Zetasizer Nano Z red (Malvern Laboratories Ltd. Malvern, UK) was utilized to determine the size of liposome particles in the presence of peptide via DLS. The relationship between particle size and Brownian motion (Stokes-Einstein relationship) is utilized by the Zetasizer to determine the average size of a population of

particles in solution. 0.1 mM POPC:PE:PS:PI (5:3:1:1) liposome was measured in a low volume disposable cell initially followed by incremental addition of peptide to achieve the same peptide-liposome ratios as in the CD measurements. Samples were incubated in the Zetasizer at 20°C for a total of 10 min prior to reading to give sufficient time for interaction between the peptide and the liposome and a consistent thermal gradient throughout the sample. Each reading consisted of 12 scans each of 10 sec duration with parameters set to measure size in a low volume disposable sizing cell. The equilibration time was set to 60 sec and was included in the incubation time.

3.3.5 Dual Polarization Interferometry (DPI).

Dual polarization interferometry is a relatively new technique, which explores the molecular layers adsorbed to the surface of a waveguide by means of an electromagnetic evanescent wave of a laser beam; it measures the refractive index and the thickness of very thin films, and is also used to study the protein adsorption at solid/water interface. Furthermore, if the refractive index of the studied film is fixed, the birefringence can be observed quantitatively so that the anisotropy of the film can be analyzed. DPI is a quantitative and real-time technique with the dimensional resolution of the order of angstroms. DPI then measures the increase of membrane mass due peptide association/integration (represented in X axis) and the decrease of membrane order when peptides are inserted into the membrane (Y axis) (Figure 3.6). DPI applications involve membrane protein and lipid studies, analyzing the formation of lipid bilayer, the understanding of lipid structures, affinity and kinetics of lipid–lipid and protein–lipid interactions, structural changes taking place during interactions, and the structural nature of protein–lipid complexes.

Liposome preparation for dual polarization interferometry. Thin lipid films of POPC (PM-like) and two MITO-like mixtures, POPC:POPE:POPS:POPI (5:3:1:1) and POPC:POPE:POPS:POPI/CL (4.8:2.8:1:1:0.4) were hydrated to 1 mM lipid concentration, 10 mM HEPES 150 mM NaCl pH 7.4 and buffer solution at 37 °C for 1 h with constant vortexing. The hydrated lipid suspension was sonicated in a water bath for ~30 min at 37 °C and extruded before use through 50 nm polycarbonate membranes (19 times) using an Avestin Lipofast extruder (Ottawa, Canada).

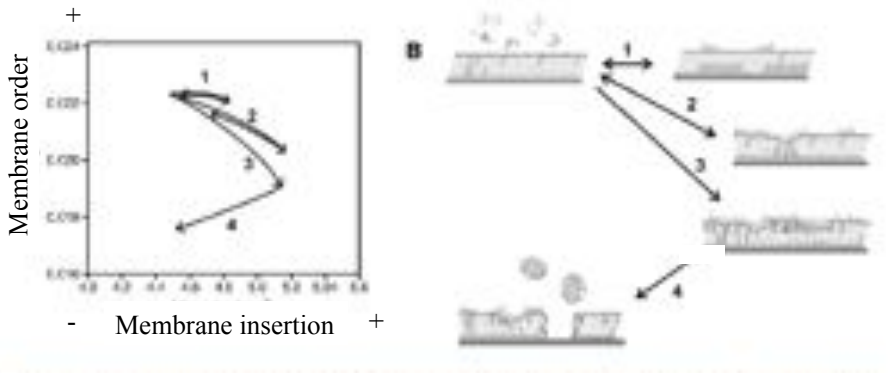

Figure 3.6. Dual Polarization Interferometry (DPI) methodology. Birefringence (Y axis) is a measure of membrane ordering. A decrease in birefringence indicates peptide insertion. Mass (X axis). Inpired by (344).

Deposition of supported lipid bilayer on sensor chips. Planar supported lipid bilayers (SLBs) were prepared via *in situ* adsorption of liposomes to a silicon oxynitride waveguide sensor chip (see Supporting information for detailed description). A fresh bilayer was used for each individual peptide measurement and 160 µL of each concentration was injected sequentially onto the SLB in increasing concentrations at a flow rate of 40 µL/min with a total of 30 min equilibration time between injections.

Data acquisition was carried out using *Ana*Light200 version 2.1.0 software and analyzed using *Ana*Light Explorer proprietary software (345, 346).

3.3.6. Small Unilamellar Liposomes (SUV) Preparation and Calcein Release Assay.

Calcein release assay was performed to study the capability of the TMD-pepts to destabilize mitochondrial membranes. Small Unilamellar Liposomes (SUV) with plasma membrane and mitochondrial composition were designed.

Small unilamellar liposomes were prepared as previously reported (347)(Figure3.6). Lipid samples were dissolved in a 2:1 (v/v) chloroform:methanol mixture and dried under N_2 stream in order to remove residual organic solvents. The dried lipid was suspended by vortexing in 150 mM Hepes buffer (pH 7.0) containing 90 mM of calcein. Lipid mixtures were incubated for 20' at a temperature above the phase transition of the major phospholipid component of the liposome. The final phospholipid concentration was about 30 mM. Disruption of multilamellar vesicle (LMV) suspensions by sonication 5 min at 4°C with a probe tip sonicator produced small unilamellar vesicles (SUV) with diameters in the range of 15-50 nm. SUV were composed of phosphatidylcholine (PC):CL (7:3, mol:mol) as MITO-like and PC:cholesterol (7:3, mol:mol) as PM-like. The lipid

suspensions, SUV were then centrifuged at 10000 rpm for 10'. Free calcein was removed by passage of the dispersion through a column of Sephadex G-50 (Sigma-Aldrich). For calcein release assays fluorescence measurements were made with a Jasco FP6600 Spectrofluorometer using 495 nm and 520 nm, as excitation and emission wavelengths respectively.

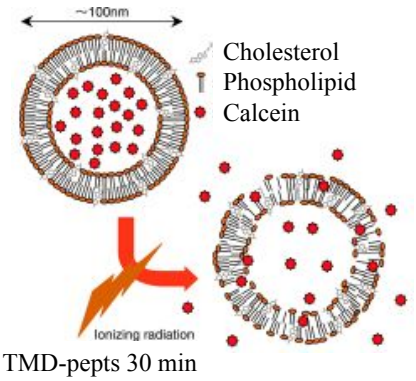

Figure 3.7. Calcein Release Assay scheme. Composition of a small unilamellar vescicle.

3.3.7. Mitochondrial Isolation and cytochrome-*c* Release Assays in MEFs.

Mitochondria were freshly isolated from MEFs (mouse embryonic fibroblast) cells by differential centrifugation steps as described previously (348). Cells were pelleted and suspended in ice-cold IB_c buffer (125 mM KCl, 5 mM KH2PO4, 2 mM MgCl2, 25 μM EGTA, 5 mM succinate, 5 μM rotenone, and 10 mM HEPES-KOH (pH 7.2)). A Douncer Tissue Grinder Homogenizer (Wheaton) was used for cell homogenization (20 strokes). Consequently samples was centrifuged at 600×g for 10 min at 4°C; the supernatant was recollected and centrifuged at 7,000×g for 10 minutes at 4°C. The pellet was washed and resuspended with ice-cold IBc and centrifuged another time at 7,000×g for 10 minutes at 4°C. Mitochondria concentration was quantified with BCA Protein Assay Kit (Thermo Scientific) and kept on ice. Isolated mitochondria (0,5 mg protein/ml) were then incubated with the different TMD-pepts (50 μM) in IB_c Buffer for 30 min at 30°C. Reaction mixtures were centrifuged at 7,000×g for 10 min. Supernatant and pellet fractions were solubilized in protein sample buffer, analyzed by SDS/PAGE (14% gel) and transferred to nitrocellulose (BioRad). Membranes were developed against cytochrome *c* antibody (#4272, Cell Signaling), α-tubulin antibody (#T8203, Sigma-Aldrich) and VDAC1/2/3 antibody (sc-98708, Santa Cruz).

3.3.8 Mitochondria Swelling measurements.

Isolated mitochondria were suspended (final concentration 0,5 mg/ml) in 100 µl of swelling buffer (120 mM KCl, 10 mM Tris-HCl, 5 mM MOPS, 5 mM KH_2PO_4, pH 7,4) in a 96-well plate. A basal signal line was assessed for 5 min and then mitochondria were treated with 50 µM of each TMD peptide and 100 µM $CaCl_2$, respectively. Changes in absorbance caused by swelling were monitored using a microplate reader at 540 nm every 5 min for 1 hour.

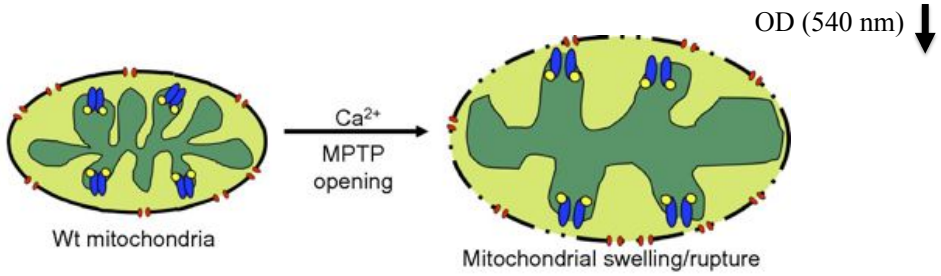

Figure 3.8. Mitochondria Swelling scheme (349).

3.3.9 Cell Lines and Cultures.

Mouse embryonic fibroblast (MEFs) *Bax/Bak KO* cell line was kindly provided by Dr. Guido Kroemer (INSERM, University of Paris). The human cervix adenocarcinoma HeLa cells were obtained from the ATCC. Wild type and *Bax/Bak KO* HCT 116 cells were kindly provided by Professors Bert Vogelstein (Howard Hughes Medical Institute) and Richard Youle (NIH, Bethesda). MEFs and HeLa were grown in Dulbecco's modified Eagle's medium plus 10% FBS. HCT116 cells were grown in McCoy´s 5A Modified Medium plus 10% FBS. Cells were incubated at standard conditions. Peptides were transfected with LipofectamineTM 2000 (Invitrogen). Briefly, peptides were combined with 2,5 µl of Lipofectamine and Opti-MEM® Reduced Serum Media (Invitrogen) for 30 min at room temperature. Then cells with confluency >70% were incubated 4 h at 37ºC with the transfection mixure. Finally, transfection mixture was discarded and CDDP treated and non-treated cells were incubated at 37ºC up to 24 hours.

3.3.10 Cell-based Caspase 3/7 Activation assays for BCL-2 TMD-pepts in different cell lines.

All cell extracts were prepared from 2×10^5 cells seeded in 6-well plates. After 24 h, cells were treated with a Lipofectamine/ peptide (3 or 10 µM) mixture for 4 h followed by administration of 35 µM cis-diammineplatinum(II) dichloride (cisplatin, CDDP). After 24

hours, cells were manipulated as described in 3.1.7. Western blot assay of caspase-3 was developed as indicate in 3.1.6.

3.3.11. Flow Cytometry assays of BCL-2 TMD-pepts in different cell lines.

Cells were harvested by centrifugation, suspended in binding buffer (10 mM HEPES pH 7.4, 140 mM NaCl, 2.5 mM $CaCl_2$) and incubated with 1 µl of tetramethylrhodamine methyl ester perchlorate (TMRM; 1 µM). To measure apoptotic or necrotic cell death, the FITC-Annexin V/PI kit (BD Biosciences) was used following manufacturer instructions (see 3.1.8). To quantify the release of cytochrome *c* from mitochondria, HeLa cells were seeded at 1.5 10^5 cell/mL and after 24 h in presence of TMD-pepts, the InnocyteTM Flow Cytometric cytochrome *c* Release kit (Calbiochem) was used according to the manufacturer's recommendations. Staining was assessed by flow cytometry on a FC500 instrument (Beckman Coulter) followed by data analysis using FlowJo software (Tree Star Inc).

3.3.12. Measurement of cellular ATP.

Relative cellular ATP content was measured by the ATPlite Kit (PerkinElmer) according to manufacturer's protocol. Cells were plated in 96-well plates at 8,000 cells per well to allow for attachment overnight. Cellular ATP content was measured using a luminescent plate reader 4 h after peptide treatment.

3.3.13. Mitochondrial dysfunction assays (MTT) upon TMD-pepts treatment in different cell lines.

MTT colorimetric assay is based on enzymatic reduction of a yellow tetrazolium salt, 3-(4,5-dimethylthiazol-2-yl)-2,5-diphenyltetrazolium bromide (MTT), generating a purple formazan crystal in metabolically active cells (Figure 3.9). Formazan is then solubilized producing a concentration related to colorimetric signal at 570 nm, proportional to the cell number and activity. Cells were cultured in sterile 96-well microtiter plates at a seeding density of 8000 cells/well for the HCT116 lines and 3000 cells/well for HeLa cells. After seeding, cells were left to adhere to the plate overnight, and then they were treated with the compounds and/or TMD-pepts of interest and incubated at 37°C for 24 h. MTT reagent (5 mg/ml in PBS) was added to each well and plates were further incubated for 4 h at 37°C. Finally, the medium was removed and the precipitated formazan crystals were dissolved in optical grade DMSO (dimethyl sulfoxide). Plates were read at 570 nm on a Wallac 1420 workstation (Perkin Elmer).

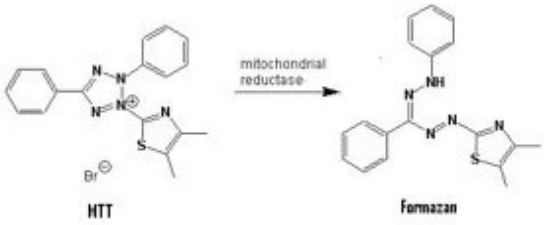

Figure 3.9. Reduction of the yellow MTT to the purple formazan.

3.3.14. Cell viability assays of TMD-pepts in different cell lines.

Cells were seeded in 96-well plates at a cellular density of 8000 cells/well for the HCT116 lines and 3000 cells/well for HeLa cells. After 24 h, cells were treated as previously described. Cells were detached and 0.5% trypan dye blue was added in solution. Live cells possess intact cell membranes that exclude the dye, whereas dead cells do not. Unstained (viable) and stained (non-viable) cells were counted separately in a hemacytometer and the total number of viable cells in the population was calculated.

3.3.15. Statistical analyses.

Statistical analyses were performed as described above (3.1.13).

3.4 CHAPTER IV

3.4.1 Cell culture, treatments and chemicals.

ABT-737 and GX15-070 drugs were purchased from Abbott Laboratories and from SelleckBio, respectively; cis-diammineplatinum(II) dichloride (cisplatin, CDDP), rapamycin and 3-methyladenine (3MA) were obtained from Sigma Aldrich. QM31 is a perhydro-1,4-diazepine-2,5-dione whose general synthetic method has been recently reported (350). The HeLa cell line was purchased from ATCC, and mouse embryonic fibroblasts MEFs wt and *KO Bax/Bak* (84, 351)) were kindly provided by Dr. Guido Kroemer (INSERM, University of Paris) and Dr. Francesco Cecconi (IRCCS Fondazione Santa Lucia in Rome) (MEFs wt and *KO Apaf-1*). All the cell lines were grown in Dulbecco's Modified Eagle's Medium (DMEM) supplemented with 10% fetal bovine serum (FBS). Cultures were maintained at 37ºC in a 5% CO_2 atmosphere. Cell media and FBS were purchased from GIBCO BRL Life Technologies. When indicated, cells were

treated with 1 μM of GX50-070, 25 μM of ABT-737, 30 μM of rapamycin or 30 μM of CDDP. When required, 10 mM MA (Methyl-adenine), 10 μM QM31 or 5 μM zVAD were administered 30 min after treatment addition, and cells were maintained in culture for 24 h. Assays were carried out between passage 6 and 10, in all cases.

3.4.2 Caspase activity expermiments for different pro-apoptotic treatments in different cell lines.

The caspase 3/7 activity assay was developed as indicated in 3.1.7.

3.4.3 Flow cytometry assays for different drugs and cell lines.

After drug treatment, cells were collected and treated following the protocol described in 3.1.8. Cells were incubated with 10 μL FITC Annexin V (BD Biosciences) and 10 μL of DRAQ7 (6 μM; Biostatus) for 10 min at 37ºC.

3.4.4 (MTT) mitochondrial dysfunction assays in different cell types.

Mitochondrial functionality was measured following the protocol described in 3.3.13. Cells were cultured in sterile 96-well microtiter plates at a seeding density of 1500 cells/well for the MEFs lines and 2000 cells/well for HeLa cells. Plates were read at 570 nm on a Wallac 1420 workstation.

3.4.5 Trypan blue exclusion assays with diverse pro-apoptotic drugs in different cell lines.

Cells were cultured in sterile 96-well microtiter plates at a seeding density of 5000 cells/well for the MEFs lines and 3000 cells/well for HeLa cells. Trypan blue was used (see 3.3.14) to determinate the percentage of viable cells.

3.4.6 Nuclei staining.

The cells cultured on coverslips were stained with 300 nM 4'-6-diamidino-2-phenylindole (DAPI) solution. Morphology of the cell nuclei was observed using a fluorescence microscope (Leica Vertical DM6000) at an excitation wavelength of 350 nm. Nuclei are considered to have the normal phenotype when they glow blue brightly and homogenously. Apoptotic nuclei can be identified by either the condensed chromatin

gathering at the periphery of the nuclear membrane or a total fragmented morphology of nuclear bodies.

3.4.7 Immunoblotting for the different pro-apoptotic treatments in different cell lines.

Whole cell extracts were obtained as indicated in 3.1.6. The antibody against LC3 (#2775) came from Cell Signaling and α-tubulin antibody (#T8203) was from Sigma-Aldrich.

3.4.8 Statistical analyses.

All the values represent the mean ± s.d. of at least three independent experiments. Statistical significance was determined by one-way ANOVA using the Graph Pad software, $p<0.05$ was designated as statistically significant.

CHAPTER

I

4.1. Introduction

Protein–protein interactions among pro-apoptotic and anti-apoptotic members of the BCL-2 family are crucial to determine the final fate of cells. However, the molecular insights of that equilibrium remain poorly understood. The role of cytosolic domains from BCL-2 proteins in the molecular network of interactions that controls MOMP have been extensively studied (121), whereas TMDs have been traditionally considered as mere membrane anchors (196, 352).

In recent years, it has been demonstrated that while some of the BCL-2 members conserve their apoptotic function in the absence of their C-terminal TMDs, others need them to modulate biological activity (63, 110, 221). Taking into account the existence of these hydrophobic regions in almost all members of the BCL-2 protein family and the fact that they exert their function within the membrane, it is reasonable to hypothesize an active role for TMDs in regulation of apoptosis.

As a first step to understand TMD molecular function, our objective was to establish the oligomerization state of these protein domains within the membrane and the interaction network among TMDs from different members of the BCL-2 protein family. All strategies have been performed maintaining proteins in its natural environment, the membrane. This is of particular interest in membrane protein interaction studies due to the existence of several interaction artifacts when proteins are extracted from the lipid bilayer.

4.2. Results and discussion

4.2.1. The oligomerization state of BCL-2 TMDs in membranes.

To test whether BCL-2 TMDs, together with soluble domains, participate in the equilibria that govern MOMP, we have first analyzed the oligomeric state of these TMDs in live cells. To address this question we have employed the prokaryotic ToxRed system (332, 353) to determine whether the TMDs of anti- (Bcl-xL, Bcl-2, Bcl-w, Mcl-1 and Diva) and pro-apoptotic (Bax, Bak, Bid, Bik, Rambo) BCL-2 proteins (Table 4.I) are sufficient to cause self-association. In this assay, the TMD tested is inserted as an in-frame fusion between the ToxR (an N-terminal transcriptional activation domain) and MBP (a C-terminal maltose-binding protein that is targeted to the periplasm) (353). ToxR is in active state when dimerizes thought BCL-2 TMD association, recognizing then the *ctx* promoter and activating the transcription of *RFP* gene (Figure 4.1). The level of fluorescence emission at 615 nm indicates the strength/intensity of TMD-mediated self-association.

Proper insertion into the membrane can be verified by the ability of periplasmic MBP to restore the capability of *E. coli MM39* mutant to grow on maltose as a sole carbon source (332).

Table 1. BCL-2 TMD sequences cloned. The aminoacids underlined are cloned only in the BiFC constructs for mitochondrial targeting. Δ G based on the Kyle and Doolittle algorithm.

BCL-2	Cloned sequence	Length	ΔG
Bcl-2	FSWLSLKTLLSLALVGACITLGAYLGHK	23	-1.356
Bcl-xL	SRKGQERFNRWFLTGMTVAGVVLLGSLFSRK	23	-0.355
Bcl-w	REGNWASVRTVLTGAVALGALVTVGAFFASK	22	-0.418
Mcl1	IRNVLLAFAGVAGVGAGLAYLIR	23	-0.275
Bcl-B	FWRKQLVQAFLSCLLTTAFIYLWTRLL	21	0.689
Bax	TWQTVTIFVAGVLTASLTIWKKMG	20	0.510
Bak	ILNVLVVLGVVLLGQFVVRRFFKS	22	-0.735
Rambo	GKSILLFGGAAAVAILAVAIGVALRKK	21	-1.403
Bik	VLLALLLLLALLLPLLSGGLHLLLK	24	-3.253
Bid	KEKTMLVLALLLAKKVA	17	2.462

In each case fluorescence ratio between the ToxRed wt construct containing the BCL-2 TM fragment (ToxR) and a ToxRed mutant construct (containing the TM domain of interest but a non functional version of the transcription factor ToxR (ToxR*)) has been included to account for basal cell fluorescence (Figure 4.1).

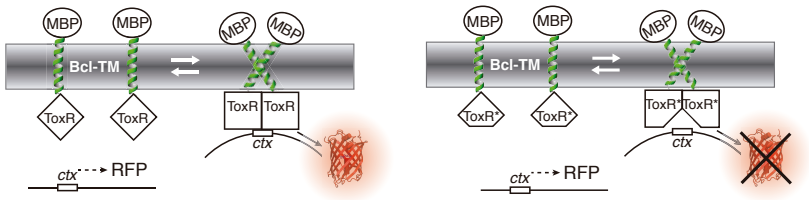

Figure 4.1. Schematic view of transmembrane interaction monitoring system (ToxR). The P1 construct consists in the N-terminal DNA binding domain of ToxR (a dimerization-dependent transcriptional activator) fused to a BCL-2 transmembrane domain and a monomeric periplasmic anchor (the maltose binding protein). Association of the TMDs results in the ToxR-mediated activation of a RFP reporter gene. The level of fluorescence indicates the strength of TMDs association. The fluorescent assay is standardized with a ToxR mutant P2 construct unable to activate the expression of RFP reporter gene.

As a positive control of interaction we used the Glycophorin A TMD (GpA TMD: EITLIIFGVMAGVIGTILLISYGI) a well characterized homo-dimeric transmembrane

protein (354, 355) and the point mutant G83I of GpA TMD as a negative control. All the BCL-2 TMDs showed the capability to form homo-oligomers within the bacterial membrane with the exception of Bid TMD. Interestingly, the TMD of apoptotic executioner protein Bax causes the highest fluorescence. Western blots of whole cell lysates detected with anti-MBP antibodies (Figure 4.2.B, bottom) demonstrate that the levels of ToxR-(Bcl-TMD)-MBP are comparable, so the different fluorescence emission levels can be interpreted to arise from differences in TMD self-association in the *E. coli* inner membrane. We conclude that the BCL-2 TMDs with the exception of Bid associate strongly in the *E. coli* inner membrane.

A

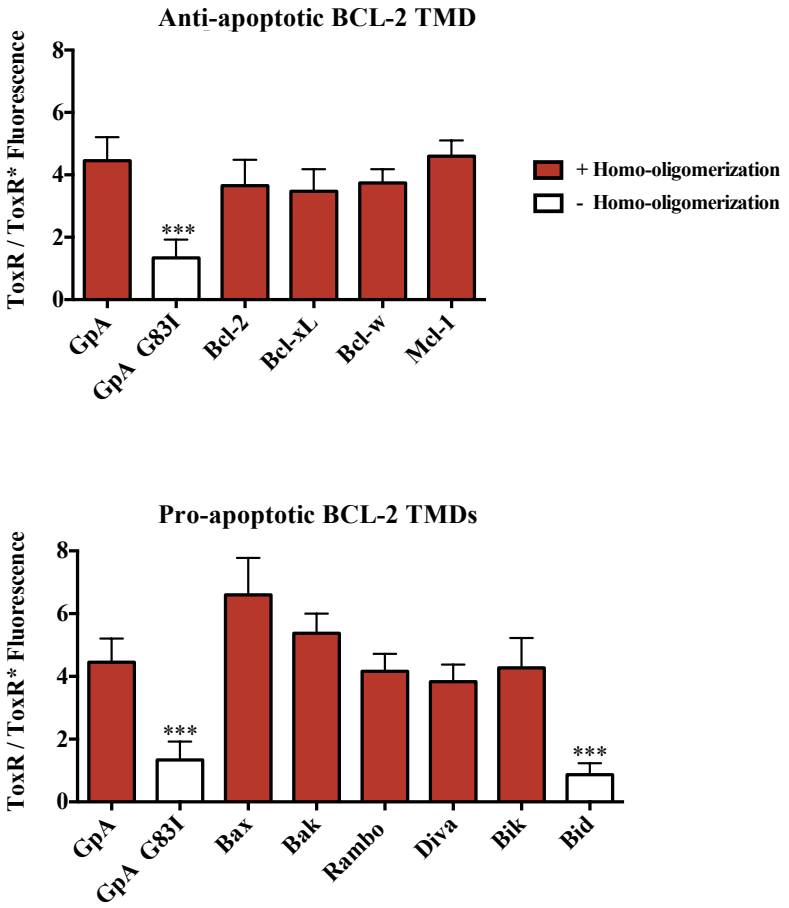

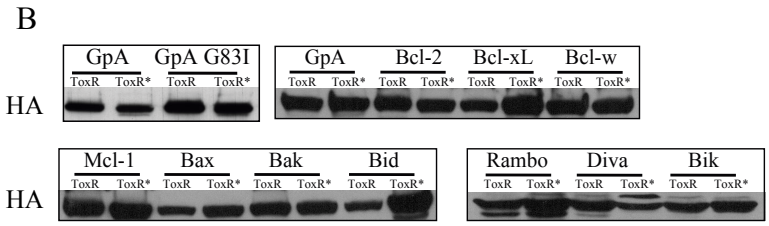

Figure 4.2. The TMDs from BCL-2 family proteins are involved in protein homo-oligomerization. (A) The formation of BCL-2 oligomers followed by the increase in fluorescence due to RFP expression mediated by ToxR transcription factor**.** The results are represented by the normalized fluorescence signal (ToxR/ToxR*) obtained with the ToxR system for the TMDs of the different BCL-2 proteins. Red bars represent positive interactions and white bars represent negative interactions. GpA positive control and point mutant GpA G83I as negative control of interaction are showed in the first and second column, respectively. All the results represent the mean of three independent experiments. Dunnett's Multiple Comparison Test (95%CI) was used to compare with a positive control Glycophorin A TMD. (B) Equivalent expression levels of all constructs were confirmed by Western blot developed against HA antibody.

The ability of the isolated TMDs to self-associate suggests that this property may underlie the previously observed functional importance of BCL-2 TMDs (356). Inspection of their amino acid sequences and comparison with previously reported interacting TM segments (357, 358) reveal glycines located roughly in the middle of TM segments as potential sources for strong helix-helix interactions. We have tested the sequence specificity of self-association using site-directed mutagenesis to find residues that were relevant in the molecular interacting interface between these quaternary structures (Figure 4.3). Several single point mutants were identified that partially disrupt formation of BCL-2 TMD homo-oligomers without affecting expression or insertion of the protein within the membrane (Figure 4.4A and B), demostrating existence of specific molecular interfaces.

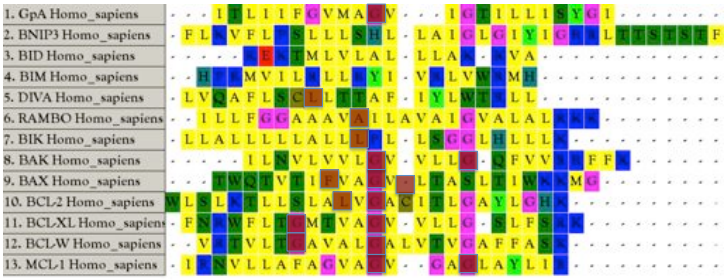

Figure 4.3. Multiple Transmembrane domain alignment for BCL-2 protein family (Homo sapiens) using CLUSTALW algorithm in MEGA 5.0 (GpA TM like outgroup). The positions of the different point mutans are highligthed in brown.

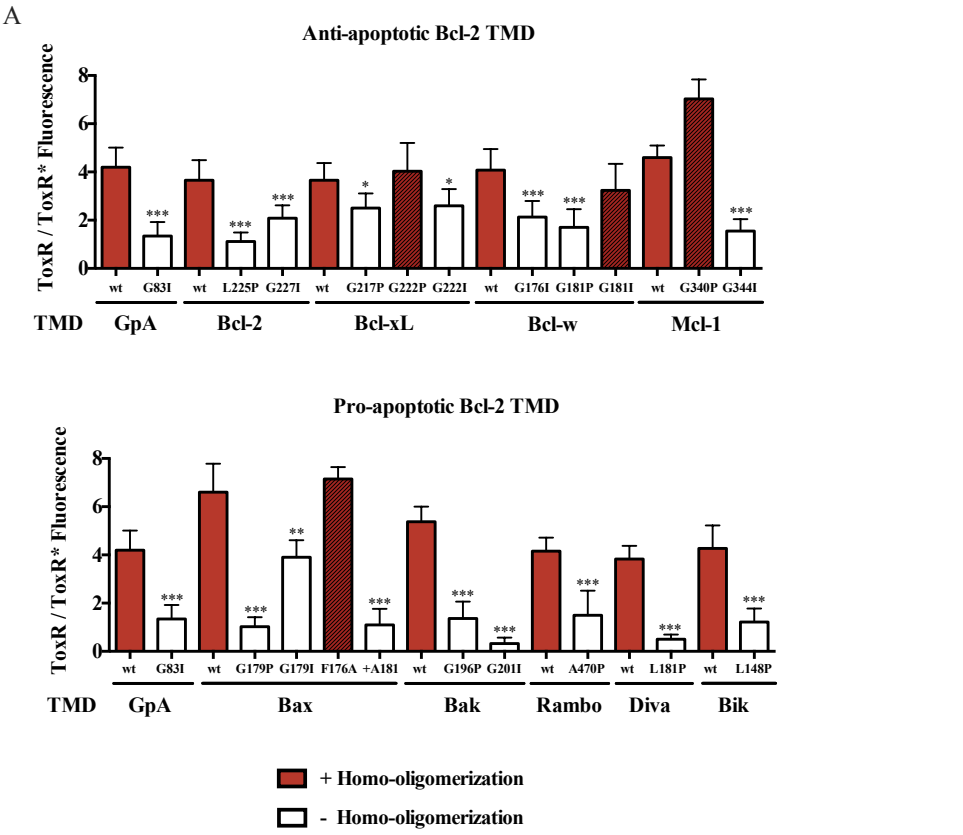

Figure 4.4. TMD mutants from BCL-2 family proteins corroborate the specificity of the homo-oligomerizations. (A) Decrease of fluorescence signal in the ToxR system induced by point mutations of BCL-2 TMDs. The drop in the fluorescence signal denotes homo-oligomer disruption. Red bars represent positive interactions and white bars represent negative interactions. GpA positive control and point mutant GpA G83I as negative control of interaction are showed in the first and second column, respectively. (B) The equal expression of all constructs was confirmed by Western blot developed against HA antibody.

Altogether these results indicate that the BCL-2 TMDs populate the membrane in a non isolated (non-monomeric) state, establishing specific interactions with other TMDs that could be relevant for the function of full length BCL-2 proteins in a physiological environment.

4.2.2. The oligomerization state of BCL-2 TMDs in the mitochondria.

Once it was demonstrated that BCL-2 TMDs have the ability to self-interact in bacterial membranes, bimolecular fluorescence complementation (BiFC) assays were used to analyze the intracellular distribution and self-association of fluorescent-protein-tagged BCL-2-TMDs. BiFC assays permit the direct visualization of protein-protein interactions (PPI) in living cells (336, 337). The principles of this methodology are illustrated in Fig 4.5A. Briefly, the proximity between two interacting molecules (BCL-2 TMDs) tagged with two complementary halves of the Venus Fluorescent protein (VN and VC) facilitates their maturation to a functional fluorescent protein, indicating oligomer formation. An improved BiFC assay with a high signal-to-noise ratio was selected to avoid background interferences (337). The system was adapted to clone BCL-2 TMDs at the C-terminal end of Venus protein fragments, according to their natural topology in full length proteins.
Both, VN- and VC- BCL-2 TMD constructs were co-transfected in the HCT 116 colon cancer cells and formation of oligomers was evidenced by reconstitution of Venus protein and appearance of green fluorescence (Fig 4.5B). Co-expression of the positive PPI pair, b-Fos and b-Jun proteins, used as a positive control of the system (359), rendered high fluorescence whereas the mutant b-ΔFos and b-Jun fusion proteins produced low fluorescence values (Fig 4.5B, + and - respectively)(337). BCL-2 TMDs were able to reconstitute Venus fluorescent protein indicating the existence of homo-oligomers in live eukaryotic cells (Figure 4.5B). Immunoblotting experiments against c-myc and HA tags confirmed equivalent expression of both VN- and VC- constructs (Figure 4.5C). Then, the different association levels, account for the different fluorescence values observed and agree with the results obtained in the ToxR system (Figure 4.2A) where self-association of pro-apoptotic protein Bax causes also the highest fluorescence.

Interactions between the BCL-2 family members via their transmembrane domain (TMD): Relevance in the apoptotic control.

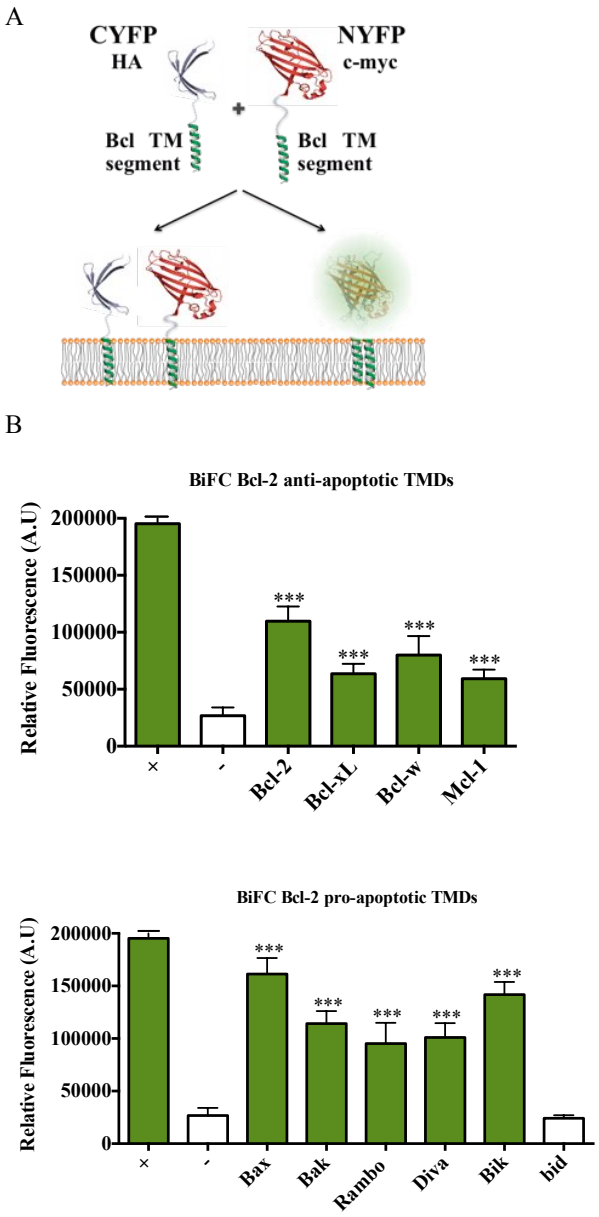

Figure 4.5. BCL-2 TMD Homo-oligomerizations in mammalian cells using BiFC strategy. (A) The Bimolecular fluorescence complementation system (BiFC) is based on the reconstitution of fluorescence from separate N- and C- terminal Venus protein fragments. This reconstitution depends on the establishment of interaction between BCL-2 TMDs. (B) BCL-2 TMD homo-oligomerization assays measured by BiFC in the HCT 116 cell line. The VC- and VN-Bcl constructs were transfected in the HCT 116 cell line and fluorescence

was measured 24 hours later. Average fluorescence intensity of three independent experiments is represented. Dunnett's Multiple Comparison Test (95%CI) was compare with negative control Δ Fos/Jun.

BCL-2 family members are targeted to the appropriate membrane either immediately after their synthesis or in response to an apoptotic stimulus. Targeting to mitochondria has been demonstrated to be mainly directed by the C-terminal region of these proteins (194, 197, 229). The role of TMDs in apoptosis modulation has been controversial. Involvement of BCL-2 interactions in apoptosis modulation clearly requires oligomer formation to occur in the mitochondrial membrane. In this context, to study the intracellular distribution of BCL-2 TMD oligomers, microscopy studies of HCT 116 cells overexpressing VC/VN TMD constructs were performed. Cells were incubated with mitotracker dye to label active mitochondria. Confocal microscopy images showed a reticular distribution of the green fluorescence for BCL-2 TMD homo-oligomers that extensive colocalized with mitochondria (Figure 4.6A). Subcellular distribution of TMDs was also corroborated by cellular fractionation studies (Figure 4.6B). In these experiments *c*-myc antibody was used to detect VN BCL-2 TMD fusion proteins while the Tom 20 protein and the Glyceraldehyde-3-phosphate dehydrogenase (GAPDH) were used as mitochondrial (M) and cytosolic (C) markers, respectively. All BCL-2 TMDs were mainly localized in the mitochondrial fraction (M), in accordance with results obtained from confocal studies.

A

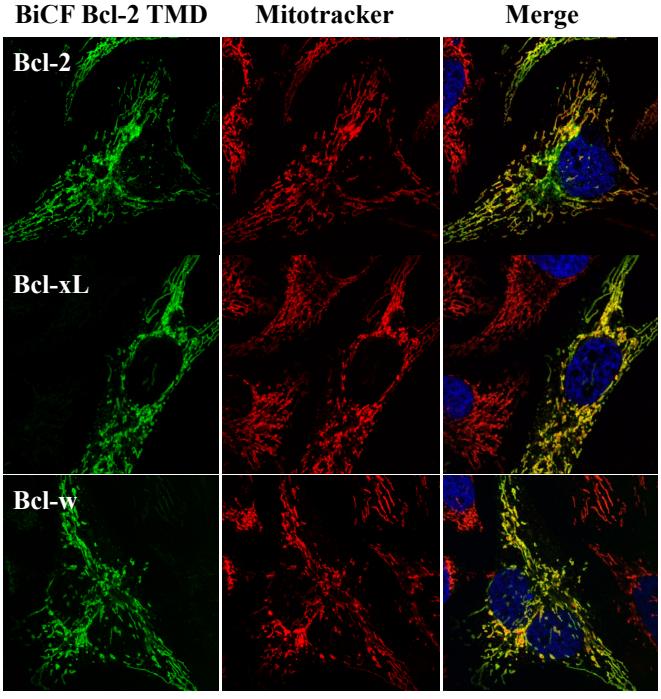

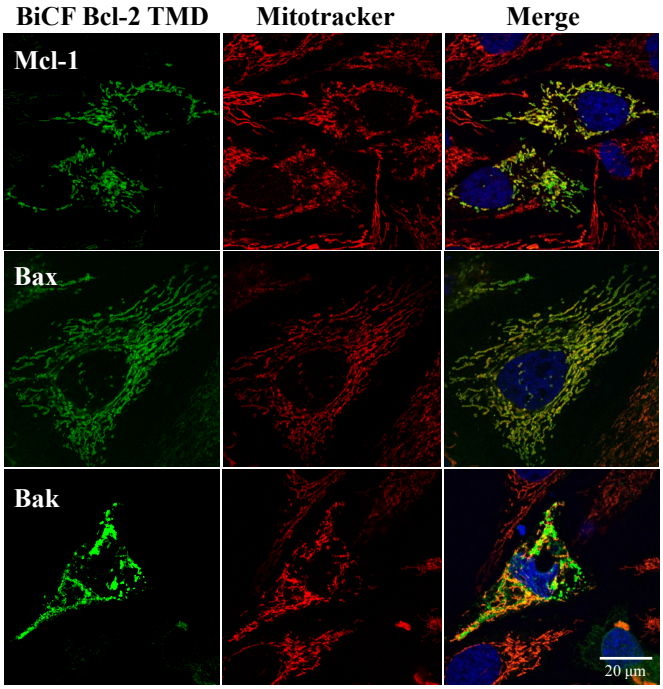

B

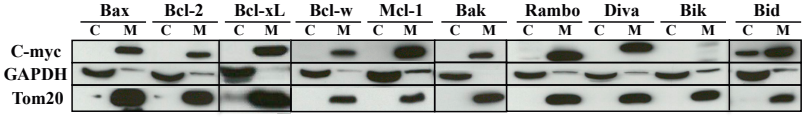

Figure 4.6. BCL-2 TMD Homo-oligomerizations take place in the mitochondria. (A) Confocal images of HCT 116 cells transfected with VC- and VN-BCL-2 constructs. The formation of homo-oligomers was observed in the green channel. Cells were incubated with Mitotracker to stain mitochondria (red channel). Co-localizations are shown in yellow. (B) Subcellular fractionation of HCT 116 cells transfected with VC- and VN-BCL-2 constructs. C-Myc antibody was used to localize the BCL-2 TMD constructs. Mitochondrial fraction (M) is monitored by the presence of Tom 20 mitochondrial protein and cytosolic fraction (C) by GAPDH.

Selected TM helix mutants, previously analyzed in the ToxR system, were also analyzed by BiFC (Fig 4.7). Those mutations which destabilize BCL-2 TM helix oligomerization faces in bacterial membranes rendered VC/VN BCL2 TMD constructs

with lower fluorescence levels, corroborating the reduced oligomer formation capacity and the relevance of these residues in the helix-helix packing interfaces.

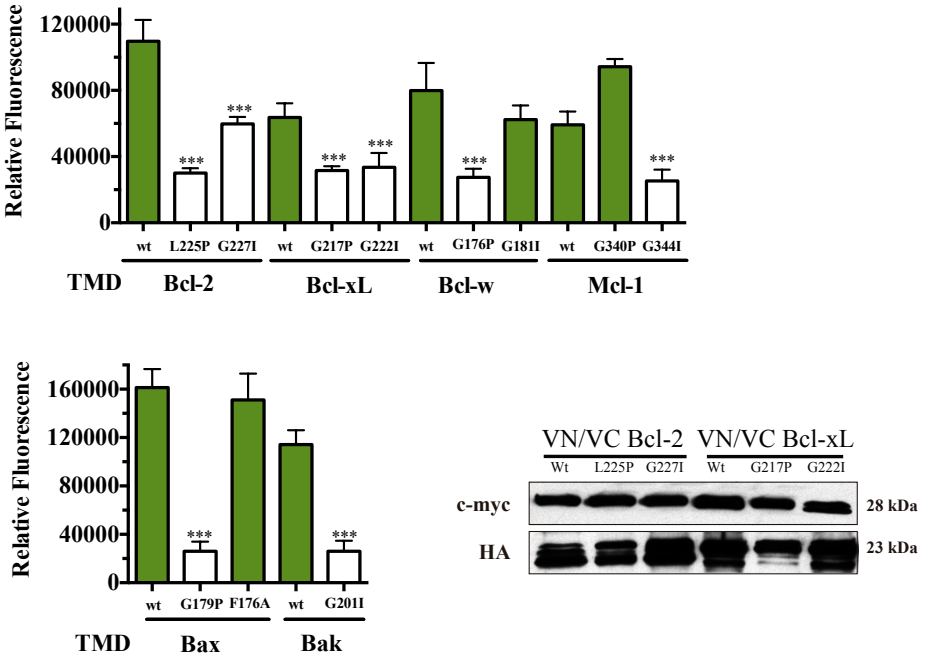

Figure 4.7. BCL-2 homo-oligomerizations also showed high specificity in eukaryotic cells. Decrease of fluorescence signal in the BiFC system induced by point mutations of BCL-2 TMDs. The drop in the fluorescence signal denotes homo-oligomer disruption. Green bars represent positive interactions and white bars represent negative interactions. Average fluorescence intensity of three independent experiments is represented. Dunnett's Multiple Comparison Test (95%CI) was used to compare with negative control Fos/ Δ Jun.

Alltogether results demonstrate the capability of the BCL-2 TMDs to form homo-oligomers in the mitochondrial membrane of eukaryotic cells. Due to the relevance of the BCL-2 family proteins for the MOMP, their structural organization within the mitochondrial membrane should be relevant for the regulation of the mitochondrial outcome.

4.2.3. The network of BCL-2 TMDs interactions.

Control of MOMP is accomplished by a complex network of interactions between members of the BCL-2 family. For this reason, once the capability of BCL-2 TMDs to homo-oligomerize was established our next question was whether hetero-oligomerizations within the membrane were also possible between the different BCL-2

TMD members.

The ToxRed system permits the study of hetero-oligomerization by setting a competion through co-transforming bacterial cells with constructs carrying one BCL-2 TMD construct fused to the ToxR and a second TMD fused to the disabled ToxR* moiety, unable to reconstitute the ToxR transcription factor (332, 353). Then, BCL-2 TMD cloned in the wild type ToxR could exclusively homo-oligomerize itself, showing the maximum level of fluoresecence (100%), or could also hetero-oligomerize with the other BCL-2 TMD fused to the disabled ToxR*, generating a fluorescence decrease (Figure 4.8). Furthermore, the GpA-TMD, a non-BCL-2 related TMD, was used as a negative control of hetero-dimerization.

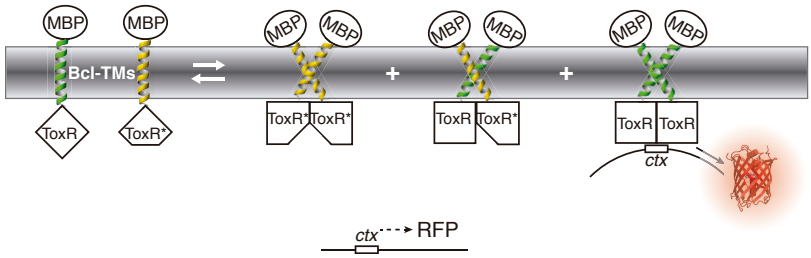

Figure 4.8. Schematic view of TM interaction monitoring system (ToxRed) adapted to evaluate hetero-oligomer formation. Co-transformation with ToxR fused to one BCL-2 TMD plasmid and a second plasmid containing disabled ToxR* fused to a different BCL-2 TMD, renders up to three different types of oligomers: fluorescent (ToxR/ToxR) combinations and non-fluorescent (ToxR/ToxR* and ToxR*/ToxR*) combinations.

Making use of this experimental procedure we studied the formation of hetero-oligomers among TMDs from the different members of the BCL-2 protein family (Figure 4.9). The results of these studies reveal a complex network of interactions among them. The network of TMD interactions obtained for the BCL-2 anti-apoptotic members reveals for example that there are not TM interactions between Bcl-2 and Bcl-xL (Figure 4.9A and 9B). Bcl-w TMD interactions (Figure 4.9C) were consistently observed with Bcl-2 TMD and Bcl-xL TMD but not with Mcl-1 TMD (Figure 4.9C). Further, Mcl-1 TMD has an interaction pattern completely different to these obtained for Bcl-2 TMD and Bcl-xL TMD, since these latter two members share a similar pattern of interactions (Figure 4.9A, B and D).

A

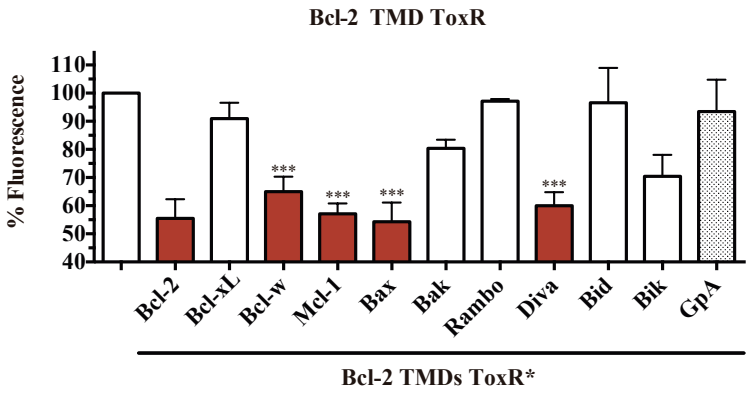
Bcl-2 TMD ToxR
% Fluorescence
110
100
90
80
70
60
50
40
***
***
***
***
Bcl-2
Bcl-xL
Bcl-w
Mcl-1
Bax
Bak
Rambo
Diva
Bid
Bik
GpA
Bcl-2 TMDs ToxR*

B

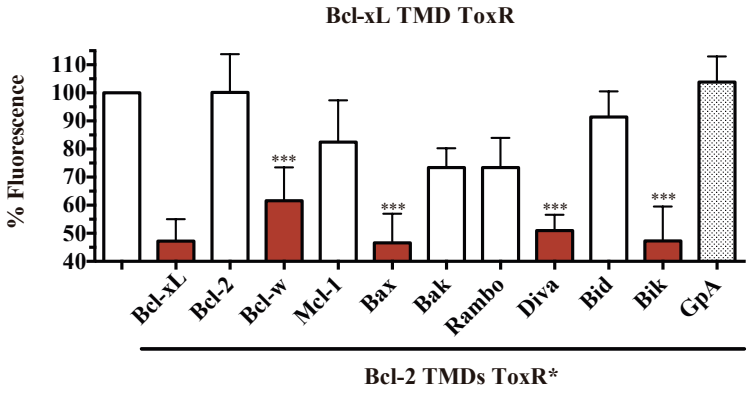
Bcl-xL TMD ToxR
% Fluorescence
110
100
90
80
70
60
50
40
***
***
***
***
Bcl-xL
Bcl-2
Bcl-w
Mcl-1
Bax
Bak
Rambo
Diva
Bid
Bik
GpA
Bcl-2 TMDs ToxR*

C

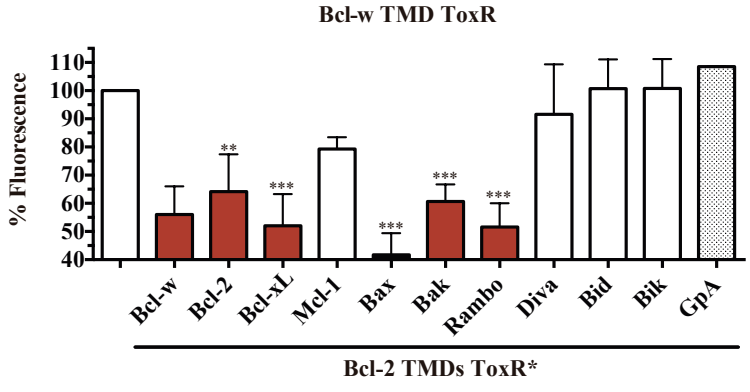
Bcl-w TMD ToxR
% Fluorescence
110
100
90
80
70
60
50
40
**
***
***
***
***
Bcl-w
Bcl-2
Bcl-xL
Mcl-1
Bax
Bak
Rambo
Diva
Bid
Bik
GpA
Bcl-2 TMDs ToxR*

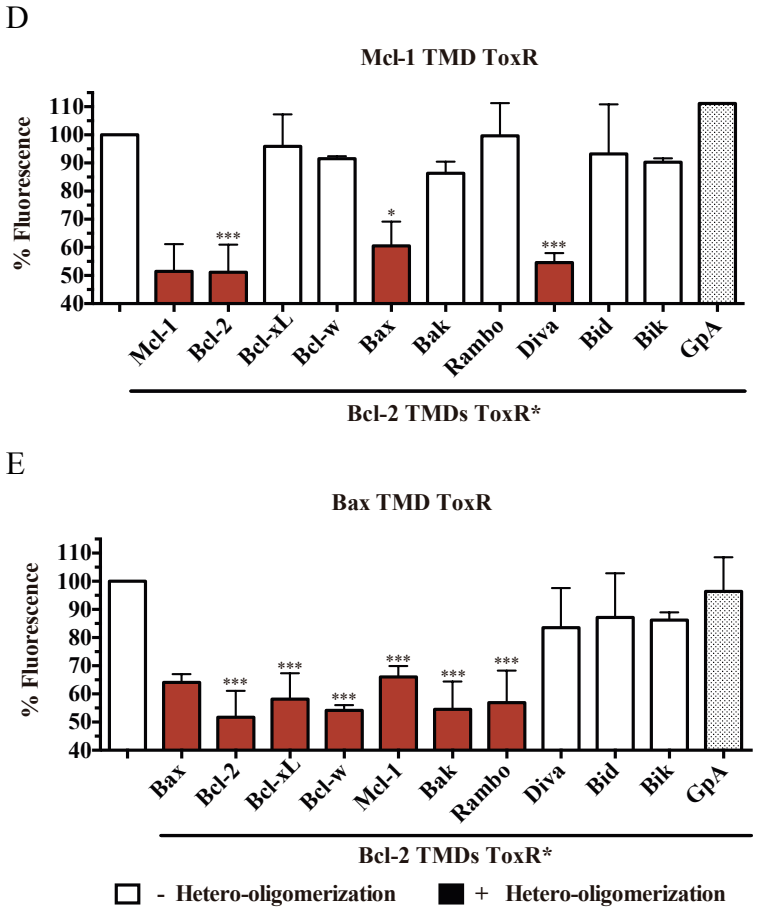

Figure 4.9. **Specific hetero-oligomerization network among TMDs from BCL-2 family proteins.** Normalized fluorescence signal obtained with the ToxR system for the combination of ToxR construct of BCL-2 TMD with ToxR* constructs from the indicated BCL-2 proteins. Red bars represent positive hetero-oligomerizations (the decrease in fluorescence indicates the formation of hetero-oligomers as described in Figure 8. ToxR*. White bars represent negative hetero-oligomerizations. The ToxR control of BCL-2 TMD (first column) represents the maximum of fluorescence (100% homo-oligomerization). GpA was used as an outgroup and represents a negative hetero-oligomerization. The same experiments are shown for the ToxR-TMD constructs of Bcl-2 (A), Bcl-xl (B), Bcl-w (C), Mcl-1(D) and Bax (E) cotransfected with ToxR* -TMD constructs from the different BCL-2 proteins.

Regarding the pro-apoptotic members, it should be noticed the differences found for Bak and Bax, while Bak TMD only interacts with Bcl-w and to a lesser extent with Bcl-xL, Bax TMD interacts with all TMDs from the anti-apoptotic members tested with the

exception of Mcl-1 TMD (Figure 4.9E).

Interestingly, we observed the formation of hetero-oligomers between the two pro-apoptotic Bax- and Bak proteins (Figure 4.9E). These two proteins have been found to be the main players in the formation of the mitochondrial pore (84, 127, 138). The relevance of their cytosolic domains for membrane permeabilization has been extensively studied but the contribution of their TMDs remains poorly understood. Our current data demonstrating the existence of hetero-oligomers between these important components could shed light onto the process of pore formation and regulation. The results obtained in the hetero-dimerization experiments with all the BCL-2 TMDs led us to define the first global network of TMD interactions among the members of the BCL-2 family (Figure 4.10).

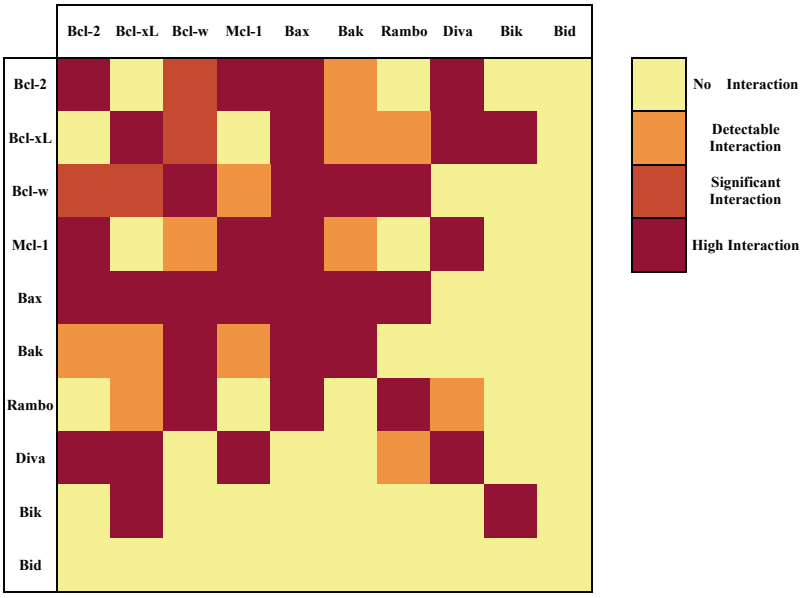

Figure 4.10. The interactome of BCL-2 TMDs. Integration of all the experimental data of homo- and hetero-oligomerization from the ToxRed system led to the classification of four levels of interaction based on the fluorescence signal, generating the interaction network map of the BCL-2 TMDs.

4.2.4. BCL-2-TMDs interactions in full-length proteins context.

Different protein domains jointly and collectively define the overall activity of a protein (360). In this sense, the studies performed with isolated TMDs from BCL-2 proteins during a stage in Dr. Frank Edlich lab in the Institute of Biochemistry and Molecular Biology of Freiburg (Germany) had permitted us to separate the putative role of their

membrane anchors from the contribution of cytosolic domains to their network of MOM interactions. Once we demonstrated the existence of heterotypic interactions between isolated anti- and pro-apoptotic TMDs from BCL-2 proteins, we went one step further to understand their contribution to global protein function and analyzed hetero-dimerization of TMDs with full-length proteins in mitochondria.

To perform these experiments self-interaction of VN/VC-BCL-2 TMDs, that reconstitutes the Venus fluorescent protein, was challenged with anti- and pro-apoptotic full length proteins (see scheme in Figure 411A). In this system a decrease of fluorescence indicates formation of hetero-oligomers between the Venus fluorescent protein and the appropriate full length protein.

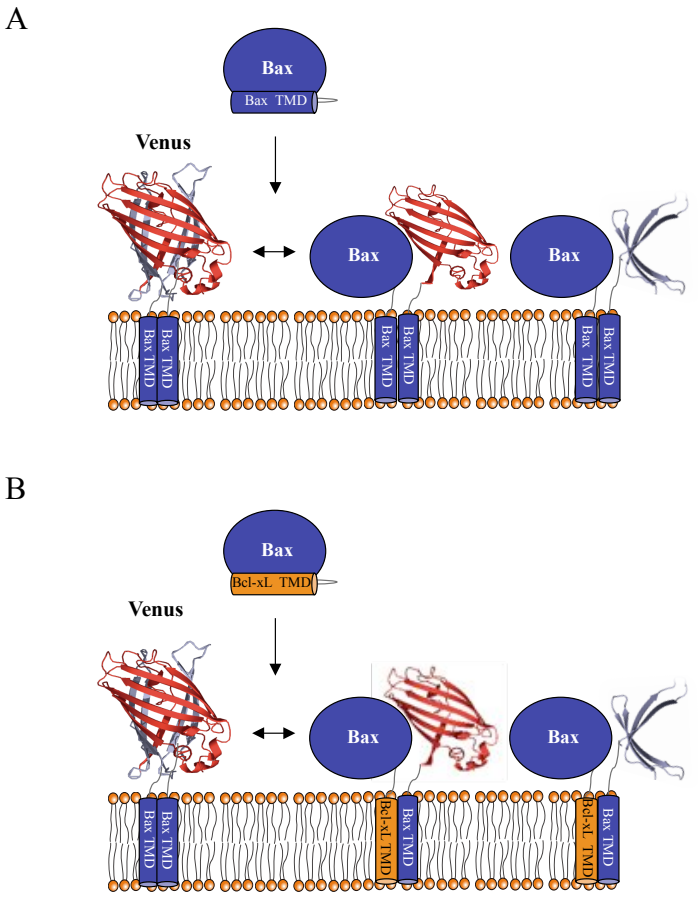

Figure 4.11. Schematic view of the interaction between some BCL-2 Full length (FL) proteins with BiFC-TMD constructs through the transmembrane region specifically. (A) Cells are co-transfected with VN/VC BiFC-TMD constructs and different BCL-2 FL proteins. Interaction between BCL-2 FL proteins and TMD

constructs produces a decrease of the fluorescence (Venus protein is not recovered). (B) In this case, the TMD of Bax FL protein was replaced to the TMD of Bcl-xL to evaluate the role of the cytosolic region in the TMD interactions.

Making use of this approach we observed that self-interaction of VN/VC-Bax TMD was competed with Bax, Bcl-2 and Bcl-xL full length proteins (Figure 4.12A). A full-length Bax protein in which the hydrophobic tail was replaced by the one from Bcl-xL (Bax-Bcl-xL tail) and the complementary Bcl-xL-Bax tail mutant also competed with Bax TMD self-interaction (Figure 4.11B). In all these experiments mitochondrial localization of VN Bax TMD recombinant protein was corroborated by cellular fractionation (Figure 4.12B, right panel). These results agree with the interaction pattern determined for isolated Bax TMD in the ToxR assay where Bax TMD interacted with TMDs from Bax, Bcl-2 and Bcl-xL (Figure 4.9E).

Interestingly, self-interaction of VN/VC-Bcl-2 TMD was only competed by Bcl-2 and Bax full-length proteins, but no competition with Bcl-xL full-length protein was observed (Figure 4.12B). Moreover, the recombinant Bax-Bcl-xL tail protein showed decreased competence when compared with the full-length Bax, whereas Bcl-xL-Bax tail protein competed similarly with Bax with Bcl-2 TMD self-interaction. These results also validate the TMD interaction pattern observed for isolated Bcl-2 TMDs (Figure 4.9A) in the context of full-length proteins.

Altogether our results demonstrate that interaction patterns observed for isolated Bcl-2, Bax, and Bcl-xL membrane anchor domains are mimicked in the presence of full-length proteins, thereby underpinning the relevance of these membrane-spanning regions in the modulation of MOM interactions among BCL-2 proteins.

A

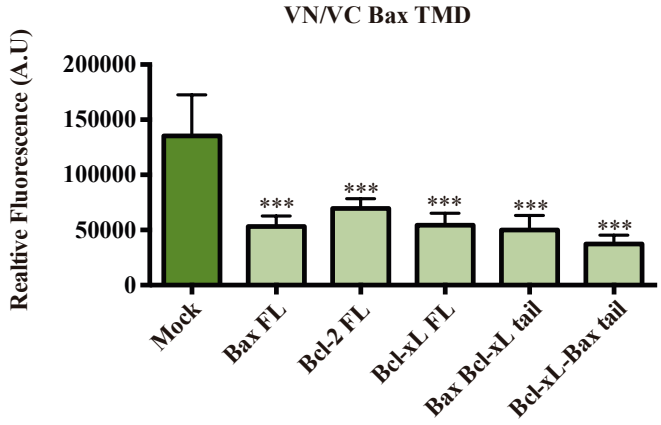

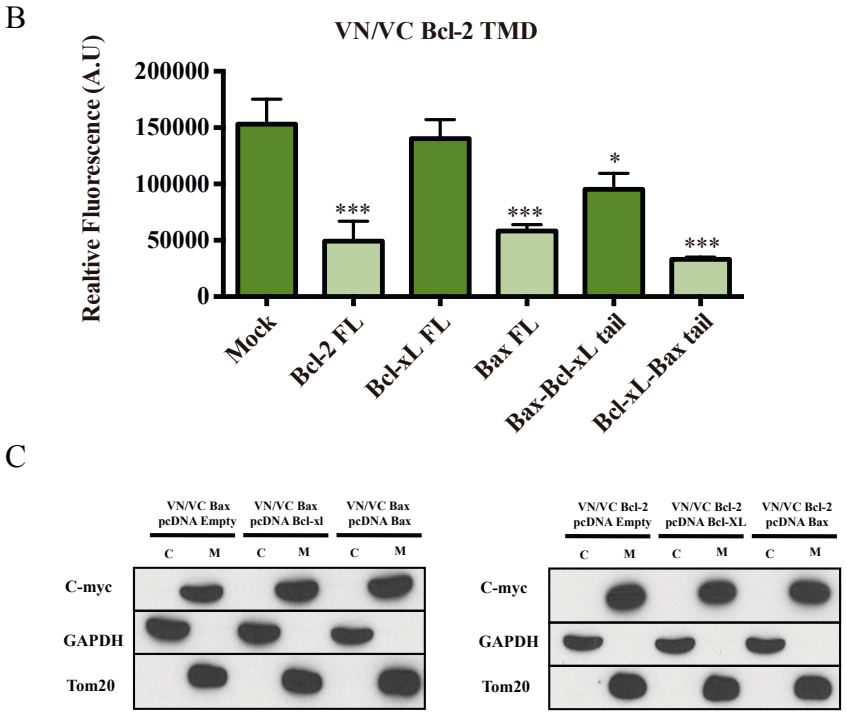

Figure 4.12. Specific interactions between BCL-2 Full-length (FL) proteins and BiFC-TMD constructs. A) HCT 116 wt cell line was co-transfected with VN/VC BiFC Bax TMD constructs and different BCL-2 FL proteins. Interaction between BCL-2 FL proteins and Bax TMD constructs produces a decrease of the fluorescence (Venus protein is not recovered). Bcl-xl FL with the TMD of Bax and Bax FL protein with the TMD of Bcl-xl were also assayed to demonstrate the specificity of the interactions. B) The same design was used for VN/VC BiFC Bcl-2 TMD assays. C) Subcellular fractionation of HCT 116 cells transfected with the BCL-2 TMD protein BiFC constructs. C-myc was used to detect BiFC constructs. GAPDH and Tom 20 was used as cytoplasmic and mitochondrial markers, respectively.

4.2.5. Relevance of BCL-2 TMDs in apoptosis.

According to the function of the BCL-2 proteins in the control of apoptosis, the role of BCL-2 TMDs in this pathway was analyzed. Previous studies have demonstrated that some BCL-2 TM regions are able to destabilize the outer mitochondrial membrane (217, 231) and/or generate pores to produce the release of apoptogenic proteins that induce apoptosis (68, 240). For that reason, the capability of these TMD to induce apoptosis was analyzed in HCT 116 Wt and HCT 116 *DKO Bax/Bax*. The results of caspase-3 activity assay and Western blot indicated that some of the TMDs, specially Bax, Bak and Mcl-1

were able to produce apoptosis (Figure 4.13A). To further explore the mechanism of BCL-2 TMDs cell death induction we analyzed different markers of apoptosis and necrosis. Increase on cytosolic lactate dehydrogenase (LDH) activity in the medium as a consequence of cell lysis is considered a marker of necrotic cell death. LDH assays showed a non-significant release of this enzyme to the extracellular media, confirming that cell death was not due to necrosis (Figure 4.13B). The capacity of some BCL-2 TMD to generate apoptosis was also evaluated by confocal microscopy, using the release of Cyt-*c* as apoptotic marker (Figure 4.13C). Bcl-2, Bcl-xL and Bcl-w did not produce apoptotic activation. On the contrary, cells transfected with Bax, Mcl-1 and Bak TMD showed the cytosolic accumulation of Cyt-*c*, indicating apoptosis.

The exposure of phosphatidylserine (PS) molecules on the outer leaflet of the plasma membrane is usually considered a hallmark of apoptosis (361). Thus, cell staining with FITC-labeled AnnexinV, which binds to PS, is a marker of early apoptotic events (AnnV+). Propidium iodide (PI) is a DNA intercalating agent that can be incorporated into cells only after major cell membrane damages (PI+). Hence, the combination of AnnV and PI cell staining is commonly used to distinguish apoptotic and necrotic cell death. Flow cytometry analyses were performed to evaluate the apoptotic profile of these TMDs (Figure 4.13D). Our results showed the characteristic profile of cells undergoing apoptosis, as both AnnV+ PI- (early apoptotic) and AnnV+ PI+ (late apoptotic) profiles were observed.

A

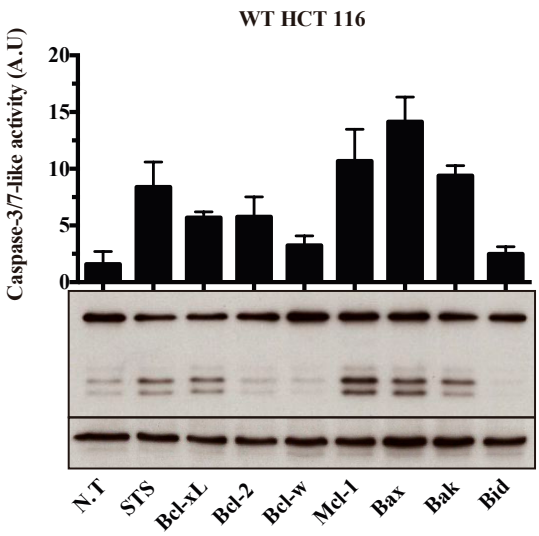

B

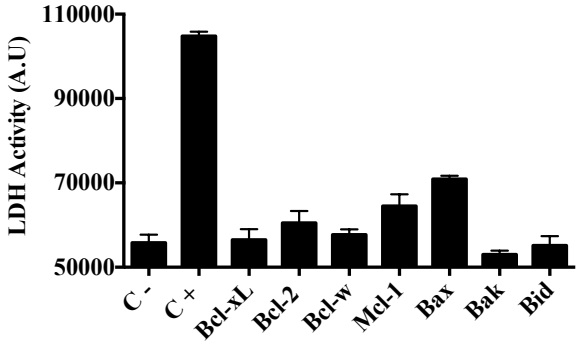
LDH Activity (A.U)
110000
90000
70000
50000
C -
C +
Bcl-xL
Bcl-2
Bcl-w
Mcl-1
Bax
Bak
Bid

C

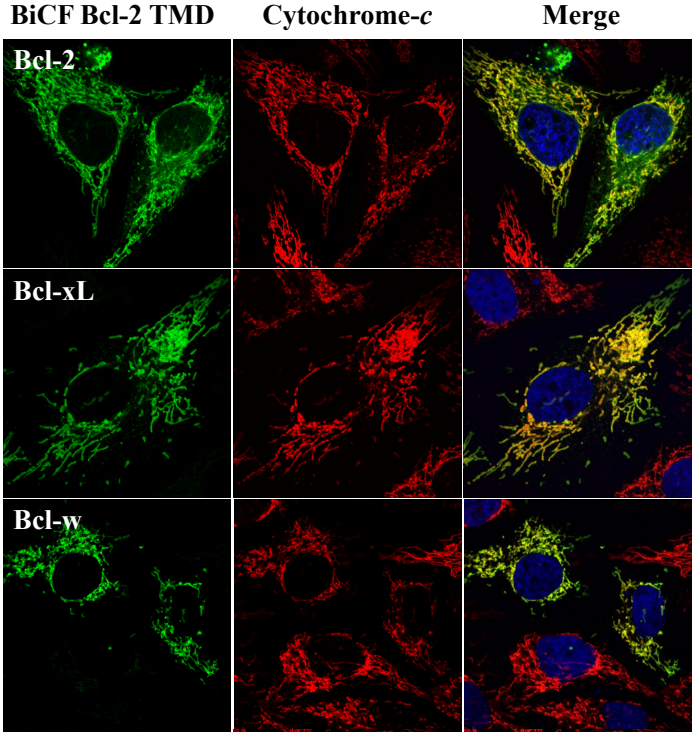
BiCF Bcl-2 TMD
Cytochrome-c
Merge
Bcl-2
Bcl-xL
Bcl-w

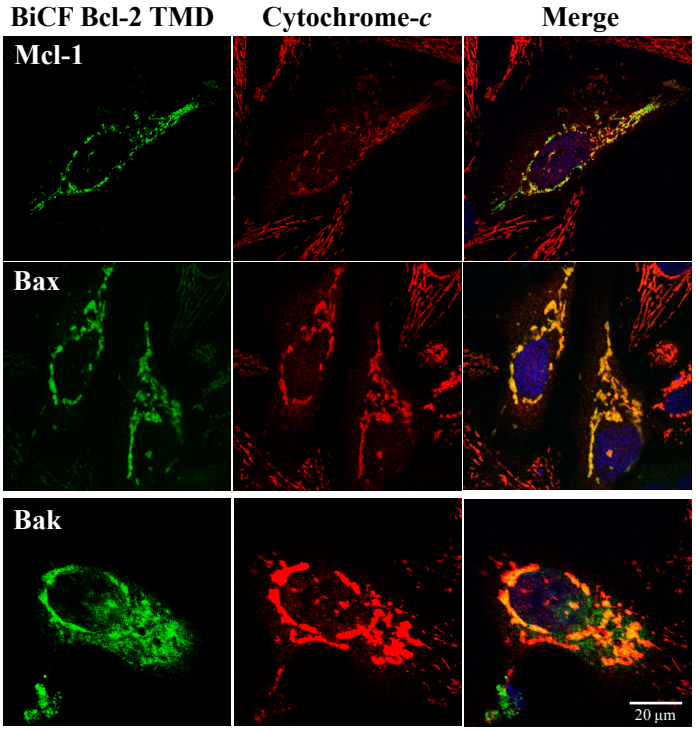
BiCF Bcl-2 TMD
Cytochrome-c
Merge
Mcl-1
Bax
Bak
20 µm

D

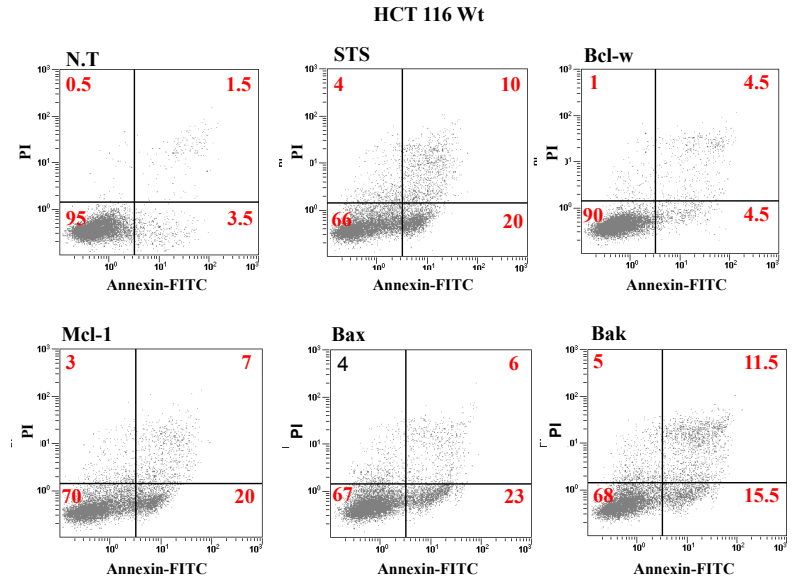
HCT 116 Wt
N.T
0.5
1.5
95
3.5
STS
4
10
66
20
Bcl-w
1
4.5
90
4.5
Mcl-1
3
7
70
20
Bax
4
6
67
23
Bak
5
11.5
68
15.5
PI
Annexin-FITC

Figure 4.13. Apoptotic effect of the BCL-2 TMD in HCT 116 Wt. (A) Caspase 3-like activity measured in the HCT 116 Wt cells. Bars represent the mean of three experiments ± s.d. (*$p < 0.1$; **$p < 0.05$; ***$p < 0.001$. STS 0.5μM was used as apoptotic inductor. Western blot was developed against Caspase-3 antibody and α-tubulin was used as load control. (B) LDH assay measured in HCT 116 Wt. Negative control represents cells transfected with empty plasmid and Triton 9% was used as posivive control. (C) Confocal images of HCT 116 Wt cells transfected with the different BiFC BCL-2 TMD constructs. Green fluorescence indicates TMD homo-oligomerization. Release of Cyt-*c* (red channel) from Mitochondria to cytosol was used as apoptotic marker. Mitochondrial co-localizations were shown in yellow. (D) Cell death profile was analyzed by flow cytometry with with FITC Annexin V and PI. Third quadrant represents the apoptotic population.

Interestingly, the capability of these BCL-2 TMDs to induce apoptosis is independent of the presence of Bax and Bak in the cell (Figure 4.14A, B and C).

A

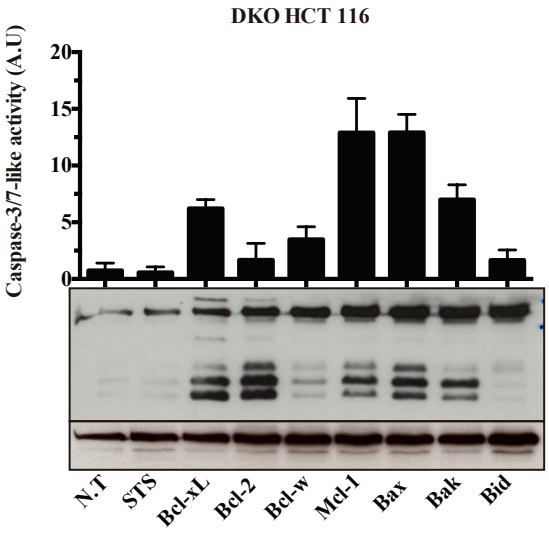

B

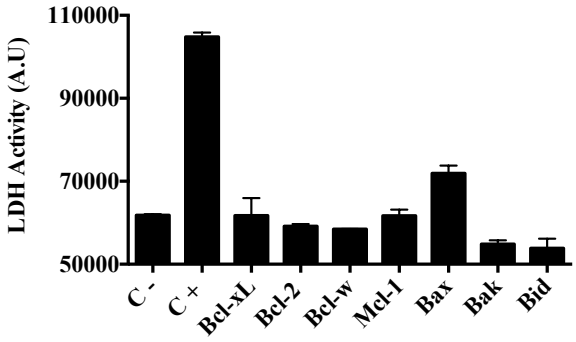

C

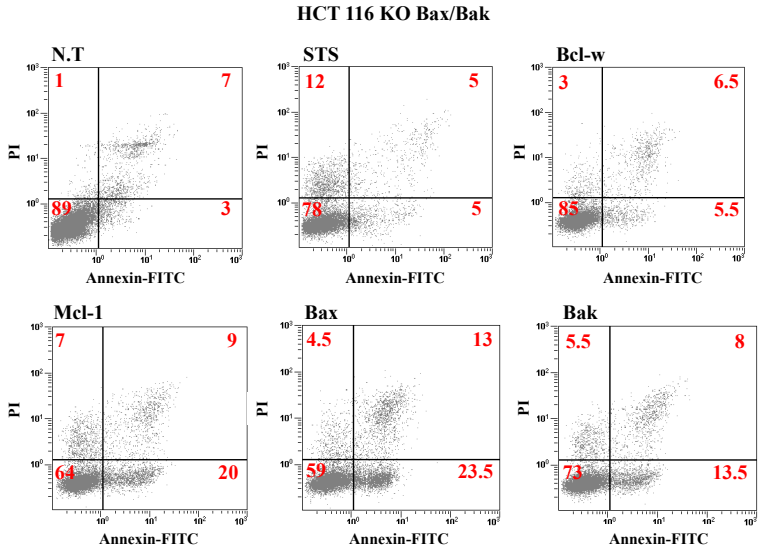

Figure 4.14. Apoptotic effect of the BCL-2 TMD in HCT 116 DKO Bax/Bak. (A) Caspase-3-like activity measured in the HCT 116 DKO cells. Bars represent the mean of three experiments ± s.d. (*$p < 0.1$; **$p < 0.05$; ***$p < 0.001$. STS 0.5μM was used as apoptotic inductor. Western blot was developed against Caspase-3 antibody and α-tubulin was used as load control. (B) LDH assay measured in HCT 116 Wt. Negative control represents cells transfected with empty plasmid and Triton 9% was used as positive control. (C) Cell death profile was analyzed by flow cytometry with with FITC Annexin V and PI. Third quadrant represents the apoptotic population.

In Bax/Bak KO HCT 116 the apoptotic profile was exactly the same as that observed for wild type cells. This result opens up two possible hypotheses:

- BCL-2 TMDs promote destabilization of the outer mitochondrial membrane inducing pores similar to that formed by Bax/Bak, and overcoming the absence of these proteins.
- Interactions established by BCL-2 TMDs within the mitochondrial membranes modify the balance between anti- and pro-apoptotic BCL-2 proteins, generating an alternative pore complex induced by other membrane complexes previously described as responsible of MOMP (362, 363).

In both cases if Bax TMD oligomerization is necessary for the formation of these mitochondrial pores, introduction of a destabilizing point mutation in the TMD sequence should therefore result in a decrease of apoptosis induction capability.

To test this hypothesis some of the Bax TMD point mutations identified as oligomer disruptors were introduced in the full-length Bax protein and in the VN/Bax TMD construct. HCT 116 cell were transfected with these mutants and caspase-3 activity at 24

hours after transfection was measured. A significant reduction of this enzymatic activity was observed for the different mutants (when compared with their wt versions Figure 4.15 A-C).

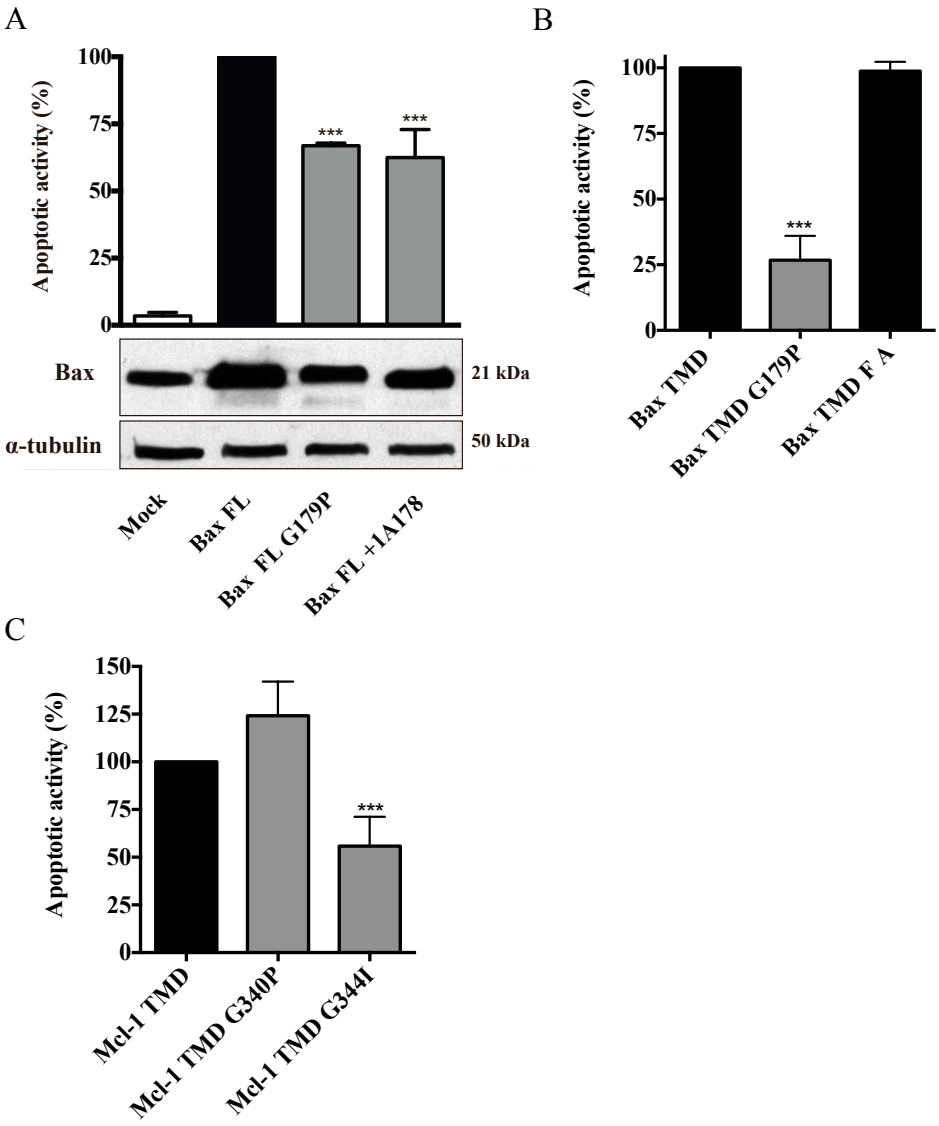

Figure 4.15. Selected point mutants of the BCL-2 TMD attenuate the apoptotic effect of the Bax FL and selected Wt TMD in HCT 116 Wt. The maximum percentage of apoptotic induction (100%) represents the caspase-3 activity referred to the wt Bax FL (A), VN/wt Bax TMD (B) and VN/wt Mcl-1. Bars represent the mean of three experiments ± s.d. (*$p < 0.1$; **$p < 0.05$; ***$p < 0.001$).

Interestingly, when these TMD mutations where introduced in the Bax FL protein, the pro-apoptotic activity was attenuated. Thus, a 30% decrease relative to the wild type Bax FL pro-apoptotic activity was achieved. Reduction on the apoptosis induction capability of Bax TMD was indeed higher (75%, Figure 4.15B). Furthermore, mutantions at the Mcl-1 TMD also decreased the apoptotic induction promoted by wild type Mcl-1 TMD (Figure 4.15C). These results demonstrate that BCL-2 TMDs, together with soluble domains, participate in the equilibria that govern MOMP.

Despite the putative existence of alternative apoptosis pathways we were interested in determining the relevance of BCL-2 TMDs in classical pathways of apoptosis induction. To accomplish this objective two different assays were performed: On one hand, the effect of some anti-apoptotic proteins (Bcl-2 and Bcl-xL) overexpressed in combination with the TMD of Mcl-1, Bax and Bak was evaluated. On the other hand, the effect of blocking anti-apoptotic proteins Bcl-2, Bcl-xL and Bcl-w (309, 364) with the BH3 mimetic ABT-263, was also analyzed. Overexpression of anti-apoptotic Bcl-xL or Bcl-2 full-length proteins reduced the apoptosis induction promoted by VN/Bax TMD (Figure 4.16A). Likely, anti-apoptotic proteins impede the formation of Bax homo-oligomers by competing through TMD hetero-oligomeric complexes that could account for the observed reduction of Bax TMD induced pro-apoptotic activity. Conversely, VN/Bak TMD apoptosis induction was not affected by the presence of these anti-apoptotic members (Figure 4.16A). Interestigly, Bcl-xL but not Bcl-2 FL protein specifically abolishes the pro-apoptotic effect induced by VN/Mcl-1 TMD, (Figure 4.16B). These findings highlight the exquisitely specific network of TMD interactions found in the apoptotic events.

A

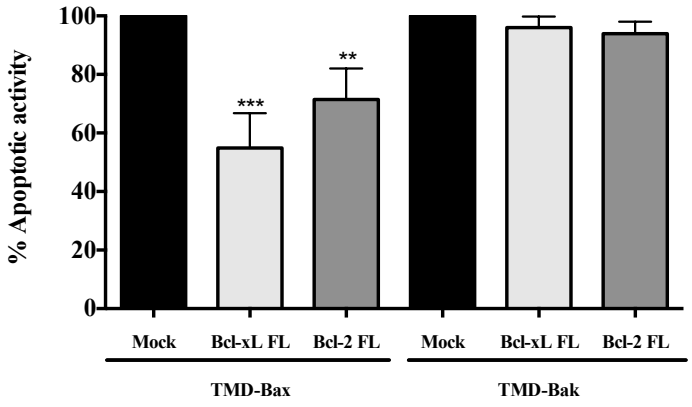

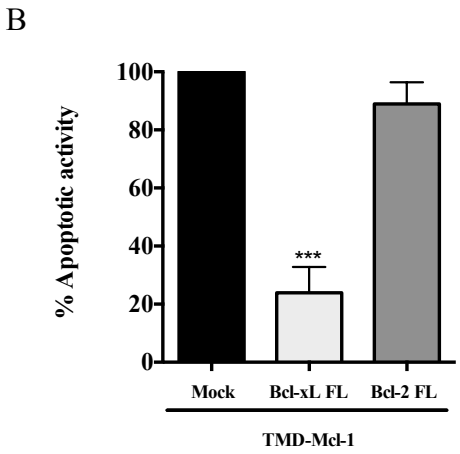

Figure 4.16. Effect of the anti-apoptotic proteins overexpression in the apoptotic activation promoted by the BCL-2 TMDs in HCT 116 Wt. The maximum percentage of apoptotic induction (100%) represents the caspase-3 activity referred to the BiFC VN Bax TMD (A), VN Bak TMD (A) and VN Mcl-1 TMD (B). Bars represent the mean of three experiments ± s.d. (*$p < 0.1$; **$p < 0.05$; ***$p < 0.001$).

Apoptosis induction based on sequestration of anti-apoptotic proteins by ABT-263 showed that combination of VN Bax TMD and ABT-263 resulted in additive apoptotic activation. In contrast, Mcl-1 and Bak TMD transfection combined with ABT-263 treatment produced a clear synergic behavior on apoptosis induction. Different behavior of Bax, Mcl-1 and Bak TMDs probably reflect different networks of protein-protein interactions established by their transmembrane anchors within the mitochondrial membrane. Furthermore, Bid TMD does not generate apoptosis by itself and does not modify the apoptotic activation promoted by ABT-263 (Figure 4.17).

Altogether these results underscore the necessity to conduct further studies regarding the interaction network that regulates MOMP to properly understand and predict cellular outcome upon anti or pro-apoptotic stimuli.

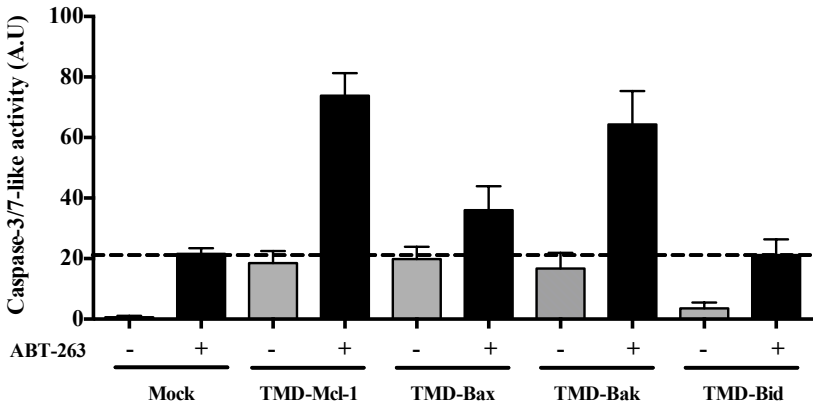

Figure 4.17. Combined treatment of the BH3 mimetic ABT-263 and the BCL-2 TMDs in HCT 116 Wt. Caspase-3 activity ((A.U) Arbitrary units) of BiFC VN BCL-2 TMDs alone and in combination with BH3 mimetic ABT-263. Bars represent the mean of three independent experiments ± s.d. (*$p < 0.1$; **$p < 0.05$; ***$p < 0.001$).

4.3. Concluding remarks.

Members of the BCL-2 family constitute the main players in the control of mitochondrial outcome, developing a crucial role in the decision of the cellular fate (57, 191). In fact several diseases, including cancer, result from an inadequate equilibrium of BCL-2 expression (365). Therefore, to gain in-depth knowledge about their interactions is the first step in the development of new pharmacological strategies (323). There is considerable evidence for implication of cytosolic domains from BCL-2 proteins in MOMP control (123, 258). However, it has been unclear whether BCL-2 TMDs play also a role in the permeabilization process, either by participation in the different models of pore complexes or by regulation of interactions between anti- and pro-apoptotic members of the BCL-2 family (366).

To answer some of these questions, this study has addressed the structural organization of BCL-2 TMDs. Making use of bacterial and eukaryotic systems it was demonstrated that most BCL-2 TMDs are non-isolated in membranes. On the contrary, they are able to interact themselves and with other members of the BCL-2 family in a highly specifical manner, generating a network of putative interactions that take place in the mitochondrial membrane and presumably participate in MOMP. We have defined for the first time a large network of BCL-2 TMD interactions. Recent works also suggest the capability of particular BCL-2 TMDs to oligomerize in the membrane, corroborating

some of the self-interactions obtained for Bax (367) and Bcl-xL (220) TMDs, as well as the existence of Bax/Bcl-2 hetero-oligomers in mitochondria (368). Some of the interactions observed in this work, as the Bax-Bak TMD hetero-oligomerization, could be crucial in the process of the pore complex formation. In addition, it is also relevant the different pattern of interactions observed for the anti-apoptotic Mcl-1 TMD when compared to other TMDs derived from anti-apoptotic proteins (i.e. Bcl-2 and Bcl-xL). Despite all three proteins exert a pro-survival function in apoptosis, several studies have demonstrated significant differences in their apoptotic behavior in different cellular systems (55, 56, 369). The present interacting network established for these BCL-2 proteins in the MOM could provide clues about the role of the TMDs in the apoptotic regulation mechanisms.

Furthermore, the work included in this chapter demonstrates the insertion of Bid TMD into different biological membranes (ToxRed and BiFC data), although the interaction map obtained shows that Bid TMD does not establish any direct interactions to any BCL-2 derived TMD. Of note, some authors have postulated a role for cardiolipin for the location of Bid at the lipidic contact sites (CS) present in mitochondria (116, 370), and probably Bid TMD actively participates in this anchoring function.

Besides elucidate the BCL-2 TMD interaction network, the putative role of several TMDs in apoptosis has been also investigated. Mcl-1, Bax and Bak TMD were able to promote apoptosis by different mechanism (68, 138). Introduction of point mutations in the TMD of Bax FL produces a decrease in the apoptosis induction capability of this protein, indicating the relevance of this domain in the regulation of apoptosis. It has also been demonstrated the capability of some BCL-2 TMDs to induce apoptosis in a genetic background, where the apoptosis effectors Bax and Bak were absent, probably by the activation of alternative MOM pores. However, the behavior of BCL-2 TMDs in a wild type context, where the capability of full length anti-apoptotic BCL-2 proteins to interfere with the TMD apoptosis induction has been demonstrated, supports the existence of intricated regulatory crossroads in the mitochondrial membrane.

Altogether the results suggested a new role in apoptosis for BCL-2 TMDs beyond serving as passive anchors. Our results are in good agreement with recent reports where, for instance, it has been demonstrated that Bax ΔTM induces membrane destabilization but the FL makes it with greater potency (371), or where it has been defined that the C-terminal of Bax could be involved in forming channels (235, 236, 240). It has also been described that Bax C-terminal mutants impaired the anti-apoptotic effect of Bcl-xL over Bax insertion (231, 232), or that the C-terminal deleted mutants of Bcl-w lose their anti-apoptotic function (63).

These results outline a mitochondrial membrane landscape where different BCL-2

members interact with each other through their TMDs and the equilibrium of BCL-2 TMD interactions contributes to the final full length BCL-2 interaction network, thereby defining the cellular fate, death or survival. In this scenario, in the same way that BH3 mimetics are being employed for cancer treatment (323), modulation of specific BCL-2–TMD-interactions emerges as a new molecular target in cancer treatment.

CHAPTER

II

5.1 Introduction.

Apoptosis is regulated by the BCL-2 family of proteins. Members of this family can be divided in three groups, depending on their function and on the presence of different BCL-2 homology domains, known as BH1-BH4. A type of pro-apoptotic BCL-2 family proteins contains only the BH3 region and hence is referred to as BH3-only proteins. Interaction of BH3-only proteins with other BCL-2 family members is critical for understanding the core machinery that controls commitment to apoptosis by mitochondrial outer membrane permeabilization. BH3-only proteins promote apoptosis by both directly activating Bax and Bak and by suppressing the anti-apoptotic proteins in the cytosol. To prevent constitutive cell death, BH3-only proteins are regulated by a variety of mechanisms including transcription and post-translational modifications that govern specific protein–protein interactions.

Some BH3-only proteins (like Bid, Bim and Puma) are termed activators, as they directly induce Bax/Bak-dependent mitochondrial outer membrane (MOM) permeabilization (372). Other BH3-only proteins (like Bad, Noxa, Bik and Bmf) are termed as sensitizers, as they promote apoptosis by binding to anti-apoptotic proteins to induce release of either activator BH3-only proteins (113) or activated Bax or Bak (373). Several BCL-2 family members also contain a carboxyl-terminal (C-terminal) hydrophobic domain to insert and anchor the BCL-2 proteins into different intracellular membranes (356), such as the nucleus, endoplasmic reticulum (ER), and the MOM, where they can promote release of apoptotic factors (374). Since interactions with the membrane play an active role in the regulation of apoptosis by changing the affinities of the interactions between partner proteins (375), it would be highly valuable to investigate if BH3-only proteins may exist as integral membrane proteins via C-terminal tail-anchor sequences. In particular, some reports have examined the anchoring capacity of BH3-only proteins to the MOM, although the existence of a transmembrane (TM) region is still unclear (207).

In this chapter we will study the ability of the TMDs from BH3-only proteins to insert in different biological membranes.

5.2 Results and discussion.

5.2.1. Putative BH3-only TMDs insertion in biological membranes *in vitro*.

To define the hydrophobic C-terminal region of human BH3-only proteins Bim, Puma, Noxa, Bik and Bmf, their amino acid sequences were parsed by the ΔG Prediction Server (http://dgpred.cbr.su.se/). Given the amino acid sequences, this algorithm provides a prediction of the corresponding apparent free energy difference, ΔGapp, for insertion of this sequence into the ER membrane by means of the Sec61 translocon (376). Table 5.I. shows the predicted ΔGapp values for the BH3-only proteins analyzed. The negative ΔGapp value for Bik C-terminal region predicts a TM disposition, whereas the positive values computed for Bim, Noxa, Bmf and Puma predicted that these sequences do not integrate into membranes.

Table 5.I.Analyzed proteins using ΔG Prediction Server v1.0 (http://dgpred.cbr.su.se/).

TM	Sequence	*Pi*	Kapp	ΔGexp	pred ΔGapp
H2	WLETGASVFPVLAIVRSFIYEP	85.9	6.2	-1.1	2.2
Bik	LLALLLLLALLLPLLSGGLHLLL	77.8	3.6	-0.8	-2.9
Bim	PRMVILRLLRYIVRLVWRM	23.2	0.3	0.7	2.5
Noxa	LLNLISKLFCSGT	1.4	0.0	2.6	5.5
Bmf	NRVWWQILLFLHNLALNG	60.4	1.5	-0.3	2.1
Puma	WRVLYNLIMGLLPLPRGHR	35.4	0.6	0.4	2.6

Subsequences with lowest ΔG marked in red. ΔG values are expressed in kcal/mol, both for the experimental (third column) and the predicted data (376, 377) (forth column). Negative and positive ΔG values are shown in green and red, respectively and denote spontaneous insertion or non-insertion, respectively. The probability of insertion (P_i) has been calculated from the experimental data as showed in Figure 5.1 and probabilities above and below 50% are shown in green and red, respectively for consistency.ΔG_{exp} (experimental); ΔG_{app} (predicted).

Membrane insertion capability of these C-terminal regions was investigated using an experimental system based on the Escherichia coli inner membrane protein leader peptidase (Lep), which accurately reports the integration of TM helices into biological membranes. Since BCL-2 family proteins are predominantly exposed to the cytosol and anchored to intracellular membranes by a C-terminal sequence, in our experimental setup we tested the candidate sequences according to its predicted topology (122). The Lep construct used consists of two TM segments (H1 and H2) connected by a cytoplasmic loop (P1) and a large C-terminal domain (P2), and inserts into ER-derived microsomal membranes with both termini located in the lumen harboring engineered acceptor sites each (G1 and G2) for N-linked glycosylation (Figure 5.1A). The BH3-only C-terminal sequence analyzed (BH3-Ct) replaced the Lep H2 domain. The glycosylation site (G2) located in the beginning of the P2 domain will be modified only if this C-terminus domain is translocated across the membrane, while G1 site, embedded in an extended N-

terminus sequence is always glycosylated. Single glycosylation (i.e., non-integration of the tested sequence) results in an increase of molecular mass of ~2.5 kDa relative to the observed molecular mass of Lep expressed in the absence of microsomes; the molecular mass shifted ~5 kDa upon double glycosylation (i.e., membrane insertion of the tested sequence). Proteinase K (PK) added to microsomal vesicles will digest the cytoplasmic exposed, non-glycosylated form of the P2 domain (Fig. 5.1A, right), or will produce a protected, glycosylated BH3 Ct/P2 fragment when the P2 domain is located in the lumen of the microsomal vesicles (Fig. 5.1A, left).

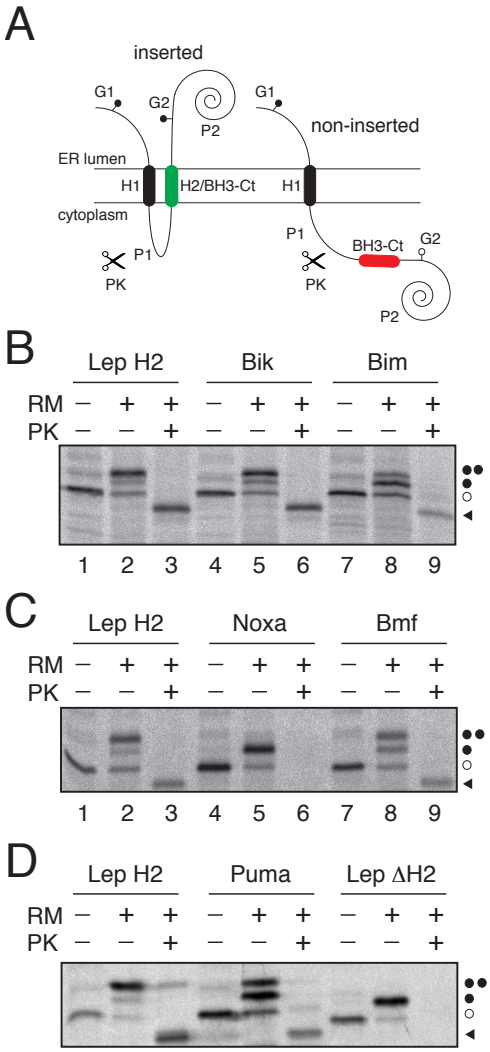

Figure 5.1. BH3 C-terminal insertion into microsomal membranes. (A) Schematic of the engineered leader peptidase (Lep) model protein. (B), (C) and (D) In vitro translation in the presence (+) or absence (−) of rough microsomes (RM) and PK. Non-glycosylated protein bands are indicated by an empty dot; single and double glycosylated proteins are indicated by one or two black dots, respectively. The protected glycosylated H2/P2 or BH3-Ct/P2 fragments are indicated by a black triangle.

The translation in the presence of membranes of constructs harboring the Bik C-terminal region (constructed as previously described (339, 378)) clearly resulted in mainly double glycosylated forms (Figure 5.1B, lane 5). PK treatment of this sample rendered a protected glycosylated Bik-Ct/P2 fragment (lane 6), indicating membrane insertion of this C-terminal region. Similar results were obtained when constructs harboring Bmf C-terminal region were assayed (Figure 5.1C lanes 7-9). In this case, as opposite to its prediction (Table 5.I), the C-terminal region of Bmf inserted efficiently into the membrane (above 60% of the molecules were doubly glycosylated, quantifications were performed as described previously (377)). Regarding Bim and Puma C-terminal regions we found that one fourth of the molecules insert into the biological membranes (Figure 5.1B, lanes 7-9 and Figure 5.1D lanes 4-6). Finally, Noxa C-terminal region transcription/translation assays in the presence of microsomal vesicles yielded singly-glycosylated forms sensitive to PK digestion (Figure 5.1C, lanes 4-6), indicative of non-TM disposition.

The dispersion of charged residues, especially in the case of Bim C-terminal sequence would explain the predicted penalty to insert into the core of the bilayer (Table 5.I). Nevertheless, the hydrophobic contribution of the neighboring residues in this sequence may reduce the free energy of membrane integration, as observed previously for some model hydrophobic/cationic sequences (339), thus allowing the low level of insertion observed.

5.2.2. BH3-only TMD insertion in bacterial systems.

The microsomal in vitro system closely mimics the conditions of in vivo membrane protein assembly. Bik, Bmf and, at a certain level, Bim and Puma C-terminal regions are properly recognized by the translocon as TM segments out of its native context (Figure 5.1). However, the presence of Lep fused domains can influence its membrane insertion capacity. Hence, we next sought to investigate whether these BH3-only C-terminal regions could direct integration into biological membranes in the absence of any membrane protein-derived domain. To this end, we used an assay for the insertion and topology in E. coli that exploits the function of maltose binding protein (MBP) in the maltose transport pathway. *E. coli MM39* cells, which lack endogenous MBP, cannot

transport maltose into the cytoplasm for metabolism, and consequently cannot grow on media in which the only available carbon source is maltose (332). If the chimeric ToxR(BH3-Ct)MBP are correctly inserted in the inner membrane (Figure 5.2A), the periplasmic MBP domain will complement MM39 malE-deficient phenotype and support growth on maltose (379). To demonstrate the requirement for periplasmic localization of MBP in the complementation assay, constructs harboring Bax C-terminal (α9) TM segment (380) or lacking a TM segment (ΔTM) were used as a positive and negative controls, respectively. Those controls and constructs harboring BH3-only C-terminal regions were transformed into MM39 cells and cultured on M9-maltose (a media that uses maltose as an only carbon source). As shown in Figure 5.2B, cells expressing Bax, Bik and Bmf C-terminal regions grow on M9-maltose.

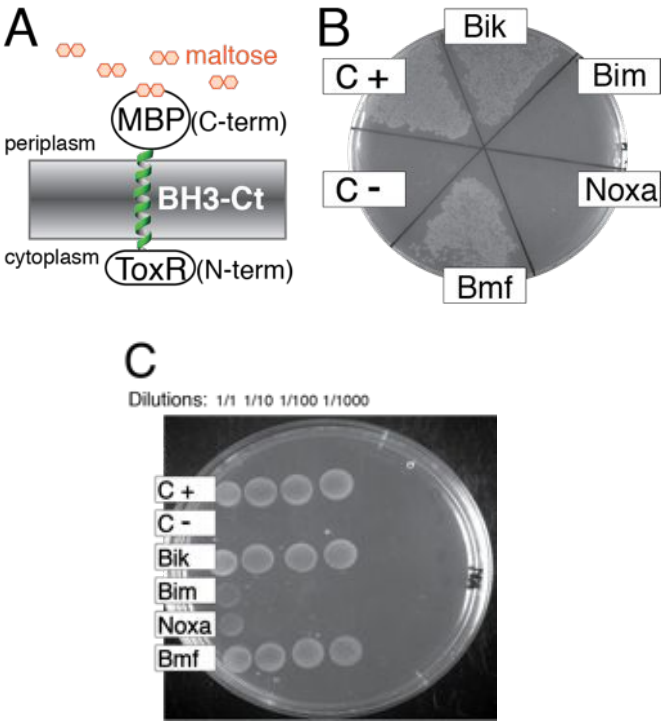

Figure 5.2. The maltose complementation assay for TM insertion and topology. (A) Schematic of the engineered cytoplasmic ToxR and periplasmic MBP domains fused to BH3 C-terminal regions at the N- and C-termini, respectively. (B) malE-deficient E. coli MM39 cells transformed with various expression constructs were cultured on M9 agar. **(C)** Serial dilutions (10-fold) from exponentially growing cultures of the *malE*-deficient strain (NT326) transformed with plasmids bearing the corresponding chimera were spotted on to M9 agar (minimal media) containing 0.4% maltose. C +, ToxR(Bax α9)MBP. C −, ToxR(ΔTM)MBP.

Cells that lack a TM segment or contain Bim or Noxa C-terminal region fail to grow (expression of all contructs was verified by growing the cells in complete media with the appropriate antibiotic selection, Figure 5.3). These experiments demonstrate that both Bik and Bmf C-terminal-containing chimerae anchor their MBP domains to the E. coli inner membrane with its proper orientation, consistent with the insertion data obtained with the microsomal system.

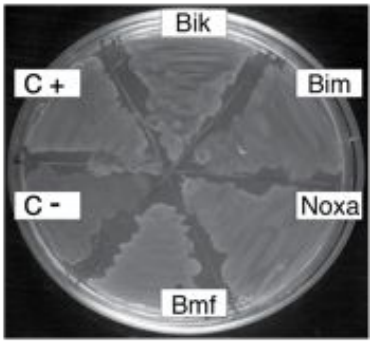

Figure 5.3. All the chimeric constructs are able to grow in LB *Amp* media.. *malE*-deficient *E. coli* MM39 (DE3) cells (*araD lacΔU1269, malEΔ444, str*^{R}; kindly supplied by W.F. DeGrado, University of Pennsylvania) transformed with various expression constructs (ampicillin resistance plasmids) were cultured on complete agar media (LB) in the presence of ampicillin as a selection marker. C +, ToxR(Bax α9)MBP. C −, ToxR(ΔTM)MBP. Bik, ToxR(Bik-Ct)MBP. Bim, ToxR(Bim-Ct)MBP. Noxa, ToxR(Noxa-Ct)MBP. Bmf, ToxR(Bmf-Ct)MBP.

5.2.3. Subcellular localization and apoptotic activity of BH3-only TMDs in human cells.

Emerging evidences indicate that the interaction of BH3-only proteins with membranes regulates binding of other Bcl-2 family members, thereby specifying function. Targeting and subcellular localization of the human BH3-only C-terminal regions were evaluated using GFP-BH3-only-Ct fusion proteins. Mitotracker dye and Grp78 protein were used to analyze the capability of the BH3-only-Ct to target GFP moiety to different cellular organelles in eukaryotic cells (Figure 5.4A and B).

GFP/Bcl-2-Ct was used as control of mitochondrial targeting (Figure 5.4A). However, some authors (195) postulated that a fraction of Bcl-2 is also localized in the ER membrane, as we found in Figure 5.4B. Bik-Ct is not present in mitochondria and

localizes exclusively in the ER membrane, which nicely correlates with the ER distribution described for the full-length Bik protein (381). Similar results were obtained in the case of Bim-Ct, therefore indicating that this C-terminal region is not enough to target MOM, at least in absence of apoptotic stimuli. Surprisingly, Bmf-Ct displayed a clear cytosolic pattern and neither mitochondrial nor ER localization was observed. This BH3-only protein probably needs association (or activation to expose its C-terminal hydrophobic upon apoptotic stimuli) with other proteins to move from the citosol to MOM. Noxa-Ct fusions showed a reticular distribution that did not co-localize neither with ER nor MOM. Some works (207, 255) have localized Noxa protein in mitochondria, usually associated throught its BH3 domain with other BCL-2 family members. Consistently, the C-terminal hydrophobic region of Noxa is not enough to target the GFP fusions to the mitochondrial membranes. Finally, Puma-Ct fusions showed partial insertion in MOM and ER, confirming the ability of this hydrophobic region to span ER membranes (Figure 5.1). These studies highlighted the different functions of the C-terminal hydrophobic regions of the BH3-only proteins, strongly suggesting that these domains could have an important role in defining each BH3-only protein as sensitizers or de-repressors.

A

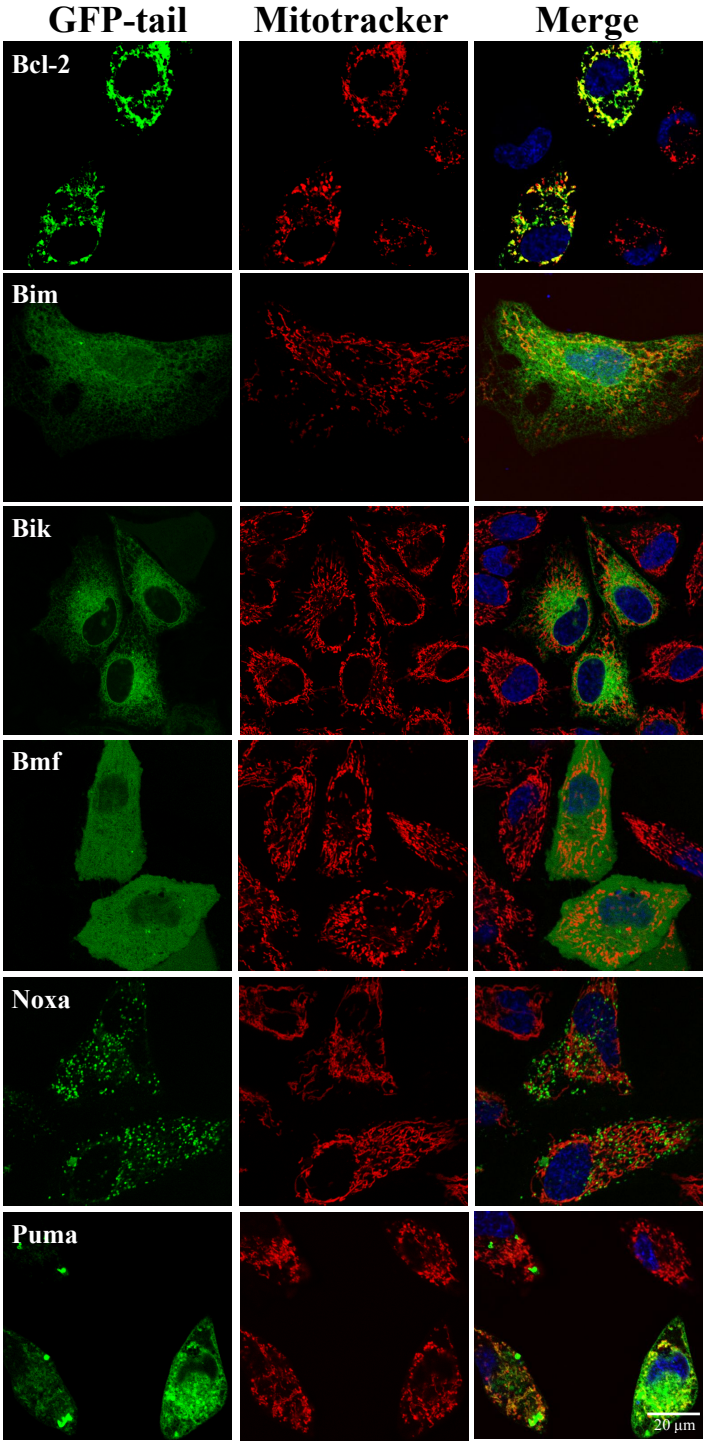

B

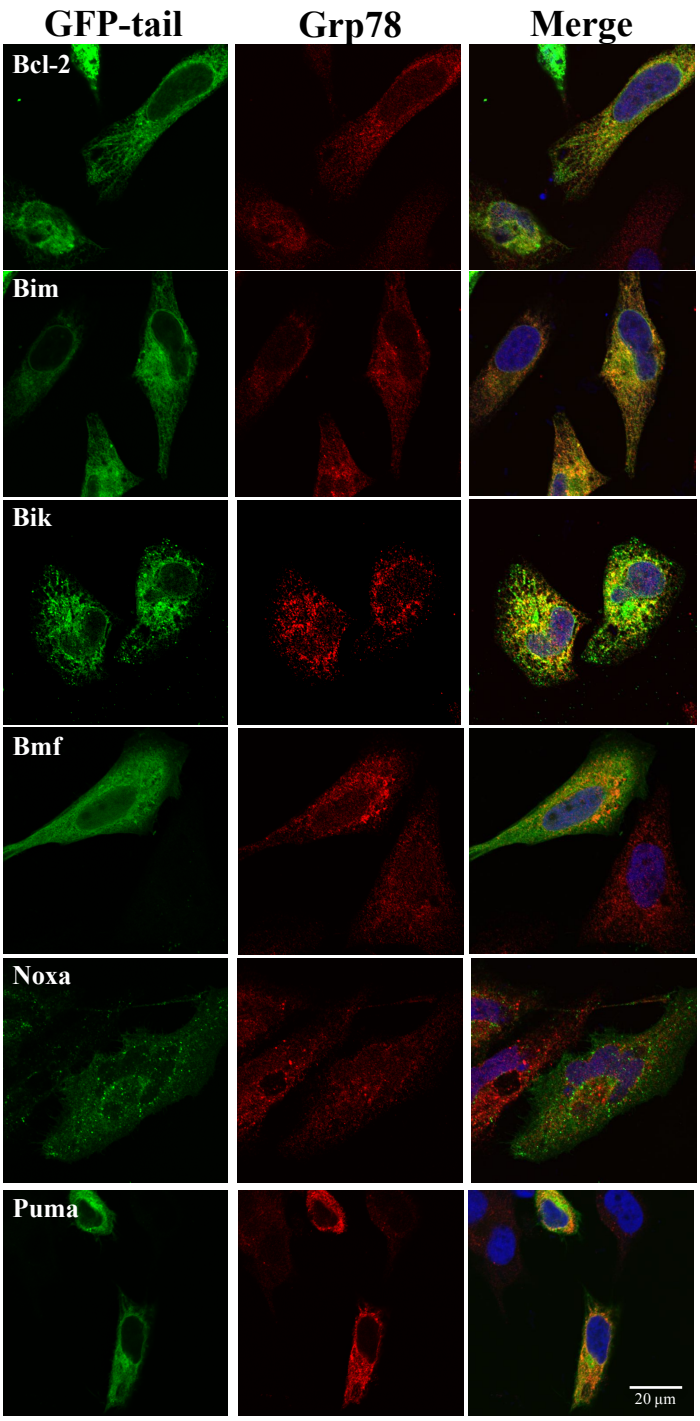

Figure 5.4. GFP/BH3-Ct targeting and insertion to different cellular organelles. Confocal images of HeLa cells transfected with the different GFP/BH3-Ct constructs (green channel). Cells were incubated with Mitotracker (A) and Grp78 (B) as mitochondrial and ER markers, respectively (red channel). Co-localizations were shown in yellow.

Function of BH3-only proteins as promoters of apoptosis has been largery analized (382). However, the role of the C-terminal hydrophobic regions of these proteins in the process is still controversial. Previous studies have demonstrated that some BCL-2 TM regions in the absence of the rest of the repective proteins are able to destabilize the outer mitochondrial membrane (217, 231) and/or generate pores to produce the release of apoptogenic proteins in order to induce apoptosis (68, 240). According to this, we analized the capability of BH3-only C-terminal regions to induce apoptosis. Overexpression of the GFP/BH3-Ct fusions in HeLa cells did not produce apoptosis (Figure 5.5A). These observations were confirmed by immunolocalization assays. The absence of Cyt-*c* release was observed in all BH3-only C-terminal regions analized in the present study by confocal microscopy (Figure 5.5B).

These results indicate that despite the hydrophobic C-terminus of these proteins are not directly related with the pro-apoptotic activity of the BH3-only proteins, they could play a relevant role in protein targeting and membrane sorting.

A

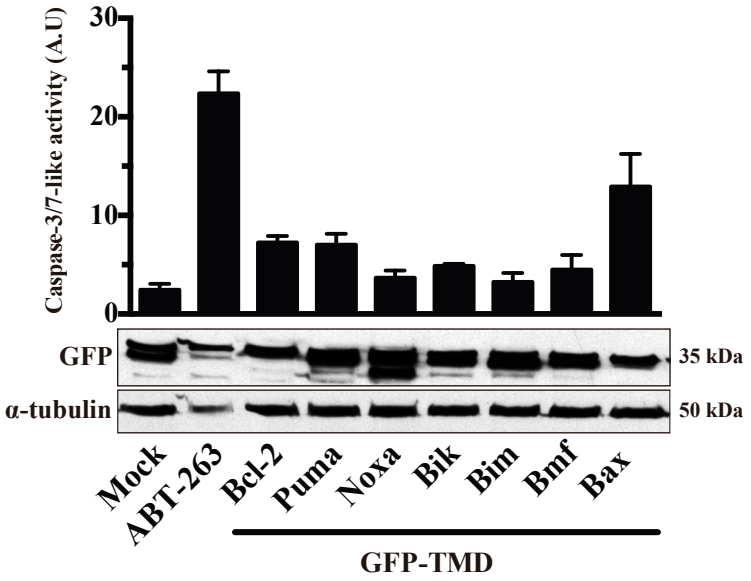

B

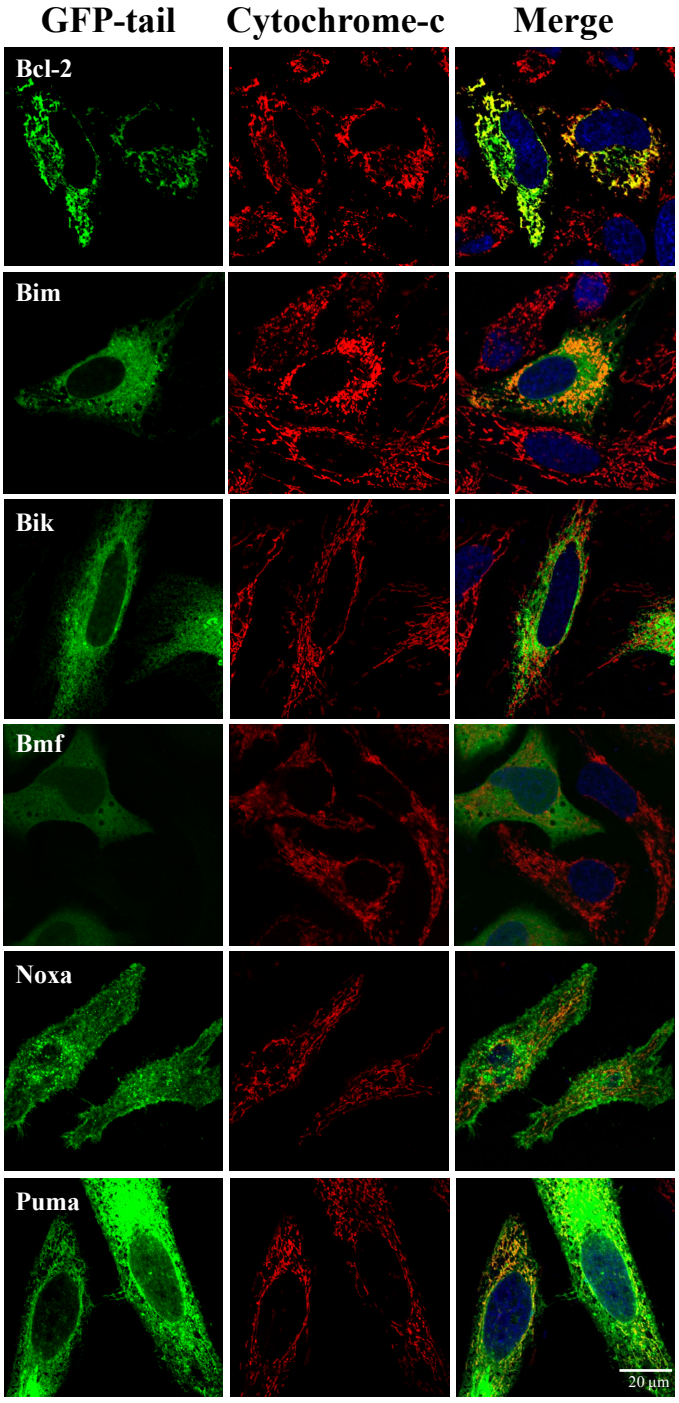

Figure 5.5. GFP/BH3-Ct fusions do not promote apoptosis activation. (A) Caspase-3-like activity measured in the HeLa cells. Bars represent the mean of three experiments ± s.d. (*$p < 0.1$; **$p < 0.05$; ***$p < 0.001$. ABT-263 10 μM was used as apoptotic inductor. Western blot was developed against GFP antibody and α-tubulin (load control). (B) Release of Cytochrome *c* in HeLa cells. Confocal images from HeLa cells transfected with different GFP/BH3-Ct constructs (green channel). Cells were fixed and incubated with Cyt-*c* antibody (apoptotic marker, red channel). Co-localizations were shown in yellow.

4.3. Concluding remarks.

Structural and biophysical studies have been invaluable in deciphering the role of BH3-only proteins (383), but gaps remain in our knowledge specially concerning the way BH3-only proteins influences on Bax/Bak membrane association (207). BH3-only proteins are crucial in the regulatory mechanism of apoptosis, inhibiting the anti-apoptotic BCL-2 members or activatying directly the pro-apoptotic effectors Bax and Bak. In this dual action mechanism the subcellular distribution of BH3-only proteins, especially their MOM localization can be of paramount relevance. The presence of C-terminal hydrophobic region in BH3-only proteins can play a role in targeting and apoptotic function of these proteins. Our results clearly show that Bik and Bmf C-termini and, to some extent, Puma and Bim insert in biological membranes *in vitro*. Similar results were obtained in the bacterial ToxR system, where Noxa C-terminal region again did not display any insertion capacity in the bacterial membranes. However, when C-terminal regions were tested in human cells some differences were observed. Insertion capacity and subcellular localization of Bik C-terminus demonstrated proper targeting to the ER membrane (106) and (Figure 5.4). Puma and Bim partially localized in the ER, altought the presence of both fusions in MOM were also observed. This distribution correlates with their apoptotic function as direct activators of Bax and Bak in MOM (100). The ER localization of BH3-only C-terminus can be related to the ER-mitochondria associated membranes (MAMs) contact sites between ER and MOM, where different ER and mitochondrial proteins are switched (384, 385).

Cytosolic Bmf C-terminus distribution indicates that this BH3-only protein did not contains MOM targeting information in its C-terminal hydrophobic region. In fact, this BH3-only sensitizer protein could interact with the anti-apoptotic proteins in the cytosol to be probably later carried to MOM, where the C-terminal hydrophobic region inserts.

Noxa C-terminus did not show capability to insertion into any of the membranes tested. However, the microscopy data indicated that the distribution of this fused protein was reticular, although neither ER nor MOM localization was observed. Recently some authors have described that the C-terminal tail of Noxa regulates the stability of both Noxa and Mcl-1 (386). Reticular distribution observed for Noxa C-terminal region is similar to that observed for some proteasome components and could be related with this recently attributed function in protein turnover. Noxa C-terminal did not then behave as a classical TM domain because did not show neither targeting neither insertion capacity to subcellular membranes.

Overall, current data describe a non-mitochondrial distribution for BH3-only C-terminal regions in clear contrast with the mitochondrial location found for the equivalent region in other pro- and anti-apoptotic BCL-2 family proteins. BH3-only proteins have to associate with other anti- or pro-apoptotic BCL-2 partners to exert their apoptotic functions (387). Through these interactions, BH3-only proteins are probably targeted to MOM only when the apoptotic machinery is activated.

The C-terminal regions of the BH3-only proteins analyzed have a moderate to low hydrophobicity score (except for Bik C-terminus) that, however, do not preclude them to insert into biological membranes. Interestingly, all the C-terminal regions analyzed lack the flanking positives charges, which have been extensively described as a signal for mitochondrial targeting (193). The ER is the preferred location for Bik, Bim and to some extent Puma, whilst their MOM translocation will probably require the enrollment of additional factors involved in mitochondrial targeting (194). For that reason, most of BH3-only C-terminal regions analyzed do not reach MOM by themselves and remain at the cytosol or inserted into the ER. Furthermore, a tight relation between the membrane of ER and mitochondrial has been recently described through the MAMs regions. These physical interaction sites between ER and mitochondria could have a role in the transmission of apoptotic signals through BH3-only proteins (384, 385). Then, BH3-only proteins could be transferred through the MAMs from the ER membrane to the MOM or stablish interactions with some BCL-2 family members located in the MOM to switch to mitochondria. In conclusion, BH3-only proteins exert their pro-apoptotic functions by differents ways and, as a consequence, their C-terminal regions have diferent targeting

and insertion capabilities in subcellular membranes. Further studies devoted to the mechanisms that control BH3-only proteins-mediated apoptotic activation need to be done in order to expand our knowledge of this puzzling and well orchestated process.

CHAPTER

III

6.1 Introduction.

Traditionally, Bcl-2 TMDs were referred to as membrane inserting domains (388). However, it is becoming apparent that the TMDs are more than mere insertion domains and may play a key role in the function of the Bcl-2 proteins (389-391). Synthetic peptides derived from such domains may thus represent useful analysis tools when analyzed in the appropriate *in vitro* assays, as demonstrated for other membrane-related biological disorders (392). Moreover, the sensitivity of tumor cells to MOMP when challenged with BH3 domain-derived peptides was recently exploited to increase the cellular response to chemotherapy (326, 393). This novel 'mitochondrial priming' concept extended to targeted membrane perturbation may therefore provide new directions in the pharmacological manipulation of cell death. We hypothesize that the BCL-2 derived TMD plays a central role in the function of Bcl-2 proteins and that characterization of the TMD membrane-binding properties will provide the initial step to understanding the specific role of the mitochondrial membrane in the apoptosis pathway. The aim of this chapter therefore was to perform a systematic evaluation of Bcl-2 TMD-derived peptides (TMD-pepts) in complementary biophysical and cellular studies to provide new insight into the role of the TMD in this prevalent cellular pathway.

6.2 Results and Discussion.

6.2.1. Peptide Design and Conformational Flexibility of Bcl-2 TMD-derived Peptides.

In order to perform a comparative study of the biophysical properties and putative in cellulo activity of the C-terminal region of Bcl-2 proteins, we designed and analyzed a series of peptides identified as TMDs (TMD-pepts). To determine the most appropriate sequence regions to synthesize, the entire sequence of anti-apoptotic (Bcl-2, Bcl-xL, Bcl-w, Mcl-1) and pro-apoptotic (Bax and Bak) proteins were analyzed using several transmembrane predicting algorithms (see Methods). The C-terminal residues of all proteins were found to be the most hydrophobic and therefore highly probable TMD segments. According to these results individual peptides were designed and N- and C-terminal lysine residues were added to facilitate synthesis, purification and characterization (Table 6.I).

Table 6.I. CD characterization of Bcl2-derived peptides

TMD-pepts	Peptide sequence	MW	ΔG (kcal/mol)[2]	Percentage of α-helix[1]	
				PO_4^{-3} Buffer 50mM	SDS 10mM
GpA	Ac-*KK*EITLIIFGVMAGVIGTILLISYGI*KK*-NH2	3317.3	-1.150	13	36
Bcl-2	Ac-*KK*KTLLSLALVGACITLGAYL*KKK*-NH2	2601.8	-1.356	22	100
Bcl-xL	Ac-*KK*RWFLTGMTVAGVVLLGSLFSRK*K*-NH2	2864.9	-0.355	8	78
Bcl-w	Ac-*KKK*RTVLTGAVALGALVTVGAFFAK*KK*-NH2	2843.9	-0.418	8	49
Mcl1	Ac-*KK*RNVLLAFAGVAGVGAGLAYLIR*KK*-NH2	2754.8	-0.275	7	79
Bax	Ac-*KK*TWQTVTIFVAGVLTASLTIWKK-NH2	2760.6	0.510	12	40
Bak	Ac-*KKK*ILNVLVVLGVVLLGQFVVRRFFK*KK*-NH2	3311.3	-0.735	46	100

[1] Percentages of α-helical secondary structure obtained from the CD data interpreted with the K2D program of Dichroweb (available on the World Wide Web).[2] Prediction of ΔG (394).obtained from ΔG prediction server 1.0 (http://dgpred.cbr.su.se) considering only the TMDs of the proteins without added flanking Lys (shown in italics) (336)(394).

The native TMD sequence of each protein contain at least one positively-charged amino acids and the insertion of additional terminal lysine residues have previously been shown to not interfere with the interacting properties of the hydrophobic sequences of many TMD core sequences (395, 396). Although the sequence alignment of the peptides derived from the TMD revealed less than 25% sequence identity, all the original sequences displayed a similar hydrophobicity profile with segregation of positive net charge balance towards the N- and C-termini while the hydrophobic residues were located in the central region (Table 6.I), a gradation of hydrophobicity statistically found in TM segments of solved integral membranes protein structures (397).

The secondary structure of each peptide in different media was evaluated by circular dichroism (CD) spectroscopy. A control peptide derived from the TMD sequence of the well characterised plasma membrane protein glycophorin A (GpA) was also included. All peptides analyzed showed conformational flexibility, adopting different secondary structures in buffers and membrane-like environments analyzed. In phosphate buffered saline (PBS), the CD spectra of the TMD-pepts showed characteristics of extended conformation except for those derived from the pro-apoptotic protein Bak (TMD-Bak), which showed a moderate percentage of secondary structure (Table 6.I and Figure 6.1). In order to initially examine the propensity of each peptide to adopt a defined secondary structure, CD spectra were also recorded in the presence of TFE (100% vol/vol), a solvent

known to induce helicity in single-stranded potentially α-helical polypeptides (398); in the presence of methanol (MeOH), which can increase β-structure population (399); and at the criticalmicellar concentrations (10 mM) of SDS (400), which may stabilize both α-helical or β-sheet conformations depending on the intrinsic secondary structure propensity of the polypeptide (401). In 100% TFE, the TMD-pepts adopted mainly α-helical conformation, while TMD-Bcl-w and TMD-Mcl-1 adopted mixed random and helical conformations (Figure 6.1). In the presence of both MeOH and 10 mM SDS, TMD-Bcl-2, TMD-Bcl-xL and TMD-Bak exhibited α-helical structure; TMD-Bcl-w and TMD-Mcl-1 adopted mixed random and helical conformations, while TMD-Bax preferentially adopted a β-sheet conformation (Table 6.I and Figure 6.1).

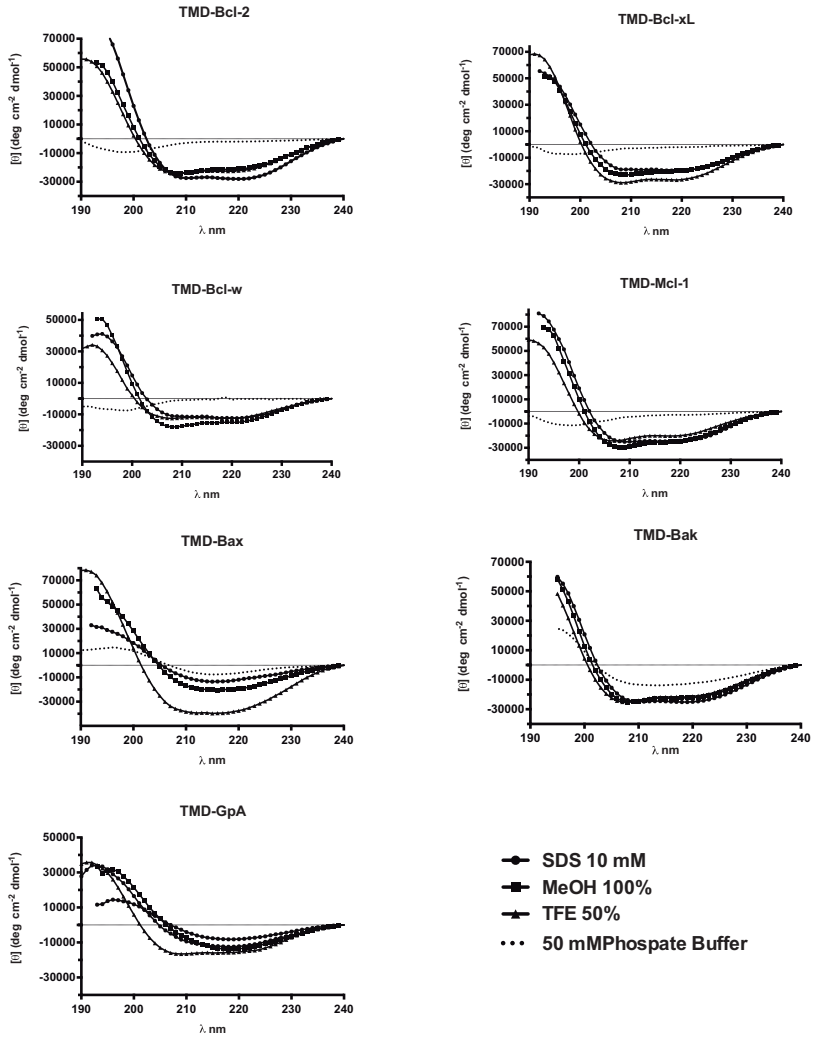

Figure 6.1. Circular Dichroism (CD) spectra of TMD derived peptides. CD spectra were measured between 190 and 240 nm at a temperature of 25° C using a Jasco J-810 spectropolarimeter. Each measurement was recorded using 2,2,2 – Trifluoroethanol (TFE 100%), Methanol (MeOH 100%), and Sodium dodecyl sulfate (SDS) 10 mM and Phosphate Buffer.

Overall, the solution CD data demonstrate that TMD-pepts, with similar hydrophobic and charge distribution characteristics, exhibit different propensities to adopt a defined secondary structure in membrane-mimetic environments suggesting conformational flexibility (402). While TMD-Bax was the only peptide that exhibited β-sheet conformation, overall, the α-helical conformation was predominant in membrane-like environments for all TMD-pepts.

6.2.2. Membrane Binding Properties of TMD-pepts.

Bcl-2 family proteins are not commonly classified as integral membrane proteins but have been recognized to act exclusively on the cytoplasmic face of mitochondria and/or ER membranes (403), where they most probably insert via their C-terminal TMD. Bcl-2 proteins are synthesized by free ribosomes as full-length proteins (including the C-terminus) in the aqueous cytosol before reaching any lipid bilayer, where C-terminal TMDs are energetically more stable. This process entails selective TMD shielding from the aqueous cytosol, targeting to the membrane surface and integration into the lipid bilayer, most likely with the assistance of as yet undiscovered chaperones. In order to evaluate the membrane affinity of the TMD of Bcl-2 proteins we analysed the binding of each TMDpept to synthetic model lipid membranes. We used the mitochondrial model membrane system (POPC/POPE/POPS/POPI/ 5/3/1/1 - Mito-like) that mimics the lipid composition of the outer mitochondrial membrane. POPC/POPE/POPS/POPI/TOCL 4.8/2.8/1/1/0.4 (Mito-like+CL) was used to determine the effect of cardiolipin, a mitochondrion-specific lipid (174, 404, 405), that is predominantly located in the inner mitochondrial membrane but may also translocate to the outer mitochondrial membrane in some circumstances (406). POPC was used as a model of the plasma membrane (PM-like). The binding of TMD-pepts to each model membrane and the effect of peptide binding on the membrane structure was analyzed by dual polarization interferometry (DPI) (407, 408) (see Methods) in collaboration with Prof. Aguilar's laboratory. The structural parameters of each supported bilayer formed via *in-situ* liposome deposition and characterized by DPI are listed in Table 6.II.

Table 6.II. Properties of the lipid bilayers formed on the planar silicon oxynitride chip surface at 20°C. (Values are averages of 12-14 repeats). Value error is one standard deviation.

	Lipid	Thickness (nm)	Birefringence	Mass (ng/mm^2)
PM-like	POPC	4.76 ± 0.03	0.0199 ± 0.0005	4.76 ± 0.03
MITO-like	POPC/POPE/POPS/POPI (5:3:1:1)	4.48 ± 0.06	0.0176 ± 0.0005	4.47 ± 0.07
MITO-like+CL	POPC/POPE/POPS/POPI/POCL (4.8.:2.8:1:1:0.4)	4.89 ± 0.18	0.0198 ± 0.0001	4.88 ± 0.33

The accumulative binding of each TMD-pepts was characterized by the transmagnetic (TM) and transelectric (TE) phase changes, which were subsequently resolved into the mass of membrane-bound peptide and birefringence for each lipid bilayer. The overall amount of bilayer-bound peptide at the end of the 20µM injection is plotted in Figure 6.2. Relative to the PM-like bilayer, only Bcl-w and Bak showed a statistically significant increase in mass bound to the Mito-like bilayer. However, there was a meaningful increase in the total amount of peptide bound in the presence of cardiolipin for all peptides except Mcl-1-derived TMD-pept. Globally, the binding experiments indicate that all peptides interact more efficiently with the cardiolipin-containing Mito-like bilayers.

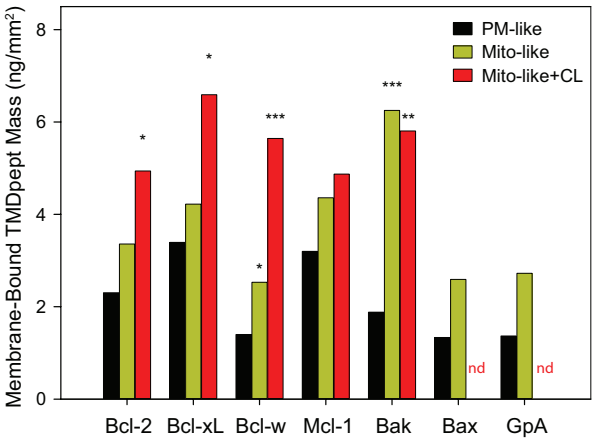

Figure 6.2. TMD-pepts preferential binding to mitochondrial membrane-derived bilayers. The total mass of TMD-pepts bound to the PM-like (POPC), Mito-like (POPC /POPE/POPS/POPI = 60:30:10:10) and Mito-like+CL (POPC/POPE/POPS/POPI/TOCL = 58:28:10:10:4) obtained at the end of 20µM injection. Values indicate mean values +/- S.E.M. (*: $p < 0.02$, **: $p < 0.005$ and ***: $p < 0.001$).

Birefringence is a measure of membrane ordering that permits a systematic analysis of changes in bilayer order (a measure of structure), and allows the impact of peptide binding on the membrane structure (346, 408, 409) to be investigated. The changes in the order of the PM-like and both Mito-like bilayers induced by the TMD-pepts

(birefringence vs mass plots) are shown in Figure 6.3, which reflect the overall profile of bilayer disordering during peptide binding. For each bilayer, injection of each peptide at increasing concentrations resulted in increased mass bound to the bilayer. There was little to no dissociation of any of TMD-pepts indicating that all peptides bound irreversibly under the conditions used. Furthermore, These plots demonstrate that all peptides caused minimal disruption to the PM-like membrane but reduced the ordering of both Mito-like membranes.

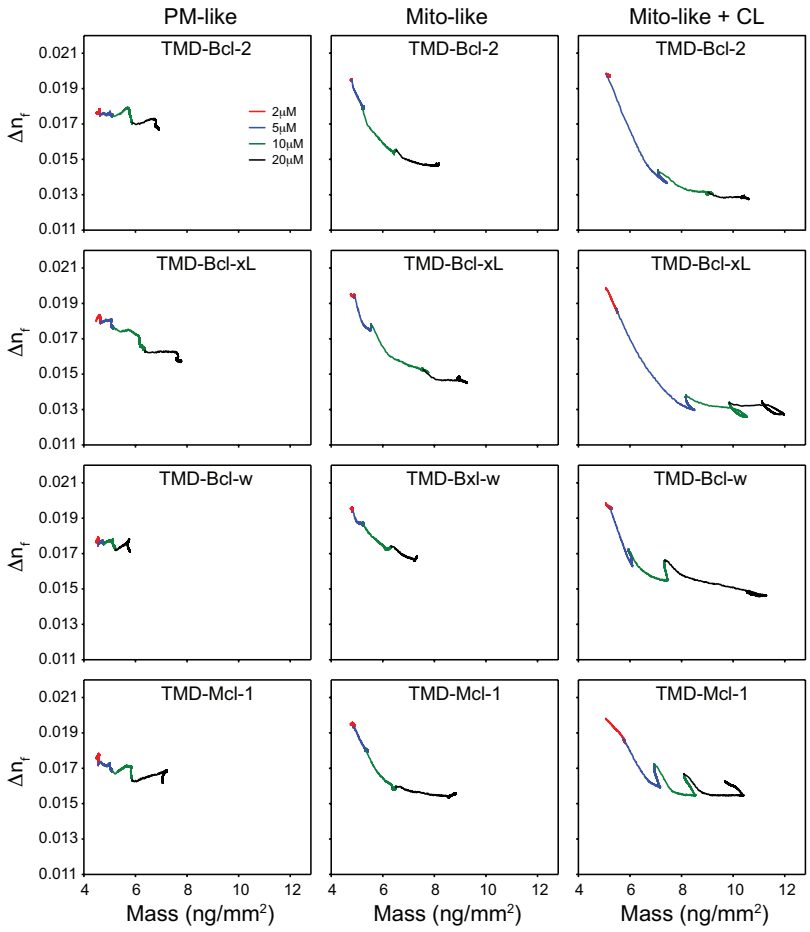

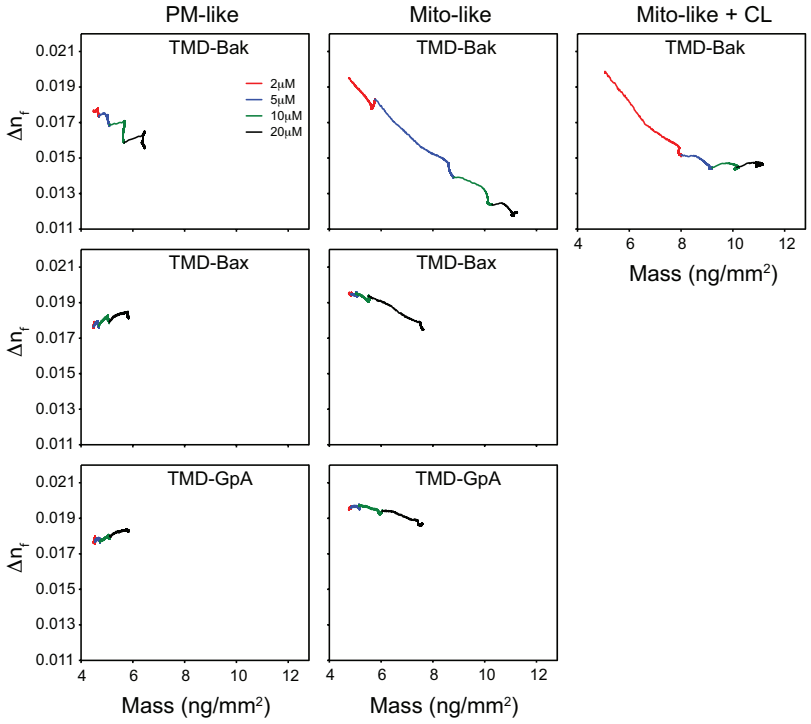

Figure 6.3. Changes in bilayer order induced by TMD-pepts. Dual Polarisation Interferometry. The effect of peptides on membrane disordering is analyzed by the changes of birefringence (D*nf*) as a function of membrane bound-peptide mass, in POPC (PM-like, left panels), in POPC/POPE/POPS/POPI (5:3:1:1) (MITO-like, central panels) and in POPC/POPE/POPS/POPI/POCL (4.8:2.8:1:1:0.4) (MITO-like/CL, right panels). A decrease in birefringence corresponds to a decrease in bilayer order, while an increase in birefringence reflects an increase bilayer ordering.

The dependence of both mass and birefringence on peptide concentration as shown in Figure 6.4 allows further analysis of the effect of each peptide on the structure of the three model membranes. On the PM-like bilayer, the membrane ordering increased slightly (increase in birefringence) or decreased (drop in birefringence), reflecting small changes in bilayer structure and demonstrating the ability of the PM-like bilayer to recover from peptide binding. However, in comparison, the Mito-like bilayer exhibited a significant degree of re-ordering to accommodate the bound peptide, which increased further in the presence of cardiolipin. For the TMD-pepts derived from anti-apoptotic proteins (TMD-Bcl-2, TMD-Bcl-xL, TMD-Bcl-w and TMD-Mcl-1), the birefringence of both mitochondrial membrane-derived bilayers approached a plateau at higher levels of bound peptide (Figure 6.3 and 6.4). In contrast, the birefringence of the Mito-like bilayer

continued to drop for the TMD-pept derived from pro-apoptotic protein Bak (Figure 6.3 and 6.4), suggesting a higher membrane perturbing effect on this mitochondrial membrane-derived bilayer. As expected, the GpA-derived TMD-peptide, a protein that is not associated with mitochondrial membranes, caused a much smaller drop in bilayer order. In summary, the results indicate that a lower concentration of the TMD peptides is required to induce a significant change in membrane order in both mitochondrial membrane-derived bilayers, and suggests a potential role of cardiolipin for the differential localization of the Bcl-2 proteins in membranes, especially for TMD-Bcl-xL and TMD-Bak (Figure 6.4).

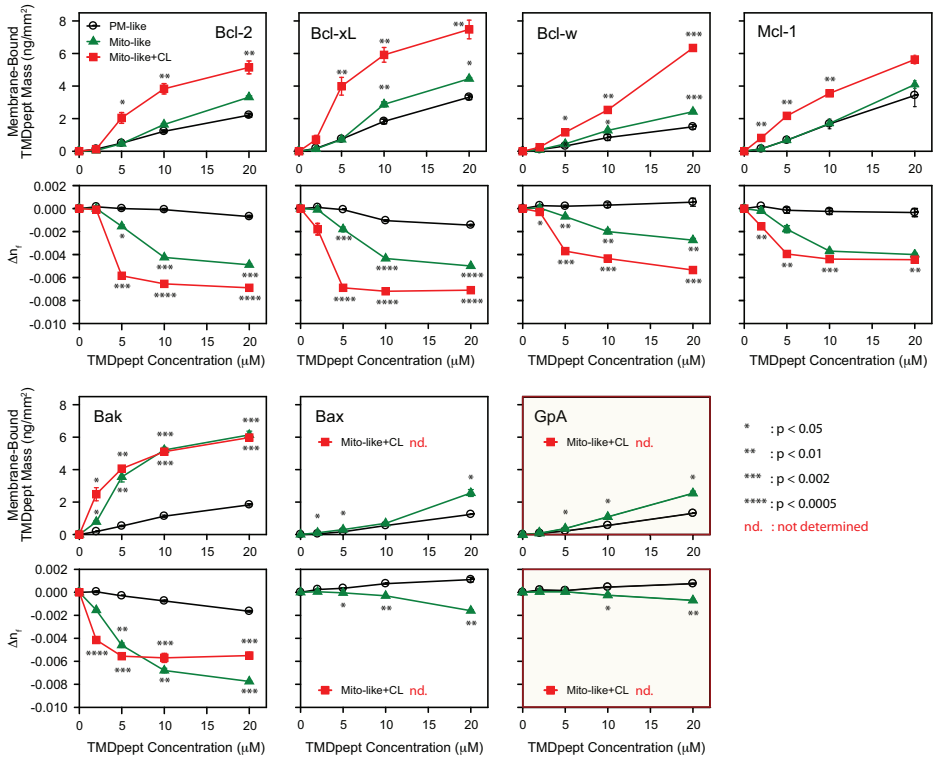

Figure 6.4. Changes in bilayer order induced by TMD-pepts. Measurements of bilayer mass and birefringence at different TMD-pept concentration. Dependence of mass (Dependence of mass (ng/mm^2) and birefringence (Δn_f) on concentration of each TMD-derived peptide PM-like (black line), Mito-like (green line) and Mito-like+CL like bilayers (red line). A decrease in birefringence corresponds to a decrease in bilayer order, while an increase in birefringence reflects an increase bilayer ordering.

Next, we analyzed the influence of the membrane environment in the secondary structure of TMD-pepts by means of CD spectroscopy. CD spectra were obtained in the presence of synthetic liposomes at different lipid:peptide molar ratios (L:P). In the presence of PM-like liposomes, TMD-pepts were found to populate random or β-sheet-like conformations characterized by a minimum centered at 217 nm (Figure 6.5).

The CD spectra in the presence of Mito-like liposomes exhibited a minimum at 222-224 nm suggesting the coexistence of dynamic mixed structures characterized by the presence of helical conformation. In addition, the 208 nm minimum characteristic of helical conformations was less defined. The less defined double minima associated with α-helical spectra is commonly observed for peptides that bind strongly to liposomes (410, 411). TMD-Bax precipitated out from solution in the presence of Mito-like liposomes precluding structural analysis by CD.

In contrast to the behavior in PM-like liposomes, all TMD-pepts caused Mito-like liposome solutions to become turbid over time and dynamic light scattering (DLS) was therefore utilized to understand this phenomenon. The size and distribution of particles present upon addition of each peptide are shown in Figure 6.6. At low lipid:peptide (L:P) ratios (red lines) we found a single species approximately 60 - 100 nm in size corresponding to the expected size for liposomes produced by extrusion through a 100 nm pore size filter. However, at higher L:P ratios, all peptides except TMD-Bax (which had low solubility under the conditions) and TMD-GpA, caused the formation of larger species in the range of 800–1000 nm and up to 5000 nm in diameter. Thus, the addition of TMD-Bcl-2, TMD-Bcl-xL, TMD-Bcl-w, TMD-Mcl-1 and TMD-Bak all caused changes in the properties of the model Mito-like membrane leading to liposome fusion.

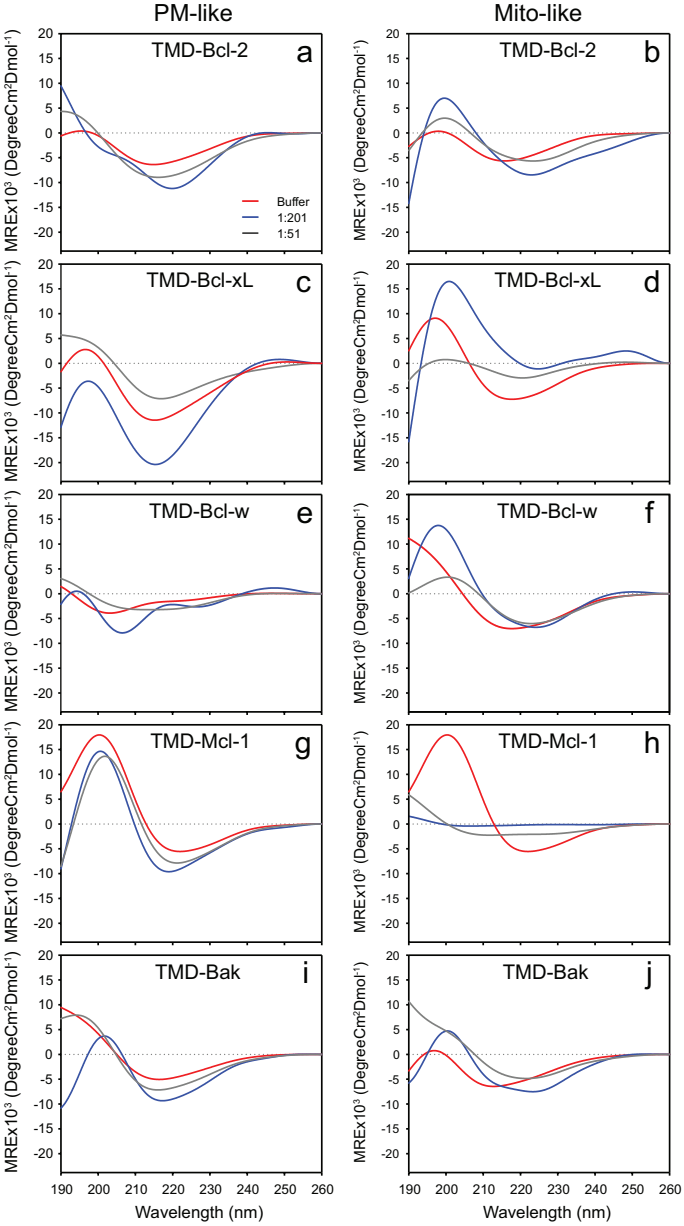

Figure 6.5. CD spectra of TMD-derived peptides in POPC (left panels) and POPC:POPE:POPS:POPI (5:3:1:1, right panels) at two different lipid:peptide ratios, 1:51 (black) and 1:201 (blue).

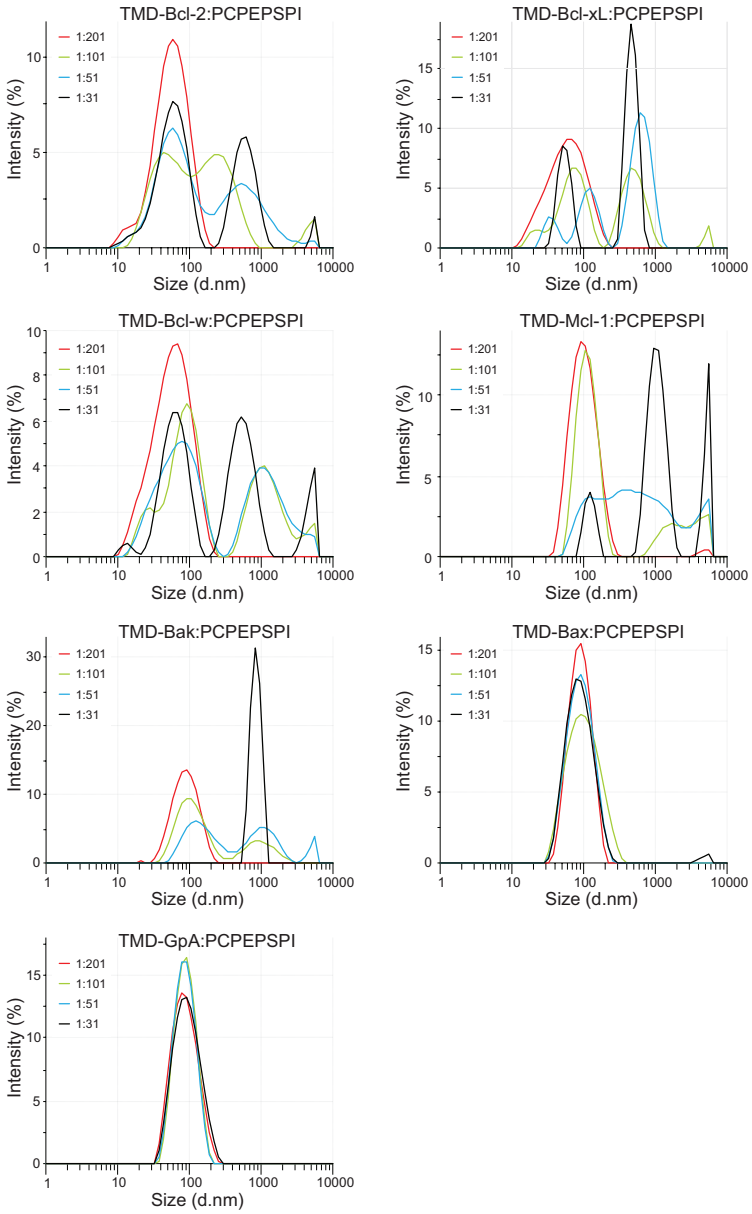

Figure 6.6. Analysis of the effect of TMD-derived peptides on liposome diameter in POPC and POPC:POPE:POPS:POPI (5:3:1:1), at four different lipid:peptide ratios, 1:31, 1:51, 1:101 and 1:201.

6.2.3. TMD-pepts promote calcein release from liposomes and Cytochrome c Release from Isolated Mitochondria.

To determine whether membrane binding of TMD-pepts induced bilayer disruption, membrane leakage was analyzed by dye release assays. We measured the rate of liposome-encapsulated calcein release from model PM-like and Mito-like membranes. The TMD-pepts were evaluated at the biologically active concentration of 10 μM (see below) and all Bcl-2-derived peptides, except Bcl-w, consistently induced higher calcein release from Mito-like than from PM-like liposomes (Table 6.III), suggesting a specific role in the perturbation of mitochondrial membranes, especially for TMD-Bcl-xL, TMD-Mcl-1, and TMD-Bax and TMD-Bak. Moreover, the control TMD-GpA peptide induced more calcein leakage from PM-like than from Mito-like membranes and can therefore be described as a mitochondrial inactive peptide. These results, together with the results obtained from DPI, suggest that TMD-pepts derived from Bcl-2 proteins are poorly active at plasma membranes inducing minor damage that can easily self-repair.

Table 6.III . TMD-pepts-induced calcein release from liposomes

TMD-pept	% of released calcein[a]		
	PM-like	Mito-like	*t-student*
Bcl-2	28 ± 4	40 ± 7	*
Bcl-xL	4 ± 7	75 ± 16	***
Bcl-w	20 ± 6	28 ± 5	n.s.
Mcl-1	15 ± 6	53 ± 6	***
Bax	6 ± 8	52 ± 7	***
Bak	41 ± 12	88 ± 3	***
GpA	47 ± 12	11 ± 6	**

[a] The % of calcein release was calculated taken into account as total release that obtained when liposomes were treated with the 10% Triton X-100. The TMD-pepts were evaluated at 10 μM.

Interestingly, the damage that these peptides induce in mitochondrial membranes may find application in the apoptotic activation of tumor cells by mitochondrial priming. We then evaluated the potential biological activity of TMD-pepts in isolated intact mitochondria purified from mouse embryonic fibroblasts (MEFs) cells. In control (N.T., non-treated) mitochondria, cytochrome *c* (Cyt-*c*) was found in the pellet that contained the mitochondrial fraction characterized by the presence of the mitochondrial voltage-dependent anion selective channel protein 1 (VDAC 1) (412) (Figure 6.7a and b). A similar result was found with the mitochondrial inactive peptide TMD-GpA. In contrast, TMD-Bcl-xL, TMD-Bax and TMD-Bak induced the highest level of mitochondrial Cyt-*c* release, while TMD-Mcl-1 was consistently the less active peptide (Figure 6.7a and b). In order to further characterize the effect of TMD-pepts on the integrity of the isolated mitochondria, we developed a mitochondrial-swelling assay. TMD-pepts did not induce swelling when compared to Ca^{2+}-only induced experiments (Figure 6.7c). Thus, although TMD-pepts induced Cyt-*c* release, the molecular mechanism by which this occurs does not disrupt mitochondrial integrity. These results correlate with previous studies, suggesting that the molecular mechanism of full length Bcl-2 proteins-induced Cyt-*c* release specifically perturbed the mitochondrial outer membrane, while the inner membrane and the ultra-structure of mitochondria remained unaffected (413). The biophysical activity of TMD-pepts in synthetic membranes, together with the Cyt-*c* release capacity from isolated mitochondria support the notion that TMD peptides not only act as membrane anchoring domains but can also be considered as biologically active agents in their own right.

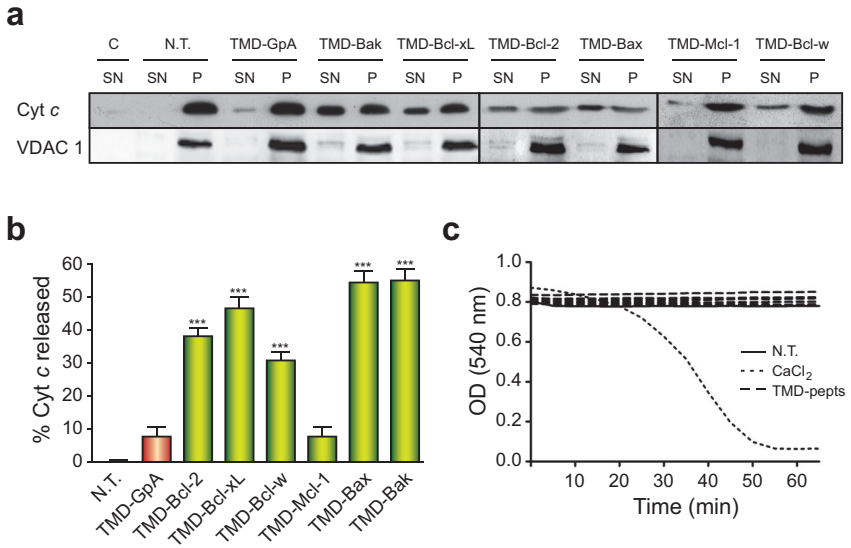

Figure 6.7. TMD-pepts promote cytochrome c release from intact isolated mitochondria. (a) VDAC and Cyt-*c* immunoblotting from pure mitochondria fractions (Pellet). Data are representative of three independent assays. (b) Western Blot quantification of Cyt-*c* release using ImageJ software. Experiments were performed independently three times (N=3) (***$p < 0.001$, compared with NT). (c) Mitochondrial swelling of TMD-pepts compared with $CaCl_2$ as positive control measured as absorbance change at 540nm.

6.2.4. Biological Activity of TMD-pepts on Human Cervix Adenocarcinoma Cells.

To further characterize the marked effect of TMD-pepts in isolated mitochondria, their biological activity in human cervix adenocarcinoma (HeLa) cells was evaluated. Firstly, HeLa cells were incubated in the presence of TMD-pepts at 10 μM for 24h. In these experimental conditions, cells were resistant to TMD-pepts and showed normal behavior. In fact, the levels of free lactate dehydrogenase (LDH) in the media revealed that cells did not lose permanent or transient membrane integrity due to TMD-pepts treatment (data not shown). In addition, the TMD-pepts did not induce plasma membrane disruption-induced cell death. As previously described (343, 414) Lipofectamine 2000 was used to facilitate the access of the peptides to the cell cytosol through the plasma membrane. We found that 10 μM TMD-Bcl-2, TMD-Bcl-xL, TMD-Bax and TMD-Bak promoted a significant increase in HeLa cell death percentages under these experimental conditions (Figure 6.8a). As expected, compromised cell viability correlated with loss of mitochondrial functionality (Figure 6.8b, Figure 6.9a), and a moderate release of Cyt-*c* from mitochondria, in particular with TMD-Bcl-xL and TMD-Bak (Figure 6.8c). These two highly active peptides also caused a significant drop in intracellular ATP levels in the early stages of treatment when the effect of the apoptotic inducer (CDDP) was still not apparent (Figure 6.8d). The drop in ATP was most probably caused by the TMD-pepts induced mitochondrial destabilization. Furthermore, we found no evidence of caspase-like activity in either case (Figure 6.8e, lanes 1-5). In this context the TMD-pepts drive cells to necrotic rather than apoptotic cell death despite having a moderate amount of Cyt-*c* released in the cytoplasm (415).

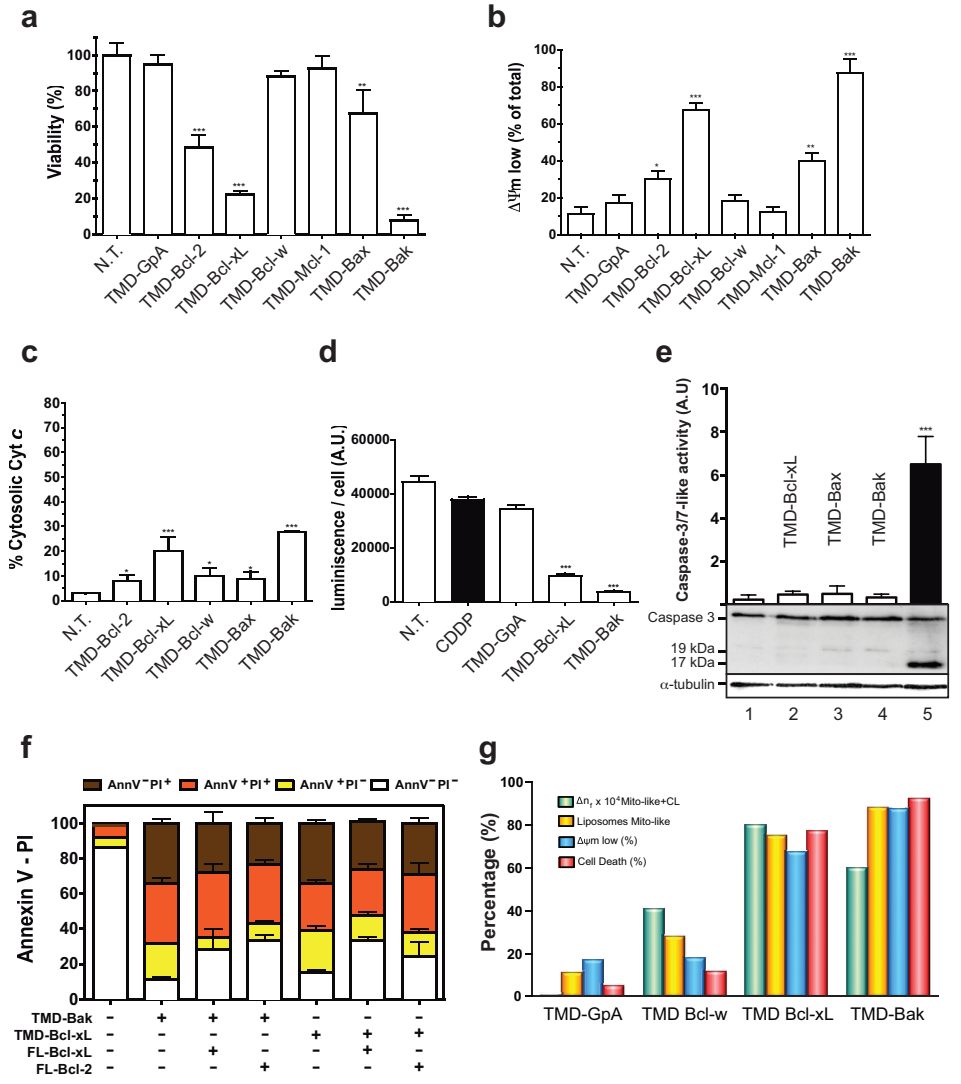

Figure 6.8. Bcl-2-derived peptides effect on viability, mitochondrial membrane potential, Cyt-*c* release and caspase 3/7 activity in HeLa cell cultures at TMD-pepts 10 μM. (a) Cell viability measured by trypan blue exclusion assay of cultures transfected with peptides at 10 μM for 24 h. (b) Mitochondrial membrane potential was measured by flow cytometry with TMRM. (c) Mitochondrial permeabilization was analyzed by flow cytometry with Cyt-*c* FITC. (d) Measurement of intracellular ATP by luminescence, peptide treatment decreased intracellular ATP levels compared with the not treated cells. Representative data are shown, bars represent the mean of three independent experiments ± s.d. (**p* < 0.1; ***p* < 0.05; ****p* < 0.001, compared with NT). (e) Caspase 3-like activity measured in the HeLa cells. Bars represent the mean of three independent experiments ± s.d. (*p < 0.1; **p < 0.05; ****p* < 0.001 compared with CDDP). Western blot developed against

caspase 3 antibody using α-tubulin like load control. The fraction at 17 and 19 KDa represents the active form of the enzyme. (f) Effect of Bcl-2 and Bcl-xL Full length on cell death was assayed by flow cytometry with FITC Annexin V and Propidium Ioride (PI). (g) Correlation Graph for HeLa cell line according to the results showed in Figure 6.7, Figure 6.8 and Table 6.III.

Accordingly, when cell fate was monitored by the combined staining with the dye Propidium iodide (PI, which is excluded from cells with intact plasma membranes) and FITC-labeled Annexin V (AnnV, which binds to phosphatidylserine moieties exposed on the surface of dying apoptotic cells) we found that the most active peptides TMD-Bcl-2, TMD,Bcl-xL, TMD-Bax and TMD-Bak generate predominantly necrotic cell death (Figure 6.9b, brown bars). Focusing on the most active peptides TMD-Bcl-xL and TMD-Bak, it should be highlighted that their behavior correlates well with their biophysical properties in the MOM. Nevertheless, their pro-death effect could not always be related to that of the full-length protein; especially for TMD-Bcl-xL, which is an anti-apoptotic member. Previous studies support the ability of Bcl-2-derived TMDs, and other natural or synthetic cytotoxic peptides (416-420) to permeabilize mitochondria, through possible pore formation (421-423).

To better understand the functional correlation between TMD-pepts and full length (FL) Bcl-2 proteins we have analyzed the effect of TMD-Bcl-xL and TMD-Bak in the presence of the anti-apoptotic proteins Bcl-2 and Bcl-xL. Flow cytometry analysis showed a slight decrease in cell death in the presence of the anti-apoptotic FL proteins, while the necrotic pathway was not significantly affected (Figure 6.8f). This indicates that anti-apoptotic proteins are able to partially block the residual apoptotic pathway promoted by Cyt-*c* release due to the presence of TMD-peptides. Based on this result we can speculate on the existence of a putative (direct or indirect) interaction among TMD-pepts and the FL Bcl-2 proteins.

As shown in Figure 6.8g, there is a good correlation between the biophysical effects of TMD-pepts on synthetic membranes and the outcome of their treatment in cell cultures. The more they perturb model membranes the larger are the cellular consequences.

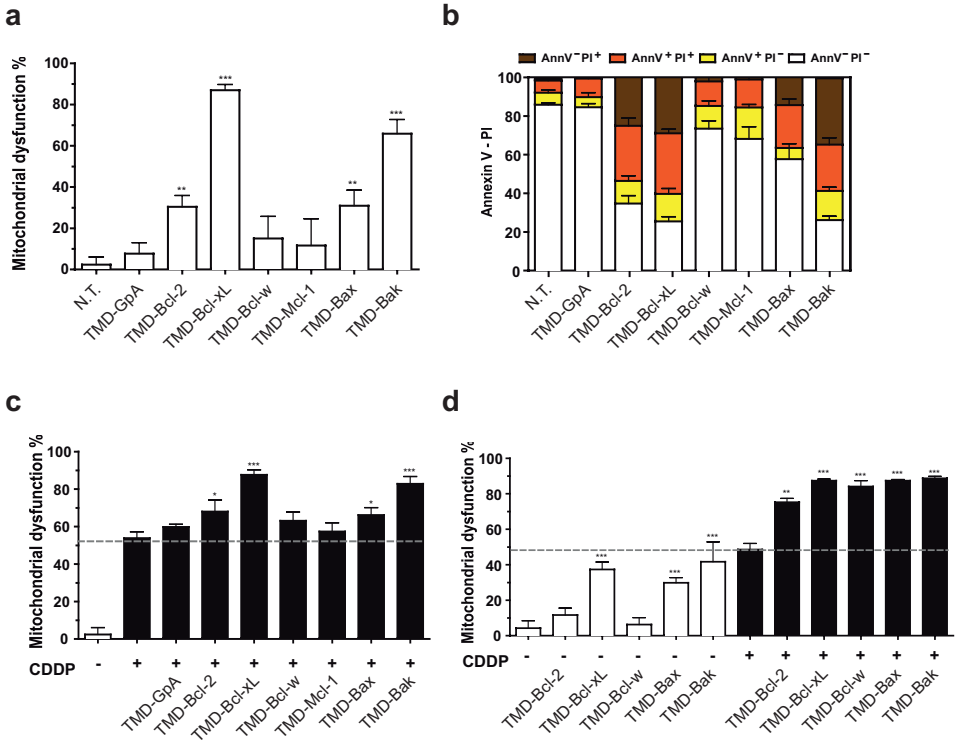

Figure 6.9. Mitochondrial dysfunction of HeLa cells co-treated with CDDP and Bcl-2 TM domain peptides (10 µM and 3 µM) measured by MTT. (a) Cells were treated with TM peptides at 10 µM for 24 h. (b) Apoptotic cell death promoted by the TMD-pepts at 10 µM was analyzed by flow cytometry with FITC Annexin V and PI. (c) Cells were treated with CDDP (40µM) for 12 h after transfection with TM peptides at 10 µM. (d) Cells treated with TM peptides at 3 µM for 24 h represented by white bars. Cells treated with CDDP (40µM) for 12 h after transfection with TM peptides at 3 µM represented by black bars. All bars represent the mean of three independent experiments ± s.d. (*$p < 0.1$; **$p < 0.05$, ***$p < 0.001$).

6.2.5. Mitochondrial priming effect of TMD-pepts.

It has been proposed that mitochondrial priming, understood as the readiness of mitochondria to actively engage the apoptotic program, inversely correlates with resistance to chemotherapy (324, 326). Mitochondrial priming can be forced by decreasing the cellular content of anti-apoptotic Bcl-2 proteins or by using BH3-mimetics such as ABT-737 (326). We were therefore interested in the evaluation of TMD-pepts as novel mitochondrial priming tools. Thus, we evaluated the sensitivity of HeLa cells to co-treatment with the chemotherapeutic agent cisplatin (cis-diammineplatinum (II) dichloride, CDDP) and TMD-pepts. Control cells treated with CDDP in the absence of TMD-pepts

showed close to 50% apoptotic cell death (Figure 6.10a) characterized by mitochondrial dysfunction (Figure 6.9c), loss of mitochondrial membrane potential (Figure 6.10b), Cyt-*c* release (Figure 6.10c) and caspase-3/7-like activity (Figure 6.10d). Interestingly, we observed that a significant decrease in cell viability correlated with an increase in apoptotic markers when CDDP treated cells where co-treated with TMD-Bcl-2, TMD-Bcl-xL, TMD-Bax and TMD-Bak peptides (Figure 6-10).

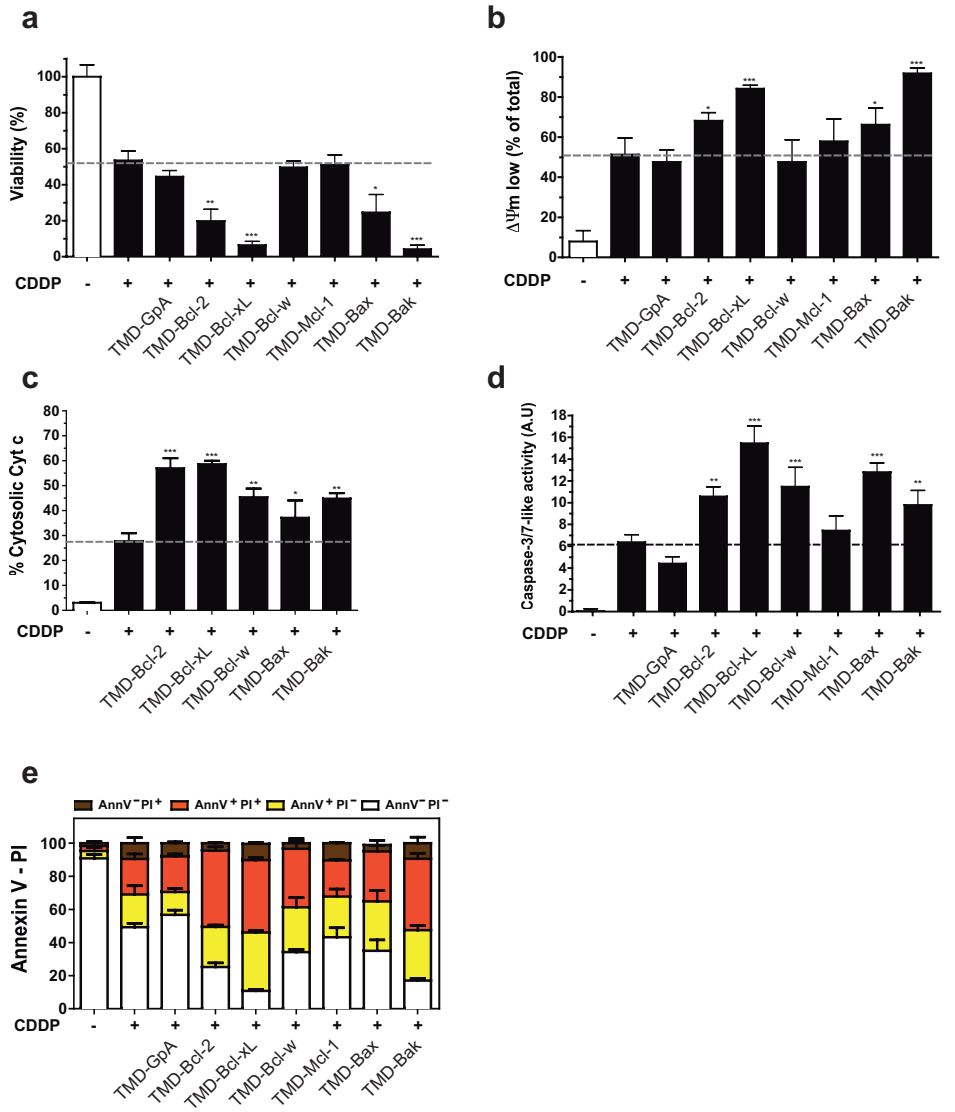

Figure 6.10. Co-treatment of TMD-pepts (10μM) with CDDP significantly enhances the effect of the chemotherapeutic drug in HeLa cells. Cells were treated with CDDP (40 μM) for 12 h after peptides

transfection protocol. (a) Viability measured by trypan blue assay. (b) Mitochondrial membrane potential was measured by flow cytometry with TMRM. (c) Mitochondrial permeabilization was analyzed by flow cytometry with anti Cyt-*c* FITC. (d) Caspase 3-like activity measured in the HeLa cells. Bars represent the mean of three independent experiments ± s.d. (*p < 0.1; **p < 0.05; ***p < 0.001 compared with CDDP). (e) Apoptotic cell death was analyzed by flow cytometry with FITC Annexin V and PI. HeLa.

Moreover, the less mitochondrial active peptide, TMD-Mcl-1, and the mitochondrial inactive peptide, TMD-GpA, did not increase the chemotherapeutic effect of CDDP (Figure 6.10). It should be noted that the effect of the co-treatment on the caspase-3/7-like activity is the result of a cooperative effect between the peptides and the drug, provided that cell treatment with TMD-pepts in the absence of CDDP did not activate caspases (Figure 6.9e lanes 2-4). The caspase-3 activity induced by the TMD-pepts in combination with CDDP was abolished in the presence of the general caspase inhibitor zVAD (Figure 6.11).

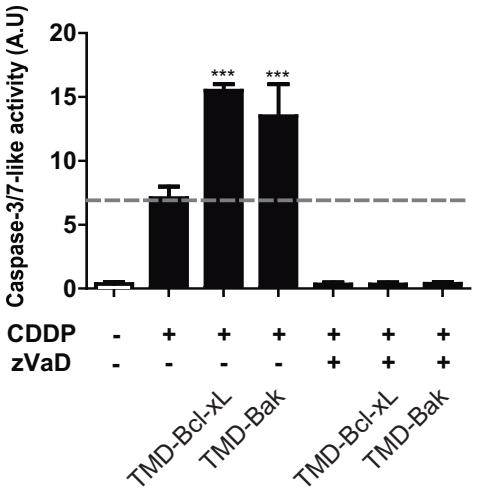

Figure 6.11. HeLa cells treated with TMD-Bcl-xL and TMD-Bak peptides and CDDP in presence of Caspase inhibitor zVaD. Cells were transfected with the peptides at 10µM. zVaD (10uM) was added before CDDP (40uM) treatment, 4 h later peptide transfection (total time 24h). (a) Apoptosis activation was measured by Caspase 3-like activity measured in HeLa cells. All bars represent the mean of three independent experiments ± s.d. (ns, no significant; *p < 0.1).

Flow cytometry analyses showed that CDDP-induced apoptotic cell death ($AnnV^+/PI^-$ and $AnnV^+/PI^+$, light and dark gray bar segments) significantly increased in the presence of the mitochondrial active peptides TMD-Bcl-2, TMD-Bcl-xL, TMD-Bax and TMD-Bak,

but was not affected by the presence of the mitochondrial inactive peptide TMD-GpA (Figure 6.10e). These results also correlated with a change in the behavior of peptides, observed by flow cytometry, from mainly necrotic when used alone (Figure 6.9b), to mainly apoptotic when used in combination with CDDP (Figure 6.10e). Altogether, these results indicate the existence of a switch from necrosis to apoptosis when TMD-pepts are used in combination with CDDP.

To better define the cooperative behavior observed in the experiments described above we studied the cell death properties at sub-lethal concentrations of TMD-pepts when used in combination with CDDP.

We then evaluated the active TMD-pepts at 3 μM in HeLa cells. At this concentration, all peptides by themselves, with the exception of TMD-Bak, showed less than 10% reduction in cell viability (Figure 6.12a, white bars), and only a partial loss of mitochondrial potential, as indicated by an increase in the number of cells with low transmembrane potential (Figure 6.12b). Moreover, neither Cyt-*c* release nor caspase-3/7-like activity was observed (Figure 6.12 panels c and d, respectively). To explore whether the priming exerted by the mitochondrial active TMD-pepts at sub-lethal concentrations could increase the sensitivity of HeLa cells to chemotherapeutic agents, we used co-treatment with CDDP (black bars). The mitochondrial priming resulted in a large increase in CDDP-induced cytotoxicity (Figure 6.12a, Figure 6.9d) accompanied by an increase in the percentage of cells with low mitochondrial transmembrane potential (Figure 6.12b), in the Cyt-*c* released to the cytosol (Figure 6.12c) and in the caspase-3/7-like activity (Figure 6.12d). Accordingly, CDDP induced apoptotic death significantly increased in the presence of the TMD-pepts (see $AnnV^+/PI^-$ and $AnnV^+/PI^+$ population in Figure 6.12e). These results confirm the behavior observed at lethal concentrations of TMD-pepts and strongly support their mitochondrial priming properties.

Interestingly, some TMD-pepts from anti-apoptotic proteins, such as Bcl-xL, show pro-death function in the tumor cell lines analyzed. It has been previously demonstrated that Bcl-xL is cleaved by caspase 3 and calpains, converting Bcl-xL from an anti-apoptotic to a pro-apoptotic factor (424).

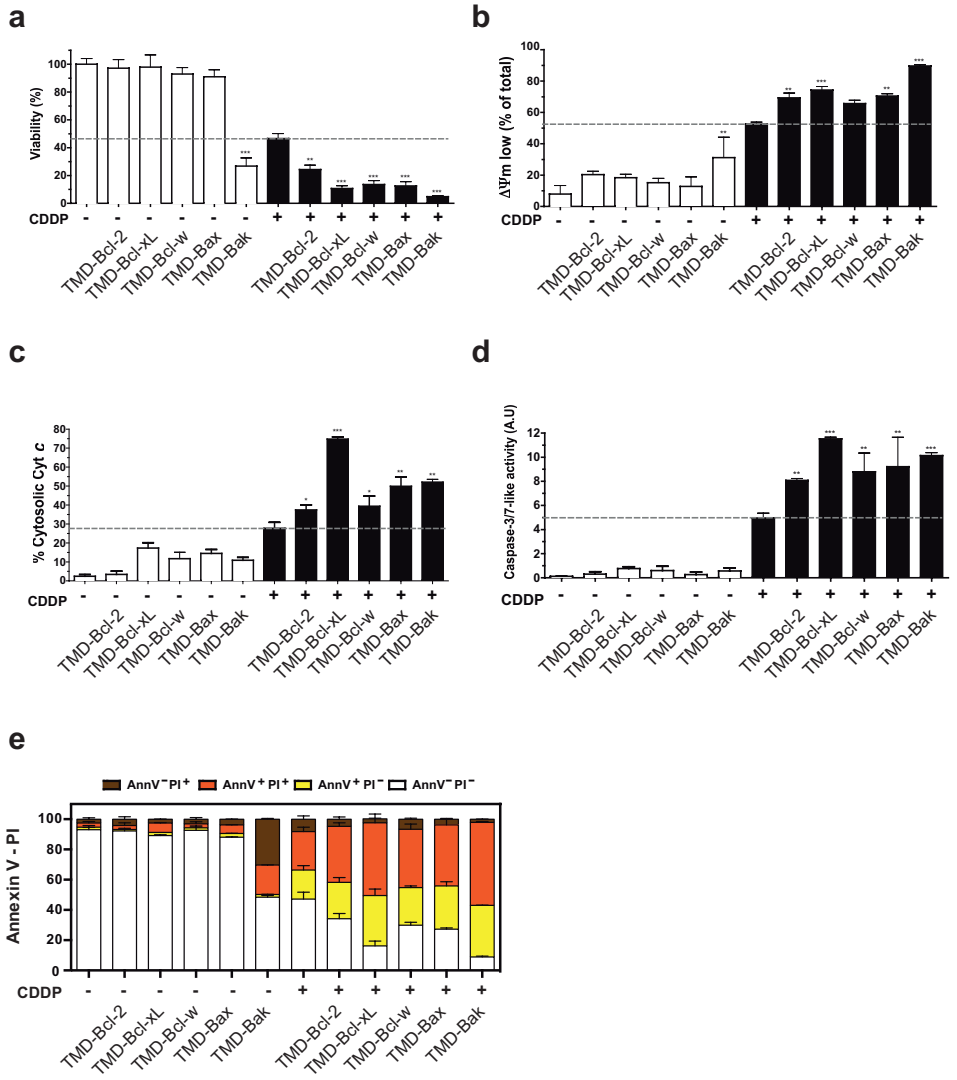

Figure 6.12. Mitochondrial priming by TMD peptides. A Sub-lethal TMDpepts doses induce a mitochondrial priming effect in co-treatments with CDDP in HeLa cells. Comparison of the effect of treatment with TMDpepts alone at 3 μM (white bars) or with co-treatment with CDDP at 40 μM for 12 h (black bars). (a) Cell viability measured by trypan blue exclusion assay of cultures treated with peptides for 24 h. (b) Mitochondrial membrane potential was measured by flow cytometry with TMRM. (c) Mitochondrial permeabilization was analyzed by flow cytometry with anti Cyt-*c* FITC. (d) Caspase 3-like activity measured in the HeLa cells. Bars represent the mean of three experiments ± s.d. (*$p < 0.1$; **$p < 0.05$; ***$p < 0.001$ NT (white bars) and CDDP (black bars)). (e) Apoptotic cell death was analyzed by flow cytometry with FITC Annexin V and PI.

Here we show that the Bcl-xL TMD could be the protein domain responsible for this switch. This behavior could be explained taking into account the common evolutionary origin of Bcl-2 proteins. The programmed cell death is executed with very few members in invertebrates but new members appear with the genomic expansion of vertebrates. In simpler systems, the same protein could be responsible for the final decision of cell death or survival depending on post-translational modifications (425, 426). All these proteins share one to four conserved Bcl-2 homology domains (BH) and most possess a C-terminal hydrophobic amino acid. The divergent evolution of pro- and anti-apoptotic members could be explained considering only the cytosolic regions of Bcl-2 proteins (425). Therefore we speculate that the pore formation capability of TMD-pepts could be modulated by the folding of their soluble regions. Overall, from these experiments we conclude that TMD-pepts clearly enhance the cell apoptosis-inducing effects of the chemotherapeutic agent CDDP in HeLa cells independently of their pro- or anti-apoptotic origin.

6.2.6. Mitochondrial priming effect can be extended to other cancer cells.

In order to generalize our findings and to better understand their physiological relevance, we analysed the behavior of the most active TMD-pepts in the human colorectal carcinoma HCT116 and HCT116 Bax/Bak double knock out (DKO) cell lines (427, 428).

We observed that HCT116 cells had a similar behavior to HeLa cells although they were slightly more resistant to TMD-pepts treatment. Hence, we characterized the effect of these TMD-pepts at 20 μM (lethal) and 10 μM (sub-lethal) concentrations (Figure 6.13).

We examinated that for both cell lines, treatment at lethal concentrations provoked loss of cell viability, which correlates with a decrease in ATP levels (Figure 6.13 a to d) and an increase in mitochondrial destabilization (Figure 6.14 panels a and b). However, there was no effect in caspase 3 activity in any case (Figure 6.13 e and f) as previously described for HeLa cells. Interestingly, in the presence of CDDP, HCT116 wt cells also showed the previously observed switch from necrosis to apoptosis (Figure 6.14c). However, there were no changes in the necrotic populations when the co-treatments were applied to the HCT116 DKO cell line (Figure 6.14d).

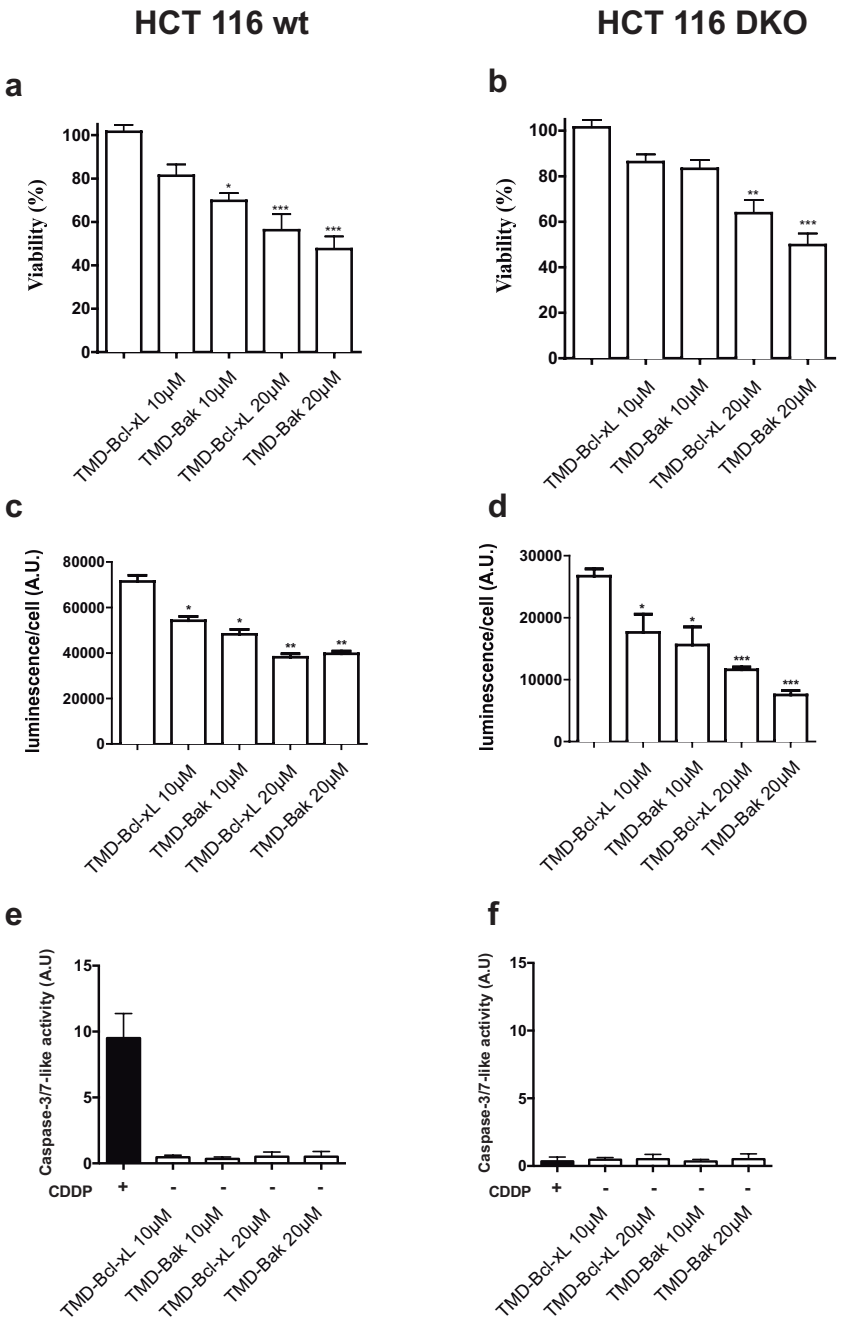

Figure 6.13. HCT116 wt and DKO were treated with TMD-Bcl-xL and TMD-Bak peptides for 24h. Cells were transfected with TMD-pepts (10 and 20 μM). (a, b) Viability was measured by trypan blue assay after 24h

of peptide transfection. (c, d) Measurement of intracellular ATP/cell by luminescence, bars represent the mean of three independent experiments ± s.d. (*p < 0.1; **p < 0.05; ***p < 0.001, compared with NT). (e, f) Apoptosis activation was measured by Caspase 3-like activity. Bars represent the mean of three experiments ± s.d. (*p < 0.1; **p < 0.05; ***p < 0.001 compared with NT (white bars) and CDDP (black bars)).

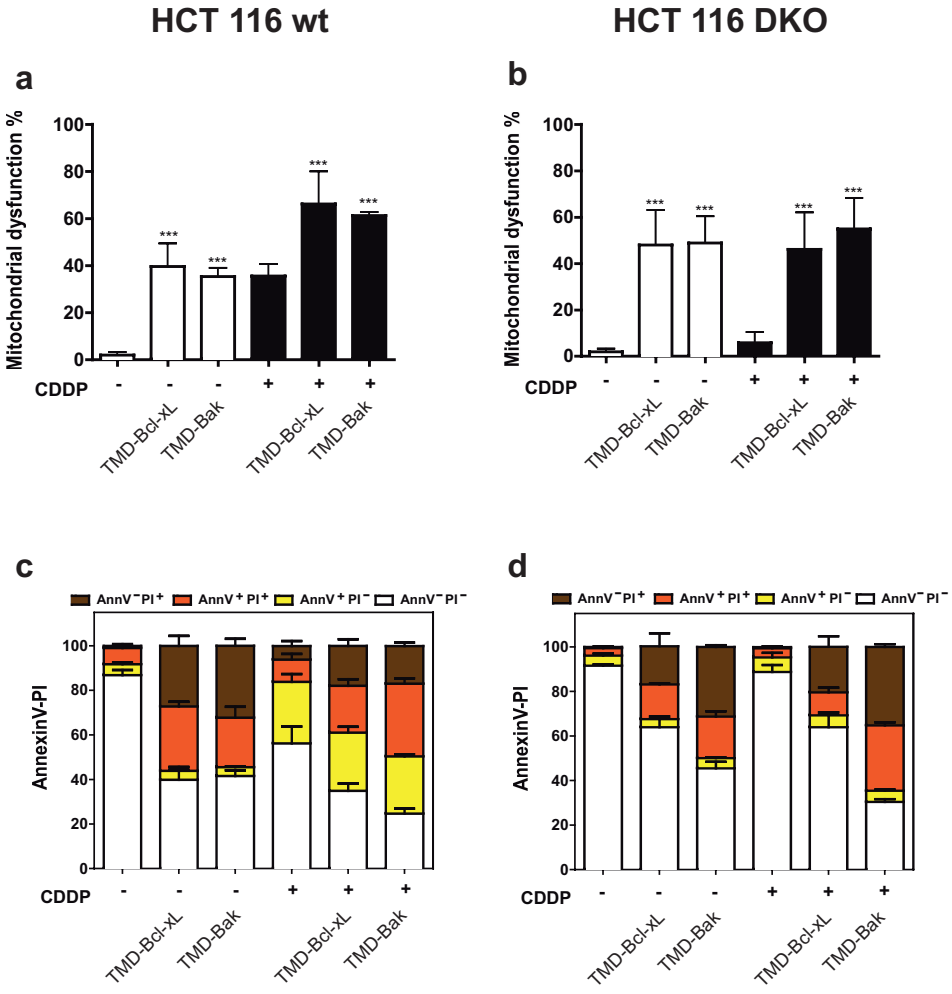

Figure 6.14. HCT116 wt and DKO were treated with TMD-Bcl-xL and TMD-Bak peptides for 24h. Cells were treated with TMD-pepts (20 μM) 4 hours after CDDP treatment. (a, b) Mitochondrial dysfunction was measured by MTT assay after 24h of peptide transfection.(c, d) Apoptotic cell death was analyzed by flow cytometry with FITC Annexin V and PI.

Similar results were obtained when peptides were assayed at sub-lethal concentrations. Under these sub-lethal conditions there was a slight effect of TMD-pepts in mitochondrial

dysfunction (Figure 6.15 panels a and b), cell viability and ATP levels (Figure 6.13 a-d) for both wild type and DKO cell lines. However, in the presence of CDDP, we observed a notable increase in caspase 3 activity for HCT116 wild type cells (Figure 6.15 panels c and e) but not for DKO cells (Figure 6.15 panels d and f). The absence of an apoptotic switch in the HCT116 DKO cell line highlights the relevance of the Bcl-2 apoptotic machinery in the TMD-pepts-mediated mitochondrial priming.

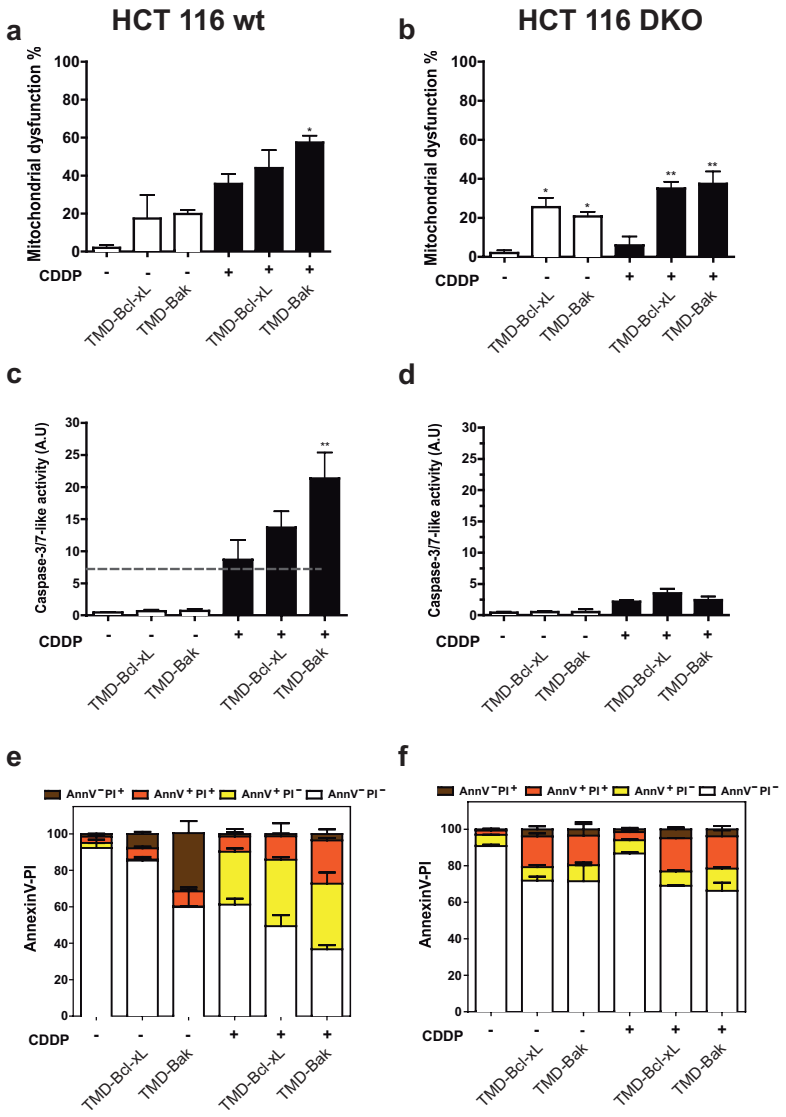

Figure 6.15 Mitochondrial priming effect of TMD-pepts in HCT 116 cell lines wt and Bax/Bak KO. Cells were treated with TMD-pepts at 10µM and CDDP is added at 20 µM. (a, b) Mitochondrial dysfunction was measured by MTT assays 24h after peptide transfection. (c, d) Caspase 3-like activity measured in HCT 116 cell lines. Bars represent the mean of three experiments ± s.d. (*$p < 0.1$; **$p < 0.05$; ***$p < 0.001$ compared with NT (white bars) and CDDP (black bars)). (e, f) Apoptotic cell death was analyzed by flow cytometry with FITC Annexin V and PI.

6.3. Concluding remarks.

The existing paradigm for Bcl-2 protein-mediated control of mitochondria and cell fate in apoptotic signaling involves protein-protein interactions among Bcl-2 members mediated by BH3 domains (123). However, there is increasing evidence the role of the membrane (120, 429) and the interaction of Bcl-2 proteins within the membrane through their TMDs (116, 196, 387, 388, 429, 430) must also be included. The present study has led to the establishment of an activity-based classification of the Bcl-2 TMD-derived peptides. Overall, both biophysical and cellular data point toward a clear correlation between mitochondrial membrane insertion/perturbation capability and cellular activity (Figure 6.8g and Figure 6.16), sustaining an active role of these peptides in MOMP.

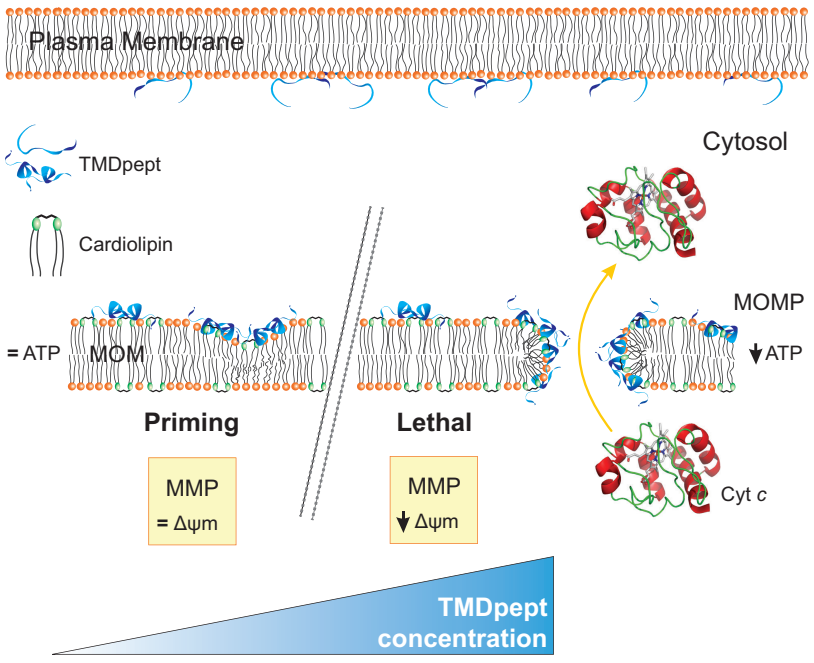

Figure 6.16. Preferential TMD-pepts binding to mitochondrial membrane induces mitochondrial membrane disruption. Schematic representation depicting the relatively low binding of TMD-pepts to the plasma membrane compared to its higher binding to the mitochondrial membrane. This preferential binding disrupts the mitochondrial membrane structure leading to Cyt-*c* release to the cytosol.

The control of apoptosis exerted by Bcl-2 proteins has led to the use of BH3-derived peptides and BH3 mimetics as potential drugs to improve cancer treatments (307, 324, 326, 431). Targeting the BH3 domain of Bcl2 proteins to induce apoptosis in cancer cells is not always effective and mostly depends on pro-survival Bcl2 members (393, 432, 433). Therefore, combination treatments have emerged as novel pharmacological strategies to avoid toxicities and increase efficacy of anti-tumor treatments (342, 394, 434). In this scenario, we demonstrate that the combination of CDDP with sub-lethal dosages of TMD-pepts, especially TMD-Bcl-xL and TMD-Bak, increases its pro-apoptotic activity, exerting a mitochondrial priming effect. We speculate that TMD-pepts need direct or indirect interactions with the Bcl-2 network to produce the apoptotic priming effect.

In light of the TMD-pepts effect in mitochondrial priming, we envisage that Bcl-2-derived TMD-pepts have the potential to make significant contributions to our understanding of apoptosis-induced clinical disorders and to establish a basis for the design of new cancer therapeutics.

CHAPTER

IV

BH3-mimetics- and cisplatin-induced cell death proceeds through different pathways depending on the availability of death-related cellular components.

7.1. Introduction.

Current anti-tumour treatments based in inducing apoptosis target cancer cells and rapidly dividing normal cells as well as other especially sensitive differentiated cells. Therefore, these treatments do not differentiate between malignant and normal cells. Chemotherapy causes toxicity, leading to side effects like those reported for apoptosis-inducing and DNA-damaging agent cisplatin (cis-diammineplatinum(II) dichloride, CDDP), which induces ototoxicity (435) and alopecia (436). These undesirable effects may be ameliorated by the discovery of new more specific cell death-inducing drugs (437), or by selectively and locally inhibiting apoptosis in defined sensitive cells.

The proposal of developing BH3-mimetics as chemotherapeutic drugs originates from understanding the role of the Bcl-2 protein family in regulating the intrinsic apoptotic pathway by controlling mitochondria outer membrane permeability (MOMP). The small molecule compounds developed as inhibitors of anti-apoptotic Bcl-2 proteins, generically named BH3-mimetics such as ABT-737 (Abbott Laboratories) or obatoclax (GX15-070, Gemin X Biotechnologies), release pro-apoptotic binding partners and suffice to induce apoptosis. ABT-737 binds selectivity to anti-apoptotic Bcl-2, but has a low affinity to Mcl-1 and A1 (307, 438). GX15-070 has been proposed to influence the activity of the Bak/Mcl-1 and Bim/Mcl-1 complexes (320) to induce mitochondrial- mediated apoptosis, which would imply Bax/Bak-mediated MOMP and apoptosome-mediated activation of caspases. However, in some cell lines that are relevant for disease, GX15-070-treatment has also been described to render phenotypic cell characteristics, which could be associated with GX15-070 activities, including autophagy, independently of mitochondrial-mediated apoptosis. The cytotoxic activity of GX15-070 and ABT-737 in Bax/Bak double knockout cells has also been reported (305, 322), while the role of the apoptosome (Figure 7.1) is unclear as it is still to be explored in detail. This is particularly relevant for studying the activity of BH3-mimetics in cells with low Apaf-1 contents that correlate with resistance to chemotherapeutic treatments (439, 440) and for preclinically evaluating a new class of apoptosis inhibitors targeting the apoptosome (441, 442), which are currently being evaluated as agents to locally prevent chemotherapy-induced secondary effects. It would then be of interest to comparatively analyze the activity of BH3-mimetics and CDDP (as a representative of established cytotoxic drugs) in cells in which Apaf-1 has been genetically deleted and to also analyze whether apoptosome inhibitors can inhibit BH3-mimetics-induced cell death.

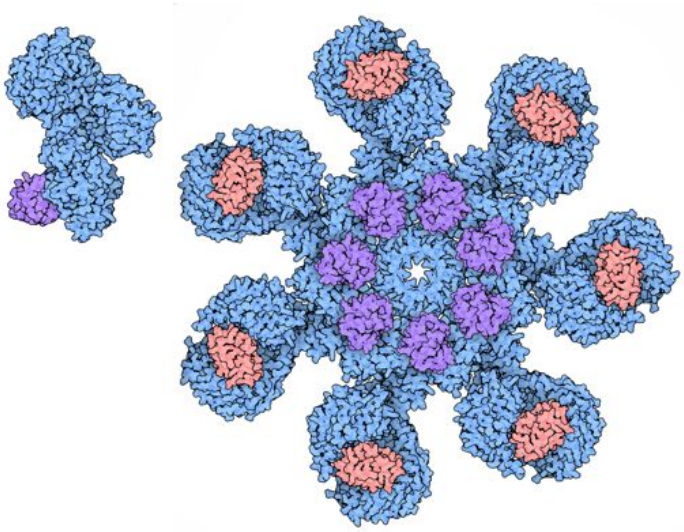

Figure 7.1. **The structure of apoptosome complex.** Cytochrome *c* (showed in red) is released from mitochondria when apoptotis is induced and it binds to the cytosolic protein Apaf-1 (blue) to facilitate the formation of apoptosome in the presence of dATP (purple), the third component of the complex. Once formed, the apoptosome can then recruit and activate the inactive pro-caspase-9. Once activated, this initiator caspase can then activate effector caspases and trigger a cascade of events leading to apoptosis. (http://www.rcsb.org/pdb/101/motm.do?momID=177)

7.2. Results and discussion.

7.2.1. Apaf-1 inhibitor QM31 reduces the activation of apoptosis promoted by different apoptotic inductors.

The immortalisation process may affect the genetic background of mouse embryonic fibroblasts (MEFs) cell lines and might be responsible for the differences observed in the behavior of the different MEFs knock out (KO) Apaf1 cellular models. For this reason, it was initially analysed the apoptotic response to ABT-737 of the embryonic fibroblast wild-type (WT) MEFs and Apaf1 KO mouse (MEFs KO Apaf1) cell lines, (351) which were previously established by spontaneous immortalisation (SIM) or by infection with SV40 antigen T (SV40IM) (443). ABT-737 treatment induced activation of caspase-3, release of Cyt-*c* and death in SV40IM-MEFs WT. However in SV40IM-MEFs KO Apaf-1 and SIM-MEFs, these parameters remain unaffected (Figure 7.2A,B and C) (444). These results suggest that ABT-737 trigger signalling is not fully perceived by the Apaf-1 SIM-MEFs cells. Thus, the immortalisation process may affect the genetic background

and might be responsible for the differences between both MEFs cellular models. For this reason, we selected SV40IM-MEFs to evaluate the response of different cells lines towards several apoptotic insults.

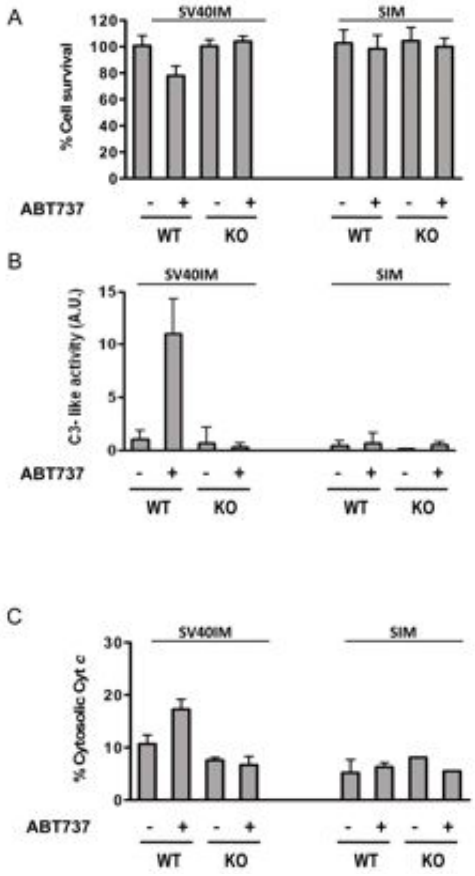

Figure 7.2. ABT-737 treatment induces cell death in SV40IM WT MEFs but not SV40IM KO MEFs and SIM MEFs. (A) Percentage of cell survival measured by the trypan blue exclusion assay in SV40IM and SIM MEFs, WT and Apaf1 depleted, in the presence or absence of ABT-737 (20 μM) for 24 h. (B) Caspase-3 like activity was measured under the same conditions described above. (C) Cells with Cyt-c released measured by the flow cytometry analysis after incubation with ABT-737 (20 μM) for 24 h. In all cases, bars represent the mean of three experiments ± s.d.

MEFs from wild-type mouse (MEFs wt Apaf-1 and MEFs wt Bax/Bak) (351) were treated with ABT-737, GX15-070 or cisplatin (cis-diammineplatinum(II) dichloride, CDDP), either alone or in combination with apoptosome inhibitor compound QM31 (441,

442), or with broad spectrum caspase inhibitor Z-Val-Ala-Asp(OMe)-fluoromethylketone (zVADfmk).

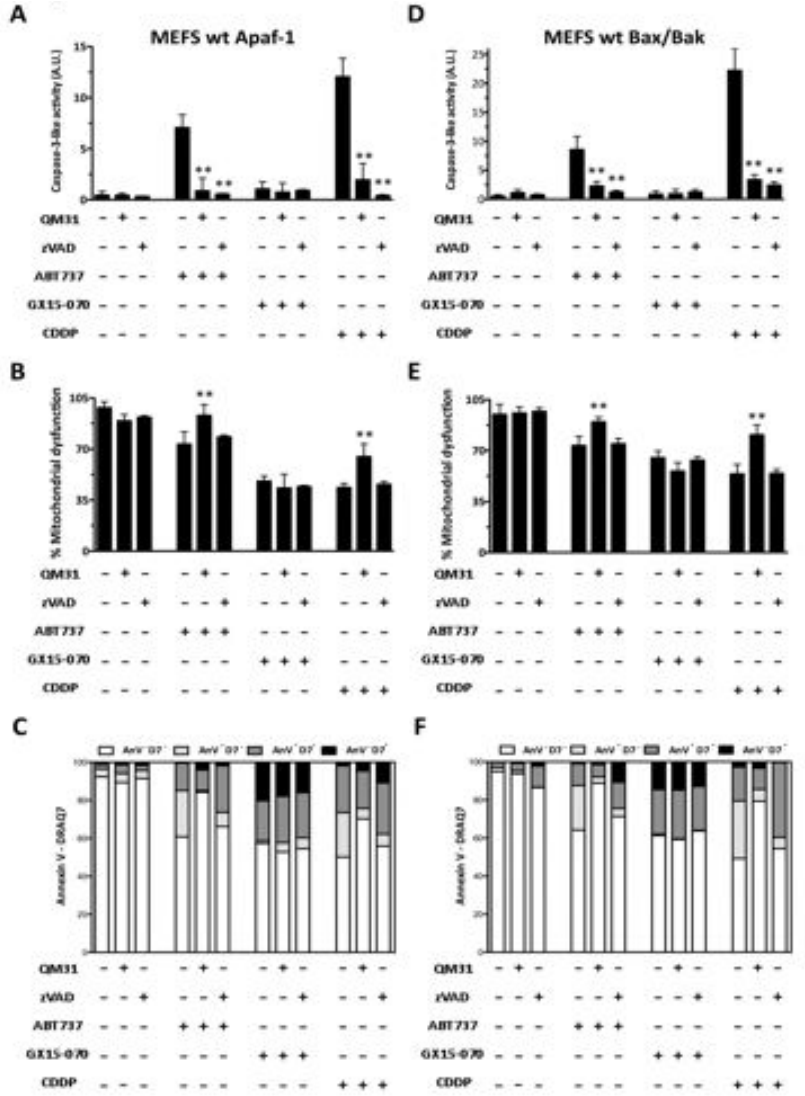

Figure 7.3. **Apaf-1 inhibitor QM31 prevents cell death in non tumor cells treated with both ABT-737 and CDDP, but not in cells treated with GX15-070**. (A and D) Caspase 3-like activity was measured in MEFs wt Apaf-1 and MEFs wt Bax/Bak treated with ABT-737 (25 μM), GX15-070 (1 μM) and CDDP (30 μM) in the presence or absence of QM31 (10 μM) and zVADfmk (5 μM). (B and E) Mitochondrial dysfunction was measured by an MTT assay under the same conditions described above. Bars represent the mean of three experiments ± s.d. (**p,0.05). (C and F) Apoptotic cell death was determined by flow cytometry with FITC Annexin V and DRAQ7. Data are representative results of three independent experiments.

Cultured cells were evaluated at 24 h post-treatment. ABT-737 and CDDP treatments induced activation of caspase-3, which was inhibited by zVADfmk and by QM31. However, when cells were treated with GX15-070, only residual caspase-3 activity was observed (Figure 7.3A and D). Cell viability was determined by MTT (Figure 7.3B and E) to find that ABT-737- and CDDP-induced death (20% and 60%, respectively) was inhibited by QM31, but not by zVADfmk, while the cell death induced by GX15-070 (around 50%) was not inhibited by either zVADfmk or QM31. Annexin V/DRAQ7 flow cytometry assays corroborate viability and apoptotic cell death results (Figure 7.3C and F).

7.2.2. QM31 needs the presence of Apaf-1 and the Bax/Bak pro-apoptotic effectors to block apoptosis. Obatoclax and CDDP induce cell death by dependent and non-dependent apoptotic mechanism.

The same experiments were conducted in Apaf-1 knockout (KO) mouse embryonic fibroblasts (MEFs KO Apaf-1) (351), in MEFs KO Bax/Bak (84) and in cervix adenocarcinoma cells (HeLa). In MEFs KO Apaf-1 (Figure 7.4A) and MEFs KO Bax/Bak (Figure 7.4D), none of the treatments induced caspase-3 activity, while cell viability was unaffected by the ABT-737 treatment, but decreased with both GX15-070 and CDDP treatments (Figure 7.4B and E). GX15-070- and CDDP- induced cell death in these cells was not inhibited upon apoptosome or caspase inhibition. Consequently, treatments with QM31 and zVADfmk did not significantly modify the percentage of Annexin V stained cells (Figure 7.4C and F).

BH3-mimetics- and cisplatin-induced cell death proceeds through different pathways depending on the availability of death-related cellular components.

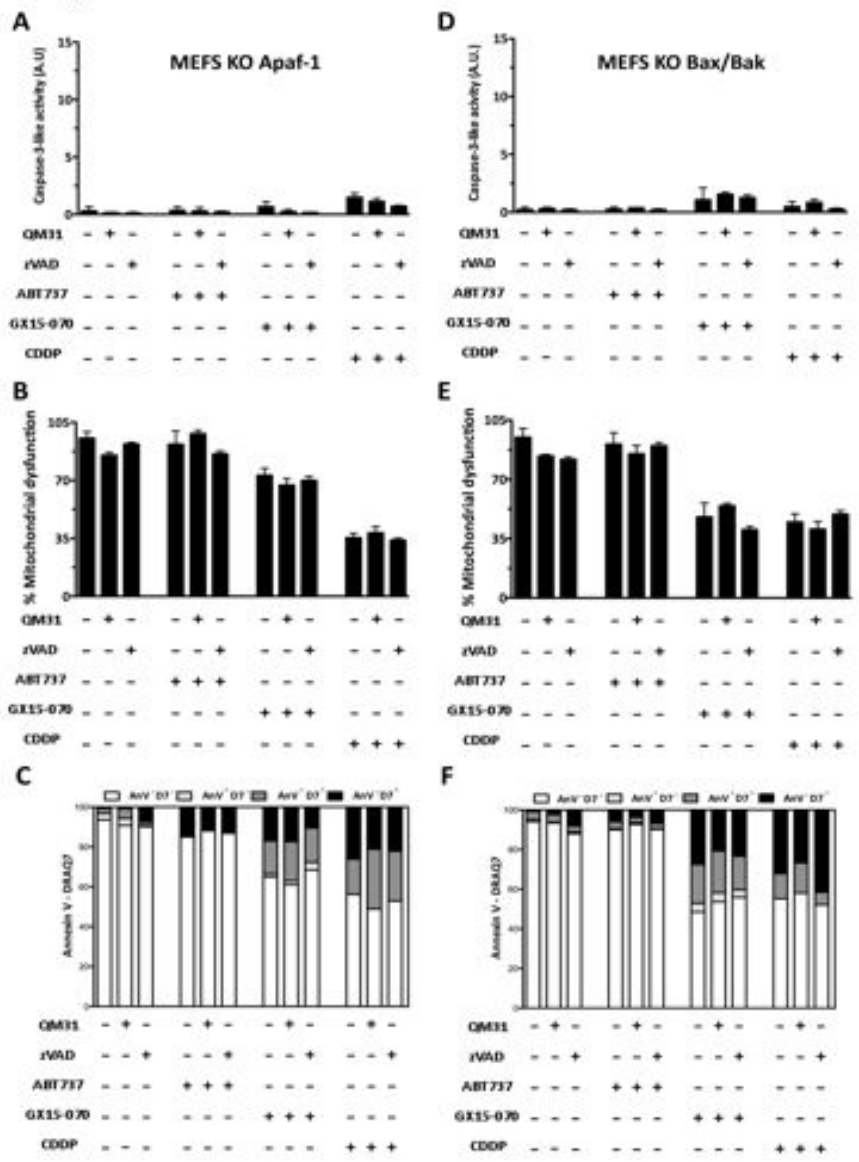

Figure 7.4. GX15-070 and CDDP induce caspase 3 independent cell death in Apaf-1 and Bax/Bak deficient cells. (A and D) Caspase 3- like activity was measured in MEFs KO Apaf-1 and MEFs KO Bax/Bak treated with ABT-737 (25 μM), GX15-070 (1 μM) and CDDP (30 μM) in the presence or absence of QM31 (10 μM) and zVADfmk (5 μM). (B and E) Mitochondrial dysfunction was measured by an MTT assay under the same conditions described above. Bars represent the mean of three experiments ± s.d. (C and F) Apoptotic cell death was analyzed by flow cytometry with FITC Annexin V and DRAQ7. Data are representative results of three independent experiments.

BH3-mimetics- and cisplatin-induced cell death proceeds through different pathways depending on the availability of death-related cellular components.

These results suggest that in the absence of key death-related cellular components, such as the Bcl-2 proteins Bax and Bak and the apoptosome constituent protein Apaf-1, ABT-737-triggering signaling is not fully perceived by the cell, while CDDP-depending signaling found caspase- independent cell death pathways. CDDP-induced cell death was partially recovered by necrostatin-1 (Nec), an inhibitor of RIPK1 in MEFs KO Apaf-1 and MEFs KO Bax/Bak (Figure 7.5A), suggesting that necroptosis (a form of programmed necrosis that depends on activity of RIPK1) could participate in CDDP-induced death in these cells. In fact, nuclear staining upon CDDP treatment showed non apoptotic cell death in MEFs KO Apaf-1 and MEFs KO Bax/Bak cells (Figure 7.5B), while treatment induced canonical apoptotic bodies in MEFs wt Apaf-1, indicating that DNA damaging agents may activate alternative cell death pathways when the intrinsic pathway of apoptosis is blocked.

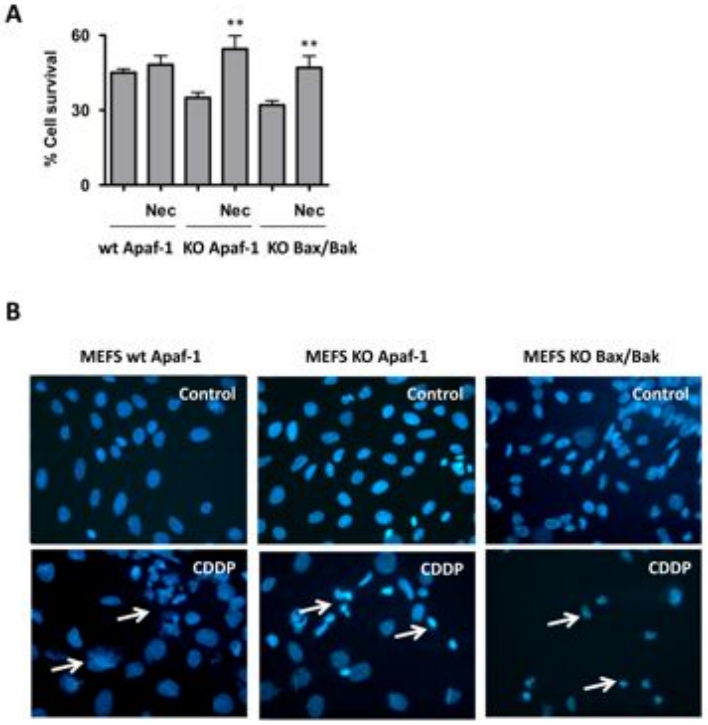

Figure 7.5. Non apoptotic cell death upon CDDP treatment in Apaf-1- and Bax/Bak-deficient cells. (A) Cell survival was measured by trypan blue exclusion upon treatment with CDDP (30 μM) in the presence or absence of necrostatin (Nec; 100 μM). Bars represent the mean of three experiments ± s.d. (**p,0.05). (B) MEFs wt Apaf-1, MEFs KO Apaf-1 and MEFs KO Bax/Bak were stained with DAPI upon CDDP (30 μM) treatment. Nuclei are considered to have the normal phenotype when glowing bright and homogenously. Apoptotic nuclei can be identified by the fragmented morphology of nuclear bodies. White arrows indicate dying cells.

BH3-mimetics- and cisplatin-induced cell death proceeds through different pathways depending on the availability of death-related cellular components.

In human cervix adenocarcinoma (HeLa) cells, rather than inducing caspase-3 activity, GX15-070 induced a type of cell death that was not inhibited by zVADfmk or QM31 (Figure 7.6A, B and C), which correlates with the phenotypes observed in all the MEFs cell lines. CDDP induced caspase-3 activation, which was inhibited in the presence of QM31 or zVADfmk (Figure 7.6A), and also generated cell death (Figure 7.6B and C). CDDP-induced death was partially prevented by QM31, but not by zVADfmk (Figure 7.6B and C). Nonetheless, the zVADfmk inhibition of ABT-737-induced cas- pase-3 activity was unable to protect cells from dying (Figure 7.6B and C). Interestingly, and unlike the results found in the MEFs wt, apoptosome inhibition by QM31 did not inhibit ABT-737-induced caspase-3 and cell death (Figure 7.6A and C).

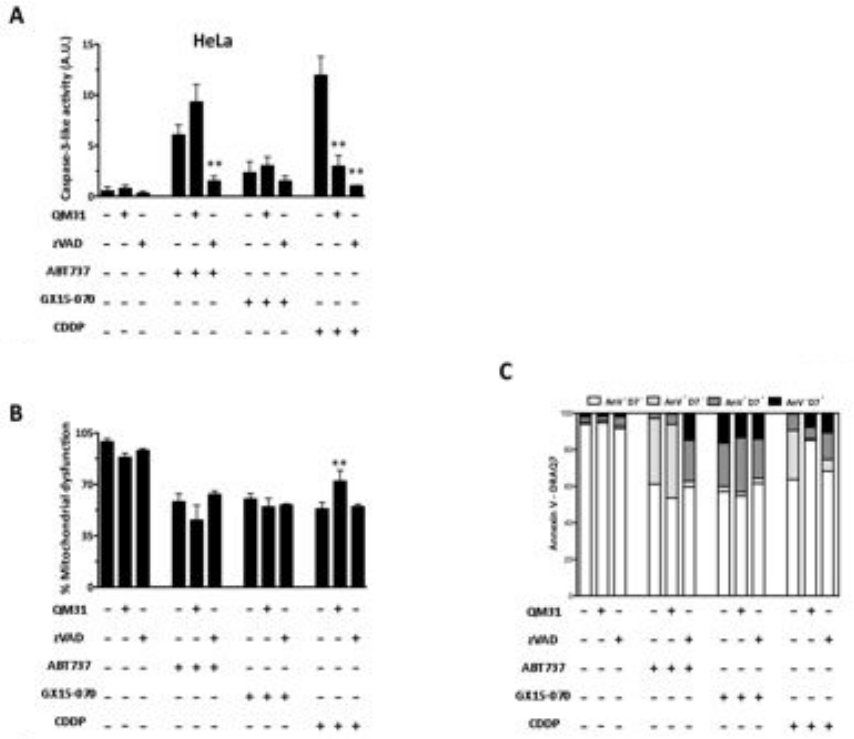

Figure 7.6. Apaf-1 inhibition does not protect tumor HeLa cells from death induced by ABT-737 and GX15-070. (A) Caspase 3-like activity was measured in the HeLa cells treated with ABT-737 (25 μM), GX15-070 (1 μM) and CDDP (30 μM) in the presence or absence of QM31 (10 μM) and zVADfmk (5 μM). (B) Mitochondrial dysfunction was measured by an MTT assay under the same conditions described above. Bars represent the mean of three experiments ± s.d. (*p,0.1; **p,0.05). (C) Apoptotic cell death was analyzed by flow cytometry with FITC Annexin V and DRAQ7. Data are representative results of three independent experiments.

BH3-mimetics- and cisplatin-induced cell death proceeds through different pathways depending on the availability of death-related cellular components.

7.2.3. Obatoclax (GX15-070) acts as autophagy activator.

To proceed with an initial analysis of the cell death pathway induced by GX15-070 in the MEFs wt Apaf-1, MEFs wt Bax/ Bak, MEFs KO Apaf-1, MEFs KO Bax/Bak, and HeLa cells, we analyzed the expression of anti-apoptotic proteins Bcl-2, Bcl-xL and Mcl-1 and found no significant changes (data not shown). We also explored the induction of autophagy. Autophagy is a catabolic process involving the formation of autophagosomes and autolysosomes. Light chain 3 (LC3, a mammalian ortholog of yeast Atg8 (445)) is essential for autophagosome formation and can be used as a reporter protein. When the process of autophagy proceeds, LC3-I (the cytosolic form) is processed to the autophagosomal membrane-bound LC3-II form (445). The LC3-II form increased considerably with GX15-070 treatment (Figure 7.7A–E), suggesting that evaluated GX15-070-induced cell death was mediated by autophagy activation in all the cell lines.

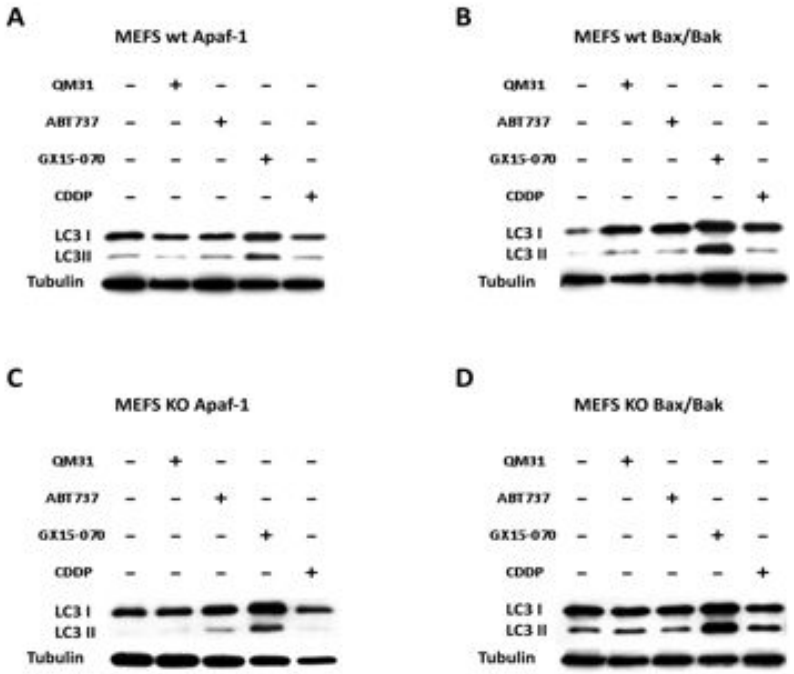

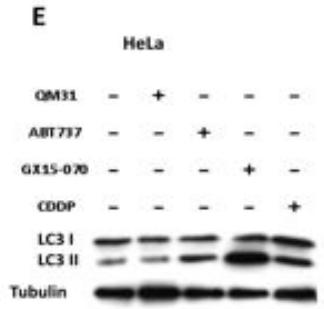

Figure 7.7. GX15-070 promotes the activation of the autophagic pathway via LC3 in all the cell lines. (A–E) LC3 detection in MEFs wt Apaf-1, MEFs wt Bax/Bak, MEFSs KO Apaf-1, MEFs KO Bax/Bak and HeLa cells treated 24h with ABT-737 (25 μM), GX15-070 (1 μM), CDDP (30 μM) and QM31 (10 μM).

The activity of III phosphoinositide 3-kinase (PI3K III) is important in Beclin-1 (the human ortholog of yeast Atg-6)-induced autophagy (446), and 3-methyladenine (3MA, an inhibitor of PI3K III) is commonly used to determine the dependence of Beclin-1 in autophagy. 3MA did not modify GX15-070-induced LC3 processing (Fig. 7.8). Therefore, GX15-070-induced autophagy in both MEFs wt and MEFs KO Apaf-1 is independent of Beclin-1, as also reported for MEFs KO Bax/Bak and HeLa cells (322). As an internal control, we induced autophagy by rapamycin and found that rapamycin-induced autophagy was inhibited by 3MA in all four cell lines analyzed (Fig. 7.8A-D).

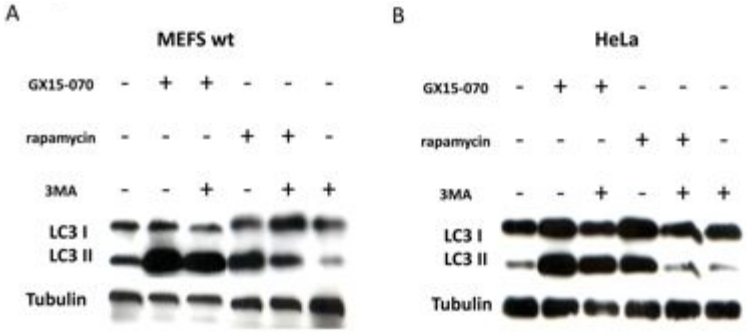

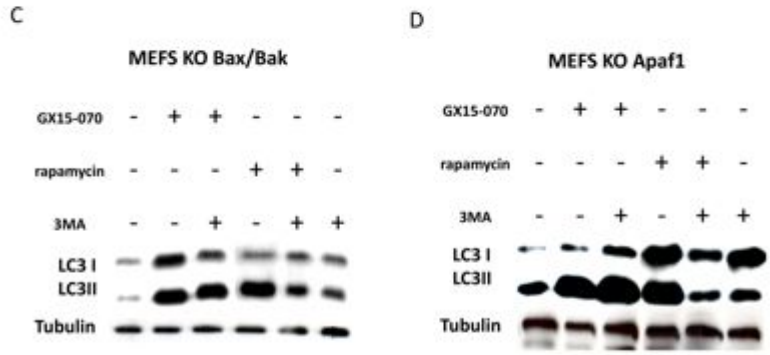

Figure 7.8. GX15-070 activates Beclin-1 non-dependent autophagy in all the cell lines. (A–D) LC3 immunoblotting in the MEFs wt Apaf-1, MEFs KO Apaf-1, MEFs KO Bax/Bak and HeLa cell lines treated with rapamycin (30 μM) and GX15-070 (1 μM) for 24 h in the presence or absence of 3MA (10 μM).

It has been reported that GX15-070 is able to induce apoptosis and autophagy in several cell lines (447). Thus we performed a time-course analysis to examine whether GX15-070-treatment induces both autophagy and apoptosis. We used LC3 conversion as a marker of autophagy (Fig. 7.7) and caspase-3 activity as a marker of apoptosis. After 24 h we did not observe GX15-070-induced caspase-3 activation in the cell lines analyzed in the present study (Fig. 7.9). At 48 h however, we noted that GX15-070- induced caspase-3 activity in both MEFs wt and in HeLa cells.

GX15-070-induced apoptosis at 48 h was inhibited by apoptosome inhibitor QM31. In contrast, GX15-070 did not induce apoptosis in MEFs KO Bax/Bak and in MEFs KO Apaf-1 at 48 h. These results suggest that GX15-070 can induce multiple cell death pathways, such as caspase-dependent apoptosis and autophagy. Nevertheless, GX15-070-induced apoptosis is not only dependent in Bax/Bak, as previously demonstrated (322, 447), but also in Apaf-1.

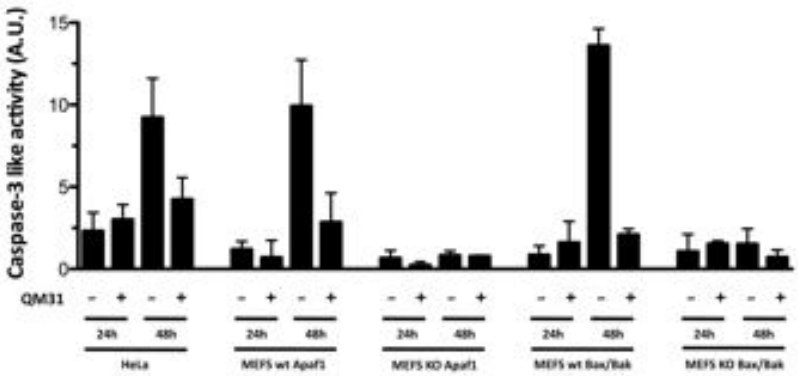

Figure 7.9. GX15-070 induces caspase 3-like activity after 48 h in HeLa and MEFs wt. Caspase 3-like activity was measured at 24 h and 48 h upon treatment with GX15-070 (1 μM) in the presence or absence of QM31 (10 μM) in HeLa, MEFs wt Apaf-1, MEFs KO Apaf-1, MEFs wt Bax/Bak and MEFs KO Bax/Bak.

7.3. Concluding remarks.

In conclusion, the present study reveals that BH3-mimetic ABT-737 not only requires Bax/Bak to exert its apoptosis-inducing effect, but also Apaf-1, indicating the exclusive targeting of ABT-737 to Bcl-2 anti-apoptotic proteins. ABT-737 upon binding to Bcl-2 and Bcl-xL removes the anti-apoptotic activity of these proteins in pro-apoptotic Bax/Bak and induces MOMP. However, MOMP-dependent signaling needs the components of the apoptotic pathway downstream of mitochondria, such as the formation of the apoptosome, to induce cell death. Hence, ABT-737 treatments to cancer cells would have less side effects to differentiated cells containing low levels of Apaf-1, such as neurons and cardiomyocytes (448, 449), than other treatments with lesser dependence of Apaf-1. In contrast, BH3-mimetic GX15-070 and DNA damage-inducing CDDP induce cell death in the absence of both Bax/Bak and Apaf-1. While GX15-070 induces mainly autophagy-based cell death at 24 h, a cell fraction dies by apoptosis at longer times post-treatment (48h). On the other hand, CDDP induces necroptosis when apoptosis signaling pathway is not available. Our results extend findings by describing not only the sensitivity of different cells to the cell-inducing agents explored, but also the behavior of current apoptosis inhibitors, which could be useful in topical applications aimed to diminish unwanted cell death. Non tumor cells, as demonstrated herein with MEFs wt, could be protected from the cytotoxic effects of ABT-737 and CDDP by the chemical inhibition of the apoptosome through QM31, which lowered caspase-3 activity and improved cell survival, while the use of caspase inhibitors prevented caspase activation, but did not improve survival. This scenario correlates with proposals in mammals that solely caspase inhibition, downstream of MOMP delays, and in defined circumstances, modifies the outcome rather than preventing cell death (450). However, the autophagy-based cell death induced by GX15-070 was not prevented by QM31 or caspase inhibitors. These results will be of interest when defining future combination therapies where the systemic administration of cytotoxic agents, which aims to kill malignant cells, could be locally counteracted by apoptosis inhibitors. For instance, dermatopic and intra-cochlear administration of apoptosome inhibitors would probably find applications as anti-alopecia and anti-ototoxic agents, respectively, for anti-cancer treatments based on ABT-7373 and CDDP.

CONCLUSIONS

- The results of this Thesis show that BCL-2 TMDs are not isolated in the mitochondrial membrane and establish for the first time the putative interaction map of BCL-2 TMDs. In addition, the potential contribution of these TMDs to apoptotic regulation has been demonstrated. BCL-2 TMDs, together with soluble domains, participate in the equilibria that govern MOMP.

- In the subfamily of BH3-only proteins, we have demonstrated that the predicted TMDs of Bik, Puma and Bim are able to insert in cellular membranes efficiently. These results open the field to study potential interactions with other Bcl-2 TMDs. In contrast, Noxa and Bmf TMD show low insertion capability in cellular membranes.

- The studies with Bcl-2 TMD derived peptides have demonstrated that some TMD-pepts can integrate specifically into mitochondrial membranes. Moreover, Bcl-2, Bcl-xL, Bax and Bak TMD-pepts induce Cyt-*c* release. Consequently, insertion of these peptides induces cell death or synergizes at sublethal concentrations with chemotherapeutic treatments.

- BH3-mimetic ABT-737 not only requires Bax/Bak to exert its apoptosis-inducing effect, but also Apaf-1, while GX15-070 and CDDP induce different modalities of cell death in the absence of Bax/Bak or Apaf-1. Apoptosome inhibitor QM31 protects from the cytosolic effects of ABT-737 and partially against CDDP but not against the autophagy-based cell death induced by GX15-070.

BIBLIOGRAPHY

1. Clarke PG & Clarke S (1995) Historic apoptosis. *Nature* 378(6554):230.
2. Lockshin RA & Williams CM (1965) Programmed Cell Death--I. Cytology of Degeneration in the Intersegmental Muscles of the Pernyi Silkmoth. *Journal of insect physiology* 11:123-133.
3. Kerr JF, Wyllie AH, & Currie AR (1972) Apoptosis: a basic biological phenomenon with wide-ranging implications in tissue kinetics. *British journal of cancer* 26(4):239-257.
4. Galluzzi L*, et al.* (2012) Molecular definitions of cell death subroutines: recommendations of the Nomenclature Committee on Cell Death 2012. *Cell Death Differ* 19(1):107-120.
5. Galluzzi L*, et al.* (2014) Essential versus accessory aspects of cell death: recommendations of the NCCD 2015. *Cell death and differentiation*.
6. Horvitz HR (1999) Genetic control of programmed cell death in the nematode Caenorhabditis elegans. *Cancer research* 59(7 Suppl):1701s-1706s.
7. Hengartner MO & Horvitz HR (1994) Programmed cell death in Caenorhabditis elegans. *Current opinion in genetics & development* 4(4):581-586.
8. Zou H, Li Y, Liu X, & Wang X (1999) An APAF-1.cytochrome c multimeric complex is a functional apoptosome that activates procaspase-9. *The Journal of biological chemistry* 274(17):11549-11556.
9. Kroemer G*, et al.* (2005) Classification of cell death: recommendations of the Nomenclature Committee on Cell Death. *Cell death and differentiation* 12 Suppl 2:1463-1467.
10. Kroemer G*, et al.* (2009) Classification of cell death: recommendations of the Nomenclature Committee on Cell Death 2009. *Cell death and differentiation* 16(1):3-11.
11. Miura M (2011) Active participation of cell death in development and organismal homeostasis. *Development, growth & differentiation* 53(2):125-136.
12. Norbury CJ & Hickson ID (2001) Cellular responses to DNA damage. *Annual review of pharmacology and toxicology* 41:367-401.
13. Adams JM & Cory S (2007) Bcl-2-regulated apoptosis: mechanism and therapeutic potential. *Current opinion in immunology* 19(5):488-496.
14. Strasser A, Cory S, & Adams JM (2011) Deciphering the rules of programmed cell death to improve therapy of cancer and other diseases. *The EMBO journal* 30(18):3667-3683.
15. Elmore S (2007) Apoptosis: a review of programmed cell death. *Toxicologic pathology* 35(4):495-516.
16. Tsujimoto Y*, et al.* (1984) Molecular cloning of the chromosomal breakpoint of B-cell lymphomas and leukemias with the t(11;14) chromosome translocation. *Science* 224(4656):1403-1406.
17. Vaux DL, Cory S, & Adams JM (1988) Bcl-2 gene promotes haemopoietic cell survival and cooperates with c-myc to immortalize pre-B cells. *Nature* 335(6189):440-442.
18. Golstein P & Kroemer G (2007) Cell death by necrosis: towards a molecular definition. *Trends in biochemical sciences* 32(1):37-43.
19. Degterev A*, et al.* (2005) Chemical inhibitor of nonapoptotic cell death with therapeutic potential for ischemic brain injury. *Nature chemical biology* 1(2):112-119.
20. Proskuryakov SY, Konoplyannikov AG, & Gabai VL (2003) Necrosis: a specific form of programmed cell death? *Experimental cell research* 283(1):1-16.
21. Whelan RS*, et al.* (2012) Bax regulates primary necrosis through mitochondrial dynamics. *Proceedings of the National Academy of Sciences of the United States of America* 109(17):6566-6571.
22. Mizushima N & Kuma A (2008) Autophagosomes in GFP-LC3 Transgenic Mice. *Methods in molecular biology* 445:119-124.

23. Meijer AJ & Codogno P (2009) Autophagy: regulation and role in disease. *Critical reviews in clinical laboratory sciences* 46(4):210-240.
24. Baehrecke EH (2005) Autophagy: dual roles in life and death? *Nature reviews. Molecular cell biology* 6(6):505-510.
25. White E (2012) Deconvoluting the context-dependent role for autophagy in cancer. *Nature reviews. Cancer* 12(6):401-410.
26. Kundu M & Thompson CB (2008) Autophagy: basic principles and relevance to disease. *Annual review of pathology* 3:427-455.
27. Levine B, Sinha S, & Kroemer G (2008) Bcl-2 family members: dual regulators of apoptosis and autophagy. *Autophagy* 4(5):600-606.
28. Maiuri MC*, et al.* (2007) BH3-only proteins and BH3 mimetics induce autophagy by competitively disrupting the interaction between Beclin 1 and Bcl-2/Bcl-X(L). *Autophagy* 3(4):374-376.
29. Gonzalez-Polo RA*, et al.* (2005) The apoptosis/autophagy paradox: autophagic vacuolization before apoptotic death. *Journal of cell science* 118(Pt 14):3091-3102.
30. Vercammen D*, et al.* (1998) Dual signaling of the Fas receptor: initiation of both apoptotic and necrotic cell death pathways. *The Journal of experimental medicine* 188(5):919-930.
31. Han W, Xie J, Li L, Liu Z, & Hu X (2009) Necrostatin-1 reverts shikonin-induced necroptosis to apoptosis. *Apoptosis : an international journal on programmed cell death* 14(5):674-686.
32. Liu P*, et al.* (2012) Dysregulation of TNFalpha-induced necroptotic signaling in chronic lymphocytic leukemia: suppression of CYLD gene by LEF1. *Leukemia* 26(6):1293-1300.
33. Lieberthal W, Triaca V, & Levine J (1996) Mechanisms of death induced by cisplatin in proximal tubular epithelial cells: apoptosis vs. necrosis. *The American journal of physiology* 270(4 Pt 2):F700-708.
34. Leontieva OV, Gudkov AV, & Blagosklonny MV (2010) Weak p53 permits senescence during cell cycle arrest. *Cell cycle* 9(21):4323-4327.
35. Salvesen GS & Renatus M (2002) Apoptosome: the seven-spoked death machine. *Developmental cell* 2(3):256-257.
36. Igney FH & Krammer PH (2002) Death and anti-death: tumour resistance to apoptosis. *Nature reviews. Cancer* 2(4):277-288.
37. Green DR (2005) Apoptotic pathways: ten minutes to dead. *Cell* 121(5):671-674.
38. Ashkenazi A & Dixit VM (1998) Death receptors: signaling and modulation. *Science* 281(5381):1305-1308.
39. Ashkenazi A (2002) Targeting death and decoy receptors of the tumour-necrosis factor superfamily. *Nature reviews. Cancer* 2(6):420-430.
40. Wajant H, Pfizenmaier K, & Scheurich P (2002) TNF-related apoptosis inducing ligand (TRAIL) and its receptors in tumor surveillance and cancer therapy. *Apoptosis : an international journal on programmed cell death* 7(5):449-459.
41. Kischkel FC*, et al.* (1995) Cytotoxicity-dependent APO-1 (Fas/CD95)-associated proteins form a death-inducing signaling complex (DISC) with the receptor. *The EMBO journal* 14(22):5579-5588.
42. Fulda S, Meyer E, & Debatin KM (2002) Inhibition of TRAIL-induced apoptosis by Bcl-2 overexpression. *Oncogene* 21(15):2283-2294.
43. Orzaez M, Gortat A, Mondragon L, & Perez-Paya E (2009) Peptides and peptide mimics as modulators of apoptotic pathways. *ChemMedChem* 4(2):146-160.
44. Green DR & Kroemer G (2004) The pathophysiology of mitochondrial cell death. *Science* 305(5684):626-629.

45. Zamzami N, *et al.* (1995) Reduction in mitochondrial potential constitutes an early irreversible step of programmed lymphocyte death in vivo. *The Journal of experimental medicine* 181(5):1661-1672.
46. Petit PX, *et al.* (1995) Alterations in mitochondrial structure and function are early events of dexamethasone-induced thymocyte apoptosis. *The Journal of cell biology* 130(1):157-167.
47. Saelens X, *et al.* (2004) Toxic proteins released from mitochondria in cell death. *Oncogene* 23(16):2861-2874.
48. Garrido C, *et al.* (2006) Mechanisms of cytochrome c release from mitochondria. *Cell death and differentiation* 13(9):1423-1433.
49. Liu X, Kim CN, Yang J, Jemmerson R, & Wang X (1996) Induction of apoptotic program in cell-free extracts: requirement for dATP and cytochrome c. *Cell* 86(1):147-157.
50. Li P, *et al.* (1997) Cytochrome c and dATP-dependent formation of Apaf-1/caspase-9 complex initiates an apoptotic protease cascade. *Cell* 91(4):479-489.
51. van Loo G, *et al.* (2002) The serine protease Omi/HtrA2 is released from mitochondria during apoptosis. Omi interacts with caspase-inhibitor XIAP and induces enhanced caspase activity. *Cell death and differentiation* 9(1):20-26.
52. Schimmer AD, *et al.* (2004) Small-molecule antagonists of apoptosis suppressor XIAP exhibit broad antitumor activity. *Cancer cell* 5(1):25-35.
53. Susin SA, *et al.* (1999) Molecular characterization of mitochondrial apoptosis-inducing factor. *Nature* 397(6718):441-446.
54. Li LY, Luo X, & Wang X (2001) Endonuclease G is an apoptotic DNase when released from mitochondria. *Nature* 412(6842):95-99.
55. Cory S & Adams JM (2002) The Bcl2 family: regulators of the cellular life-or-death switch. *Nature reviews. Cancer* 2(9):647-656.
56. Youle RJ & Strasser A (2008) The BCL-2 protein family: opposing activities that mediate cell death. *Nat Rev Mol Cell Biol* 9(1):47-59.
57. Chipuk JE, Moldoveanu T, Llambi F, Parsons MJ, & Green DR (2010) The BCL-2 family reunion. *Molecular cell* 37(3):299-310.
58. Huang DC & Strasser A (2000) BH3-Only proteins-essential initiators of apoptotic cell death. *Cell* 103(6):839-842.
59. Chen L, *et al.* (2005) Differential targeting of prosurvival Bcl-2 proteins by their BH3-only ligands allows complementary apoptotic function. *Molecular cell* 17(3):393-403.
60. Hinds MG, *et al.* (2007) Bim, Bad and Bmf: intrinsically unstructured BH3-only proteins that undergo a localized conformational change upon binding to prosurvival Bcl-2 targets. *Cell death and differentiation* 14(1):128-136.
61. Borner C, *et al.* (1994) The protein bcl-2 alpha does not require membrane attachment, but two conserved domains to suppress apoptosis. *The Journal of cell biology* 126(4):1059-1068.
62. Schlesinger PH, *et al.* (1997) Comparison of the ion channel characteristics of proapoptotic BAX and antiapoptotic BCL-2. *Proceedings of the National Academy of Sciences of the United States of America* 94(21):11357-11362.
63. Hinds MG, *et al.* (2003) The structure of Bcl-w reveals a role for the C-terminal residues in modulating biological activity. *Embo J* 22(7):1497-1507.
64. Suzuki M, Youle RJ, & Tjandra N (2000) Structure of Bax: coregulation of dimer formation and intracellular localization. *Cell* 103(4):645-654.
65. Muchmore SW, *et al.* (1996) X-ray and NMR structure of human Bcl-xL, an inhibitor of programmed cell death. *Nature* 381(6580):335-341.
66. Hossini AM, Geilen CC, Fecker LF, Daniel PT, & Eberle J (2006) A novel Bcl-x splice product, Bcl-xAK, triggers apoptosis in human melanoma cells without BH3 domain. *Oncogene* 25(15):2160-2169.

67. Plotz M, Gillissen B, Hossini AM, Daniel PT, & Eberle J (2012) Disruption of the VDAC2-Bak interaction by Bcl-x(S) mediates efficient induction of apoptosis in melanoma cells. *Cell death and differentiation* 19(12):1928-1938.
68. Basanez G*, et al.* (2001) Pro-apoptotic cleavage products of Bcl-xL form cytochrome c-conducting pores in pure lipid membranes. *The Journal of biological chemistry* 276(33):31083-31091.
69. Day CL*, et al.* (2005) Solution structure of prosurvival Mcl-1 and characterization of its binding by proapoptotic BH3-only ligands. *The Journal of biological chemistry* 280(6):4738-4744.
70. Liu Q*, et al.* (2010) Apoptotic regulation by MCL-1 through heterodimerization. *The Journal of biological chemistry* 285(25):19615-19624.
71. Smits C, Czabotar PE, Hinds MG, & Day CL (2008) Structural plasticity underpins promiscuous binding of the prosurvival protein A1. *Structure* 16(5):818-829.
72. Petros AM*, et al.* (2001) Solution structure of the antiapoptotic protein bcl-2. *Proceedings of the National Academy of Sciences of the United States of America* 98(6):3012-3017.
73. Petros AM, Olejniczak ET, & Fesik SW (2004) Structural biology of the Bcl-2 family of proteins. *Biochimica et biophysica acta* 1644(2-3):83-94.
74. Aouacheria A, Brunet F, & Gouy M (2005) Phylogenomics of life-or-death switches in multicellular animals: Bcl-2, BH3-Only, and BNip families of apoptotic regulators. *Molecular biology and evolution* 22(12):2395-2416.
75. Zhu W*, et al.* (1996) Bcl-2 mutants with restricted subcellular location reveal spatially distinct pathways for apoptosis in different cell types. *The EMBO journal* 15(16):4130-4141.
76. Bouillet P, Cory S, Zhang LC, Strasser A, & Adams JM (2001) Degenerative disorders caused by Bcl-2 deficiency prevented by loss of its BH3-only antagonist Bim. *Developmental cell* 1(5):645-653.
77. Motoyama N*, et al.* (1995) Massive cell death of immature hematopoietic cells and neurons in Bcl-x-deficient mice. *Science* 267(5203):1506-1510.
78. Print CG*, et al.* (1998) Apoptosis regulator bcl-w is essential for spermatogenesis but appears otherwise redundant. *Proceedings of the National Academy of Sciences of the United States of America* 95(21):12424-12431.
79. Rinkenberger JL, Horning S, Klocke B, Roth K, & Korsmeyer SJ (2000) Mcl-1 deficiency results in peri-implantation embryonic lethality. *Genes & development* 14(1):23-27.
80. Opferman JT*, et al.* (2005) Obligate role of anti-apoptotic MCL-1 in the survival of hematopoietic stem cells. *Science* 307(5712):1101-1104.
81. Griffiths GJ*, et al.* (1999) Cell damage-induced conformational changes of the pro-apoptotic protein Bak in vivo precede the onset of apoptosis. *The Journal of cell biology* 144(5):903-914.
82. Kvansakul M*, et al.* (2008) Vaccinia virus anti-apoptotic F1L is a novel Bcl-2-like domain-swapped dimer that binds a highly selective subset of BH3-containing death ligands. *Cell death and differentiation* 15(10):1564-1571.
83. Wang H*, et al.* (2009) Novel dimerization mode of the human Bcl-2 family protein Bak, a mitochondrial apoptosis regulator. *Journal of structural biology* 166(1):32-37.
84. Wei MC*, et al.* (2001) Proapoptotic BAX and BAK: a requisite gateway to mitochondrial dysfunction and death. *Science* 292(5517):727-730.
85. Lindsten T*, et al.* (2000) The combined functions of proapoptotic Bcl-2 family members bak and bax are essential for normal development of multiple tissues. *Molecular cell* 6(6):1389-1399.

86. Knudson CM, Tung KS, Tourtellotte WG, Brown GA, & Korsmeyer SJ (1995) Bax-deficient mice with lymphoid hyperplasia and male germ cell death. *Science* 270(5233):96-99.
87. Day CL*, et al.* (2008) Structure of the BH3 domains from the p53-inducible BH3-only proteins Noxa and Puma in complex with Mcl-1. *Journal of molecular biology* 380(5):958-971.
88. Chou JJ, Li H, Salvesen GS, Yuan J, & Wagner G (1999) Solution structure of BID, an intracellular amplifier of apoptotic signaling. *Cell* 96(5):615-624.
89. Gross A*, et al.* (1999) Caspase cleaved BID targets mitochondria and is required for cytochrome c release, while BCL-XL prevents this release but not tumor necrosis factor-R1/Fas death. *The Journal of biological chemistry* 274(2):1156-1163.
90. Willis SN*, et al.* (2007) Apoptosis initiated when BH3 ligands engage multiple Bcl-2 homologs, not Bax or Bak. *Science* 315(5813):856-859.
91. Ludwinski MW*, et al.* (2009) Critical roles of Bim in T cell activation and T cell-mediated autoimmune inflammation in mice. *The Journal of clinical investigation* 119(6):1706-1713.
92. Coultas L*, et al.* (2007) Hrk/DP5 contributes to the apoptosis of select neuronal populations but is dispensable for haematopoietic cell apoptosis. *Journal of cell science* 120(Pt 12):2044-2052.
93. Jeffers JR*, et al.* (2003) Puma is an essential mediator of p53-dependent and -independent apoptotic pathways. *Cancer cell* 4(4):321-328.
94. Ranger AM*, et al.* (2003) Bad-deficient mice develop diffuse large B cell lymphoma. *Proceedings of the National Academy of Sciences of the United States of America* 100(16):9324-9329.
95. Labi V*, et al.* (2008) Loss of the BH3-only protein Bmf impairs B cell homeostasis and accelerates gamma irradiation-induced thymic lymphoma development. *The Journal of experimental medicine* 205(3):641-655.
96. Coultas L*, et al.* (2005) Concomitant loss of proapoptotic BH3-only Bcl-2 antagonists Bik and Bim arrests spermatogenesis. *The EMBO journal* 24(22):3963-3973.
97. Villunger A, Scott C, Bouillet P, & Strasser A (2003) Essential role for the BH3-only protein Bim but redundant roles for Bax, Bcl-2, and Bcl-w in the control of granulocyte survival. *Blood* 101(6):2393-2400.
98. Kuwana T*, et al.* (2002) Bid, Bax, and lipids cooperate to form supramolecular openings in the outer mitochondrial membrane. *Cell* 111(3):331-342.
99. Wei MC*, et al.* (2000) tBID, a membrane-targeted death ligand, oligomerizes BAK to release cytochrome c. *Genes & development* 14(16):2060-2071.
100. Ren D*, et al.* (2010) BID, BIM, and PUMA are essential for activation of the BAX- and BAK-dependent cell death program. *Science* 330(6009):1390-1393.
101. Inohara N, Ding L, Chen S, & Nunez G (1997) harakiri, a novel regulator of cell death, encodes a protein that activates apoptosis and interacts selectively with survival-promoting proteins Bcl-2 and Bcl-X(L). *The EMBO journal* 16(7):1686-1694.
102. Nakano K & Vousden KH (2001) PUMA, a novel proapoptotic gene, is induced by p53. *Molecular cell* 7(3):683-694.
103. Oda E*, et al.* (2000) Noxa, a BH3-only member of the Bcl-2 family and candidate mediator of p53-induced apoptosis. *Science* 288(5468):1053-1058.
104. Puthalakath H*, et al.* (2001) Bmf: a proapoptotic BH3-only protein regulated by interaction with the myosin V actin motor complex, activated by anoikis. *Science* 293(5536):1829-1832.
105. Yang E*, et al.* (1995) Bad, a heterodimeric partner for Bcl-XL and Bcl-2, displaces Bax and promotes cell death. *Cell* 80(2):285-291.

106. Chinnadurai G, Vijayalingam S, & Rashmi R (2008) BIK, the founding member of the BH3-only family proteins: mechanisms of cell death and role in cancer and pathogenic processes. *Oncogene* 27 Suppl 1:S20-29.
107. Kataoka T*, et al.* (2001) Bcl-rambo, a novel Bcl-2 homologue that induces apoptosis via its unique C-terminal extension. *The Journal of biological chemistry* 276(22):19548-19554.
108. Oltvai ZN, Milliman CL, & Korsmeyer SJ (1993) Bcl-2 heterodimerizes in vivo with a conserved homolog, Bax, that accelerates programmed cell death. *Cell* 74(4):609-619.
109. Willis SN*, et al.* (2005) Proapoptotic Bak is sequestered by Mcl-1 and Bcl-xL, but not Bcl-2, until displaced by BH3-only proteins. *Genes & development* 19(11):1294-1305.
110. Cheng EH, Sheiko TV, Fisher JK, Craigen WJ, & Korsmeyer SJ (2003) VDAC2 inhibits BAK activation and mitochondrial apoptosis. *Science* 301(5632):513-517.
111. Vogel S*, et al.* (2012) Cytosolic Bax: does it require binding proteins to keep its pro-apoptotic activity in check? *The Journal of biological chemistry* 287(12):9112-9127.
112. Chi X, Kale J, Leber B, & Andrews DW (2014) Regulating cell death at, on, and in membranes. *Biochimica et biophysica acta* 1843(9):2100-2113.
113. Letai A*, et al.* (2002) Distinct BH3 domains either sensitize or activate mitochondrial apoptosis, serving as prototype cancer therapeutics. *Cancer cell* 2(3):183-192.
114. Bleicken S*, et al.* (2010) Molecular details of Bax activation, oligomerization, and membrane insertion. *The Journal of biological chemistry* 285(9):6636-6647.
115. Tan C*, et al.* (2006) Auto-activation of the apoptosis protein Bax increases mitochondrial membrane permeability and is inhibited by Bcl-2. *The Journal of biological chemistry* 281(21):14764-14775.
116. Lovell JF*, et al.* (2008) Membrane binding by tBid initiates an ordered series of events culminating in membrane permeabilization by Bax. *Cell* 135(6):1074-1084.
117. Basanez G & Hardwick JM (2008) Unravelling the bcl-2 apoptosis code with a simple model system. *PLoS biology* 6(6):e154.
118. Leber B, Lin J, & Andrews DW (2010) Still embedded together binding to membranes regulates Bcl-2 protein interactions. *Oncogene* 29(38):5221-5230.
119. Annis MG*, et al.* (2005) Bax forms multispanning monomers that oligomerize to permeabilize membranes during apoptosis. *The EMBO journal* 24(12):2096-2103.
120. Garcia-Saez AJ, Ries J, Orzaez M, Perez-Paya E, & Schwille P (2009) Membrane promotes tBID interaction with BCL(XL). *Nat Struct Mol Biol* 16(11):1178-1185.
121. Terrones O*, et al.* (2004) Lipidic pore formation by the concerted action of proapoptotic BAX and tBID. *The Journal of biological chemistry* 279(29):30081-30091.
122. Shamas-Din A, Kale J, Leber B, & Andrews DW (2013) Mechanisms of action of Bcl-2 family proteins. *Cold Spring Harbor perspectives in biology* 5(4):a008714.
123. Llambi F*, et al.* (2011) A unified model of mammalian BCL-2 protein family interactions at the mitochondria. *Molecular cell* 44(4):517-531.
124. Gavathiotis E, Reyna DE, Davis ML, Bird GH, & Walensky LD (2010) BH3-triggered structural reorganization drives the activation of proapoptotic BAX. *Molecular cell* 40(3):481-492.
125. Chipuk JE*, et al.* (2012) Sphingolipid metabolism cooperates with BAK and BAX to promote the mitochondrial pathway of apoptosis. *Cell* 148(5):988-1000.
126. Basanez G, Soane L, & Hardwick JM (2012) A new view of the lethal apoptotic pore. *PLoS biology* 10(9):e1001399.
127. Kim H*, et al.* (2009) Stepwise activation of BAX and BAK by tBID, BIM, and PUMA initiates mitochondrial apoptosis. *Mol Cell* 36(3):487-499.
128. Ferrer PE, Frederick P, Gulbis JM, Dewson G, & Kluck RM (2012) Translocation of a Bak C-terminus mutant from cytosol to mitochondria to mediate cytochrome C release: implications for Bak and Bax apoptotic function. *PLoS One* 7(3):e31510.

129. Oh KJ, *et al.* (2010) Conformational changes in BAK, a pore-forming proapoptotic Bcl-2 family member, upon membrane insertion and direct evidence for the existence of BH3-BH3 contact interface in BAK homo-oligomers. *The Journal of biological chemistry* 285(37):28924-28937.
130. Dewson G, *et al.* (2009) Bak activation for apoptosis involves oligomerization of dimers via their alpha6 helices. *Molecular cell* 36(4):696-703.
131. Karbowski M, Norris KL, Cleland MM, Jeong SY, & Youle RJ (2006) Role of Bax and Bak in mitochondrial morphogenesis. *Nature* 443(7112):658-662.
132. Hsu YT, Wolter KG, & Youle RJ (1997) Cytosol-to-membrane redistribution of Bax and Bcl-X(L) during apoptosis. *Proc Natl Acad Sci U S A* 94(8):3668-3672.
133. Edlich F, *et al.* (2011) Bcl-x(L) retrotranslocates Bax from the mitochondria into the cytosol. *Cell* 145(1):104-116.
134. Czabotar PE, *et al.* (2013) Bax crystal structures reveal how BH3 domains activate Bax and nucleate its oligomerization to induce apoptosis. *Cell* 152(3):519-531.
135. Kroemer G, Galluzzi L, & Brenner C (2007) Mitochondrial membrane permeabilization in cell death. *Physiol Rev* 87(1):99-163.
136. Godlewski MM, Gajkowska B, Lamparska-Przybysz M, & Motyl T (2002) Colocalization of BAX with BID and VDAC-1 in nimesulide-induced apoptosis of human colon adenocarcinoma COLO 205 cells. *Anti-cancer drugs* 13(10):1017-1029.
137. Basanez G, *et al.* (2002) Bax-type apoptotic proteins porate pure lipid bilayers through a mechanism sensitive to intrinsic monolayer curvature. *The Journal of biological chemistry* 277(51):49360-49365.
138. Bleicken S, Landeta O, Landajuela A, Basanez G, & Garcia-Saez AJ (2013) Proapoptotic Bax and Bak proteins form stable protein-permeable pores of tunable size. *The Journal of biological chemistry* 288(46):33241-33252.
139. Shoshan-Barmatz V, Keinan N, & Zaid H (2008) Uncovering the role of VDAC in the regulation of cell life and death. *Journal of bioenergetics and biomembranes* 40(3):183-191.
140. Shoshan-Barmatz V & Mizrachi D (2012) VDAC1: from structure to cancer therapy. *Frontiers in oncology* 2:164.
141. Baines CP, *et al.* (2005) Loss of cyclophilin D reveals a critical role for mitochondrial permeability transition in cell death. *Nature* 434(7033):658-662.
142. Shoshan-Barmatz V & Gincel D (2003) The voltage-dependent anion channel: characterization, modulation, and role in mitochondrial function in cell life and death. *Cell biochemistry and biophysics* 39(3):279-292.
143. Tsujimoto Y & Shimizu S (2007) Role of the mitochondrial membrane permeability transition in cell death. *Apoptosis : an international journal on programmed cell death* 12(5):835-840.
144. Kokoszka JE, *et al.* (2004) The ADP/ATP translocator is not essential for the mitochondrial permeability transition pore. *Nature* 427(6973):461-465.
145. Belizario JE, Alves J, Occhiucci JM, Garay-Malpartida M, & Sesso A (2007) A mechanistic view of mitochondrial death decision pores. *Brazilian journal of medical and biological research = Revista brasileira de pesquisas medicas e biologicas / Sociedade Brasileira de Biofisica ... [et al.]* 40(8):1011-1024.
146. Baines CP, Kaiser RA, Sheiko T, Craigen WJ, & Molkentin JD (2007) Voltage-dependent anion channels are dispensable for mitochondrial-dependent cell death. *Nature cell biology* 9(5):550-555.
147. Banerjee J & Ghosh S (2004) Bax increases the pore size of rat brain mitochondrial voltage-dependent anion channel in the presence of tBid. *Biochemical and biophysical research communications* 323(1):310-314.

148. Shimizu S, Narita M, & Tsujimoto Y (1999) Bcl-2 family proteins regulate the release of apoptogenic cytochrome c by the mitochondrial channel VDAC. *Nature* 399(6735):483-487.
149. Tajeddine N*, et al.* (2008) Hierarchical involvement of Bak, VDAC1 and Bax in cisplatin-induced cell death. *Oncogene* 27(30):4221-4232.
150. Rostovtseva TK*, et al.* (2004) Bid, but not Bax, regulates VDAC channels. *The Journal of biological chemistry* 279(14):13575-13583.
151. Tsujimoto Y & Shimizu S (2000) VDAC regulation by the Bcl-2 family of proteins. *Cell death and differentiation* 7(12):1174-1181.
152. Shimizu S, Matsuoka Y, Shinohara Y, Yoneda Y, & Tsujimoto Y (2001) Essential role of voltage-dependent anion channel in various forms of apoptosis in mammalian cells. *The Journal of cell biology* 152(2):237-250.
153. Debatin KM, Poncet D, & Kroemer G (2002) Chemotherapy: targeting the mitochondrial cell death pathway. *Oncogene* 21(57):8786-8803.
154. Malia TJ & Wagner G (2007) NMR structural investigation of the mitochondrial outer membrane protein VDAC and its interaction with antiapoptotic Bcl-xL. *Biochemistry* 46(2):514-525.
155. Zalk R, Israelson A, Garty ES, Azoulay-Zohar H, & Shoshan-Barmatz V (2005) Oligomeric states of the voltage-dependent anion channel and cytochrome c release from mitochondria. *The Biochemical journal* 386(Pt 1):73-83.
156. Keinan N, Tyomkin D, & Shoshan-Barmatz V (2010) Oligomerization of the mitochondrial protein voltage-dependent anion channel is coupled to the induction of apoptosis. *Molecular and cellular biology* 30(24):5698-5709.
157. Lemasters JJ & Holmuhamedov E (2006) Voltage-dependent anion channel (VDAC) as mitochondrial governator--thinking outside the box. *Biochimica et biophysica acta* 1762(2):181-190.
158. Feldmann G*, et al.* (2000) Opening of the mitochondrial permeability transition pore causes matrix expansion and outer membrane rupture in Fas-mediated hepatic apoptosis in mice. *Hepatology* 31(3):674-683.
159. Wigdal SS, Kirkland RA, Franklin JL, & Haak-Frendscho M (2002) Cytochrome c release precedes mitochondrial membrane potential loss in cerebellar granule neuron apoptosis: lack of mitochondrial swelling. *Journal of neurochemistry* 82(5):1029-1038.
160. Dejean LM, Martinez-Caballero S, & Kinnally KW (2006) Is MAC the knife that cuts cytochrome c from mitochondria during apoptosis? *Cell death and differentiation* 13(8):1387-1395.
161. Martinez-Caballero S, Dejean LM, & Kinnally KW (2004) Some amphiphilic cations block the mitochondrial apoptosis-induced channel, MAC. *FEBS letters* 568(1-3):35-38.
162. Martinez-Caballero S*, et al.* (2009) Assembly of the mitochondrial apoptosis-induced channel, MAC. *The Journal of biological chemistry* 284(18):12235-12245.
163. Stiban J, Fistere D, & Colombini M (2006) Dihydroceramide hinders ceramide channel formation: Implications on apoptosis. *Apoptosis : an international journal on programmed cell death* 11(5):773-780.
164. Yuan H, Williams SD, Adachi S, Oltersdorf T, & Gottlieb RA (2003) Cytochrome c dissociation and release from mitochondria by truncated Bid and ceramide. *Mitochondrion* 2(4):237-244.
165. Birbes H*, et al.* (2005) A mitochondrial pool of sphingomyelin is involved in TNFalpha-induced Bax translocation to mitochondria. *The Biochemical journal* 386(Pt 3):445-451.
166. Oh HL, Seok JY, Kwon CH, Kang SK, & Kim YK (2006) Role of MAPK in ceramide-induced cell death in primary cultured astrocytes from mouse embryonic brain. *Neurotoxicology* 27(1):31-38.

167. Beverly LJ*, et al.* (2013) BAK activation is necessary and sufficient to drive ceramide synthase-dependent ceramide accumulation following inhibition of BCL2-like proteins. *The Biochemical journal* 452(1):111-119.
168. Galluzzi L & Kroemer G (2007) Mitochondrial apoptosis without VDAC. *Nature cell biology* 9(5):487-489.
169. Betaneli V, Petrov EP, & Schwille P (2012) The role of lipids in VDAC oligomerization. *Biophysical journal* 102(3):523-531.
170. Claypool SM & Koehler CM (2012) The complexity of cardiolipin in health and disease. *Trends in biochemical sciences* 37(1):32-41.
171. Van Brocklyn JR & Williams JB (2012) The control of the balance between ceramide and sphingosine-1-phosphate by sphingosine kinase: oxidative stress and the seesaw of cell survival and death. *Comparative biochemistry and physiology. Part B, Biochemistry & molecular biology* 163(1):26-36.
172. Colbeau A, Nachbaur J, & Vignais PM (1971) Enzymic characterization and lipid composition of rat liver subcellular membranes. *Biochimica et biophysica acta* 249(2):462-492.
173. Schlame M, Rua D, & Greenberg ML (2000) The biosynthesis and functional role of cardiolipin. *Progress in lipid research* 39(3):257-288.
174. Ardail D*, et al.* (1990) Mitochondrial contact sites. Lipid composition and dynamics. *J Biol Chem* 265(31):18797-18802.
175. Lutter M, Perkins GA, & Wang X (2001) The pro-apoptotic Bcl-2 family member tBid localizes to mitochondrial contact sites. *BMC cell biology* 2:22.
176. Gonzalvez F*, et al.* (2008) Cardiolipin provides an essential activating platform for caspase-8 on mitochondria. *The Journal of cell biology* 183(4):681-696.
177. Esposti MD, Erler JT, Hickman JA, & Dive C (2001) Bid, a widely expressed proapoptotic protein of the Bcl-2 family, displays lipid transfer activity. *Molecular and cellular biology* 21(21):7268-7276.
178. Hekman M*, et al.* (2006) Reversible membrane interaction of BAD requires two C-terminal lipid binding domains in conjunction with 14-3-3 protein binding. *The Journal of biological chemistry* 281(25):17321-17336.
179. Montero J*, et al.* (2010) Cholesterol and peroxidized cardiolipin in mitochondrial membrane properties, permeabilization and cell death. *Biochimica et biophysica acta* 1797(6-7):1217-1224.
180. Lucken-Ardjomande S, Montessuit S, & Martinou JC (2008) Bax activation and stress-induced apoptosis delayed by the accumulation of cholesterol in mitochondrial membranes. *Cell death and differentiation* 15(3):484-493.
181. Lee SK, Kim YC, Song SB, & Kim YS (2010) Stabilization and translocation of p53 to mitochondria is linked to Bax translocation to mitochondria in simvastatin-induced apoptosis. *Biochemical and biophysical research communications* 391(4):1592-1597.
182. Montero J*, et al.* (2008) Mitochondrial cholesterol contributes to chemotherapy resistance in hepatocellular carcinoma. *Cancer research* 68(13):5246-5256.
183. Obeid LM, Linardic CM, Karolak LA, & Hannun YA (1993) Programmed cell death induced by ceramide. *Science* 259(5102):1769-1771.
184. Cremesti A*, et al.* (2001) Ceramide enables fas to cap and kill. *The Journal of biological chemistry* 276(26):23954-23961.
185. Zhang T & Saghatelian A (2013) Emerging roles of lipids in BCL-2 family-regulated apoptosis. *Biochimica et biophysica acta* 1831(10):1542-1554.
186. Beddoe T & Lithgow T (2002) Delivery of nascent polypeptides to the mitochondrial surface. *Biochimica et biophysica acta* 1592(1):35-39.

187. Horie C, Suzuki H, Sakaguchi M, & Mihara K (2002) Characterization of signal that directs C-tail-anchored proteins to mammalian mitochondrial outer membrane. *Molecular biology of the cell* 13(5):1615-1625.
188. Wattenberg B & Lithgow T (2001) Targeting of C-terminal (tail)-anchored proteins: understanding how cytoplasmic activities are anchored to intracellular membranes. *Traffic* 2(1):66-71.
189. Antonsson B (2001) Bax and other pro-apoptotic Bcl-2 family "killer-proteins" and their victim the mitochondrion. *Cell and tissue research* 306(3):347-361.
190. Hardwick JM, Chen YB, & Jonas EA (2012) Multipolar functions of BCL-2 proteins link energetics to apoptosis. *Trends in cell biology* 22(6):318-328.
191. Borner C (2003) The Bcl-2 protein family: sensors and checkpoints for life-or-death decisions. *Molecular immunology* 39(11):615-647.
192. Puthalakath H & Strasser A (2002) Keeping killers on a tight leash: transcriptional and post-translational control of the pro-apoptotic activity of BH3-only proteins. *Cell death and differentiation* 9(5):505-512.
193. Motz C, Martin H, Krimmer T, & Rassow J (2002) Bcl-2 and porin follow different pathways of TOM-dependent insertion into the mitochondrial outer membrane. *Journal of molecular biology* 323(4):729-738.
194. Lindsay J, Esposti MD, & Gilmore AP (2011) Bcl-2 proteins and mitochondria--specificity in membrane targeting for death. *Biochimica et biophysica acta* 1813(4):532-539.
195. Lithgow T, van Driel R, Bertram JF, & Strasser A (1994) The protein product of the oncogene bcl-2 is a component of the nuclear envelope, the endoplasmic reticulum, and the outer mitochondrial membrane. *Cell growth & differentiation : the molecular biology journal of the American Association for Cancer Research* 5(4):411-417.
196. Nguyen M, Millar DG, Yong VW, Korsmeyer SJ, & Shore GC (1993) Targeting of Bcl-2 to the mitochondrial outer membrane by a COOH-terminal signal anchor sequence. *J Biol Chem* 268(34):25265-25268.
197. Kaufmann T*, et al.* (2003) Characterization of the signal that directs Bcl-x(L), but not Bcl-2, to the mitochondrial outer membrane. *The Journal of cell biology* 160(1):53-64.
198. O'Reilly LA*, et al.* (2001) Tissue expression and subcellular localization of the pro-survival molecule Bcl-w. *Cell death and differentiation* 8(5):486-494.
199. Wilson-Annan J*, et al.* (2003) Proapoptotic BH3-only proteins trigger membrane integration of prosurvival Bcl-w and neutralize its activity. *The Journal of cell biology* 162(5):877-887.
200. Shirane M & Nakayama KI (2003) Inherent calcineurin inhibitor FKBP38 targets Bcl-2 to mitochondria and inhibits apoptosis. *Nature cell biology* 5(1):28-37.
201. Yang T, Kozopas KM, & Craig RW (1995) The intracellular distribution and pattern of expression of Mcl-1 overlap with, but are not identical to, those of Bcl-2. *The Journal of cell biology* 128(6):1173-1184.
202. Scorrano L*, et al.* (2003) BAX and BAK regulation of endoplasmic reticulum Ca2+: a control point for apoptosis. *Science* 300(5616):135-139.
203. Breckenridge DG, Germain M, Mathai JP, Nguyen M, & Shore GC (2003) Regulation of apoptosis by endoplasmic reticulum pathways. *Oncogene* 22(53):8608-8618.
204. Echeverry N*, et al.* (2013) Intracellular localization of the BCL-2 family member BOK and functional implications. *Cell death and differentiation* 20(6):785-799.
205. Bouillet P & Strasser A (2002) BH3-only proteins - evolutionarily conserved proapoptotic Bcl-2 family members essential for initiating programmed cell death. *J Cell Sci* 115(Pt 8):1567-1574.

206. Schinzel A, Kaufmann T, & Borner C (2004) Bcl-2 family members: integrators of survival and death signals in physiology and pathology [corrected]. *Biochimica et biophysica acta* 1644(2-3):95-105.
207. Wilfling F*, et al.* (2012) BH3-only proteins are tail-anchored in the outer mitochondrial membrane and can initiate the activation of Bax. *Cell death and differentiation* 19(8):1328-1336.
208. Datta SR*, et al.* (2002) Survival factor-mediated BAD phosphorylation raises the mitochondrial threshold for apoptosis. *Developmental cell* 3(5):631-643.
209. Puthalakath H, Huang DC, O'Reilly LA, King SM, & Strasser A (1999) The proapoptotic activity of the Bcl-2 family member Bim is regulated by interaction with the dynein motor complex. *Molecular cell* 3(3):287-296.
210. Gonzalvez F*, et al.* (2010) Mechanistic issues of the interaction of the hairpin-forming domain of tBid with mitochondrial cardiolipin. *PloS one* 5(2):e9342.
211. Hockenbery DM, Oltvai ZN, Yin XM, Milliman CL, & Korsmeyer SJ (1993) Bcl-2 functions in an antioxidant pathway to prevent apoptosis. *Cell* 75(2):241-251.
212. Nguyen M*, et al.* (1994) Role of membrane anchor domain of Bcl-2 in suppression of apoptosis caused by E1B-defective adenovirus. *The Journal of biological chemistry* 269(24):16521-16524.
213. Peng J*, et al.* (2009) Oligomerization of membrane-bound Bcl-2 is involved in its pore formation induced by tBid. *Apoptosis : an international journal on programmed cell death* 14(10):1145-1153.
214. Schendel SL*, et al.* (1997) Channel formation by antiapoptotic protein Bcl-2. *Proceedings of the National Academy of Sciences of the United States of America* 94(10):5113-5118.
215. Thuduppathy GR, Craig JW, Kholodenko V, Schon A, & Hill RB (2006) Evidence that membrane insertion of the cytosolic domain of Bcl-xL is governed by an electrostatic mechanism. *Journal of molecular biology* 359(4):1045-1058.
216. Aisenbrey C*, et al.* (2007) Helix orientations in membrane-associated Bcl-X(L) determined by 15N-solid-state NMR spectroscopy. *European biophysics journal : EBJ* 37(1):71-80.
217. Zheng JY*, et al.* (2008) The C-terminal transmembrane domain of Bcl-xL mediates changes in mitochondrial morphology. *Biophysical journal* 94(1):286-297.
218. Hossini AM, Eberle J, Fecker LF, Orfanos CE, & Geilen CC (2003) Conditional expression of exogenous Bcl-X(S) triggers apoptosis in human melanoma cells in vitro and delays growth of melanoma xenografts. *FEBS letters* 553(3):250-256.
219. Plotz M*, et al.* (2012) Mutual regulation of Bcl-2 proteins independent of the BH3 domain as shown by the BH3-lacking protein Bcl-x(AK). *PloS one* 7(4):e34549.
220. Ospina A, Lagunas-Martinez A, Pardo J, & Carrodeguas JA (2011) Protein oligomerization mediated by the transmembrane carboxyl terminal domain of Bcl-XL. *FEBS letters* 585(19):2935-2942.
221. Todt F, Cakir Z, Reichenbach F, Youle RJ, & Edlich F (2013) The C-terminal helix of Bcl-x(L) mediates Bax retrotranslocation from the mitochondria. *Cell Death Differ* 20(2):333-342.
222. Herold MJ*, et al.* (2006) The stability and anti-apoptotic function of A1 are controlled by its C terminus. *The Journal of biological chemistry* 281(19):13663-13671.
223. Brien G*, et al.* (2009) C-terminal residues regulate localization and function of the antiapoptotic protein Bfl-1. *The Journal of biological chemistry* 284(44):30257-30263.
224. Ko JK*, et al.* (2011) Amphipathic tail-anchoring peptide and Bcl-2 homology domain-3 (BH3) peptides from Bcl-2 family proteins induce apoptosis through different mechanisms. *The Journal of biological chemistry* 286(11):9038-9048.

225. Weng C, Li Y, Xu D, Shi Y, & Tang H (2005) Specific cleavage of Mcl-1 by caspase-3 in tumor necrosis factor-related apoptosis-inducing ligand (TRAIL)-induced apoptosis in Jurkat leukemia T cells. *The Journal of biological chemistry* 280(11):10491-10500.
226. Rautureau GJ, Day CL, & Hinds MG (2010) The structure of Boo/Diva reveals a divergent Bcl-2 protein. *Proteins* 78(9):2181-2186.
227. Ke N, Godzik A, & Reed JC (2001) Bcl-B, a novel Bcl-2 family member that differentially binds and regulates Bax and Bak. *The Journal of biological chemistry* 276(16):12481-12484.
228. Kang Y*, et al.* (2007) NM23-H2 involves in negative regulation of Diva and Bcl2L10 in apoptosis signaling. *Biochemical and biophysical research communications* 359(1):76-82.
229. Valentijn AJ, Upton JP, & Gilmore AP (2008) Analysis of endogenous Bax complexes during apoptosis using blue native PAGE: implications for Bax activation and oligomerization. *The Biochemical journal* 412(2):347-357.
230. Fresquet V, Rieger M, Carolis C, Garcia-Barchino MJ, & Martinez-Climent JA (2014) Acquired mutations in BCL2 family proteins conferring resistance to the BH3 mimetic ABT-199 in lymphoma. *Blood* 123(26):4111-4119.
231. Oliver L*, et al.* (2000) The substitution of the C-terminus of bax by that of bcl-xL does not affect its subcellular localization but abrogates its pro-apoptotic properties. *FEBS letters* 487(2):161-165.
232. Arokium H, Camougrand N, Vallette FM, & Manon S (2004) Studies of the interaction of substituted mutants of BAX with yeast mitochondria reveal that the C-terminal hydrophobic alpha-helix is a second ART sequence and plays a role in the interaction with anti-apoptotic BCL-xL. *The Journal of biological chemistry* 279(50):52566-52573.
233. Ausili A, de Godos A, Torrecillas A, Corbalan-Garcia S, & Gomez-Fernandez JC (2009) The interaction of the Bax C-terminal domain with membranes is influenced by the presence of negatively charged phospholipids. *Biochimica et biophysica acta* 1788(9):1924-1932.
234. Gahl RF, He Y, Yu S, & Tjandra N (2014) Conformational Rearrangements in the Pro-apoptotic Protein, Bax, as It Inserts into Mitochondria: A CELLULAR DEATH SWITCH. *The Journal of biological chemistry* 289(47):32871-32882.
235. Lin SH*, et al.* (2011) Bax forms two types of channels, one of which is voltage-gated. *Biophysical journal* 101(9):2163-2169.
236. Torrecillas A, Martinez-Senac MM, Ausili A, Corbalan-Garcia S, & Gomez-Fernandez JC (2007) Interaction of the C-terminal domain of Bcl-2 family proteins with model membranes. *Biochimica et biophysica acta* 1768(11):2931-2939.
237. del Mar Martinez-Senac M, Corbalan-Garcia S, & Gomez-Fernandez JC (2001) Conformation of the C-terminal domain of the pro-apoptotic protein Bax and mutants and its interaction with membranes. *Biochemistry* 40(33):9983-9992.
238. Oldfield E & Chapman D (1972) Dynamics of lipids in membranes: Heterogeneity and the role of cholesterol. *FEBS letters* 23(3):285-297.
239. Garg P, Nemec KN, Khaled AR, & Tatulian SA (2013) Transmembrane pore formation by the carboxyl terminus of Bax protein. *Biochimica et biophysica acta* 1828(2):732-742.
240. Tatulian SA, Garg P, Nemec KN, Chen B, & Khaled AR (2012) Molecular basis for membrane pore formation by Bax protein carboxyl terminus. *Biochemistry* 51(46):9406-9419.
241. Boohaker RJ*, et al.* (2012) Rational development of a cytotoxic peptide to trigger cell death. *Molecular pharmaceutics* 9(7):2080-2093.
242. Kiefer MC*, et al.* (1995) Modulation of apoptosis by the widely distributed Bcl-2 homologue Bak. *Nature* 374(6524):736-739.

243. Martinez-Senac Mdel M, Corbalan-Garcia S, & Gomez-Fernandez JC (2002) The structure of the C-terminal domain of the pro-apoptotic protein Bak and its interaction with model membranes. *Biophysical journal* 82(1 Pt 1):233-243.
244. Hsu SY, Kaipia A, McGee E, Lomeli M, & Hsueh AJ (1997) Bok is a pro-apoptotic Bcl-2 protein with restricted expression in reproductive tissues and heterodimerizes with selective anti-apoptotic Bcl-2 family members. *Proceedings of the National Academy of Sciences of the United States of America* 94(23):12401-12406.
245. Hsu SY & Hsueh AJ (1998) A splicing variant of the Bcl-2 member Bok with a truncated BH3 domain induces apoptosis but does not dimerize with antiapoptotic Bcl-2 proteins in vitro. *The Journal of biological chemistry* 273(46):30139-30146.
246. Kim TH*, et al.* (2004) Bid-cardiolipin interaction at mitochondrial contact site contributes to mitochondrial cristae reorganization and cytochrome C release. *Molecular biology of the cell* 15(7):3061-3072.
247. Schendel SL*, et al.* (1999) Ion channel activity of the BH3 only Bcl-2 family member, BID. *The Journal of biological chemistry* 274(31):21932-21936.
248. Kudla G*, et al.* (2000) The destabilization of lipid membranes induced by the C-terminal fragment of caspase 8-cleaved bid is inhibited by the N-terminal fragment. *The Journal of biological chemistry* 275(30):22713-22718.
249. Oh KJ*, et al.* (2005) Conformational changes in BID, a pro-apoptotic BCL-2 family member, upon membrane binding. A site-directed spin labeling study. *The Journal of biological chemistry* 280(1):753-767.
250. Polzien L*, et al.* (2011) Pore-forming activity of BAD is regulated by specific phosphorylation and structural transitions of the C-terminal part. *Biochimica et biophysica acta* 1810(2):162-169.
251. Bernabeu A, Guillen J, Perez-Berna AJ, Moreno MR, & Villalain J (2007) Structure of the C-terminal domain of the pro-apoptotic protein Hrk and its interaction with model membranes. *Biochimica et biophysica acta* 1768(6):1659-1670.
252. Barrera-Vilarmau S, Obregon P, & de Alba E (2011) Intrinsic order and disorder in the bcl-2 member harakiri: insights into its proapoptotic activity. *PloS one* 6(6):e21413.
253. Kim JY, So KJ, Lee S, & Park JH (2012) Bcl-rambo induces apoptosis via interaction with the adenine nucleotide translocator. *FEBS letters* 586(19):3142-3149.
254. Rashmi R, Pillai SG, Vijayalingam S, Ryerse J, & Chinnadurai G (2008) BH3-only protein BIK induces caspase-independent cell death with autophagic features in Bcl-2 null cells. *Oncogene* 27(10):1366-1375.
255. Weber A, Auslander D, & Hacker G (2013) Mouse Noxa uses only the C-terminal BH3-domain to inactivate Mcl-1. *Apoptosis : an international journal on programmed cell death* 18(9):1093-1105.
256. Yee KS & Vousden KH (2008) Contribution of membrane localization to the apoptotic activity of PUMA. *Apoptosis : an international journal on programmed cell death* 13(1):87-95.
257. Hanahan D & Weinberg RA (2000) The hallmarks of cancer. *Cell* 100(1):57-70.
258. Rooswinkel RW*, et al.* (2014) Antiapoptotic potency of Bcl-2 proteins primarily relies on their stability, not binding selectivity. *Blood* 123(18):2806-2815.
259. Liu Y, Hernandez AM, Shibata D, & Cortopassi GA (1994) BCL2 translocation frequency rises with age in humans. *Proceedings of the National Academy of Sciences of the United States of America* 91(19):8910-8914.
260. Campos L*, et al.* (1993) Peripheral blood stem cells harvested after chemotherapy and GM-CSF for treatment intensification in patients with advanced lymphoproliferative diseases. *Leukemia* 7(9):1409-1415.
261. Weller M, Malipiero U, Aguzzi A, Reed JC, & Fontana A (1995) Protooncogene bcl-2 gene transfer abrogates Fas/APO-1 antibody-mediated apoptosis of human malignant

glioma cells and confers resistance to chemotherapeutic drugs and therapeutic irradiation. *The Journal of clinical investigation* 95(6):2633-2643.
262. Joensuu H, Pylkkanen L, & Toikkanen S (1994) Bcl-2 protein expression and long-term survival in breast cancer. *The American journal of pathology* 145(5):1191-1198.
263. McDonnell TJ*, et al.* (1992) Expression of the protooncogene bcl-2 in the prostate and its association with emergence of androgen-independent prostate cancer. *Cancer research* 52(24):6940-6944.
264. Sinicrope FA, Hart J, Michelassi F, & Lee JJ (1995) Prognostic value of bcl-2 oncoprotein expression in stage II colon carcinoma. *Clinical cancer research : an official journal of the American Association for Cancer Research* 1(10):1103-1110.
265. Henderson S*, et al.* (1993) Epstein-Barr virus-coded BHRF1 protein, a viral homologue of Bcl-2, protects human B cells from programmed cell death. *Proceedings of the National Academy of Sciences of the United States of America* 90(18):8479-8483.
266. Boise LH*, et al.* (1993) bcl-x, a bcl-2-related gene that functions as a dominant regulator of apoptotic cell death. *Cell* 74(4):597-608.
267. Kirsh EJ, Baunoch DA, & Stadler WM (1998) Expression of bcl-2 and bcl-X in bladder cancer. *The Journal of urology* 159(4):1348-1353.
268. Naik P, Karrim J, & Hanahan D (1996) The rise and fall of apoptosis during multistage tumorigenesis: down-modulation contributes to tumor progression from angiogenic progenitors. *Genes & development* 10(17):2105-2116.
269. Castilla C*, et al.* (2006) Bcl-xL is overexpressed in hormone-resistant prostate cancer and promotes survival of LNCaP cells via interaction with proapoptotic Bak. *Endocrinology* 147(10):4960-4967.
270. Nagane M, Levitzki A, Gazit A, Cavenee WK, & Huang HJ (1998) Drug resistance of human glioblastoma cells conferred by a tumor-specific mutant epidermal growth factor receptor through modulation of Bcl-XL and caspase-3-like proteases. *Proceedings of the National Academy of Sciences of the United States of America* 95(10):5724-5729.
271. Shigemasa K*, et al.* (2002) Increased MCL-1 expression is associated with poor prognosis in ovarian carcinomas. *Japanese journal of cancer research : Gann* 93(5):542-550.
272. Kaufmann SH*, et al.* (1998) Elevated expression of the apoptotic regulator Mcl-1 at the time of leukemic relapse. *Blood* 91(3):991-1000.
273. Rampino N*, et al.* (1997) Somatic frameshift mutations in the BAX gene in colon cancers of the microsatellite mutator phenotype. *Science* 275(5302):967-969.
274. Pohland T, Wagner S, Mahyar-Roemer M, & Roemer K (2006) Bax and Bak are the critical complementary effectors of colorectal cancer cell apoptosis by chemopreventive resveratrol. *Anti-cancer drugs* 17(4):471-478.
275. Du X, Xiang L, Mackall C, & Pastan I (2011) Killing of resistant cancer cells with low Bak by a combination of an antimesothelin immunotoxin and a TRAIL Receptor 2 agonist antibody. *Clinical cancer research : an official journal of the American Association for Cancer Research* 17(18):5926-5934.
276. Jackson S, Harwood C, Thomas M, Banks L, & Storey A (2000) Role of Bak in UV-induced apoptosis in skin cancer and abrogation by HPV E6 proteins. *Genes & development* 14(23):3065-3073.
277. Rosen K*, et al.* (1998) Downregulation of the pro-apoptotic protein Bak is required for the ras-induced transformation of intestinal epithelial cells. *Current biology : CB* 8(24):1331-1334.
278. Ionov Y, Yamamoto H, Krajewski S, Reed JC, & Perucho M (2000) Mutational inactivation of the proapoptotic gene BAX confers selective advantage during tumor clonal evolution. *Proceedings of the National Academy of Sciences of the United States of America* 97(20):10872-10877.

279. Manoochehri M, Karbasi A, Bandehpour M, & Kazemi B (2013) Down-Regulation of BAX Gene During Carcinogenesis and Acquisition of Resistance to 5-FU in Colorectal Cancer. *Pathology oncology research : POR*.
280. Erler JT, *et al.* (2004) Hypoxia-mediated down-regulation of Bid and Bax in tumors occurs via hypoxia-inducible factor 1-dependent and -independent mechanisms and contributes to drug resistance. *Molecular and cellular biology* 24(7):2875-2889.
281. Wang X, *et al.* (2014) BAX and CDKN1A polymorphisms correlated with clinical outcomes of gastric cancer patients treated with postoperative chemotherapy. *Medical oncology* 31(11):249.
282. Shibue T, *et al.* (2003) Integral role of Noxa in p53-mediated apoptotic response. *Genes & development* 17(18):2233-2238.
283. Li J, Lee B, & Lee AS (2006) Endoplasmic reticulum stress-induced apoptosis: multiple pathways and activation of p53-up-regulated modulator of apoptosis (PUMA) and NOXA by p53. *The Journal of biological chemistry* 281(11):7260-7270.
284. Fricker M, O'Prey J, Tolkovsky AM, & Ryan KM (2010) Phosphorylation of Puma modulates its apoptotic function by regulating protein stability. *Cell death & disease* 1:e59.
285. Villunger A, *et al.* (2003) p53- and drug-induced apoptotic responses mediated by BH3-only proteins puma and noxa. *Science* 302(5647):1036-1038.
286. Sinicrope FA, *et al.* (2008) Prognostic impact of bim, puma, and noxa expression in human colon carcinomas. *Clinical cancer research : an official journal of the American Association for Cancer Research* 14(18):5810-5818.
287. Bouillet P, *et al.* (1999) Proapoptotic Bcl-2 relative Bim required for certain apoptotic responses, leukocyte homeostasis, and to preclude autoimmunity. *Science* 286(5445):1735-1738.
288. Upton JP, *et al.* (2008) Caspase-2 cleavage of BID is a critical apoptotic signal downstream of endoplasmic reticulum stress. *Molecular and cellular biology* 28(12):3943-3951.
289. Kamer I, *et al.* (2005) Proapoptotic BID is an ATM effector in the DNA-damage response. *Cell* 122(4):593-603.
290. Desagher S, *et al.* (2001) Phosphorylation of bid by casein kinases I and II regulates its cleavage by caspase 8. *Molecular cell* 8(3):601-611.
291. Zinkel SS, *et al.* (2003) Proapoptotic BID is required for myeloid homeostasis and tumor suppression. *Genes & development* 17(2):229-239.
292. Kaufmann T, *et al.* (2007) The BH3-only protein bid is dispensable for DNA damage- and replicative stress-induced apoptosis or cell-cycle arrest. *Cell* 129(2):423-433.
293. Blume-Jensen P, Janknecht R, & Hunter T (1998) The kit receptor promotes cell survival via activation of PI 3-kinase and subsequent Akt-mediated phosphorylation of Bad on Ser136. *Current biology : CB* 8(13):779-782.
294. She QB, *et al.* (2005) The BAD protein integrates survival signaling by EGFR/MAPK and PI3K/Akt kinase pathways in PTEN-deficient tumor cells. *Cancer cell* 8(4):287-297.
295. Schmelzle T, *et al.* (2007) Functional role and oncogene-regulated expression of the BH3-only factor Bmf in mammary epithelial anoikis and morphogenesis. *Proceedings of the National Academy of Sciences of the United States of America* 104(10):3787-3792.
296. Olie RA & Zangemeister-Wittke U (2001) Targeting tumor cell resistance to apoptosis induction with antisense oligonucleotides: progress and therapeutic potential. *Drug resistance updates : reviews and commentaries in antimicrobial and anticancer chemotherapy* 4(1):9-15.
297. Jansen B, *et al.* (1998) bcl-2 antisense therapy chemosensitizes human melanoma in SCID mice. *Nature medicine* 4(2):232-234.

298. Bedikian AY, *et al.* (2006) Bcl-2 antisense (oblimersen sodium) plus dacarbazine in patients with advanced melanoma: the Oblimersen Melanoma Study Group. *Journal of clinical oncology : official journal of the American Society of Clinical Oncology* 24(29):4738-4745.
299. Heere-Ress E, *et al.* (2002) Bcl-X(L) is a chemoresistance factor in human melanoma cells that can be inhibited by antisense therapy. *International journal of cancer. Journal international du cancer* 99(1):29-34.
300. Zangemeister-Wittke U, *et al.* (2000) A novel bispecific antisense oligonucleotide inhibiting both bcl-2 and bcl-xL expression efficiently induces apoptosis in tumor cells. *Clinical cancer research : an official journal of the American Association for Cancer Research* 6(6):2547-2555.
301. Sieghart W, *et al.* (2006) Mcl-1 overexpression in hepatocellular carcinoma: a potential target for antisense therapy. *Journal of hepatology* 44(1):151-157.
302. Piche A, *et al.* (1998) Modulation of Bcl-2 protein levels by an intracellular anti-Bcl-2 single-chain antibody increases drug-induced cytotoxicity in the breast cancer cell line MCF-7. *Cancer research* 58(10):2134-2140.
303. Wang JL, *et al.* (2000) Cell permeable Bcl-2 binding peptides: a chemical approach to apoptosis induction in tumor cells. *Cancer research* 60(6):1498-1502.
304. Sattler M, *et al.* (1997) Structure of Bcl-xL-Bak peptide complex: recognition between regulators of apoptosis. *Science* 275(5302):983-986.
305. van Delft MF, *et al.* (2006) The BH3 mimetic ABT-737 targets selective Bcl-2 proteins and efficiently induces apoptosis via Bak/Bax if Mcl-1 is neutralized. *Cancer cell* 10(5):389-399.
306. Wesarg E, *et al.* (2007) Targeting BCL-2 family proteins to overcome drug resistance in non-small cell lung cancer. *International journal of cancer. Journal international du cancer* 121(11):2387-2394.
307. Oltersdorf T, *et al.* (2005) An inhibitor of Bcl-2 family proteins induces regression of solid tumours. *Nature* 435(7042):677-681.
308. Hann CL, *et al.* (2008) Therapeutic efficacy of ABT-737, a selective inhibitor of BCL-2, in small cell lung cancer. *Cancer research* 68(7):2321-2328.
309. Park CM, *et al.* (2008) Discovery of an orally bioavailable small molecule inhibitor of prosurvival B-cell lymphoma 2 proteins. *Journal of medicinal chemistry* 51(21):6902-6915.
310. Wang G, *et al.* (2006) Structure-based design of potent small-molecule inhibitors of anti-apoptotic Bcl-2 proteins. *Journal of medicinal chemistry* 49(21):6139-6142.
311. Zaidi R & Hadi SM (1992) Complexes involving gossypol, DNA and Cu(II). *Biochemistry international* 28(6):1135-1143.
312. Wei J, *et al.* (2010) Synthesis and biological evaluation of Apogossypolone derivatives as pan-active inhibitors of antiapoptotic B-cell lymphoma/leukemia-2 (Bcl-2) family proteins. *Journal of medicinal chemistry* 53(22):8000-8011.
313. Wang Z, *et al.* (2008) TW-37, a small-molecule inhibitor of Bcl-2, inhibits cell growth and invasion in pancreatic cancer. *International journal of cancer. Journal international du cancer* 123(4):958-966.
314. Mohammad RM, *et al.* (2007) Preclinical studies of TW-37, a new nonpeptidic small-molecule inhibitor of Bcl-2, in diffuse large cell lymphoma xenograft model reveal drug action on both Bcl-2 and Mcl-1. *Clinical cancer research : an official journal of the American Association for Cancer Research* 13(7):2226-2235.
315. Hu ZY, Sun J, Zhu XF, Yang D, & Zeng YX (2009) ApoG2 induces cell cycle arrest of nasopharyngeal carcinoma cells by suppressing the c-Myc signaling pathway. *Journal of translational medicine* 7:74.

316. Paoluzzi L*, et al.* (2008) Targeting Bcl-2 family members with the BH3 mimetic AT-101 markedly enhances the therapeutic effects of chemotherapeutic agents in in vitro and in vivo models of B-cell lymphoma. *Blood* 111(11):5350-5358.
317. Wei J*, et al.* (2009) Apogossypol derivatives as antagonists of antiapoptotic Bcl-2 family proteins. *Molecular cancer therapeutics* 8(4):904-913.
318. Wei J*, et al.* (2011) An optically pure apogossypolone derivative as potent pan-active inhibitor of anti-apoptotic bcl-2 family proteins. *Frontiers in oncology* 1:28.
319. Trudel S*, et al.* (2007) The Bcl-2 family protein inhibitor, ABT-737, has substantial antimyeloma activity and shows synergistic effect with dexamethasone and melphalan. *Clinical cancer research : an official journal of the American Association for Cancer Research* 13(2 Pt 1):621-629.
320. Nguyen M*, et al.* (2007) Small molecule obatoclax (GX15-070) antagonizes MCL-1 and overcomes MCL-1-mediated resistance to apoptosis. *Proc Natl Acad Sci U S A* 104(49):19512-19517.
321. Konopleva M*, et al.* (2008) Mechanisms of antileukemic activity of the novel Bcl-2 homology domain-3 mimetic GX15-070 (obatoclax). *Cancer research* 68(9):3413-3420.
322. McCoy F*, et al.* (2010) Obatoclax induces Atg7-dependent autophagy independent of beclin-1 and BAX/BAK. *Cell death & disease* 1:e108.
323. Thomas S*, et al.* (2013) Targeting the Bcl-2 family for cancer therapy. *Expert opinion on therapeutic targets* 17(1):61-75.
324. Ni Chonghaile T*, et al.* (2011) Pretreatment mitochondrial priming correlates with clinical response to cytotoxic chemotherapy. *Science* 334(6059):1129-1133.
325. Opferman JT & Korsmeyer SJ (2003) Apoptosis in the development and maintenance of the immune system. *Nature immunology* 4(5):410-415.
326. Vo TT*, et al.* (2012) Relative mitochondrial priming of myeloblasts and normal HSCs determines chemotherapeutic success in AML. *Cell* 151(2):344-355.
327. Ryan J & Letai A (2013) BH3 profiling in whole cells by fluorimeter or FACS. *Methods* 61(2):156-164.
328. Brunelle JK, Ryan J, Yecies D, Opferman JT, & Letai A (2009) MCL-1-dependent leukemia cells are more sensitive to chemotherapy than BCL-2-dependent counterparts. *The Journal of cell biology* 187(3):429-442.
329. Deng J*, et al.* (2007) BH3 profiling identifies three distinct classes of apoptotic blocks to predict response to ABT-737 and conventional chemotherapeutic agents. *Cancer cell* 12(2):171-185.
330. Yip KW & Reed JC (2008) Bcl-2 family proteins and cancer. *Oncogene* 27(50):6398-6406.
331. Chonghaile TN*, et al.* (2014) Maturation stage of T-cell acute lymphoblastic leukemia determines BCL-2 versus BCL-XL dependence and sensitivity to ABT-199. *Cancer discovery* 4(9):1074-1087.
332. Russ WP & Engelman DM (1999) TOXCAT: a measure of transmembrane helix association in a biological membrane. *Proceedings of the National Academy of Sciences of the United States of America* 96(3):863-868.
333. Li R*, et al.* (2004) Dimerization of the transmembrane domain of Integrin alphaIIb subunit in cell membranes. *The Journal of biological chemistry* 279(25):26666-26673.
334. Yin H*, et al.* (2007) Computational design of peptides that target transmembrane helices. *Science* 315(5820):1817-1822.
335. Kerppola TK (2008) Bimolecular fluorescence complementation (BiFC) analysis as a probe of protein interactions in living cells. *Annual review of biophysics* 37:465-487.
336. Kerppola TK (2009) Visualization of molecular interactions using bimolecular fluorescence complementation analysis: characteristics of protein fragment complementation. *Chemical Society reviews* 38(10):2876-2886.

337. Kodama Y & Hu CD (2010) An improved bimolecular fluorescence complementation assay with a high signal-to-noise ratio. *BioTechniques* 49(5):793-805.
338. Hessa T*, et al.* (2005) Recognition of transmembrane helices by the endoplasmic reticulum translocon. *Nature* 433(7024):377-381.
339. Martinez-Gil L, Perez-Gil J, & Mingarro I (2008) The surfactant peptide KL4 sequence is inserted with a transmembrane orientation into the endoplasmic reticulum membrane. *Biophysical journal* 95(6):L36-38.
340. Navarro JA*, et al.* (2006) RNA-binding properties and membrane insertion of Melon necrotic spot virus (MNSV) double gene block movement proteins. *Virology* 356(1-2):57-67.
341. Sauri A, Tamborero S, Martinez-Gil L, Johnson AE, & Mingarro I (2009) Viral membrane protein topology is dictated by multiple determinants in its sequence. *Journal of molecular biology* 387(1):113-128.
342. Orzaez M, Guevara T, Sancho M, & Perez-Paya E (2012) Intrinsic caspase-8 activation mediates sensitization of erlotinib-resistant tumor cells to erlotinib/cell-cycle inhibitors combination treatment. *Cell death & disease* 3:e415.
343. Palacios-Rodriguez Y*, et al.* (2011) Polypeptide modulators of caspase recruitment domain (CARD)-CARD-mediated protein-protein interactions. *The Journal of biological chemistry* 286(52):44457-44466.
344. Hall K, Lee TH, Mechler AI, Swann MJ, & Aguilar MI (2014) Real-time measurement of membrane conformational states induced by antimicrobial peptides: balance between recovery and lysis. *Scientific reports* 4:5479.
345. Hirst DJ*, et al.* (2011) Effect of acyl chain structure and bilayer phase state on binding and penetration of a supported lipid bilayer by HPA3. *European biophysics journal : EBJ* 40(4):503-514.
346. Lee TH*, et al.* (2010) Real-time quantitative analysis of lipid disordering by aurein 1.2 during membrane adsorption, destabilisation and lysis. *Biochimica et biophysica acta* 10(86):30.
347. Sila M, Au S, & Weiner N (1986) Effects of Triton X-100 concentration and incubation temperature on carboxyfluorescein release from multilamellar liposomes. *Biochimica et Biophysica Acta (BBA) - Biomembranes* 859(2):165-170.
348. Frezza C, Cipolat S, & Scorrano L (2007) Organelle isolation: functional mitochondria from mouse liver, muscle and cultured fibroblasts. *Nat Protoc* 2(2):287-295.
349. Karch J*, et al.* (2013) Bax and Bak function as the outer membrane component of the mitochondrial permeability pore in regulating necrotic cell death in mice. *eLife* 2:e00772.
350. Moure A*, et al.* (2011) Chemical modulation of peptoids: synthesis and conformational studies on partially constrained derivatives. *Chemistry* 17(28):7927-7939.
351. Cecconi F, Alvarez-Bolado G, Meyer BI, Roth KA, & Gruss P (1998) Apaf1 (CED-4 homolog) regulates programmed cell death in mammalian development. *Cell* 94(6):727-737.
352. Valentijn AJ, Upton JP, Bates N, & Gilmore AP (2008) Bax targeting to mitochondria occurs via both tail anchor-dependent and -independent mechanisms. *Cell death and differentiation* 15(8):1243-1254.
353. Berger BW*, et al.* (2010) Consensus motif for integrin transmembrane helix association. *Proc Natl Acad Sci U S A* 107(2):703-708.
354. Adair BD & Engelman DM (1994) Glycophorin A helical transmembrane domains dimerize in phospholipid bilayers: a resonance energy transfer study. *Biochemistry* 33(18):5539-5544.
355. Treutlein HR, Lemmon MA, Engelman DM, & Brunger AT (1992) The glycophorin A transmembrane domain dimer: sequence-specific propensity for a right-handed supercoil of helices. *Biochemistry* 31(51):12726-12732.

356. Gomez-Fernandez JC (2014) Functions of the C-terminal domains of apoptosis-related proteins of the Bcl-2 family. *Chemistry and physics of lipids* 183:77-90.
357. Russ WP & Engelman DM (2000) The GxxxG motif: a framework for transmembrane helix-helix association. *Journal of molecular biology* 296(3):911-919.
358. Vilar M*, et al.* (2009) Activation of the p75 neurotrophin receptor through conformational rearrangement of disulphide-linked receptor dimers. *Neuron* 62(1):72-83.
359. Nakagawa C, Inahata K, Nishimura S, & Sugimoto K (2011) Improvement of a Venus-based bimolecular fluorescence complementation assay to visualize bFos-bJun interaction in living cells. *Bioscience, biotechnology, and biochemistry* 75(7):1399-1401.
360. Merabet S*, et al.* (2011) Insights into Hox protein function from a large scale combinatorial analysis of protein domains. *PLoS genetics* 7(10):e1002302.
361. Corsten MF, Hofstra L, Narula J, & Reutelingsperger CP (2006) Counting heads in the war against cancer: defining the role of annexin A5 imaging in cancer treatment and surveillance. *Cancer research* 66(3):1255-1260.
362. Suh DH, Kim MK, Kim HS, Chung HH, & Song YS (2013) Mitochondrial permeability transition pore as a selective target for anti-cancer therapy. *Frontiers in oncology* 3:41.
363. Shoshan-Barmatz V, Mizrachi D, & Keinan N (2013) Oligomerization of the mitochondrial protein VDAC1: from structure to function and cancer therapy. *Progress in molecular biology and translational science* 117:303-334.
364. Tahir SK*, et al.* (2010) Identification of expression signatures predictive of sensitivity to the Bcl-2 family member inhibitor ABT-263 in small cell lung carcinoma and leukemia/lymphoma cell lines. *Molecular cancer therapeutics* 9(3):545-557.
365. Coultas L & Strasser A (2003) The role of the Bcl-2 protein family in cancer. *Seminars in cancer biology* 13(2):115-123.
366. Gomez-Fernandez JC (2014) Functions of the C-terminal domains of apoptosis-related proteins of the Bcl-2 family. *Chemistry and physics of lipids* 183C:77-90.
367. Gahl RF, He Y, Yu S, & Tjandra N (2014) Conformational Rearrangements in the Pro-Apoptotic Protein, Bax, as it inserts into mitochondria: A Cellular Death Switch. *The Journal of biological chemistry*.
368. Mahajan NP*, et al.* (1998) Bcl-2 and Bax interactions in mitochondria probed with green fluorescent protein and fluorescence resonance energy transfer. *Nature biotechnology* 16(6):547-552.
369. Dzhagalov I, Dunkle A, & He YW (2008) The anti-apoptotic Bcl-2 family member Mcl-1 promotes T lymphocyte survival at multiple stages. *Journal of immunology* 181(1):521-528.
370. Gonzalvez F*, et al.* (2005) tBid interaction with cardiolipin primarily orchestrates mitochondrial dysfunctions and subsequently activates Bax and Bak. *Cell death and differentiation* 12(6):614-626.
371. Basanez G*, et al.* (1999) Bax, but not Bcl-xL, decreases the lifetime of planar phospholipid bilayer membranes at subnanomolar concentrations. *Proc Natl Acad Sci U S A* 96(10):5492-5497.
372. Kim H*, et al.* (2006) Hierarchical regulation of mitochondrion-dependent apoptosis by BCL-2 subfamilies. *Nature cell biology* 8(12):1348-1358.
373. Uren RT*, et al.* (2007) Mitochondrial permeabilization relies on BH3 ligands engaging multiple prosurvival Bcl-2 relatives, not Bak. *The Journal of cell biology* 177(2):277-287.
374. Andreu-Fernandez V*, et al.* (2014) Peptides derived from the transmembrane domain of Bcl-2 proteins as potential mitochondrial priming tools. *ACS chemical biology* 9(8):1799-1811.
375. Aranovich A*, et al.* (2012) Differences in the mechanisms of proapoptotic BH3 proteins binding to Bcl-XL and Bcl-2 quantified in live MCF-7 cells. *Molecular cell* 45(6):754-763.

376. Hessa T*, et al.* (2007) Molecular code for transmembrane-helix recognition by the Sec61 translocon. *Nature* 450(7172):1026-1030.
377. Tamborero S, Vilar M, Martinez-Gil L, Johnson AE, & Mingarro I (2011) Membrane insertion and topology of the translocating chain-associating membrane protein (TRAM). *Journal of molecular biology* 406(4):571-582.
378. Martinez-Gil L, Sauri A, Vilar M, Pallas V, & Mingarro I (2007) Membrane insertion and topology of the p7B movement protein of Melon Necrotic Spot Virus (MNSV). *Virology* 367(2):348-357.
379. Bano-Polo M*, et al.* (2012) Polar/Ionizable residues in transmembrane segments: effects on helix-helix packing. *PloS one* 7(9):e44263.
380. Garcia-Saez AJ, Mingarro I, Perez-Paya E, & Salgado J (2004) Membrane-insertion fragments of Bcl-xL, Bax, and Bid. *Biochemistry* 43(34):10930-10943.
381. Germain M, Mathai JP, McBride HM, & Shore GC (2005) Endoplasmic reticulum BIK initiates DRP1-regulated remodelling of mitochondrial cristae during apoptosis. *The EMBO journal* 24(8):1546-1556.
382. Shamas-Din A, Brahmbhatt H, Leber B, & Andrews DW (2011) BH3-only proteins: Orchestrators of apoptosis. *Biochimica et biophysica acta* 1813(4):508-520.
383. Kvansakul M & Hinds MG (2014) The structural biology of BH3-only proteins. *Methods in enzymology* 544:49-74.
384. Garofalo T*, et al.* (2015) Role of mitochondrial raft-like microdomains in the regulation of cell apoptosis. *Apoptosis : an international journal on programmed cell death*.
385. Grimm S (2012) The ER-mitochondria interface: the social network of cell death. *Biochimica et biophysica acta* 1823(2):327-334.
386. Pang X*, et al.* (2014) The carboxyl-terminal tail of Noxa protein regulates the stability of Noxa and Mcl-1. *The Journal of biological chemistry* 289(25):17802-17811.
387. Shamas-Din A, Brahmbhatt H, Leber B, & Andrews DW (2011) BH3-only proteins: Orchestrators of apoptosis. *Biochimica et biophysica acta* 4:508-520.
388. Garcia-Saez AJ (2012) The secrets of the Bcl-2 family. *Cell death and differentiation* 19(11):1733-1740.
389. Edlich F*, et al.* (2011) Bcl-xL Retrotranslocates Bax from the Mitochondria into the Cytosol. *Cell* 145(1):104-116.
390. Todt F, Cakir Z, Reichenbach F, Youle RJ, & Edlich F (2013) The C-terminal helix of Bcl-xL mediates Bax retrotranslocation from the mitochondria. *Cell death and differentiation* 20(2):333-342.
391. Wilfling F*, et al.* (2012) BH3-only proteins are tail-anchored in the outer mitochondrial membrane and can initiate the activation of Bax. *Cell Death Differ* 19(8):1328-1336.
392. Slivka PF, Wong J, Caputo GA, & Yin H (2008) Peptide probes for protein transmembrane domains. *ACS chemical biology* 3(7):402-411.
393. Chonghaile TN & Letai A (2008) Mimicking the BH3 domain to kill cancer cells. *Oncogene* 27 Suppl 1:S149-157.
394. Michels J*, et al.* (2013) Synergistic interaction between cisplatin and PARP inhibitors in non-small cell lung cancer. *Cell cycle* 12(6):877-883.
395. Rath A, Tulumello DV, & Deber CM (2009) Peptide models of membrane protein folding. *Biochemistry* 48(14):3036-3045.
396. Orzaez M, Salgado J, Gimenez-Giner A, Perez-Paya E, & Mingarro I (2004) Influence of proline residues in transmembrane helix packing. *Journal of molecular biology* 335(2):631-640.
397. Baeza-Delgado C, Marti-Renom MA, & Mingarro I (2013) Structure-based statistical analysis of transmembrane helices. *European biophysics journal : EBJ* 42(2-3):199-207.

398. Vilar M, Esteve V, Pallas V, Marcos JF, & Perez-Paya E (2001) Structural properties of carnation mottle virus p7 movement protein and its RNA-binding domain. *The Journal of biological chemistry* 276(21):18122-18129.
399. Pastor MT, Lopez de la Paz M, Lacroix E, Serrano L, & Perez-Paya E (2002) Combinatorial approaches: a new tool to search for highly structured beta-hairpin peptides. *Proceedings of the National Academy of Sciences of the United States of America* 99(2):614-619.
400. Orzaez M, Perez-Paya E, & Mingarro I (2000) Influence of the C-terminus of the glycophorin A transmembrane fragment on the dimerization process. *Protein science : a publication of the Protein Society* 9(6):1246-1253.
401. Blondelle SE, Forood B, Houghten RA, & Perez-Paya E (1997) Secondary structure induction in aqueous vs membrane-like environments. *Biopolymers* 42(4):489-498.
402. Vilar M, Sauri A, Marcos JF, Mingarro I, & Perez-Paya E (2005) Transient structural ordering of the RNA-binding domain of carnation mottle virus p7 movement protein modulates nucleic acid binding. *Chembiochem* 6(8):1391-1396.
403. Schinzel A, Kaufmann T, & Borner C (2004) Bcl-2 family members: integrators of survival and death signals in physiology and pathology [corrected]. *Biochimica et biophysica acta* 1:2-3.
404. Osman C, Voelker DR, & Langer T (2011) Making heads or tails of phospholipids in mitochondria. *The Journal of cell biology* 192(1):7-16.
405. de Kroon AI, Dolis D, Mayer A, Lill R, & de Kruijff B (1997) Phospholipid composition of highly purified mitochondrial outer membranes of rat liver and Neurospora crassa. Is cardiolipin present in the mitochondrial outer membrane? *Biochimica et biophysica acta* 3(1):108-116.
406. Schug Z & Gottlieb E (2009) Cardiolipin acts as a mitochondrial signalling platform to launch apoptosis. *Biochimica et biophysica acta* 1788(10):2022-2031.
407. Lee TH*, et al.* (2009) Molecular imaging and orientational changes of antimicrobial peptides in membranes. *Adv Exp Med Biol* 611:313-315.
408. Lee TH*, et al.* (2010) The membrane insertion of helical antimicrobial peptides from the N-terminus of Helicobacter pylori ribosomal protein L1. *Biochimica et biophysica acta* 3:544-557.
409. Fernandez DI, Lee TH, Sani MA, Aguilar MI, & Separovic F (2013) Proline Facilitates Membrane Insertion of the Antimicrobial Peptide Maculatin 1.1 via Surface Indentation and Subsequent Lipid Disordering. *Biophysical journal* 104(7):1495-1507.
410. Ouellet M, Otis F, Voyer N, & Auger M (2006) Biophysical studies of the interactions between 14-mer and 21-mer model amphipathic peptides and membranes: insights on their modes of action. *Biochimica et biophysica acta* 1758(9):1235-1244.
411. Biron E, Voyer N, Meillon JC, Cormier ME, & Auger M (2000) Conformational and orientation studies of artificial ion channels incorporated into lipid bilayers. *Biopolymers* 55(5):364-372.
412. Borgne-Sanchez A*, et al.* (2007) Targeted Vpr-derived peptides reach mitochondria to induce apoptosis of alphaVbeta3-expressing endothelial cells. *Cell death and differentiation* 14(3):422-435.
413. Von Ahsen O, Waterhouse NJ, Kuwana T, Newmeyer DD, & Green DR (2000) The 'harmless' release of cytochrome c. *Cell death and differentiation* 7(12):1192-1199.
414. Hayashida W, Horiuchi M, & Dzau VJ (1996) Intracellular third loop domain of angiotensin II type-2 receptor. Role in mediating signal transduction and cellular function. *The Journal of biological chemistry* 271(36):21985-21992.
415. Eguchi Y, Shimizu S, & Tsujimoto Y (1997) Intracellular ATP levels determine cell death fate by apoptosis or necrosis. *Cancer research* 57(10):1835-1840.

416. Ellerby HM*, et al.* (1999) Anti-cancer activity of targeted pro-apoptotic peptides. *Nature medicine* 5(9):1032-1038.
417. Law B, Quinti L, Choi Y, Weissleder R, & Tung CH (2006) A mitochondrial targeted fusion peptide exhibits remarkable cytotoxicity. *Molecular cancer therapeutics* 5(8):1944-1949.
418. Mai JC, Mi Z, Kim SH, Ng B, & Robbins PD (2001) A proapoptotic peptide for the treatment of solid tumors. *Cancer research* 61(21):7709-7712.
419. Marks AJ*, et al.* (2005) Selective apoptotic killing of malignant hemopoietic cells by antibody-targeted delivery of an amphipathic peptide. *Cancer research* 65(6):2373-2377.
420. Rege K, Patel SJ, Megeed Z, & Yarmush ML (2007) Amphipathic peptide-based fusion peptides and immunoconjugates for the targeted ablation of prostate cancer cells. *Cancer research* 67(13):6368-6375.
421. Torrecillas A, Martinez-Senac MM, Ausili A, Corbalan-Garcia S, & Gomez-Fernandez JC (2007) Interaction of the C-terminal domain of Bcl-2 family proteins with model membranes. *Biochimica et biophysica acta* 1768(11):2931-2939.
422. Valero JG*, et al.* (2011) Bax-derived membrane-active peptides act as potent and direct inducers of apoptosis in cancer cells. *Journal of cell science* 124(Pt 4):556-564.
423. Garg P, Nemec KN, Khaled AR, & Tatulian SA (2013) Transmembrane pore formation by the carboxyl terminus of Bax protein. *Biochimica et biophysica acta* 1828(2):732-742.
424. Basanez G, Soane L, & Hardwick JM (2012) A new view of the lethal apoptotic pore. *PLoS biology* 10(9):25.
425. Lanave C, Santamaria M, & Saccone C (2004) Comparative genomics: the evolutionary history of the Bcl-2 family. *Gene* 333:71-79.
426. Aouacheria A, Rech de Laval V, Combet C, & Hardwick JM (2013) Evolution of Bcl-2 homology motifs: homology versus homoplasy. *Trends in cell biology* 23(3):103-111.
427. Zhang L, Yu J, Park BH, Kinzler KW, & Vogelstein B (2000) Role of BAX in the apoptotic response to anticancer agents. *Science* 290(5493):989-992.
428. Wang C & Youle RJ (2012) Predominant requirement of Bax for apoptosis in HCT116 cells is determined by Mcl-1's inhibitory effect on Bak. *Oncogene* 31(26):3177-3189.
429. Kale J, Liu Q, Leber B, & Andrews DW (2012) Shedding light on apoptosis at subcellular membranes. *Cell* 151(6):1179-1184.
430. Garg P, Nemec KN, Khaled AR, & Tatulian SA (2013) Transmembrane pore formation by the carboxyl terminus of Bax protein. *Biochimica et Biophysica Acta (BBA) - Biomembranes* 1828(2):732-742.
431. Ni Chonghaile T & Letai A (2008) Mimicking the BH3 domain to kill cancer cells. *Oncogene* 27(1):52.
432. Kang MH & Reynolds CP (2009) Bcl-2 inhibitors: targeting mitochondrial apoptotic pathways in cancer therapy. *Clinical cancer research : an official journal of the American Association for Cancer Research* 15(4):1126-1132.
433. Roy MJ, Vom A, Czabotar PE, & Lessene G (2013) Cell death and the mitochondria: therapeutic targeting of the BCL-2 family-driven pathway. *British journal of pharmacology*.
434. Lee MJ*, et al.* (2012) Sequential application of anticancer drugs enhances cell death by rewiring apoptotic signaling networks. *Cell* 149(4):780-794.
435. Slattery EL & Warchol ME (2010) Cisplatin ototoxicity blocks sensory regeneration in the avian inner ear. *The Journal of neuroscience : the official journal of the Society for Neuroscience* 30(9):3473-3481.
436. Trueb RM (2009) Chemotherapy-induced alopecia. *Seminars in cutaneous medicine and surgery* 28(1):11-14.
437. Hellwig CT & Rehm M (2012) TRAIL signaling and synergy mechanisms used in TRAIL-based combination therapies. *Molecular cancer therapeutics* 11(1):3-13.

438. Zhai D, Jin C, Satterthwait AC, & Reed JC (2006) Comparison of chemical inhibitors of antiapoptotic Bcl-2-family proteins. *Cell death and differentiation* 13(8):1419-1421.
439. Soengas MS*, et al.* (2001) Inactivation of the apoptosis effector Apaf-1 in malignant melanoma. *Nature* 409(6817):207-211.
440. Soengas MS, Gerald WL, Cordon-Cardo C, Lazebnik Y, & Lowe SW (2006) Apaf-1 expression in malignant melanoma. *Cell death and differentiation* 13(2):352-353.
441. Mondragon L*, et al.* (2009) A chemical inhibitor of Apaf-1 exerts mitochondrioprotective functions and interferes with the intra-S-phase DNA damage checkpoint. *Apoptosis : an international journal on programmed cell death* 14(2):182-190.
442. Mondragon L*, et al.* (2008) Modulation of cellular apoptosis with apoptotic protease-activating factor 1 (Apaf-1) inhibitors. *Journal of medicinal chemistry* 51(3):521-529.
443. Ferraro E*, et al.* (2011) Apaf1 plays a pro-survival role by regulating centrosome morphology and function. *Journal of cell science* 124(Pt 20):3450-3463.
444. Sancho M*, et al.* (2014) Altered mitochondria morphology and cell metabolism in Apaf1-deficient cells. *PloS one* 9(1):e84666.
445. Kuma A, Matsui M, & Mizushima N (2007) LC3, an autophagosome marker, can be incorporated into protein aggregates independent of autophagy: caution in the interpretation of LC3 localization. *Autophagy* 3(4):323-328.
446. Maiuri MC, Criollo A, & Kroemer G (2010) Crosstalk between apoptosis and autophagy within the Beclin 1 interactome. *The EMBO journal* 29(3):515-516.
447. Heidari N, Hicks MA, & Harada H (2010) GX15-070 (obatoclax) overcomes glucocorticoid resistance in acute lymphoblastic leukemia through induction of apoptosis and autophagy. *Cell death & disease* 1:e76.
448. Johnson CE*, et al.* (2007) Differential Apaf-1 levels allow cytochrome c to induce apoptosis in brain tumors but not in normal neural tissues. *Proceedings of the National Academy of Sciences of the United States of America* 104(52):20820-20825.
449. Potts MB, Vaughn AE, McDonough H, Patterson C, & Deshmukh M (2005) Reduced Apaf-1 levels in cardiomyocytes engage strict regulation of apoptosis by endogenous XIAP. *The Journal of cell biology* 171(6):925-930.
450. Kroemer G & Martin SJ (2005) Caspase-independent cell death. *Nature medicine* 11(7):725-730.
451. Hanahan D & Weinberg RA (2011) Hallmarks of cancer: the next generation. *Cell* 144(5):646-674.
452. Grover R & Wilson GD (1996) Bcl-2 expression in malignant melanoma and its prognostic significance. *European journal of surgical oncology : the journal of the European Society of Surgical Oncology and the British Association of Surgical Oncology* 22(4):347-349.
453. Mestre-Escorihuela C*, et al.* (2007) Homozygous deletions localize novel tumor suppressor genes in B-cell lymphomas. *Blood* 109(1):271-280.
454. Rudin CM*, et al.* (2012) Phase II study of single-agent navitoclax (ABT-263) and biomarker correlates in patients with relapsed small cell lung cancer. *Clinical cancer research : an official journal of the American Association for Cancer Research* 18(11):3163-3169.
455. Tse C*, et al.* (2008) ABT-263: a potent and orally bioavailable Bcl-2 family inhibitor. *Cancer research* 68(9):3421-3428.
456. Kodama Y & Hu CD (2012) Bimolecular fluorescence complementation (BiFC): a 5-year update and future perspectives. *BioTechniques* 53(5):285-298.
457. Perez-Gil J, Nag K, Taneva S, & Keough KM (1992) Pulmonary surfactant protein SP-C causes packing rearrangements of dipalmitoylphosphatidylcholine in spread monolayers. *Biophysical journal* 63(1):197-204.

SUMMARY

IN

SPANISH

10.1. INTRODUCCIÓN

La apoptosis ha sido definida clásicamente como un programa de muerte celular programada esencial para el mantenimiento de la homeostasis de los tejidos, los mecanismos inmunitarios así como la reorganización tisular durante el desarrollo del organismo. Este mecanismo de suicidio celular es ejecutado a través de la activación de una cascada de proteasas llamadas caspasas (3). Puede ser desencadenado a través de la activación de receptores de muerte celular situados en la membrana plasmática (vía extrínseca) o a través de un proceso de señalización celular originado desde la mitocondria (vía intrínseca) (38, 55). Principalmente la ruta intrínseca, aunque también la extrínseca, está regulada por una familia de proteínas llamadas BCL-2, cuya localización es mayoritariamente mitocondrial (55).

La modulación del proceso apoptótico por parte de las proteínas de la familia BCL-2 tiene lugar mediante una compleja red de interacciones entre sus miembros que desemboca en último término en la permeabilización de la membrana mitocondrial externa (MOM) o en evitar dicha permeabilización. Esta permeabilización de la MOM resulta crítica, ya que es considerada como el punto de no retorno para la activación de la apoptosis (48) . Una vez permeabilizada la MOM se produce la liberación desde la matriz mitocondrial al citosol de factores pro-apoptóticos tales como SMAC, Diablo y citocromo *c*. Ya en el citosol, y en presencia de ATP, el citocromo *c* interactúa con Apaf-1 y con procaspasa-9 para formar el apoptosoma (49, 50) (ver Figura 7.1). En este complejo macromolecular la proteasa procaspasa-9 es procesada y activada para a su vez activar procaspasa-3, desencadenado una cascada de proteasas que genera la destrucción final de la célula.

La familia de proteínas BCL-2 se caracteriza porque todos sus miembros comparten homología de secuencia en al menos una (el dominio BH3) de las cuatro regiones o dominios de homología de BCL-2 llamados BH1, BH2, BH3, y BH4. Además, muchos de los miembros de la familia poseen una región hidrófobica C-terminal cuya función es anclarse a las membranas intracelulares. Atendiendo a criterios funcionales y estructurales existen tres subgrupos dentro de esta familia de proteínas que son: proteínas anti-apoptóticas (Bcl-2, Bcl-xL, Mcl-1, A1, Bcl-w), pro-apoptóticas (Bax, Bak y Bok) y proteínas con un único dominio BH3, llamadas *BH3-only* (Bim, Rambo, Bik, Bad, Bmf, HRK (Harakiri) Puma y Noxa) (382)(Figura 10.1.1).

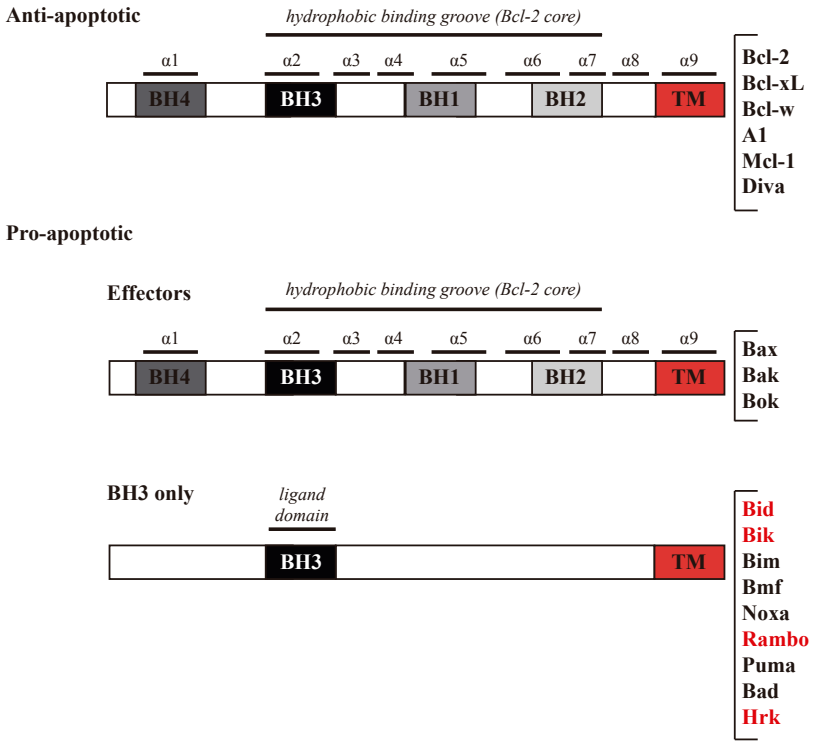

Figura 10.1.1. Organización estructural y funcional de las proteínas de la familia BCL-2. Se divide en tres subfamilias de proteínas con funciones anti y pro-apoptóticas. Los miembros anti-apoptóticos incluyen A1, Bcl-2, Bcl-xL, Bcl-w, MCL-1 y Diva y comparten los 4 dominios de homología de Bcl-2 (BH1-4). Los miembros pro-apoptóticos se subdividen en proteínas "multidominio" y proteínas *BH3-only*. Las proteínas multidominio también presentan dominios de homología 1 a 4, mientras que las *BH3-only* contienen sólo un dominio BH, el BH3, que es el responsable de la unión a las proteínas anti-apoptóticas. La mayoría de las proteínas BCL-2 también presentan un dominio transmembrana hidrofóbico (TMD). En el grupo *BH3-only*, el TMD esta confirmado en Bid, Bik, Rambo y Hrk (marcadas en rojo).

A menudo el subgrupo de las proteínas *BH3-only* es dividido en dos dependiendo de su capacidad para interactuar bien con las proteínas anti-apoptóticas, o bien con las proteínas efectoras Bax y Bak. Uno de estos subgrupos está formado por los denominados activadores directos Bid, Bim y Puma, capaces de inhibir a las BCL-2 anti-apoptóticas, pero también de unirse a las proteínas efectoras para activarlas y favorecer su oligomerización entre sí, desencadenando la permeabilización de la membrana mitocondrial externa (MOMP). El segundo grupo está integrado por las proteínas sensibilizadoras/de-represoras (Bad, Bmf, Hrk y Noxa). Estas proteínas carecerían de la

capacidad para activar directamente Bak o Bax. Sin embargo, son capaces de unirse e inhibir a las proteínas anti-apoptóticas favoreciendo con ello la activación de las efectoras Bax y Bak, para promover el MOMP.

En células sanas no sometidas a ningún tipo de estrés, la proteína pro-apoptótica Bax reside inactiva en el citosol, con su dominio C-terminal secuestrado dentro del llamado surco hidrofóbica (64). Tras la activación de la cascada de señalización apoptótica, Bax pasa a su forma activa tras uno o varios cambios conformacionales derivados de su interacción con otros miembros de la familia BCL-2; estos cambios conformacionales liberan el dominio C-terminal el cual dirige y ancla a Bax en la MOM. Una vez en la membrana, las proteínas efectoras Bax y Bak homo- y hetero-oligomerizan formando poros proteolíticos y/o proteolipídicos que promueven la permeabilización y la liberación de diversos factores apoptogénicos.

En cualquiera de los tipos celulares existentes en el organismo el delicado equilibrio que se establece entre supervivencia o muerte es el que determina el destino celular. Por tanto, ligeros desajustes que alteran este balance hacia un destino u otro son responsables de un gran número de enfermedades. De hecho, las alteraciones que experimentan algunos de los mecanismos de muerte celular han sido reconocidos como una de las seis características que definen los procesos tumorales (451). Por tanto, la desregulación de las proteínas de la familia BCL-2, que actúan como moduladores cruciales del proceso de apoptosis, han sido relacionadas con el desarrollo de varios tipos de tumores (258). Estas proteínas podrían ser responsables directas de la enfermedad (conductores), aunque también podrían estar implicadas en la resistencia adquirida a los tratamientos anti-tumorales. Este es el motivo por el que tradicionalmente muchos de los fármacos desarrollados contra el cáncer, independientemente de su mecanismo de acción principal, tengan como dianas las proteínas de la familia BCL-2, ya sean para tratar de activar a las proteínas efectoras Bax y Bak (153) como para bloquear la acción de las anti-apoptóticas que constituyen una forma de quimioresistencia intrínseca.

El papel de las proteínas BCL-2 ha sido demostrado en diversos tumores hematológicos (260, 303). También se ha establecido la correlación entre la elevada expresión de la proteína anti-apoptotica Bcl-2 y el mal pronóstico en melanoma (452), cáncer de mama (262) y próstata (263). Por otro lado, la disminución de la expresión de la *BH3-only* Bim también se relaciona con varios tipos de cáncer, incluyendo el linfoma de células B y el cáncer de colon (286, 453). Debido a la amplia implicación de la familia BCL-2 en los procesos tumorales existen numerosas líneas de investigación en curso cuyo objetivo es restaurar la sensibilidad de las células cancerosas a las señales pro-apoptóticas.

Uno de los primeros fármacos desarrollados para inhibir la acción de las proteínas antiapoptóticas de la familia Bcl-2 se denomina Oblimersen. Se trata de un

oligonucleótido antisentido modificado complementario al gen de la proteína Bcl-2 (298). Sin embargo, la eficacia de este fármaco es todavía objeto de estudio y presenta algunos problemas de toxicidad. Diversos estudios estructurales de las proteínas de la familia BCL-2 mostraron que las interacciones citosólicas de estas proteínas se basan en la unión del dominio BH3 de miembros pro-apoptóticos con la región del surco hidrofóbico presente en las proteína anti-apoptóticas (59). Por este motivo uno de los puntos centrales en el diseño de fármacos antitumorales se focalizó en imitar el dominio BH3 de las proteínas *BH3-only*, surgiendo varias moléculas denominadas "miméticos de BH3" (305). Estos "miméticos de BH3" se unen a uno o varios de los miembros anti-apoptóticos de la familia BCL-2 para bloquear su acción pro-supervivencia, generando la liberación de Bax y Bak para crear poros en el MOM y activar el proceso apoptótico. Uno de los "miméticos de BH3" más eficientes hasta la fecha es un compuesto desarrollado por Abbott, llamado ABT-737, y su variante de ingesta oral ABT-263 (307). Ambos son inhibidores de las proteínas anti-apoptóticas Bcl-xL, Bcl-w y Bcl-2. En ensayos clínicos, ABT-263 ha mostrado prometedores resultados en algunos tipos de neoplasias linfoides (307, 454, 455). Una variante de estos compuestos llamada ABT-199, que actúa específicamente sobre la proteína Bcl-2, también muestra resultados prometedores en ensayos de leucemia linfocítica crónica, en la actualidad en fase I de desarrollo.

Aunque la aparición de estos "miméticos de BH3" representa un gran avance en el desarrollo de estrategias antitumorales, existen diversos tipos de cáncer dependientes de los niveles de proteínas BCL-2 que no responden al tratamiento con éstos compuestos. Recientemente ha sido introducido el concepto de 'cebado' mitocondrial para referirse la inducción de la permeabilización de las mitocondrias de células tumorales, lo conduciría a su muerte. Dependiendo de los niveles de expresión de proteínas anti-apoptóticas y de su presencia en la mitocondrias, las células tumorales serán más o menos susceptibles a los tratamientos antitumorales que tienen como diana a éstas BCL-2 anti-apoptóticas.

Durante los últimos años se han propuesto diferentes modelos para la formación de poros en la membrana mitocondrial externa (140): PTP (poro transitorio para la permeabilización), MAC (canal mitocondrial inducido por apoptosis), oligomerización de VDAC1, de Bax y Bak, y de ceramidas. La evolución de estos modelos ha provocado dos cambios fundamentales, por un lado la relevancia que adquiere la red de interacciones que se establecen entre las proteínas de la familia BCL-2 que regulan la formación de la mayor parte de estos poros mitocondriales; y por otro lado la inclusión de la propia membrana mitocondrial como un participante activo en el mantenimiento del equilibrio de esta red de interacciones que regulan todo el proceso apoptótico.

Actualmente existe un mapa bastante completo de la red de interacciones en la que se comprende bien la contribución de las regiones citosólicas de las proteínas de la familia

BCL-2. Sin embargo, a pesar de que una gran parte de estas interacciones proteína-proteína tienen lugar en el contexto de la membrana mitocondrial, la contribución de los regiones hidrofóbicas de estas proteínas BCL-2 (BCL-2 TMDs) a esta red está lejos de estar resuelta. Además, existen evidencias que sugieren un papel relevante de estas regiones transmembrana (TMD) en el control de la apoptosis. Estas y otras cuestiones que implican a los BCL-2 TMDs son las que hemos abordado durante el transcurso de la presente Tesis Doctoral.

10.2. OBJETIVOS

La apoptosis se define clásicamente como un tipo de muerte celular programada. La activación de este proceso está mayoritariamente regulada por las proteínas de la familia BCL-2. Los miembros de esta familia se localizan en citoplasma, ER y MOM en las células sanas. Sin embargo, durante la apoptosis, la mayor parte de las interacciones entre estas proteínas ocurren en las membranas de orgánulos intracelulares. El objetivo central de esta Tesis Doctoral es ampliar nuestros conocimientos del mecanismo de acción de las proteínas de la familia BCL-2 en presencia de membranas. Este objetivo general ha sido abordado mediante los siguientes objetivos específicos:

- El primer objetivo de este trabajo ha sido determinar la participación de los BCL-2 TMDs en la red de interacciones que establecen los diferentes miembros de la familia BCL-2. Así mismo, Se ha estudiado la importancia de las interacciones de los BCL-2 TMDs en el contexto de las proteínas BCL-2 completas así como la relevancia funcional de estos TMDs en las rutas apoptóticas.
- La capacidad de inserción en la membrana mitocondrial de las proteínas BH3-only es actualmente muy controvertida. Por ello, el segundo objetivo de esta tesis ha sido investigar la capacidad de las regiones hidrofóbicas del extremo C-terminal de proteínas *BH3-only* para insertarse en diferentes membranas biológicas.
- El papel de los dominios citosólicos de las proteínas BCL-2 como sensibilizadores de la permeabilización mitocondrial (MOMP) en quimioterapia ha sido ampliamente estudiado. Sin embargo, poco se sabe acerca del papel de los BCL-2 TMDs en este proceso. Así, el tercer objetivo de esta tesis ha sido investigar la contribución de péptidos sintéticos derivados de BCL-2 TMDs en el proceso de permeabilización de la membrana mitocondrial externa (MOMP).

- Este trabajo también aborda el estudio de las diferentes rutas de muerte celular que son activadas en respuesta a diferentes fármacos pro-apoptóticos, dependiendo de la maquinaria apoptótica disponible en la célula.

10.3. MATERIAL Y MÉTODOS

10.3.1. Metodología utilizada para el estudio de las interacciones entre dominios transmembrana de las proteínas de la familia BCL-2.

Durante la realización de esta Tesis Doctoral se han abordado diferentes estrategias para el estudio y análisis de las regiones TM de las proteínas de la familia BCL-2. En lo referente a la determinación de posibles interacciones entre los diferentes TMDs se han realizado los análisis utilizando dos tecnologías que permiten estudiar interacciones proteína-proteína en célula vivas. En primer lugar se ha utilizado el sistema de complementación ToxRed en bacterias para la realización de un rastreo de interacciones entre los diferentes TMDs. En segundo lugar, se ha empleado la metodología de BiFC basada en complementación bimolecular de fluorescencia con el objetivo de analizar las interacciones en células eucariotas y determinar su localización subcelular.

10.3.1.1. Diseño, clonaje, expresión y análisis de los BCL-2 TMD en el sistema ToxRed.

El ensayo de complementación de maltosa (Figura10.3.1) fue realizado de acuerdo a un protocolo previamente descrito (332, 333). El objetivo de los experimentos realizados en este sistema fue determinar la correcta orientación, la capacidad de inserción así como la habilidad de los dominios TM de las proteínas BCL-2 de establecer asociaciones hélice-hélice para formar homo y/o hetero-oligómeros en la membrana interna de las bacterias de la cepa MM39 de *E. coli*. Los plásmidos ToxR originales fueron proporcionados por el laboratorio del Profesor William De Grado (UCSF). En estas construcciones la clonación de las diferentes secuencias correspondientes a los TMD estudiados se llevó a cabo entre la secuencia que codifica para el dominio de activación del factor de transcripción de *Vibrio cholerae* ToxR y la secuencia que codifica para el dominio periplásmico del translocador de maltosa (MBP). Para determinar si las proteínas de fusión ToxR-TM-MBP estaban correctamente insertadas y orientadas en la membrana bacteriana, se realizó el crecimiento de MM39, transformadas con las diferentes construcciones, en un medio que contenía maltosa como única fuente de carbono. La cepa MM39 presenta deleccionado el gen *malE* que codifica para la MBP, de tal forma que solo aquellas

bacterias que expresen las construcciones ToxR-TM-MBP y que las tengan correctamente insertadas y orientadas en su membrana interna (de tal manera que el dominio MBP quede en el espacio periplásmico), podrán captar maltosa del medio y por ello serán capaces de crecer en este medio restrictivo. La capacidad de homo- y hetero-oligomerización de las diferentes proteínas de fusión se determinó mediante la expresión del gen *RFP* que codifica la proteína de fluorescencia roja (RFP), el cual se encuentra bajo el control del promotor *ctx* que es a su vez reconocido por el factor de transcripción ToxR. No obstante, el reconocimiento de la secuencia del promotor sólo tiene lugar cuando ToxR se encuentra en forma de dímero, y esta dimerización solo es posible si los segmentos TM ensayados interaccionan y acercan los monómeros de ToxR. Como control de este sistema, se realizaron las mismas construcciones con el mutante de ToxR R96K (ToxR*), que permite la dimerización del factor de transcripción pero no su unión al promotor *ctx* , por lo que RFP no se expresa (334) (Figura 10.3.1).

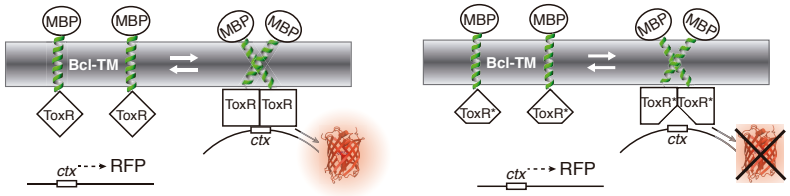

Figura 10.3.1. Vista esquemática del sistema ToxR para el análisis de interacciones TM. Las construcciones están formadas por el activador transcripcional dependiente de dimerización ToxR, un dominio TM BCL-2 y el translocador de maltosa MBP. La interacción de los TMDs produce la activación mediada por ToxR de un gen reportero, en este caso *RFP*. El nivel de fluorescencia indica la afinidad de la asociación entre los TMDs. Este ensayo de fluorescencia ha sido normalizado con una construcción mutante ToxR* incapaz de activar la expresión del gen reportero.

Para generar las diferentes construcciones quiméricas de ToxR, se diseñaron cebadores con las secuencias completas de los TMDs flanqueadas por los sitios de restricción *Hind*III/*Xho*I presentes en el plásmido ToxR (Tabla 10.I.). Una vez hibridados los cebadores, fueron tratados con polinucleótido quinasa para añadir los grupos fosfato y posteriormente se ligaron con la ligasa del bacteriófago T4 (Promega). Para facilitar la inserción de los TMD en los plásmidos ToxR se utilizó fosfatasa alcalina (Roche) para eliminar el fosfato 5' en el vector de ToxR sin inserto.

Para confirmar la especificidad de las interacciones, se diseñaron mutantes puntuales de cada BCL-2 TMD estudiado utilizando el kit Stratagene Quikchange II disponible comercialmente (Agilent, CA, EE.UU.).

Tabla 10.I. Secuencia de los BCL-2 TMD clonados. Los aminoácidos subrayados fueron añadidos en la clonación para el sistema BiFC por su relevancia en el direccinamiento de los TMD a mitocondria. ΔG representa una medida de hidrofobicidad en las secuencias analizadas, valores negativos son indicativos de inserción en membranas biológicas.

BCL-2	Cloned sequence	Length	ΔG
Bcl-2	FSWLSLKTLLSLALVGACITLGAYLGHK	23	-1.356
Bcl-xL	SRKGQERFNRWFLTGMTVAGVVLLGSLFSRK	23	-0.355
Bcl-w	REGNWASVRTVLTGAVALGALVTVGAFFASK	22	-0.418
Mcl1	IRNVLLAFAGVAGVGAGLAYLIR	23	-0.275
Bcl-B	FWRKQLVQAFLSCLLTTAFIYLWTRLL	21	0.689
Bax	TWQTVTIFVAGVLTASLTIWKKMG	20	0.510
Bak	ILNVLVVLGVVLLGQFVVRRFFKS	22	-0.735
Rambo	GKSILLFGGAAAVAILAVAIGVALRKK	21	-1.403
Bik	VLLALLLLLALLLPLLSGGLHLLLK	24	-3.253
Bid	KEKTMLVLALLLAKKVA	17	2.462

Las construcciones ToxR-TM-MBP (200 ng) fueron transformadas en células competentes MM39 mediante choque térmico a 42°C durante 90 seg. Tras crecer las células en agitación 1 h en LB, fueron sembradas en medio mínimo con agar y ampicilina 100 mg/ml. Tras 48 h, las células MM39, que expresaron las proteínas quiméricas ToxR-TM-MBP fueron cultivadas medio LB con ampicilina durante 6 h. Los cultivos fueron sedimentados y se incubaron con agitación a 37°C durante 48 h en medio mínimo hasta obtener una OD_{600} 0,8. Las mediciones de fluorescencia de RFP se realizaron utilizando el espectrofotómetro Wallac 1420 con una longitud de onda de excitación de 570nm y longitud de onda de emisión de 620nm en placas de 24 pocillos (Thermo Scientific).

Para evaluar los niveles de expresión de todas las construcciones ToxR-TM-MBP , las células MM39 se sedimentaron por centrifugación durante 5 min a 3000×g, se eliminó el sobrenadante y los sedimentos celulares se resuspendieron en 10× del reactivo de lisis FastBreak (Promega). A continuación, la mezcla se incubó a temperatura ambiente en agitación suave durante 30 min y posteriormente las muestras se centrifugaron durante 10 min para separar la fracciones esferoplásmica y periplásmicas. Se cuantificaron todas las muestras con el kit de cuantificación de BCA (Thermo Scientific). 50 µg de proteína total de cada muestra fueron cargados en geles SDS-PAGE de acrilamida al 12%, se transfirieron a membranas de nitrocelulosa, se bloquearon con leche en TBS-Tween 20 5%, y se incubaron durante la noche con el anticuerpo primario correspondiente (MBP de New England Biolabs (#E8038S); HA C29F4 (#3724S) y c-myc 9B11 (#2276S) de cell-

signalling). Las membranas se incubaron con el anticuerpo secundario apropiado conjugado con peroxidasa para la detección de la cantidad de proteína por quimioluminiscencia (Amersham Pharmacia Biotech).

A modo de ejemplo se muestran los resultados que se obtuvieron siguiendo esta metodología para los TMD de Bcl-2, Bcl-xL y Bax (Figura 10.3.2). En todos los ensayos realizados se utilizó como control positivo de homo-oligomerización el fragmento TM de glicoforina (GpA), cuya dimerización ha sido ampliamente demostrada en la bibliografía (332). En la misma línea, el mutante de GpA G83I fue empleado como control negativo. Además, la señal de fluorescencia obtenida fue normalizada respecto a la señal obtenida por respectivas las construcciones ToxR*.

Los resultados obtenidos muestran que los TMDs de Bcl-2, Bcl-xL y Bax homo-oligomerizan (Figura 10.3.2A). Mas aún, estas interacciones entre hélices TM presentan una elevada especificidad, dado que encontramos mutantes puntuales de las superfícies de interacción TMD-TMD capaces de romper estas homo-oligomerizaciones (10.3.2B).

A

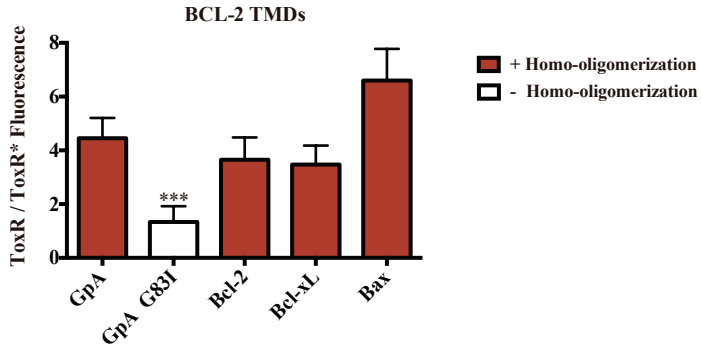

B

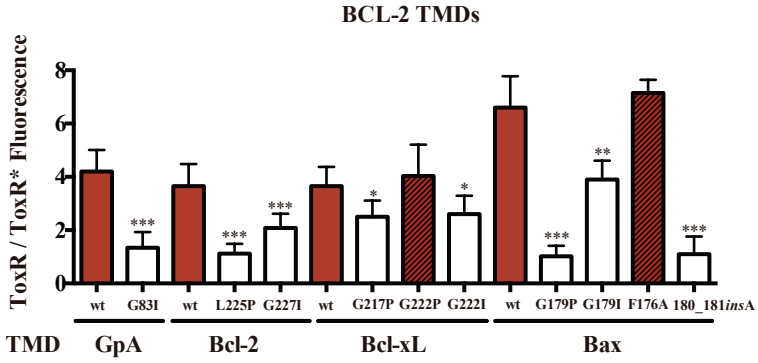

Figura 10.3.2. Los TMDs de las proteínas de la familia BCL-2 son capaces de homo-oligomerizar. (A) La formación de oligómeros entre BCL-2 TMDs produce un aumento de la fluorescencia debido a la expresión RFP mediada por el factor de transcripción ToxR. Los resultados representan la señal de fluorescencia normalizada (ToxR / ToxR *). (B) Disminución de la señal de fluorescencia en el sistema ToxR inducida por mutaciones puntuales de BCL-2 TMDs. La caída de la señal de fluorescencia indica que los TMD no homo-oligomerizan. Las barras rojas representan las interacciones positivas y barras blancas representan las interacciones negativas. GpA actúa como control positivo y el mutante puntual GpA G83I negativo. Todos los resultados representan la media de tres experimentos independientes. Se utilizó el test de comparación múltiple de Dunnett (CI 95%) para la comparación con el control positivo glicoforina A TMD.

Para analizar las interacciones entre diferentes BCL-2 TMDs se modificó la metodología descrita para el sistema ToxR en el caso de las homo-oligomerizaciones desarrollándose un ensayo de competencia (Figura 10.3.3B). Se transformó la cepa MM39 con dos construcciones: por un lado ToxR-TMD1-MBP, capaz de oligomerizar y de activar la expresión de RFP; por otro ToxR*-TMD2-MBP, capaz de oligomerizar pero no de reconocer la secuencia del promotor *ctx*. De esta forma, si consideramos que los TMD1 y TMD2 hetero-oligomerizan, la interacción de estas construcciones no producirá la expresión de RFP, ya que es necesario que ambos ToxR sean completamente funcionales para unirse al DNA del promotor. Por ello, se producirá un descenso en la señal de fluorescencia roja correspondiente a RFP. Si por el contrario no existe interacción, la construcción ToxR-TMD1-MBP interaccionará únicamente consigo misma y se mantendrá la señal de fluorescencia al mismo nivel que en el caso de las homo-oligomerizaciones.

Siguiendo el ejemplo para los TMDs de Bcl-2, Bcl-xL y Bax podemos observar que tanto Bcl-2 como Bcl-xL son capaces de hetero-oligomerizar con el TMD de Bax (Figura 10.3.3B, C y D). Sin embargo los TMD de Bcl-2 y Bcl-xL no interaccionan entre sí como se observa en la figura 10.3.3B y C. En estos ensayos el TMD de GpA es usado como control negativo de interacción ya que no presenta ninguna relación con los TMD analizados.

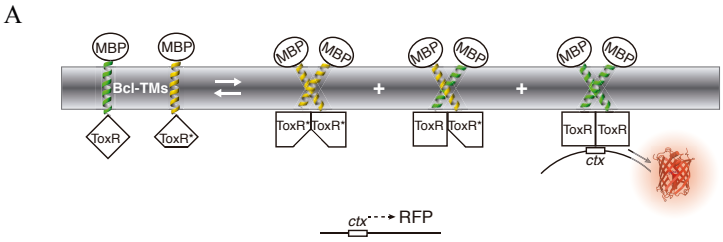

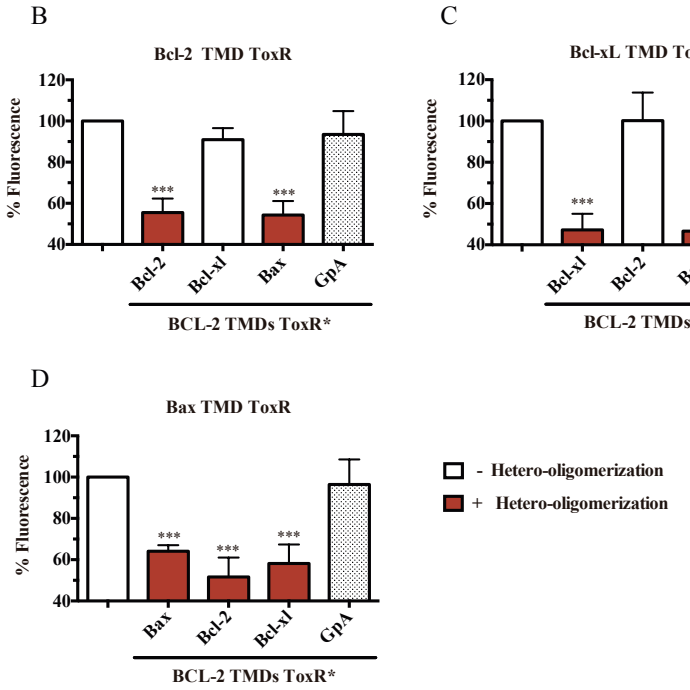

Figura 10.3.3 hetero-oligomerizaciones entre TMDs de las proteínas de la familia BCL-2. (A) Vista esquemática del sistema ToxR adaptado para evaluar la formación de hetero-oligómeros. La cotransformación de una construcción ToxR de un BCL-2 TMD y ToxR * de otro TMD , genera tres posibles oligómeros diferentes: combinaciones fluorescentes (ToxR / ToxR) y no fluorescentes (ToxR / ToxR * y ToxR * / ToxR *).(B,C y D). El control de la construcción ToxR del TMD analizado en cada caso (primera columna) representa la máxima señal de fluorescencia (100% homo-oligomerización). Las barras rojas representan hetero-oligomerizaciones positivas. La disminución de la fluorescencia indica la formación de hetero-oligómeros con las construcciones ToxR* evaluadas. Las barras blancas representan hetero-oligomerizaciones negativas. GpA es una proteína no relacionada y se utilizó como control negativo de hetero-oligomerización. los experimentos se realizaron para las construcciones ToxR-TMD-MBP de Bcl-2 (B), Bcl-xL (C) y Bax (D) cotransfectadas con ToxR*-TMD-MBP de las diferentes proteínas BCL-2.

10.3.1.2. Diseño, clonaje, expresión y análisis de segmentos TM en el sistema BiFC.

Toda la metodología basada en el sistema de complementación bimolecular de fluorescencia (BiFC) ha sido realizada como se describió previamente en la bibliografía (335, 456). El objetivo de estos ensayos ha sido el análisis de la capacidad de interacción entre los TMD de las proteínas BCL-2 en células eucariotas, así como la localización subcelular de estas interacciones. Estos experimentos están basados en la idea de que la proteína Venus (un mutante de la proteína YFP que emite fluorescencia verde en lugar de amarilla) puede ser dividida en dos fragmentos: VN, que comprende la región desde el

aminoácido 1 al 155, y que además presenta la mutación I152L que disminuye considerablemente el ruido de fondo inespecífico, y VC (155-238, A206K). Cuando estos fragmentos se encuentran lo suficientemente próximos en el interior de la célula son capaces de reconstituir la proteína completa, que emite fluorescencia verde (Figura 10.3.4). Esta propiedad permite que al fusionar a cada fragmento diferentes proteínas, podamos determinar si interaccionan dependiendo de si se produce o no la emisión de fluorescencia derivada de la reconstitución de la proteína fluorescente. Por ello, hemos fusionado tanto a VN como a VC cada uno de los TMDs de las proteínas BCL-2. Dado que la topología de los TMD en todas las BCL-2 es C-terminal, han sido clonados tras las regiones VN y VC de Venus, separándose de ellas por medio de una serie de aminoácidos que actúan a modo de espaciadores. Como control positivo de oligomerización se utilizó la interacción conocida de las proteínas nucleares b-Jun y b-fos, así como una forma truncada de b-fos que no se asocia a b-jun para establecer un control negativo.

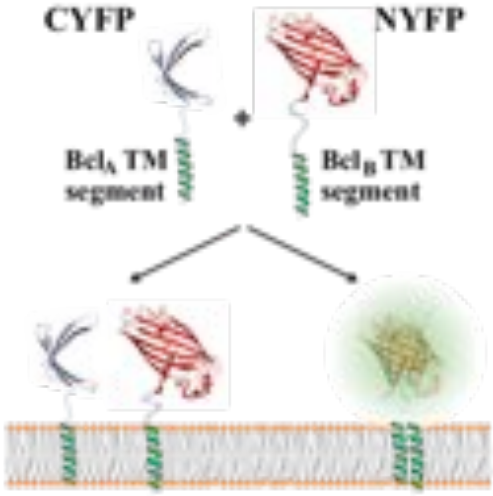

Figura 10.3.4. Representación esquemática del sistema de complementación bimolecular de fluorescencia (BiFC) en células de mamífero para el análisis de interacciones TM de proteínas de la familia BCL-2. El sistema esta basado en la reconstitución de la fluorescencia a partir de los fragmentos VN y VC en los que se ha sido dividida la proteína Venus. Esta reconstitución depende del establecimiento de la interacción entre los TMDs.

Para la clonación de las diferentes construcciones de BiFC se diseñaron cebadores con las secuencias completas de los TMDs flanqueadas por el sitio de restricción *Not*I, presente en la región C-terminal de los plásmidos de BiFC. Una vez hibridados los cebadores (95ºC 10 min, 60ºC 8 h), fueron tratados con polinucleótido quinasa para

añadir los grupos fosfato y posteriormente se ligaron con T4 DNA ligasa (Promega). Para facilitar la inserción de los TMD en los plásmidos BiFC se utilizó fosfatasa alcalina (Roche) para eliminar el 5' fosfato.

Para confirmar la especificidad de las interacciones en este sistema, se utilizaron aquellos mutantes puntuales de cada BCL-2 TMD que rompieron la interacción en el sistema ToxR. Se utilizó de nuevo el kit Stratagene Quikchange II (Agilent, CA, EE.UU.). Finalmente, todas las construcciones fueron verificadas por secuenciación del DNA.

La líneas celulares utilizadas para todos los ensayos fueron HeLa y HCT 116 que fueron mantenidas en las condiciones recomendadas por la *American Type Culture Collection*. Los ensayos se realizaron en placas de seis pocillos al 60% de confluencia celular y se cotransfectaron usando Lipofectamine 2000 (Invitrogen) o Turbofect (Thermo scientific) con cantidades desde 0,25 a 1 μg de cada plásmido VN/VC. Las células transfectadas se incubaron a 37°C durante 24 h y a continuación fue medida la emisión de fluorescencia de Venus a 535 nm, excitando a la longitud de onda de 500 nm utilizando el espectrofotómetro Wallac 1420.

Para evaluar los niveles de expresión de todas las construcciones VN/VC BiFC-TMD se obtuvieron extractos celulares mediante lisis celular en un tampón que contiene: Tris-HCl 25 mM pH 7,4, EDTA 1 mM, EGTA 1 mM, 1% SDS, así como inhibidores de proteasas. La concentración de proteína se determinó utilizando el kit de cuantificación de BCA (Thermo Scientific). 60 μg de cada lisado celular se resolvieron mediante electroforesis SDS-PAGE y se transfirieron a membranas de nitrocelulosa. Tras la transferencia, las membranas se bloquearon utilizando 5% de leche en polvo en TBS-Tween 20 y se incubaron durante la noche con el anticuerpo primario correspondiente. Tras tres lavados con TBS-Tween 20, las membranas se incubaron con el anticuerpo secundario apropiado conjugado con la enzima peroxidasa para la detección de proteína por quimioluminiscencia (Amersham Pharmacia Biotech). Los anticuerpos contra el epítopo de VC HA C29F4 (# 3724S), de VN c-myc 9B11 (# 2276S) , Bax (#2772) y caspasa-3 (# 9662S) proceden de Cell Signalling y α-tubulina (# T8203) de Sigma-Aldrich.

Para determinar la localización subcelular de todas esta red de interacciones mediadas por los BCL-2 TMDs, se llevaron a cabo ensayos de localización subcelular e inmunolocalización por microscopía confocal de las construcciones de BiFC. Las células fueron sembradas y transfectadas sobre cubreobjetos de vidrio y tras la expresión de las construcciones durante 24 h, se lavaron repetidas veces en PBS para eliminar los restos celulares y de medio de cultivo. El proceso de fijación se realizó con paraformaldehído al 4% durante 20 min. Después de tres lavados con PBS, las células se permeabilizaron con 0,1% de Triton X-100 y posteriormente se llevó a cabo el bloqueo en 2% de gelatina en

PBS. Para el ensayo de liberación de citocromo *c*, las células se incubaron con el anticuerpo contra Cyt-*c* (1: 200; SC13561; Santa Cruz) durante 12h a 4ºC seguido de una incubación con el anticuerpo secundario anti-IgG de ratón-Alexa 555 (1: 400)(Invitrogen) durante 2 h. Los cristales fueron montados en portaobjetos de vidrio con Mowiol/DAPI (Sigma). Las imágenes se obtuvieron utilizando un microscopio confocal LSM 510 con un objetivo de 63x. Cada experimento fue repetido al menos tres veces. Se analizaron al menos 30 imágenes de cada muestra. Para la determinación de salida de citocromo *c* se contaron doscientas células y se clasificaron de acuerdo a la localización de Cyt-*c* en las mitocondrias (morfología tubular) o citosol (patrón difuso). Las imágenes de fluorescencia se analizaron y cuantificaron por colocalización con el software ImageJ. La colocalización de las construcciones BiFC-TMD y la sonda Mitotracker (500 nM, 20 min, 37°C, Invitrogen) o el anticuerpo Grp78 (1:1000, Abcam, revelado con Alexa555 1:400) se definió como la superposición parcial o total de las señales verde y roja.

Como aplicación de toda esta metodología pondremos dos ejemplos: la interacción y localización subcelular de los BCL-2 TMDs de Bcl-2, Bcl-xL y Bax (Figura 10.3.5); y un trabajo realizado en el transcurso de esta tesis doctoral con el TMD de la proteína SP-C del surfactante pulmonar que no ha sido incluido en la misma debido a que la temática abordada se aleja del tema principal de esta tesis.

A

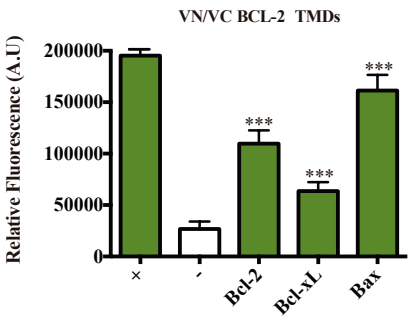

B

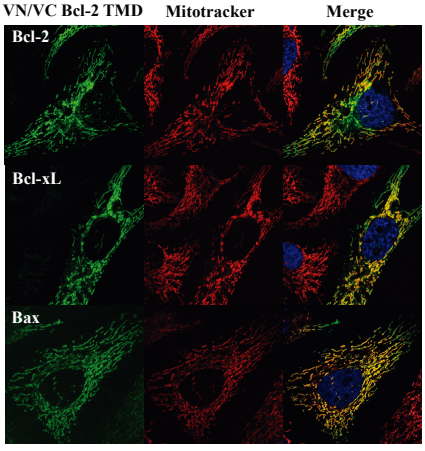

Figura 10.3.5. Homodimerización de los segmentos transmembrana de Bcl-2, Bcl-xL y Bax en células HCT 116 usando el sistema BiFC. (A) Medida de fluorescencia de BiFC para los TMDs de Bcl-2, Bcl-xL y Bax. Las construcciones VC y VN se transfectaron HCT 116 y la fluorescencia (A.U. unidades relativas) se midió a las 24 h. Las Barras representan La intensidad media de fluorescencia de tres experimentos independientes. El test de comparación múltiple de Dunnett (CI 95%) se utilizó para comparar la señal media

con el control negativo de fluorescencia Jun /ΔFos (control positivo Jun/Fos). (B) Imágenes de microcopia confocal en células HCT 116 transfectadas con construcciones VC y VN para Bcl-2, Bcl-xL y Bax TMD. La formación de homo-oligómeros se observa en el canal verde. El canal rojo (Mitotracker) corresponde al marcador mitocondrial. La colocalización se muestra en amarillo.

El surfactante pulmonar se compone en un 90-95% de lípidos (80% fosfolípidos y 5%-10% lípidos neutros, en particular el colesterol), y un 8%-10% de proteínas. Estas proteínas son específicas de esta película biológica, e incluyen a la proteína surfactante A1 (SPA1), SPA2, SPB, SPC y SPD. Las SPA y SPD son hidrofílicas y las SPB y SPC (proteína del sulfactante pulmonar C) directamente afectan las propiedades biofísicas de los lípidos que constituyen el surfactante. La alteración tanto a nivel génico como proteico de alguna de éstas proteínas es la responsable de diferentes patologías respiratorias.

SPC humana es un péptido de 35 aminoácidos altamente hidrofóbico que se sintetiza como una proteína precursora mucho mayor de 21 kD. La SPC adopta una conformacional en hélice α con capacidad de inserción en las membranas alveolares (457). Alteraciones en la proteína SPC se asocian al síndrome de distress respiratorio en infantes prematuros y a la proteinosis alveolar pulmonar. Por este motivo resulta de gran importancia el estudio de la dinámica de membranas en la cual la dimerización de la SPC juega un papel esencial, así como su capacidad de asociación a otras proteínas y a los lípidos de la membrana alveolar.

La figura 10.3.5. describe la capacidad de homo-oligomerización de la región TM de la proteína SPC en células humanas. Esta interacción es además específica ya que no se asocia con otros fragmentos TM como el de Bcl-2 (Figura 10.3.5A). SPC se localiza normalmente en el retículo endoplasmático y como se observa en los resultados de microscopia confocal es en este orgánulo donde tiene lugar la dimerización (Figura 10.3.5B).

A

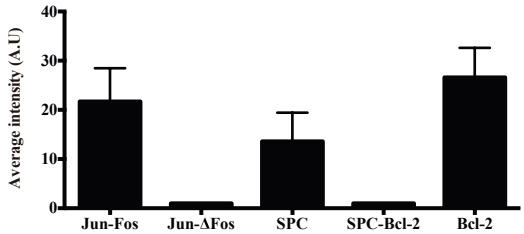

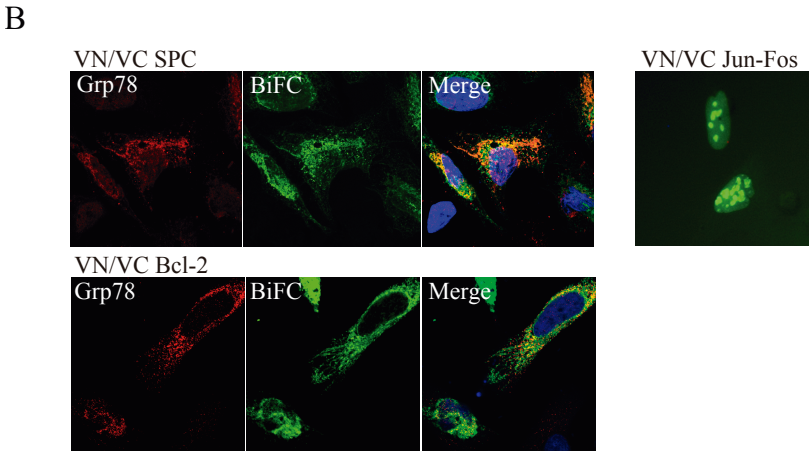

Figura 10.3.6. Homodimerización de segmentos TM de SPC en células HeLa usando el sistema BiFC. (A) Medida de fluorescencia de BiFC para los TMDs de SPC y Bcl-2. Las construcciones VC y VN se transfectaron HeLa y la fluorescencia (A.U. unidades relativas) se midió a las 24 h. Las Barras representan La intensidad media de fluorescencia de tres experimentos independientes. El test de comparación múltiple de Dunnett (CI 95%) se utilizó para comparar la señal media con el control negativo de fluorescencia Jun /ΔFos (control positivo Jun/Fos) . (B) Imágenes de microcopia confocal en células HeLa transfectadas con construcciones VC y VN para SPC y Bcl-2. La formación de homo-oligómeros se observa en el canal verde. El canal rojo corresponde al marcador de retículo endoplasmático Grp78. La colocalización se muestra en amarillo.

10.3.2. Metodología utilizada para el estudio de la función apoptótica de los dominios TM de las proteínas de la familia BCL-2.

La función principal de las proteínas de la familia BCL-2 es el control de la ruta apoptótica. Por tanto, uno de los objetivos de esta Tesis fue determinar la relevancia de los BCL-2 TMD en apoptosis. Para ello, se emplearon diferentes estrategias y protocolos de medición de la activación apoptótica entre los que destacaremos aquí el ensayo de actividad enzimática para la proteasa ejecutora caspasa-3 y los experimentos de salida de citocromo *c* en mitocondrias aisladas.

10.3.2.1 Determinación de la actividad de caspasa-3 frente a diferentes tratamientos.

Esta metodología se basa en la extracción del contenido citosólico de células sometidas a diferentes tratamientos, para incubarlos posteriormente en presencia de un sustrato fluorogénico específico de caspasa-3, la cual sólo se encuentra activa en el citosol cuando ha sido procesada por la maquinaria apoptótica. Los extractos celulares se prepararon a partir de 2×10^5 células sembradas en placas de 6 pocillos. Después de 24 h, se llevaron a

cabo los tratamientos farmacológicos pertinentes según el diseño del ensayo. Tras el tratamiento, las células fueron recogidas con tripsina, lavadas con tampón salino (PBS) y sedimentadas por centrifugación a 400 g 5 min. Los sedimentos se resuspendieron en tampón de extracción (PIPES 50 mM, KCl 50 mM, EDTA 5 mM, $MgCl_2$ 2 mM, DTT 2 mM) suplementado con un cóctel de inhibidores de proteasas (Sigma) y se mantuvieron en hielo durante 5 min. A continuación se congelaron y descongelaron tres veces en nitrógeno liquido para facilitar la lisis celular. Los lisados celulares se centrifugaron a 14.000 rpm durante 5 min y se recogieron los sobrenadantes, que corresponden al extracto citosólico. La concentración de proteína total fue cuantificada utilizando el kit de proteína BCA (basado en el ácido bicinconínico, Thermo Scientific). 60 µg proteína total se mezclaron con 200 µL de tampón de ensayo de caspasa (PBS 10% de glicerol, EDTA 0,1 mM, DTT 2 mM) que contenía 100 µM del sustrato específico de caspase-3 (Ac-DEVD-AFC (Enzo Life Sciences)). Finalmente la actividad caspasa-3 fue medida mediante liberación del grupo fluorescente AFC del sustrato a 37°C de forma continua utilizando un Wallac 1420 Workstation (λexc 400 nm; λem 508 nm). La actividad de esta proteasa se expresó como el incremento de unidades de fluorescencia relativa por minuto (AU).

A modo de ejemplo se muestran los resultados obtenidos en las líneas celulares MEFs Wt Apaf-1 y Wt Bax/Bak del capítulo IV frente a diferentes tratamientos antitumorales (Figura 10.3.7.)

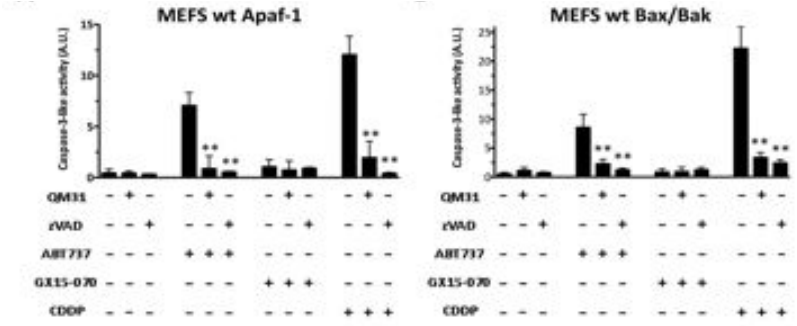

Figura 10.3.7. Actividad caspasa-3 en MEFs Wt de Bax/Bak y Apaf-1. QM31 evita la apoptosis en células no tumorales tratadas tanto con ABT737 como con CDDP, pero no en las tratadas con GX15-070. La actividad caspasa-3 se midió en MEFs sometidas a los siguientes tratamientos: ABT737 (25 µM), GX15-070 (1 µM) y CDDP (30 µM) en presencia o ausencia de QM31 (10 µM) y zVADfmk (5 µM). Las barras representan la media de al menos tres experimentos independientes ± sd (** p, 0,05).

10.3.2.2 Liberación de citocromo *c* en mitocondrias aisladas tratadas con diferentes péptidos derivados de los TMD de proteínas BCL-2.

Para realizar estos ensayos las mitocondrias fueron aisladas a partir de células MEFs mediante diferentes etapas de centrifugación como ha sido previamente descrito (348). Brevemente, $6x10^6$ células por placa de 150 mm fueron sembradas dos días antes de realizar el experimento. A continuación, fueron recogidas con tripsina y tras tres lavados con PBS se centrifugaron a 600 g 10 min a 4ºC. Descartado el sobrenadante, los sedimentos fueron resuspendidos en 3 ml de tampón IB_C (125 mM KCl, 5 mM KH2PO4, 2 mM MgCl2, 25 µM EGTA, 5 mM de succinato, rotenona 5 µM, y 10 mM HEPES-KOH (pH 7.2)). La lisis celular se llevó a cabo mediante rotura mecánica, utilizando el *douncer* adecuado y entre 20-30 golpes. Los lisados se centrifugaron a 600 g 10 min a 4ºC para eliminar las fracciones nucleares. El sobrenadante fue centrifugado a 7000 g 10 min a 4º. Se descartó el sobrenadante y se resuspendió el sedimento en IB_C para volver a centrifugar a 7000 g 10 min a 4º. Volvimos a quedarnos con el sedimento que fue finalmente resuspendido en 20 µL de IB_C. Una vez aisladas, las mitocondrias fueron incubadas con los diferentes TMD-pepts (50 µM) sintetizados químicamente en el tampón IB_C durante 30 min a 30°C. A continuación se centrifugaron a 14.000 g durante 10 min. Las fracciones mitocondriales del sobrenadante y del sedimento fueron cuantificadas y analizadas por Western blot utilizando anticuerpos contra citocromo *c* (#4272, Cell Signalling), α-tubulina (#T8203,Sigma-Aldrich) y VDAC 1/2/3 (sc-98708, Santa Cruz), siendo estos dos últimos marcadores de citosol y mitocondria, respectivamente. Su utilidad reside en servir como referencia para mostrar la pureza de las diferentes fracciones obtenidas.

La presencia de citocromo *c* en la fracción citosólica es indicativa de un proceso de desestabilización/permeabilización mitocondrial, por lo que aquellos TMD-pepts que promuevan este fenómeno tendrán funciones pro-apoptóticas. Como puede observarse a modo de ejemplo en la figura 10.3.8., algunos de los BCL-2 TMD-pepts son capaces de generar una desestabilización en la MOM que produce la salida de citocromo *c*, especialmente en el caso de Bcl-xL y Bak. En otros casos como Mcl-1 y Bcl-w, estos TMD-pepts no producen una permeabilización mitocondrial significativa, lo que además nos indica que los BCL-2 TMD-pepts no son fragmentos hidrofóbicos genéricos, sino que existe una especificidad en su secuencia para ejercer una función determinada. Como control negativo de la permeabilización mitocondrial se utilizó el péptido de GpA, cuyo TMD no tiene afinidad por las membranas mitocondriales ni funciones apoptóticas conocidas.

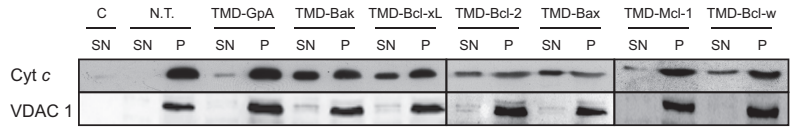

Figura 10.3.8. Liberación de citocromo *c* en mitocondrias aisladas. (A) Las mitocondrias aisladas fueron tratadas con 50 μM del TMD-pept que se indica en la parte superior durante 30 min a 30ºC. El Western blot de las diferentes fracciones mitocondrias purificadas fue revelado contra los anticuerpos de VDAC 1/2/3, utilizado como marcador mitocondrial, y citocromo *c* para determinar la permeabilización mitocondrial ejercida por los diferentes TMD-pepts. GpA TMD-pept fue utilizado como control negativo al tratarse de una proteína no relacionada con apoptosis y sin funciones mitocondriales descritas. Los datos son representativos de tres ensayos independientes.

10.4. CONCLUSIONES

- Los resultados de esta Tesis muestran que los dominios TM de las proteínas BCL-2 no se encuentran aislados en la membrana mitocondrial sino que son capaces de asociarse entre ellos. Los estudios de hetero-oligomerizaciones nos han permitido establecer por primera vez el mapa de interacciones de los TMD de las proteínas BCL-2. Además, se ha demostrado la contribución potencial de estos TMD a la regulación del proceso apoptótico. Por todo ello, concluimos que los BCL-2 TMDs, junto con los dominios solubles, participan en el delicado equilibrio que regula la permeabilización de la membrana mitocondrial (MOMP).

- En la subfamilia de las proteínas *BH3-only* hemos demostrado que las regiones hidrofóbicas C-terminales de Bik, Bim y Puma son capaces de insertarse en las membranas celulares de manera eficiente. Estos resultados abren un campo de estudio sobre las posibles interacciones con otros Bcl-2 TMDs. Por el contrario, las regiones C-terminales de Noxa y Bmf muestran una capacidad de inserción baja en las membranas celulares.

- Los estudios con péptidos derivados de los BCL-2 TMD han demostrado que algunos TMD-pepts pueden integrarse de manera específica en las membranas mitocondriales. Por otra parte, los TMD-pepts de Bcl-2, Bcl-xL, Bax y Bak inducen la liberación de citocromo *c*. En consecuencia, la introducción de estos péptidos induce muerte celular o bien establecen sinergismos con tratamientos

quimioterapéuticos cuando son empleados a concentraciones subletales, lo que les capacita para su potencial uso terapéutico.

- El BH3 mimético ABT737 no sólo requiere Bax/Bak para inducir apoptosis, sino también Apaf-1, mientras que GX15-070 y CDDP inducen diferentes modalidades de muerte celular en ausencia de las proteínas pro-apoptóticas Bax y Bak o Apaf-1. Por otro lado, el inhibidor del apoptosoma QM31 protege a la célula de los efectos derivados del tratamiento con ABT737 y parcialmente de los de CDDP, pero no logra bloquear la inducción de muerte celular por autofagia inducida por GX15-070.

APPENDIX I

- Andreu-Fernández V1, Genovés A, Lee TH, Stellato M, Lucantoni F, Orzáez M, Mingarro I, Aguilar MI, Pérez-Payá E. "**Peptides derived from the transmembrane domain of Bcl-2 proteins as potential mitochondrial priming tools.**" ACS Chem Biol. 2014. doi: 10.1021/cb5002679.

All the results of this publication are contained within this thesis. Vicente Andreu has performed the experiments and contributed to their design and to the writing of the manuscript.

ACS chemical biology

Articles

pubs.acs.org/acschemicalbiology

Peptides Derived from the Transmembrane Domain of Bcl-2 Proteins as Potential Mitochondrial Priming Tools

Vicente Andreu-Fernández,[†,⊥] Ainhoa Genoves,[*,†,⊥,▲] Tzong-Hsien Lee,[§] Matthew Stellato,[§] Federico Lucantoni,[†] Mar Orzáez,[†] Ismael Mingarro,[‖] Marie-Isabel Aguilar,[*,§] and Enrique Pérez-Payá[†,⊥,#]

[†]Laboratory of Peptide and Protein Chemistry, Centro de Investigación Príncipe Felipe, E-46012 Valencia, Spain

[⊥]Instituto de Biomedicina de Valencia, IBV-CSIC, E-46010 Valencia, Spain

[§]Department of Biochemistry and Molecular Biology, Monash University, Clayton, Victoria 3800 Australia

[‖]Departament de Bioquímica i Biologia Molecular, Universitat de València, 46100 Burjassot, Spain

Supporting Information

ABSTRACT: The Bcl-2 family of proteins is crucial for apoptosis regulation. Members of this family insert through a specific C-terminal anchoring transmembrane domain (TMD) in the mitochondrial outer membrane where they hierarchically interact to determine cell fate. While the mitochondrial membrane has been proposed to actively participate in these protein−protein interactions, the influence of the TMD in the membrane-mediated interaction is poorly understood. Synthetic peptides (TMD-pepts) corresponding to the putative TMD of anti-apoptotic (Bcl-2, Bcl-xL, Bcl-w, and Mcl-1) and pro-apoptotic (Bax, Bak) members were synthesized and characterized. TMD-pepts bound more efficiently to mitochondria-like bilayers than to plasma membrane-like bilayers, and higher binding correlated with greater membrane perturbation. The Bcl-2 TMD peptides promoted mitochondrial outer membrane permeabilization (MOMP) and cytochrome c release from isolated mitochondria and different cell lines. TMD-pepts exhibited nonapoptotic pro-death activity when apoptosis stimuli were absent. In addition, the peptides enhanced the apoptotic pathway induced by chemotherapeutic agents in cotreatment. Overall, the membrane perturbation effects of the TMD-pepts observed in the present study open the way for their use as new chemical tools to sensitise tumor cells to chemotherapeutic agents, in accordance with the concept of mitochondria priming.

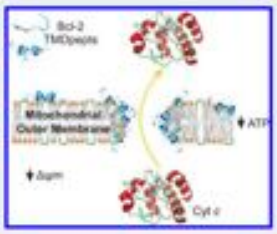

The function of the Bcl-2 proteins in apoptosis has been linked to their direct interaction with the mitochondrial membrane. Mitochondrial outer membrane permeabilization (MOMP) is considered the initial step that leads to the formation of the apoptotic pore, which has been related to the release of pro-apoptotic mitochondrial resident proteins including cytochrome c (cyt c) and smac/diablo to the cytosol and subsequent activation of caspases.[1−3] Proteins of the Bcl-2 family are divided into anti- and pro-apoptotic and a third class known as BH3-only proteins. Antiapoptotic members of this family (Bcl-2, Bcl-xL, Bcl-w, and Mcl-1) share four homology regions defined as Bcl-2 homology domains (BH1, BH2, BH3, and BH4). The pro-apoptotic members Bax and Bak contain the BH1−3 domains while the BH3-only proteins (e.g., Bid and Bim) only contain the BH3 domain.[4] BH3-only proteins promote apoptosis either by suppressing the antiapoptotic proteins or by direct activation of pro-apoptotic members.[5] Bcl-2 family protein dysfunctions have been associated with human diseases and several compounds targeting these proteins are under development as potential therapeutics for novel cancer treatments.[6]

The mechanism by which Bcl-2 proteins are directed to, and interact with, the membranes is still controversial, particularly because these proteins do not contain organelle specific targeting sequences.[7−10] The C-terminal amino acid sequence of most of the Bcl-2 proteins, in particular, the antiapoptotic and pro-apoptotic members, contains a stretch of highly hydrophobic residues that are likely to correspond to a transmembrane domain (TMD).[11] Furthermore, a recent study proposed that the BH3-only proteins can also be inserted into the mitochondrial outer membrane (MOM) by the C-terminal hydrophobic region.[12] Traditionally, Bcl-2 TMDs were referred to as membrane inserting domains.[7] However, it is becoming apparent that the TMDs are more than mere insertion domains and may play a key role in the function of the Bcl-2 proteins.[12−14] Synthetic peptides derived from such domains may thus represent useful tools when analyzed in the appropriate *in vitro* assays, as demonstrated for other membrane-related biological disorders.[15] Moreover, the sensitivity of tumor cells to MOMP when challenged with BH3 domain-derived peptides was recently exploited to increase the cellular response to chemotherapy.[16,17] This novel "mitochondrial priming" concept extended to targeted membrane perturbation may therefore provide new directions in the

Received: July 10, 2013
Accepted: June 6, 2014
Published: June 6, 2014

dx.doi.org/10.1021/cb400679r | ACS Chem. Biol. 2014, 9, 1799−1811

Table 1. CD Characterization of Bcl2-Derived Peptides

TMD-pept	peptide sequence	MW	ΔG (kcal/mol)[a]	percentage of α-helix[b]	
				PO_4^{-3} buffer 50 mM	SDS 10 mM
GpA	Ac-KKEITLIIFGVMGVIGTILLISYIKK-NH2	3167.5	−1.150	15	36
Bcl-2	Ac-KKETLLSLALVACITLGAYLKKK-NH2	2601.8	−1.356	32	100
Bcl-xL	Ac-KKRNFLTGMTVAGVVLLGSLFSRKK-NH2	2864.9	−0.353	8	78
Bcl-w	Ac-KKERTVLTGAVALGALYTVGAFFAKKK-NH2	2843.9	−0.418	8	49
Mcl1	Ac-KKENVLLAFAGVAGVGAGLAYLIRKK-NH2	2754.8	−0.273	7	79
Bax	Ac-KKTWQTVTIFVAGVLTASLTIWKK-NH2	2760.6	0.510	12	40
Bak	Ac-KKRILNVLVVLGVVLLGQFVVRRFFKKK-NH2	3311.3	−0.735	46	100

[a]Percentages of α-helical secondary structure obtained from the CD data interpreted with the K2D program of Dichroweb (available on the World Wide Web). [b]Prediction of ΔG.[42] Obtained from ΔG prediction server 1.0 (http://dgpred.cbr.su.se) considering only the TMDs of the proteins without added flanking Lys (shown in italics).[40,41,43,44]

pharmacological manipulation of cell death. We hypothesize that the TMD plays a central role in the function of Bcl-2 proteins and that characterization of the TMD membrane-binding properties will provide the initial step to understanding the specific role of the mitochondrial membrane in the apoptosis pathway. The aim of this study therefore was to perform a systematic evaluation of Bcl-2 TMD-derived peptides (TMD-pepts) in complementary biophysical and cellular studies to provide new insight into the role of the TMD in this prevalent cellular pathway.

RESULTS AND DISCUSSION

Peptide Design and Conformational Flexibility of Bcl-2 TMD-Derived Peptides. In order to perform a comparative study of the biophysical properties and putative in cellulo activity of the C-terminal region of Bcl-2 proteins, we designed and analyzed a series of peptides identified as TMD-pepts. To determine the most appropriate sequence regions to synthesize, the entire sequence of antiapoptotic (Bcl-2, Bcl-xL, Bcl-w, Mcl-1) and pro-apoptotic (Bax and Bak) proteins were analyzed using several transmembrane predicting algorithms (see Methods). The C-terminal residues of all proteins were found to be the most hydrophobic and therefore highly probable TMD segments. According to these results, individual peptides were designed and N- and C-terminal lysine residues were added to facilitate synthesis, purification, and characterization (Table 1). The native TMD sequence of each protein contain at least one positively charged amino acid and the insertion of additional terminal lysine residues have previously been shown to not interfere with the interacting properties of the hydrophobic sequences of many TMD core sequences.[14,19] Although the sequence alignment of the peptides derived from the TMD revealed less than 25% sequence identity, all the original sequences displayed a similar hydrophobicity profile with segregation of positive net charge balance toward the N- and C-termini while the hydrophobic residues were located in the central region (Table 1), a gradation of hydrophobicity statistically found in TM segments of solved integral membranes protein structures.[20]

The secondary structure of each peptide in different media was evaluated by circular dichroism (CD) spectroscopy. A control peptide derived from the TMD sequence of the well characterized plasma membrane protein glycophorin A (GpA) was also included. All peptides analyzed showed conformational flexibility, adopting different secondary structures in buffers and membrane-like environments analyzed. In phosphate buffered saline (PBS), the CD spectra of the TMD-pepts showed characteristics of extended conformation except for those derived from the pro-apoptotic protein Bak (TMD-Bak), which showed a moderate percentage of secondary structure (Table 1 and Supporting Information Figure S1). In order to initially examine the propensity of each peptide to adopt a defined secondary structure, CD spectra were also recorded in the presence of TFE (100% vol/vol), a solvent known to induce helicity in single-stranded potentially α-helical polypeptides;[21] in the presence of methanol (MeOH), which can increase β-structure population;[22] and at the critical micellar concentrations (10 mM) of SDS,[23] which may stabilize both α-helical or β-sheet conformations depending on the intrinsic secondary structure propensity of the polypeptide.[24] In 100% TFE, the TMD-pepts adopted mainly α-helical conformation, while TMD-Bcl-w and TMD-Mcl-1 adopted mixed random and helical conformations (Supporting Information Figure S1). In the presence of both MeOH and 10 mM SDS, TMD-Bcl-2, TMD-Bcl-xL and TMD-Bak exhibited α-helical structure; TMD-Bcl-w and TMD-Mcl-1 adopted mixed random and helical conformations, while TMD-Bax preferentially adopted a β-sheet conformation (Table 1 and Supporting Information Figure S1). Overall, the solution CD data demonstrate that TMD-pepts, with similar hydrophobic and charge distribution characteristics, exhibited different propensities to adopt a defined secondary structure in membrane-mimetic environments suggesting conformational flexibility.[25] While TMD-Bax was the only peptide that exhibited β-sheet conformation, overall, the α-helical conformation was predominant in membrane-like environments for all TMD-pepts.

Membrane Binding Properties of TMD-pepts. Bcl-2 family proteins are not commonly classified as integral membrane proteins but have been recognized to act exclusively on the cytoplasmic face of mitochondria and/or ER membranes,[26] where they most probably insert via their C-terminal TMD. Bcl-2 proteins are synthesized by free ribosomes as full-length proteins (including the C-terminus) in the aqueous cytosol before reaching any lipid bilayer, where C-terminal TMDs are energetically more stable. This process entails selective TMD shielding from the aqueous cytosol, targeting to the membrane surface and integration into the lipid bilayer, most likely with the assistance of as yet undiscovered chaperones. In order to evaluate the membrane affinity of the TMD of Bcl-2 proteins, we analyzed the binding of each TMD-pept to synthetic model lipid membranes. We used the mitochondrial model membrane system (POPC/POPE/POPS/POPI/S/3/1/1, mito-like) that mimics the lipid composition of the outer mitochondrial membrane. POPC/POPE/POPS/POPI/TOCL 48/28/1/1/0.4 (mito-like+CL) was used to determine the effect of cardiolipin, a mitochondrion-specific

dx.doi.org/10.1021/cb500267t | ACS Chem. Biol. 2014, 9, 1799−1811

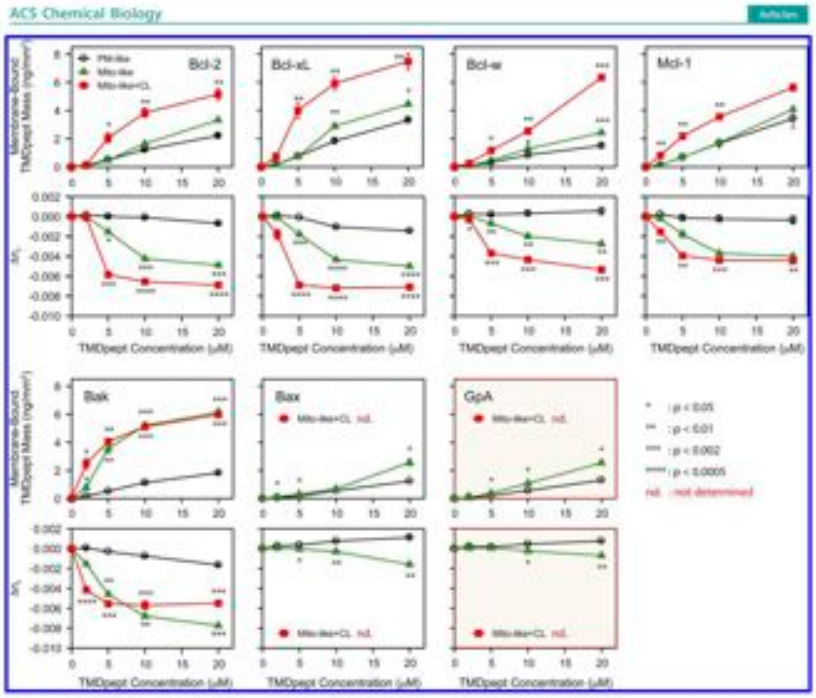

Figure 1. Changes in bilayer order induced by TMD-pepts. Measurements of bilayer mass and birefringence at different TMD-pept concentration. Dependence of mass (dependence of mass (ng/mm^2) and birefringence (Δn_0) on concentration of each TMD-derived peptide PM-like (black line), mito-like (green line), and mito-like+CL-like bilayers (red line). A decrease in birefringence corresponds to a decrease in bilayer order, while an increase in birefringence reflects an increase in bilayer ordering.

lipid,[17−19] which is predominantly located in the inner mitochondrial membrane but may also translocate to the outer mitochondrial membrane in some circumstances.[20] POPC was used as a model of the plasma membrane (PM-like). The binding of TMD-pepts to each model membrane and the effect of peptide binding on the membrane structure was analyzed by dual polarization interferometry (DPI)[21,22] (see Methods). The structural parameters of each supported bilayer formed *via in situ* liposome deposition and characterized by DPI are listed in Supporting Information Table S1. The accumulative binding of each TMD-pepts was characterized by the transmagnetic (TM) and transelectric (TE) phase changes, which were subsequently resolved into the mass of membrane-bound peptide and birefringence for each lipid bilayer. Plots of mass and birefringence changes versus time are shown in the Supporting Information (Figure S2). For each bilayer, injection of each peptide at increasing concentrations resulted in increased mass bound to the bilayer. There was little to no dissociation of any of TMD-pepts indicating that all peptides bound irreversibly under the conditions used. The overall amount of bilayer-bound peptide at the end of the 20 μM injection is plotted in Supporting Information Figure S3. Relative to the PM-like bilayer, only Bcl-w and Bak showed an statistically significant increase in mass bound to the mito-like bilayer. However, there was a meaningful increase in the total amount of peptide bound in the presence of cardiolipin for all peptides except Mcl-1-derived TMD-pept (Supporting Information Figure S3). Globally, the binding experiments indicate that all peptides interact more efficiently with the cardiolipin-containing mito-like bilayers.

Birefringence is a measure of membrane ordering that permits a systematic analysis of changes in bilayer order (a measure of structure) and allows the impact of peptide binding on the membrane structure[21−24] to be investigated. The changes in the order of the PM-like and both mito-like bilayers induced by the TMD-pepts (birefringence vs mass plots) are shown in Supporting Information Figure S4, which reflect the overall profile of bilayer disordering during peptide binding. These plots demonstrate that all peptides caused minimal disruption to the PM-like membrane but reduced the ordering of both mito-like

dx.doi.org/10.1021/cb500267t | ACS Chem. Biol. 2014, 9, 1799−1811

membranes. The dependence of both mass and birefringence on peptide concentration, as shown in Figure 1, allows further analysis of the effect of each peptide on the structure of the three model membranes. On the PM-like bilayer, the membrane ordering increased slightly (increase in birefringence) or decreased (drop in birefringence), reflecting small changes in bilayer structure and demonstrating the ability of the PM-like bilayer to recover from peptide binding. However, in comparison, the mito-like bilayer exhibited a significant degree of reordering to accommodate the bound peptide, which increased further in the presence of cardiolipin. For the TMD-pepts derived from antiapoptotic proteins (TMD-Bcl-2, TMD-Bcl-xL, TMD-Bcl-w, and TMD-Mcl-1), the birefringence of both mitochondrial membrane-derived bilayers approached a plateau at higher levels of bound peptide (Supporting Information Figure S4a). In contrast, the birefringence of the mito-like bilayer continued to drop for the TMD-pept derived from pro-apoptotic protein Bak (Supporting Information Figure S4b), suggesting a higher membrane perturbing effect on this mitochondrial membrane-derived bilayer. As expected, the GpA-derived TMD-peptide, a protein that is not associated with mitochondrial membranes, caused a much smaller drop in bilayer order. In summary, the results indicate that a lower concentration of the TMD peptides is required to induce a significant change in membrane order in both mitochondrial membrane-derived bilayers, and suggests a potential role of cardiolipin for the differential localisation of the Bcl-2 proteins in membranes, especially for TMD-Bcl-xL and TMD-Bak (Figure 1).

Next, we analyzed the influence of the membrane environment in the secondary structure of TMD-pepts by means of CD spectroscopy. CD spectra were obtained in the presence of synthetic liposomes at different lipid/peptide molar ratios (L/P). In the presence of PM-like liposomes, TMD-pepts were found to populate random or β-sheet-like conformations characterized by a minimum centered at 217 nm (Supporting Information Figure S5). The CD spectra in the presence of mito-like liposomes exhibited a minimum at 222−224 nm suggesting the coexistence of dynamic mixed structures characterized by the presence of helical conformation. In addition, the 208 nm minimum characteristic of helical conformations was less defined. The less defined double minima associated with α-helical spectra is commonly observed for peptides that bind strongly to liposomes.[35,36] TMD-Bax precipitated out from solution in the presence of mito-like liposomes precluding structural analysis by CD.

In contrast to the behavior in PM-like liposomes, all TMD-pepts caused mito-like liposome solutions to become turbid over time and dynamic light scattering (DLS) was therefore utilized to understand this phenomenon. The size and distribution of particles present upon addition of each peptide are shown in Supporting Information Figure S6. At low lipid/peptide (L/P) ratios (red lines), we found a single species approximately 60−100 nm in size corresponding to the expected size for liposomes produced by extrusion through a 100 nm pore size filter. However, at higher L/P ratios, all peptides except TMD-Bax (which had low solubility under the conditions) and TMD-GpA, caused the formation of larger species in the range of 800−1000 nm and up to 5000 nm in diameter. Thus, the addition of TMD-Bcl-2, TMD-Bcl-xL, TMD-Bcl-w, TMD-Mcl-1, and TMD-Bak all caused changes in the properties of the model mito-like membrane leading to liposome fusion.

TMD-pepts Promote Calcein Release from Liposomes and Cytochrome *c* Release from Isolated Mitochondria. To determine whether membrane binding of TMD-pepts induced bilayer disruption, membrane leakage was analyzed by dye release assays. We measured the rate of liposome-encapsulated calcein release from model PM-like and mito-like membranes. The TMD-pepts were evaluated at the biologically active concentration of 10 μM (see below) and all Bcl-2-derived peptides, except Bcl-w, consistently induced higher calcein release from mito-like than from PM-like liposomes (Table 2), suggesting a specific role in the perturbation

Table 2. TMD-pepts-Induced Calcein Release from Liposomes

	% of released calcein[a]		
TMD-pept	PM-like	mito-like	*t*-Student
Bcl-2	28 ± 4	40 ± 7	*
Bcl-xL	4 ± 7	75 ± 16	***
Bcl-w	20 ± 6	28 ± 5	n.s.
Mcl-1	15 ± 8	53 ± 6	***
Bax	8 ± 8	52 ± 7	***
Bak	41 ± 12	88 ± 3	***
GpA	47 ± 12	11 ± 6	**

[a]The % of calcein release was calculated as a fraction of the total release obtained when liposomes were treated with 10% Triton X-100. The TMD-pepts were evaluated at 10 μM.

of mitochondrial membranes, especially for TMD-Bcl-xL, TMD-Mcl-1, and TMD-Bax, and TMD-Bak. Moreover, the control TMD-GpA peptide induced more calcein leakage from PM-like than from mito-like membranes and can therefore be described as a mitochondrial inactive peptide. These results, together with the results obtained from DPI, suggest that TMD-pepts derived from Bcl-2 proteins are poorly active at plasma membranes inducing minor damage that can easily self-repair. Interestingly, the damage that these peptides induce in mitochondrial membranes may find application in the apoptotic activation of tumor cells by mitochondrial priming. We then evaluated the potential biological activity of TMD-pepts in isolated intact mitochondria purified from mouse embryonic fibroblasts (MEFs) cells. In control (NT, nontreated) mitochondria, cytochrome *c* (cyt *c*) was found in the pellet that contained the mitochondrial fraction characterized by the presence of the mitochondrial voltage-dependent anion selective channel protein 1 (VDAC 1)[37] (Figures 2a and 3a). A similar result was found with the mitochondrial inactive peptide TMD-GpA. In contrast, TMD-Bcl-xL, TMD-Bax, and TMD-Bak induced the highest level of mitochondrial cyt *c*-release, while TMD-Mcl-1 was consistently the least active peptide (Figure 2b). In order to further characterize the effect of TMD-pepts on the integrity of the isolated mitochondria, we developed a mitochondrial-swelling assay. TMD-pepts did not induce swelling when compared to Ca^{2+}-only induced experiments (Figure 2c). Thus, although TMD-pepts induced cyt *c* release, the molecular mechanism by which this occurs does not disrupt mitochondrial integrity. These results correlate with previous studies, suggesting that the molecular mechanism of full length Bcl-2 proteins-induced cyt *c* release specifically perturbed the mitochondrial outer membrane, while the inner membrane and the ultrastructure of mitochondria remained unaffected.[38] The biophysical activity of TMD-pepts in synthetic membranes, together with the cyt *c* release capacity

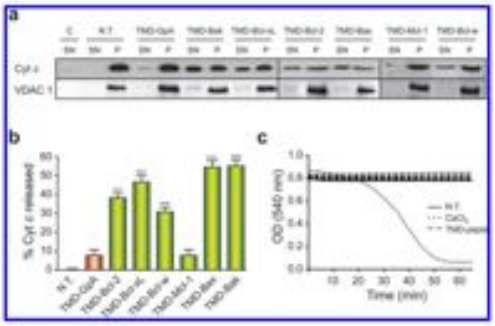

Figure 2. TMD-pepts promote cytochrome c release from intact isolated mitochondria. (a) VDAC and cyt *c* immunoblotting from pure mitochondria fractions (pellet). Data are representative of three independent assays. (b) Western blot quantification of cyt *c* release using ImageJ software. Experiments were performed independently three times ($N = 3$) (***$p < 0.001$, compared with NT). (c) Mitochondrial swelling of TMD-pepts compared with $CaCl_2$ as positive control measured as absorbance change at 540 nm.

from isolated mitochondria support the notion that TMD peptides not only act as membrane anchoring domains but can also be considered as biologically active agents in their own right.

Biological Activity of TMD-pepts on Human Cervix Adenocarcinoma Cells. To further characterize the marked effect of TMD-pepts in isolated mitochondria, their biological activity in human cervix adenocarcinoma (HeLa) cells was evaluated. First, HeLa cells were incubated in the presence of TMD-pepts at 10 μM for 24 h. In these experimental conditions, cells were resistant to TMD-pepts and showed normal behavior. In fact, the levels of free lactate dehydrogenase (LDH) in the media revealed that cells did not lose permanent or transient membrane integrity due to TMD-pepts treatment (data not shown). In addition, the TMD-pepts did not induce plasma membrane disruption-induced cell death. As previously described,[39,40] Lipofectamine 2000 was used to facilitate the access of the peptides to the cell cytosol through the plasma membrane. We found that 10 μM TMD-Bcl-2, TMD-Bcl-xL, TMD-Bax, and TMD-Bak promoted a significant increase in HeLa cell death percentages under these experimental conditions (Figure 3a). As expected, compromised cell viability correlated with loss of mitochondrial functionality (Figure 3b, Supporting Information Figure S7a), and a moderate release of cyt c from mitochondria, in particular with TMD-Bcl-xL and TMD-Bak (Figure 3c). These two highly active peptides also caused a significant drop in intracellular ATP levels in the early stages of treatment when the effect of the apoptotic inducer (CDDP) was still not apparent (Figure 3d). The drop in ATP was most probably caused by the TMD-pepts induced mitochondrial destabilization. Furthermore, we found no evidence of caspase-like activity in either case (Figure 3e, lanes 1−5). In this context the TMD-pepts drive cells to necrotic rather than apoptotic cell death despite having a moderate amount of cyt c released in the cytoplasm.[41] Accordingly, when cell fate was monitored by the combined staining with the dye Propidium iodide (PI, which is excluded from cells with intact plasma membranes) and FITC-labeled Annexin V (AnnV, which binds to phosphatidylserine moieties exposed on the surface of dying apoptotic cells) we found that the most active peptides TMD-Bcl-2, TMD,Bcl-xL, TMD-Bax, and TMD-Bak generate predominantly necrotic cell death (Supporting Information Figure S7b, black bars). Focusing on the most active peptides TMD-Bcl-xL and TMD-Bak, it should be highlighted that their behavior correlates well with their biophysical properties in the MOM. Nevertheless, their pro-death effect could not always be related to that of the full-length protein; especially for TMD-Bcl-xL, which is an antiapoptotic member. Previous studies support the ability of Bcl-2-derived TMDs, and other natural or synthetic cytotoxic peptides[42−46] to permeabilize mitochondria, through possible pore formation.[47−49]

To better understand the functional correlation between TMD-pepts and full length (FL) Bcl-2 proteins, we have analyzed the effect of TMD-Bcl-xL and TMD-Bak in the presence of the antiapoptotic proteins Bcl-2 and Bcl-xL. Flow cytometry analysis showed a slight decrease in cell death in the presence of the antiapoptotic FL proteins, while the necrotic pathway was not significantly affected (Figure 3f). This indicates that antiapoptotic proteins are able to partially block the residual apoptotic pathway promoted by cyt c release due to the presence of TMD-peptides. Based on this result, we can speculate on the existence of a putative (direct or indirect) interaction among TMD-pepts and the FL Bcl-2 proteins.

As shown in Figure 3g, there is a good correlation between the biophysical effects of TMD-pepts on synthetic membranes and the outcome of their treatment in cell cultures. The more they perturb model membranes, the larger are the cellular consequences.

Mitochondrial Priming Effect of TMD-pepts. It has been proposed that mitochondrial priming, understood as the readiness of mitochondria to actively engage the apoptotic program, inversely correlates with resistance to chemotherapy.[17,50] Mitochondrial priming can be forced by decreasing the cellular content of antiapoptotic Bcl-2 proteins or by using BH3-mimetics such as ABT-737.[17] We were therefore interested in the evaluation of TMD-pepts as novel mitochondrial priming tools. Thus, we evaluated the sensitivity of HeLa cells to cotreatment with the chemotherapeutic agent cisplatin (cis-diamminedichloroplatinum(II) dichloride, CDDP) and

dx.doi.org/10.1021/cb500267t | ACS Chem. Biol. 2014, 9, 1799−1811

ACS Chemical Biology

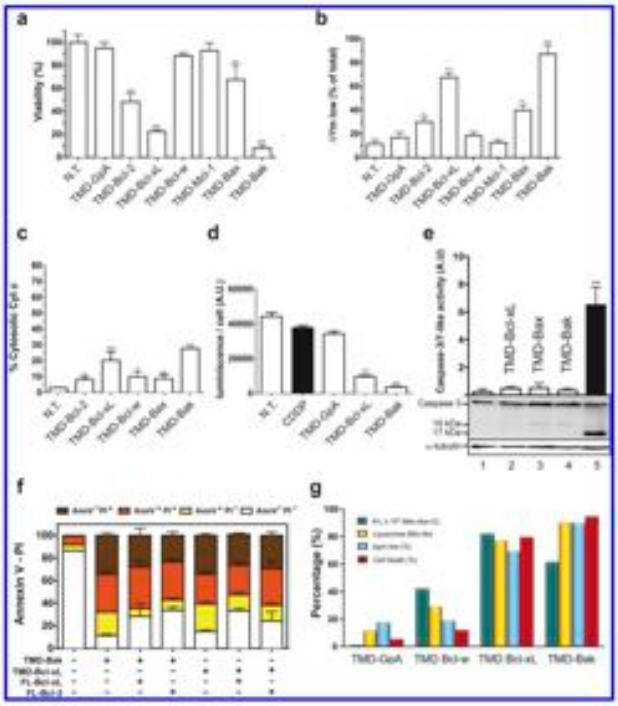

Figure 3. Bcl-2-derived peptides effect on viability, mitochondrial membrane potential, cyt *c* release, and caspase-3/7 activity in HeLa cell cultures at TMD-pepts 10 μM. (a) Cell viability measured by trypan blue exclusion assay of cultures transfected with peptides at 10 μM for 24 h. (b) Mitochondrial membrane potential was measured by flow cytometry with TMRM. (c) Mitochondrial permeabilization was analyzed by flow cytometry with cyt *c*-FITC. (d) Measurement of intracellular ATP by luminescence, peptide treatment decreased intracellular ATP levels compared with the not treated cells. Representative data are shown, bars represent the mean of three independent experiments ± standard deviation (SD) ($^{*}p < 0.1$; $^{**}p < 0.05$; $^{***}p < 0.001$, compared with NT). (e) Caspase-3-like activity measured in the HeLa cells. Bars represent the mean of three independent experiments ± SD ($^{*}p < 0.1$; $^{**}p = 0.05$; $^{***}p < 0.001$ compared with CDDP). Western blot developed against caspase-3 antibody using α-tubulin like load control. The fraction at 17 and 19 kDa represents the active form of the enzyme. (f) Effect of Bcl-2 and Bcl-xL Full length on cell death was assayed by flow cytometry with FITC Annexin V and Propidium Ioride (PI). (g) Correlation graph for HeLa cell line according to the results shown in Figure 2, this figure, and Table 2.

TMD-pepts. Control cells treated with CDDP in the absence of TMD-pepts showed close to 50% apoptotic cell death (Figure 4a) characterized by mitochondrial dysfunction (Supporting Information Figure S7c), loss of mitochondrial membrane potential (Figure 4b), cyt *c* release (Figure 4c), and caspase-3/7-like activity (Figure 4d). Interestingly, we observed that a significant decrease in cell viability correlated with an increase in apoptotic markers when CDDP treated cells where cotreated with TMD-Bcl-2, TMD-Bcl-xL, TMD-Bax, and TMD-Bak peptides (Figure 4). Moreover, the less mitochondrial active peptide, TMD-Mcl-1, and the mitochondrial inactive peptide, TMD-GpA, did not increase the chemotherapeutic effect of CDDP (Figure 4).

It should be noted that the effect of the cotreatment on the caspase-3/7-like activity is the result of a cooperative effect between the peptides and the drug, provided that cell treatment with TMD-pepts in the absence of CDDP did not activate caspases (Figure 3e lanes 2−4). The caspase-3 activity induced by the TMD-pepts in combination with CDDP was abolished in the presence of the general caspase inhibitor zVAD (Supporting Information Figure S8).

Flow cytometry analyses showed that CDDP-induced apoptotic cell death ($AnnV^{+}/PI^{-}$ and $AnnV^{+}/PI^{+}$, light and dark gray bar segments) significantly increased in the presence of the mitochondrial active peptides TMD-Bcl-2, TMD-Bcl-xL, TMD-Bax, and TMD-Bak but was not affected by the presence

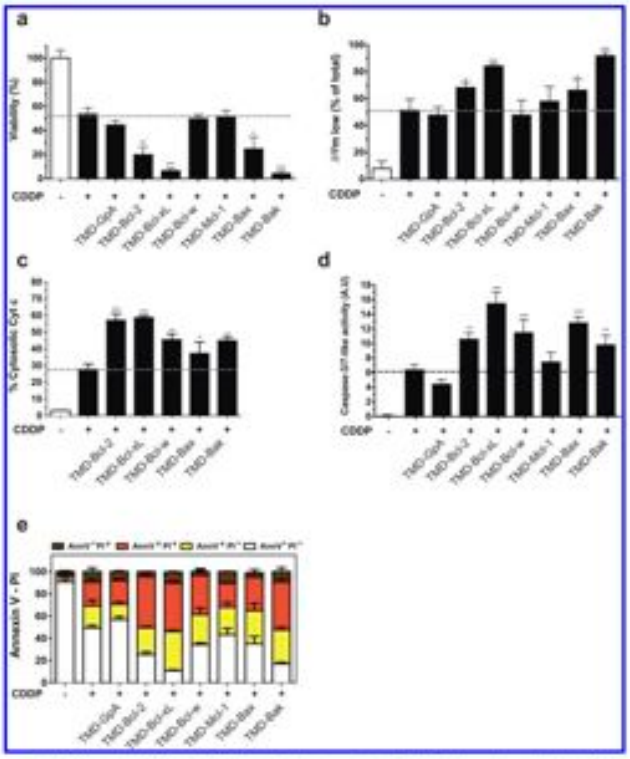

Figure 6. Co-treatment of TMD-pepts (10 μM) with CDDP significantly enhances the effect of the chemotherapeutic drug in HeLa cells. Cells were treated with CDDP (40 μM) for 12 h after peptide transfection protocol. (a) Viability measured by trypan blue assay. (b) Mitochondrial membrane potential was measured by flow cytometry with TMRM. (c) Mitochondrial permeabilization was analyzed by flow cytometry with anti-cyt c-FITC. (d) Caspase-3-like activity measured in the HeLa cells. Bars represent the mean of three independent experiments ± SD (*$p < 0.1$; **$p < 0.05$; ***$p < 0.001$ compared with CDDP). (e) Apoptotic cell death was analyzed by flow cytometry with FITC Annexin V and PI HeLa.

of the mitochondrial inactive peptide TMD-GpA (Figure 4c). These results also correlated with a change in the behavior of peptides, observed by flow cytometry, from mainly necrotic when used alone (Supporting Information Figure S7b) to mainly apoptotic when used in combination with CDDP (Figure 4e). Altogether, these results indicate the existence of a switch from necrosis to apoptosis when TMD-pepts are used in combination with CDDP.

To better define the cooperative behavior observed in the experiments described above, we studied the cell death properties at sublethal concentrations of TMD-pepts when used in combination with CDDP.

We then evaluated the active TMD-pepts at 3 μM in HeLa cells. At this concentration, all peptides by themselves, with the exception of TMD-Bak, showed less than 10% reduction in cell viability (Figure 5a, white bars), and only a partial loss of mitochondrial potential, as indicated by an increase in the number of cells with low transmembrane potential (Figure 5b). Moreover, neither cyt c release nor caspase-3/7-like activity was observed (Figure 5 panels c and d, respectively). To explore whether the priming exerted by the mitochondrial active TMD-pepts at sublethal concentrations could increase the sensitivity of HeLa cells to chemotherapeutic agents, we used cotreatment with CDDP (black bars). The mitochondrial priming resulted in a large increase in CDDP-induced cytotoxicity (Figure 5a, Supporting Information Figure S7d) accompanied by an increase in the percentage of cells with low mitochondrial transmembrane potential (Figure 5b), in the cyt c released to

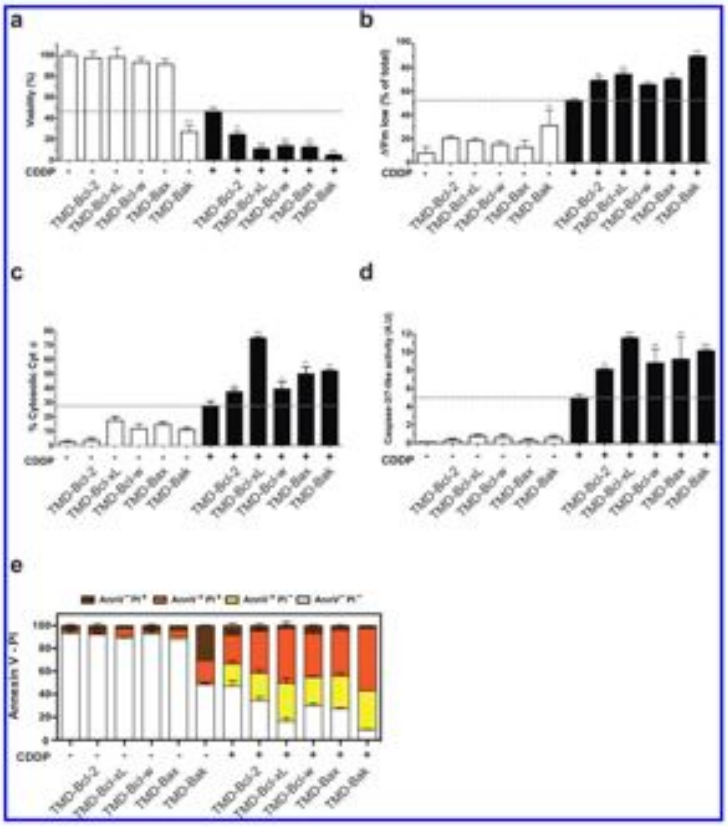

Figure 5. Mitochondrial priming by TMD peptides. Sublethal TMD-pepts doses induce a mitochondrial priming effect in cotreatments with CDDP in HeLa cells. Comparison of the effect of treatment with TMD-pepts alone at 5 μM (white bars) or with cotreatment with CDDP at 40 μM for 12 h (black bars). (a) Cell viability measured by trypan blue exclusion assay of cultures treated with peptides for 24 h. (b) Mitochondrial membrane potential was measured by flow cytometry with TMRM. (c) Mitochondrial permeabilization was analyzed by flow cytometry with anti-cyt *c*-FITC. (d) Caspase-3-like activity measured in the HeLa cells. Bars represent the mean of three experiments ± SD (°$p < 0.1$; **$p < 0.05$; ***$p < 0.001$ NT (white bars) and CDDP (black bars)). (e) Apoptotic cell death was analyzed by flow cytometry with FITC Annexin V and PI.

the cytosol (Figure 5c) and in the caspase-3/7-like activity (Figure 5d). Accordingly, CDDP induced apoptotic death significantly increased in the presence of the TMD-pepts (see $AnnV^+/PI^-$ and $AnnV^+/PI^+$ population in Figure 5e). These results confirm the behavior observed at lethal concentrations of TMD-pepts and strongly support their mitochondrial priming properties.

Interestingly, some TMD-pepts from antiapoptotic proteins, such as Bcl-xL, show pro-death function in the tumor cell lines analyzed. It has been previously demonstrated that Bcl-xL is cleaved by caspase-3 and calpains, converting Bcl-xL from an antiapoptotic to a pro-apoptotic factor.[3] Here, we show that the Bcl-xL TMD could be the protein domain responsible for this switch. This behavior could be explained taking into account the common evolutionary origin of Bcl-2 proteins. The programmed cell death is executed with very few members in invertebrates but new members appear with the genomic expansion of vertebrates. In simpler systems, the same protein

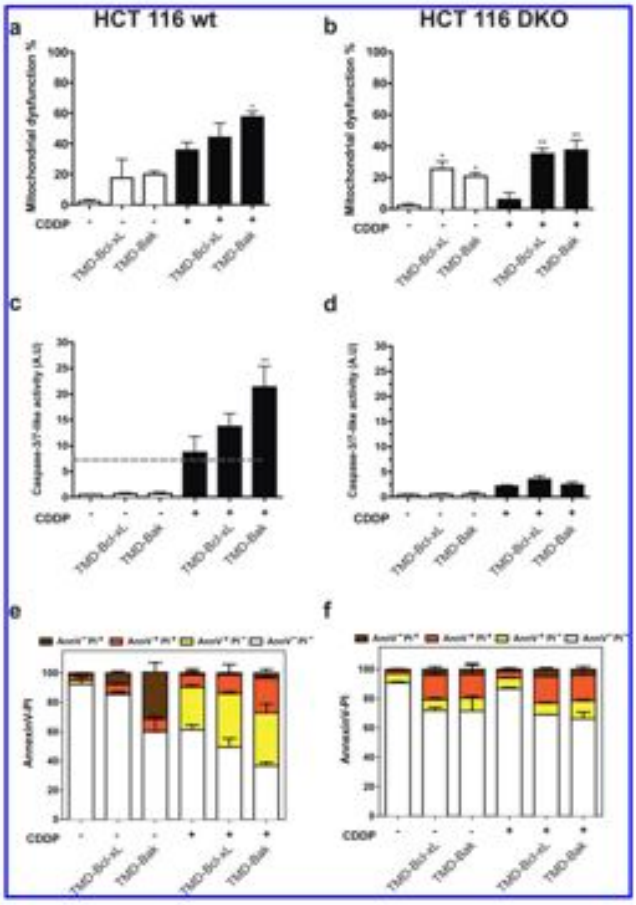

Figure 6. Mitochondrial priming effect of TMD-pepts in HCT 116 cell lines wt and Bax/Bak KO. Cells were treated with TMD-pepts at 10 μM and CDDP is added at 20 μM. (a, b) Mitochondrial dysfunction was measured by MTT assays 24 h after peptide transfection. (c, d) Caspase-3-like activity measured in HCT 116 cell lines. Bars represent the mean of three experiments ± SD (*$p < 0.1$; **$p < 0.05$); ***$p < 0.001$ compared with NT (white bars) and CDDP (black bars)). (e, f) Apoptotic cell death was analyzed by flow cytometry with FITC Annexin V and PI.

could be responsible for the final decision of cell death or survival depending on post-translational modifications.[51,52] All these proteins share one to four conserved Bcl-2 homology domains (BH) and most possess a C-terminal hydrophobic amino acid. The divergent evolution of pro- and anti-apoptotic members could be explained considering only the cytosolic regions of Bcl-2 proteins.[51] Therefore, we speculate that the pore formation capability of TMD-pepts could be modulated by the folding of their soluble regions. Overall, from these experiments we conclude that TMD-pepts clearly enhance the cell apoptosis-inducing effects of the chemotherapeutic agent CDDP in HeLa cells independently of their pro- or anti-apoptotic origin.

Mitochondrial Priming Effect Can Be Extended to Other Cancer Cells. In order to generalize our findings and to better understand their physiological relevance, we analyzed the behavior of the most active TMD-pepts in the human colorectal carcinoma HCT116 and HCT116 Bax/Bak double knock out (DKO) cell lines.[53,54]

We observed that HCT116 cells had a similar behavior to HeLa cells although they were slightly more resistant to TMD-pepts treatment. Hence, we characterized the effect of these TMD-pepts at 20 μM (lethal) and 10 μM (sublethal) concentrations (Supporting Information Figure S9).

We observed that for both cell lines, treatment at lethal concentrations provoked loss of cell viability, which correlates with a decrease in ATP levels (Supporting Information Figure S9) and an increase in mitochondrial destabilization (Supporting Information Figure S10 panels a and b). However, there was no effect in caspase-3 activity in any case (Supporting Information Figure S9 e and f), as previously described for HeLa cells. Interestingly, in the presence of CDDP, HCT116 wt cells also showed the previously observed switch from necrosis to apoptosis (Supporting Information Figure S10c). However, there were no changes in the necrotic populations when the cotreatments were applied to the HCT116 DKO cell line (Supporting Information Figure S10d). Similar results were obtained when peptides were assayed at sublethal concentrations. Under these sublethal conditions, there was a slight effect of TMD-pepts in mitochondrial dysfunction (Figure 6 panels a and b), cell viability, and ATP levels (Supporting Information Figure S9 a–d) for both wild type and DKO cell lines. However, in the presence of CDDP, we observed a notable increase in caspase-3 activity for HCT116 wild type cells (Figure 6 panels c and e) but not for DKO cells (Figure 6 panels d and f). The absence of an apoptotic switch in the HCT116 DKO cell line highlights the relevance of the Bcl-2 apoptotic machinery in the TMD-pepts-mediated mitochondrial priming.

Conclusions. The existing paradigm for Bcl-2 protein-mediated control of mitochondria and cell fate in apoptotic signaling involves protein–protein interactions among Bcl-2 members mediated by BH3 domains.[55] However, there is increasing evidence the role of the membrane[8,56] and the interaction of Bcl-2 proteins within the membrane through their TMDs[5,7,9,10,57,58] must also be included. The present study has led to the establishment of an activity-based classification of the Bcl-2 TMD-derived peptides. Overall, both biophysical and cellular data point toward a clear correlation between mitochondrial membrane insertion/perturbation capability and cellular activity (Figure 3g and Figure 7), sustaining an active role of these peptides in MOMP.

The control of apoptosis exerted by Bcl-2 proteins has led to the use of BH3-derived peptides and BH3 mimetics as potential drugs to improve cancer treatments.[17,50,59,60] Targeting the BH3 domain of Bcl2 proteins to induce apoptosis in cancer cells is not always effective and mostly depends on pro-survival Bcl2 members.[18,61,62] Therefore, combination treatments have emerged as novel pharmacological strategies to avoid toxicities and increase efficacy of antitumor treatments.[63−65] In this scenario, we demonstrate that the combination of CDDP with sublethal dosages of TMD-pepts, especially TMD-Bcl-xL and TMD-Bak, increases its pro-apoptotic activity, exerting a mitochondrial priming effect. We speculate that TMD-pepts need direct or indirect interactions with the Bcl-2 network to produce the apoptotic priming effect.

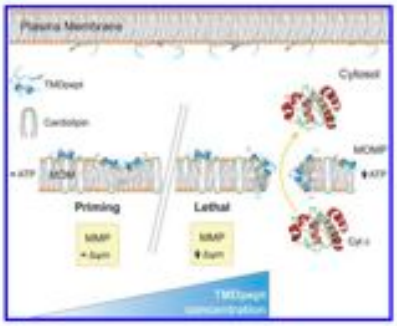

Figure 7. Preferential TMD-pepts binding to mitochondrial membrane induces mitochondrial membrane disruption. Schematic representation depicting the relatively low binding of TMD-pepts to the plasma membrane compared to its higher binding to the mitochondrial membrane. This preferential binding disrupts the mitochondrial membrane structure leading to cyt c release to the cytosol. MMP: mitochondrial membrane potential. MOM: mitochondrial outer membrane. MOMP: mitochondrial outer membrane permeabilization.

In light of the TMD-pepts effect in mitochondrial priming, we envisage that Bcl-2-derived TMD-pepts have the potential to make significant contributions to our understanding of apoptosis-induced clinical disorders and to establish a basis for the design of new cancer therapeutics.

METHODS

Bioinformatics Analysis. The prediction of TMDs was done using two of the most common methods available on the Internet: Dense Alignment Surface method[66] in DAS server (http://www.sbc.su.se/~miklos/DAS/) and TransMembrane Hidden Markov Model[23] at the TMHMM Server v. 2.0 (http://www.cbs.dtu.dk/services/TMHMM/). Prediction of Gibbs Free Energy (ΔG) was obtained with ΔG prediction server v1.0 (http://dgpred.cbr.su.se/) using standard parameters in all cases.[67] The entire protein sequences were obtained from UniProt (http://www.uniprot.org) and analyzed with these programs.

Dual Polarization Interferometry (DPI). *Liposome Preparation for Dual Polarization Interferometry.* Thin lipid films of POPC (PM-like) and two mito-like mixtures, POPC:POPE:POPS:POPI (5:3:1:1) and POPC:POPE:POPS:POPI:TOCL (4.8:2.8:1:1:0.4) were hydrated to 1 mM lipid concentration with 10 mM HEPES 150 mM NaCl pH 7.4), buffer solution at 37 °C for 1 h with constant vortexing. The hydrated lipid suspension was sonicated in a water bath for ~30 min at 37 °C and extruded before use through 50 nm polycarbonate membranes (19 times) using an Avestin Liposfast extruder (Ottawa, Canada).

Deposition of Supported Lipid Bilayer on Sensor Chips. Planar supported lipid bilayers (SLBs) were prepared via in situ adsorption of liposomes to a silicon oxynitride waveguide sensor chip (see Supporting Information for detailed description). A fresh bilayer was used for each individual peptide measurement and 180 μL of each concentration was injected sequentially onto the SLB in increasing concentrations at a flow rate of 40 μL/min with a total of 30 min equilibration time between injections.

Data acquisition was carried out using AnaLight200 version 2.1.0 software and analyzed using AnaLight Explorer proprietary software.[68,69]

Small Unilamellar Liposomes (SUV) Preparation and Calcein Release Assay. Small unilamellar liposomes were prepared as previously reported.[48] Lipid samples were dissolved in a 2:1 (v/v) chloroform:methanol mixture and dried under N_2 stream in order to remove residual. The dried lipid was suspended by vortexing in 150 mM Hepes buffer (pH 7.0) containing 90 mM of calcein. Lipid mixtures were incubated for 20 min at a temperature above the phase transition temperature of the major phospholipid component of the liposome. The final phospholipid concentration was about 30 mM. Disruption of multilamellar vesicle (LMV) suspensions by sonication 5 min at 4 °C with a probe tip sonicator produced small unilamellar vesicles (SUV) with diameters in the range 15−50 nm. SUV were composed of phosphatidylcholine (PC):Cl (7:3, mol/mol) as mito-like and PC/cholesterol (7:3, mol/mol) as PM-like. The lipid suspensions, SUV were then centrifuged at 10000 rpm for 10 min. Free calcein was removed by passage of the dispersion through a column of Sephadex G-50 (Sigma-Aldrich). For calcein release assays fluorescence measurements were made with a Jasco FP6600 spectrofluorometer (495 and 520 nm, excitation and emission wavelengths).

Mitochondrial Isolation and Cytochrome c Release Assays. Mitochondria were freshly isolated from MEFS cells by differential centrifugation steps as described previously.[49] Isolated mitochondria were incubated with the different TMD-pepts (50 μM) in I_b buffer (125 mM KCl, 5 mM KH_2PO_4, 2 mM $MgCl_2$, 25 μM EGTA, 5 mM succinate, 5 μM rotenone, and 10 mM HEPES-KOH (pH 7.2)) for 30 min at 30 °C. Reaction mixtures were centrifuged at 14 000*g* for 10 min. Supernatant and pellet fractions were subjected Western blotting using cytochrome c antibody (14 kDa, cell signaling ref:4272), α-tubulin antibody (Sigma-Aldrich, ref #T8203) and VDAC1/2/3 antibody (26 kDa, Santa Cruz ref sc-98708).

Mitochondria Swelling Measurements. Isolated mitochondria were suspended (*final* concentration 0.5 mg mL^{-1}) in 100 μL of swelling buffer (120 mM KCl, 10 mM tris-HCl, 5 mM MOPS, 5 mM KH_2PO_4, pH 7.4) in a 96-well plate. A basal signal line was assessed for 5 min and then mitochondria were treated with 50 μM of each TMD peptide and 100 μM $CaCl_2$, respectively. Changes in absorbance caused by swelling were monitored using a microplate reader at 540 nm every 5 min for 1 h.

Cell Lines and Cultures. The mouse embryonic fibroblast (MEFs) KO Bax/Bak cell lines were kindly provided by Dr. Guido Kroemer. The human cervix adenocarcinoma (HeLa) cells were obtained from the ATCC. HCT-116 wt and Bak-/Bax- were kindly provided by Professors Bert Vogelstein and Richard Youle. MEFs and HeLa were grown in Dulbecco's modified Eagle's medium plus 10% FBS. HCT116 were grown in McCoy's 5A Modified Medium plus 10% FBS. Cells were incubated at standard conditions. Peptides were transfected with Lipofectamine 2000 (Invitrogen). Briefly, peptides were combined with 2,5 μL of lipofectamine and Opti-MEM Reduced Serum Media (Invitrogen) for 30 min at room temperature (RT) and then incubated with cells >70% confluency during 4 h at 37 °C. Finally, transfection mixture was discarded and CDDP treated and non-treated cells incubated at 37 °C up to 24 h.

Cell-based Caspase-3/7 Activation Assay. All cell extracts were prepared from 1.5×10^5 cells seeded in 6-well plates. After 24 h, cells were treated with a Lipofectamine/peptide (10 μM) mixture for 4 h followed by administration of 35 μM cis-diamminoplatinum(II) dichloride (cisplatin, CDDP). After 24 h, cells were scrapped and washed with PBS. Pellets were resuspended in extraction buffer (50 mM PIPES, 50 mM KCl, 5 mM EDTA, 2 mM $MgCl_2$, 2 mM DTT), kept on ice for 5 min and frozen and thawed three times. Cell lysates were centrifuged at 14 000 rpm for 5 min and supernatants were collected. Total protein (50 μg) was mixed with 200 μL of caspase assay buffer (PBS, 10% glycerol, 0.1 mM EDTA, 2 mM DTT) containing 20 μM of the Ac-DEVD-afc (Enzo Life Sciences) caspase-3 specific substrate. Caspase activity was continuously monitored following the release of fluorescent afc at 37 °C using a Wallac 1420 Workstation (λ_{ex} = 400 nm; λ_{em} = 508 nm).

Flow Cytometry. Cells were harvested by centrifugation, suspended in binding buffer (10 mM HEPES pH 7.4, 140 mM NaCl, 2.5 mM $CaCl_2$) and incubated with 1 μL of tetramethylrhodamine methyl ester perchlorate (TMRM; 1 μM). To measure apoptotic or necrotic cell death, the FITC-Annexin V/PI kit (BD Biosciences) was used following manufacturer instructions. To quantify the release of cytochrome c from mitochondria, HeLa cells were seeded at 1.5×10^5 cell/mL, and after 24 h in the presence of the TMD-pepts at the concentrations indicated, the InnocyteTM Flow Cytometric cytochrome c Release kit (Calbiochem) was used according to the manufacturer's recommendations. Staining was assessed by flow cytometry on a FC500 instrument (Beckman Coulter) followed by data analysis using FlowJo software (Tree Star Inc.).

Measurement of Cellular ATP. Relative cellular ATP content was measured by the ATPlite Kit (PerkinElmer) accordingly with manufacturer's protocol. Cells were plated in 96-well plates at 8,000 cells per well to allow for attachment overnight. Cellular ATP content was measured by a luminescent plate reader 4 h post peptide treatment.

Mitochondrial Dysfunction Assay (MTT). Cell viability was measured by a 3-[4,5-dimethylthiazol-2-yl]-2,5-diphenyltetrazolium bromide (MTT) colorimetric assay. Cells were cultured in sterile 96-well microtiter plates at a seeding density of 12000 cells/well for the HCT116 lines and 3000 cells/well for HeLa cells. Plates were read at 570 nm on a Wallac 1420 workstation.

Cell Viability Assay. Cells were cultured in sterile 96-well microtiter plates at a seeding density of 12000 cells/well for the HCT116 lines and 3000 cells/well for HeLa cells. Trypan blue exclusion assay was used to determinate the percentage of cell viability.

Statistical Analysis. All the values represent the mean ± SD of at least three independent experiments. Statistical significance was determined by one-way ANOVA using the Graph Pad software $p < 0.01$ was designated as statistically significant.

■ ASSOCIATED CONTENT

Supporting Information

Supporting figures and general experimental procedures. This material is available free of charge via the Internet at http://pubs.acs.org.

■ AUTHOR INFORMATION

Corresponding Authors

*Email: agenoves@cipf.es.

*Email: mibel.aguilar@monash.edu.

Author Contributions

[‡]V.A.-F. and A.G. contributed equally to this study.

Notes

The authors declare no competing financial interest.

■ ACKNOWLEDGMENTS

This work was supported by grants from the Spanish Ministry of Science and Innovation (MICINN-BIO2007-60066, -SAF2010-15512, -SAF2008-00048, BFU2012-39482, and CSD2008-00005C), and by Generalitat Valenciana Prometeo/2010/005. A.G. is recipient of JAE-Doc position (CSIC). The financial support of the Australian Research Council is gratefully acknowledged.

■ DEDICATION

[#]The authors wish to dedicate this paper to the memory of our friend and colleague, Professor Enrique Pérez Payá.

■ REFERENCES

(1) Westphal, D., Dewson, G., Czabotar, P. E., and Kluck, R. M. (2011) Molecular biology of Bax and Bak activation and action. *Biochim. Biophys. Acta 4*, 521−531.

(2) Basanez, G., Soane, L., and Hardwick, J. M. (2012) A new view of the lethal apoptotic pore. *PLoS Biol. 10*, 25.

(3) Li, P., Nijhawan, D., Budihardjo, I., Srinivasula, S. M., Ahmad, M., Alnemri, E. S., and Wang, X. (1997) Cytochrome c and dATP-dependent formation of Apaf-1/caspase-9 complex initiates an apoptotic protease cascade. *Cell 91*, 479−489.
(4) Hardwick, J. M., and Youle, R. J. (2009) SnapShot: BCL-2 proteins. *Cell 138*, 0e03.
(5) Shamas-Din, A., Brahmbhatt, H., Leber, B., and Andrews, D. W. (2011) BH3-only proteins: Orchestrators of apoptosis. *Biochim. Biophys. Acta 4*, 508−520.
(6) Kelly, P. N., and Strasser, A. (2011) The role of Bcl-2 and its pro-survival relatives in tumourigenesis and cancer therapy. *Cell Death Differ. 18*, 1414−1424.
(7) Garcia-Saez, A. J. (2012) The secrets of the Bcl-2 family. *Cell Death Differ. 19*, 1733−1740.
(8) Kale, J., Liu, Q., Lebet, B., and Andrews, D. W. (2012) Shedding light on apoptosis at subcellular membranes. *Cell 151*, 1179−1184.
(9) Lindsay, J., Esposti, M. D., and Gilmore, A. P. (2011) Bcl-2 proteins and mitochondria−specificity in membrane targeting for death. *Biochim. Biophys. Acta 4*, 532−539.
(10) Nguyen, M., Millar, D. G., Yong, V. W., Korsmeyer, S. J., and Shore, G. C. (1993) Targeting of Bcl-2 to the mitochondrial outer membrane by a COOH-terminal signal anchor sequence. *J. Biol. Chem. 268*, 25265−25268.
(11) Garcia-Saez, A. J., Mingarro, I., Perez-Paya, E., and Salgado, J. (2004) Membrane-insertion fragments of Bcl-xL, Bax, and Bid. *Biochemistry 43*, 10930−10943.
(12) Willfling, F., Weber, A., Potthoff, S., Vogtle, F. N., Meisinger, C., Paschen, S. A., and Hacker, G. (2012) BH3-only proteins are tail-anchored in the outer mitochondrial membrane and can initiate the activation of Bax. *Cell Death Differ. 19*, 1328−1336.
(13) Edlich, F., Banerjee, S., Suzuki, M., Cleland, M. M., Arnoult, D., Wang, C., Neutzner, A., Tjandra, N., and Youle, R. J. (2011) Bcl-xL retrotranslocates Bax from the mitochondria into the cytosol. *Cell 145*, 104−116.
(14) Todt, F., Cakir, Z., Reichenbach, F., Youle, R. J., and Edlich, F. (2013) The C-terminal helix of Bcl-xL mediates Bax retrotranslocation from the mitochondria. *Cell Death Differ. 20*, 333−342.
(15) Slivka, P. F., Wong, J., Caputo, G. A., and Yin, H. (2008) Peptide probes for protein transmembrane domains. *ACS Chem. Biol. 3*, 402−411.
(16) Chonghaile, T. N., and Letai, A. (2008) Mimicking the BH3 domain to kill cancer cells. *Oncogene 27* (Suppl1), S149−157.
(17) Vo, T. T., Ryan, J., Carrasco, R., Neuberg, D., Rossi, D. J., Stone, R. M., Deangelo, D. J., Frattini, M. G., and Letai, A. (2012) Relative mitochondrial priming of myeloblasts and normal HSCs determines chemotherapeutic success in AML. *Cell 151*, 344−355.
(18) Rath, A., Tulumello, D. V., and Deber, C. M. (2009) Peptide models of membrane protein folding. *Biochemistry 48*, 3036−3043.
(19) Ortizzo, M., Salgado, J., Gimenez-Giner, A., Perez-Paya, E., and Mingarro, I. (2004) Influence of proline residues in transmembrane helix packing. *J. Mol. Biol. 335*, 631−640.
(20) Baeza-Delgado, C., Marti-Renom, M. A., and Mingarro, I. (2013) Structure-based statistical analysis of transmembrane helices. *Eur. Biophys J. 42*, 199−207.
(21) Vilar, M., Esteve, V., Pallas, V., Marcos, J. F., and Perez-Paya, E. (2001) Structural properties of carnation mottle virus p7 movement protein and its RNA-binding domain. *J. Biol. Chem. 276*, 18122−18129.
(22) Pastor, M. T., Lopez de la Paz, M., Lacroix, E., Serrano, L., and Perez-Paya, E. (2002) Combinatorial approaches: A new tool to search for highly structured β-hairpin peptides. *Proc. Natl. Acad. Sci. U.S.A. 99*, 614−619.
(23) Ortizzo, M., Perez-Paya, E., and Mingarro, I. (2000) Influence of the C-terminus of the glycophorin A transmembrane fragment on the dimerization process. *Protein Sci. 9*, 1246−1253.
(24) Biondello, S. E., Fernood, B., Houghten, R. A., and Perez-Paya, E. (1997) Secondary structure induction in aqueous vs membrane-like environments. *Biopolymers 42*, 489−498.
(25) Vilar, M., Saurí, A., Marcos, J. F., Mingarro, I., and Perez-Paya, E. (2005) Transient structural ordering of the RNA-binding domain of carnation mottle virus p7 movement protein modulates nucleic acid binding. *ChemBioChem 6*, 1391−1396.
(26) Schimmel, A., Kaufmann, T., and Borner, C. (2004) Bcl-2 family members: integrators of survival and death signals in physiology and pathology. *Biochim. Biophys. Acta 1*, 2−3.
(27) Ardail, D., Privat, J. P., Egret-Charlier, M., Levrat, C., Lerme, F., and Louisot, P. (1990) Mitochondrial contact sites. Lipid composition and dynamics. *J. Biol. Chem. 265*, 18797−18802.
(28) Osman, C., Voelker, D. R., and Langer, T. (2011) Making heads or tails of phospholipids in mitochondria. *J. Cell Biol. 192*, 7−16.
(29) de Kroon, A. I., Dolis, D., Mayer, A., Lill, R., and de Kruijff, B. (1997) Phospholipid composition of highly purified mitochondrial outer membranes of rat liver and Neurospora crassa. Is cardiolipin present in the mitochondrial outer membrane? *Biochim. Biophys. Acta 3*, 108−116.
(30) Schug, Z., and Gottlieb, E. (2009) Cardiolipin acts as a mitochondrial signalling platform to launch apoptosis. *Biochim. Biophys. Acta 1788*, 2022−2031.
(31) Lee, T. H., Hall, K., Mechler, A., Martin, L., Popplewell, J., Ronan, G., and Aguilar, M. I. (2009) Molecular imaging and orientational changes of antimicrobial peptides in membranes. *Adv. Exp. Med. Biol. 611*, 313−315.
(32) Lee, T. H., Hall, K. N., Swann, M. J., Popplewell, J. F., Unabia, S., Park, Y., Hahm, K. S., and Aguilar, M. I. (2010) The membrane insertion of helical antimicrobial peptides from the N-terminus of *Helicobacter pylori* ribosomal protein L1. *Biochim. Biophys. Acta 3*, 544−557.
(33) Fernandez, D. I., Lee, T. H., Sani, M. A., Aguilar, M. I., and Separovic, F. (2013) Proline facilitates membrane insertion of the antimicrobial peptide maculatin 1.1 via surface indentation and subsequent lipid disordering. *Biophys. J. 104*, 1495−1507.
(34) Lee, T. H., Heng, C., Swann, M. J., Gehman, J. D., Separovic, F., and Aguilar, M. I. (2010) Real-time quantitative analysis of lipid disordering by aurein 1.2 during membrane adsorption, destabilisation, and lysis. *Biochim. Biophys. Acta 10*, 30.
(35) Ouellet, M., Otis, F., Voyer, N., and Auger, M. (2006) Biophysical studies of the interactions between 14-mer and 21-mer model amphipathic peptides and membranes: Insights on their modes of action. *Biochim. Biophys. Acta 1758*, 1231−1244.
(36) Biron, E., Voyer, N., Meillon, J. C., Cormier, M. E., and Auger, M. (2008) Conformational and orientation studies of artificial ion channels incorporated into lipid bilayers. *Biopolymers 55*, 364−372.
(37) Borgne-Sanchez, A., Dupont, S., Langonne, A., Baux, L., Lecoeur, H., Chavrier, D., Lasalle, M., Dvas, O., Bttere, J. J., Brabant, M., Roux, P., Pechoux, C., Brtand, J. P., Hoebeke, J., Deniaud, A., Brenner, C., Rustin, P., Edelman, L., Rebouillat, D., and Jacotot, E. (2007) Targeted Vpr-derived peptides reach mitochondria to induce apoptosis of αVβ3-expressing endothelial cells. *Cell Death Differ. 14*, 422−435.
(38) Von Ahsen, O., Waterhouse, N. J., Kuwana, T., Newmeyer, D. D., and Green, D. R. (2000) The 'harmless' release of cytochrome c. *Cell Death Differ. 7*, 1192−1199.
(39) Palacios-Rodriguez, Y., Garcia-Lainez, G., Sancho, M., Gortat, A., Orzaez, M., and Perez-Paya, E. (2011) Polypeptide modulators of caspase recruitment domain (CARD):CARD-mediated protein−protein interactions. *J. Biol. Chem. 286*, 44457−44466.
(40) Hayashida, W., Horiuchi, M., and Dzau, V. J. (1996) Intracellular third loop domain of angiotensin II type-2 receptor. Role in mediating signal transduction and cellular function. *J. Biol. Chem. 271*, 21985−21992.
(41) Eguchi, Y., Shimizu, S., and Tsujimoto, Y. (1997) Intracellular ATP levels determine cell death fate by apoptosis or necrosis. *Cancer Res. 57*, 1835−1840.
(42) Ellerby, H. M., Arap, W., Ellerby, L. M., Kain, R., Andrusiak, R., Rio, G. D., Krajewski, S., Lombardo, C. R., Rao, R., Ruoslahti, E., Bredesen, D. E., and Pasqualini, R. (1999) Anti-cancer activity of targeted pro-apoptotic peptides. *Nat. Med. 5*, 1032−1038.

(43) Law, B., Quinti, L., Choi, Y., Weissleder, R., and Tung, C. H. (2006) A mitochondrial targeted fusion peptide exhibits remarkable cytotoxicity. *Mol. Cancer Ther. 5*, 1944−1949.
(44) Mai, J. C., Mi, Z., Kim, S. H., Ng, B., and Robbins, P. D. (2001) A proapoptotic peptide for the treatment of solid tumors. *Cancer Res. 61*, 7709−7712.
(45) Marks, A. J., Cooper, M. S., Anderson, R. J., Orchard, K. H., Hale, G., North, J. M., Ganeshaguru, K., Steele, A. J., Mehta, A. B., Lowdell, M. W., and Wickremasinghe, R. G. (2005) Selective apoptotic killing of malignant hemopoietic cells by antibody-targeted delivery of an amphipathic peptide. *Cancer Res. 65*, 2373−2377.
(46) Rege, K., Patel, S. J., Megeed, Z., and Yarmush, M. L. (2007) Amphipathic peptide-based fusion peptides and immunoconjugates for the targeted ablation of prostate cancer cells. *Cancer Res. 67*, 6368−6376.
(47) Torrecillas, A., Martínez-Senac, M. M., Aunló, A., Corbalán-García, S., and Gomez-Fernandez, J. C. (2007) Interaction of the C-terminal domain of Bcl-2 family proteins with model membranes. *Biochim. Biophys. Acta 1768*, 2931−2939.
(48) Valero, J. G., Sancey, L., Kucharczak, J., Guillemin, Y., Gimenez, D., Prudent, J., Gillet, G., Salgado, J., Coll, J. L., and Aouacheria, A. (2011) Bax-derived membrane-active peptides act as potent and direct inducers of apoptosis in cancer cells. *J. Cell Sci. 124*, 556−564.
(49) Garg, P., Nemec, K. N., Khaled, A. R., and Tatulian, S. A. (2013) Transmembrane pore formation by the carboxyl terminus of Bax protein. *Biochim. Biophys. Acta 1828*, 732−742.
(50) Ní Chonghaile, T., Sarosiek, K. A., Vo, T. T., Ryan, J. A., Tammareddi, A., Moore Vdel, G., Deng, J., Anderson, K. C., Richardson, P., Tai, Y. T., Mitsiades, C. S., Matulonis, U. A., Drapkin, R., Stone, R., Deangelo, D. J., McConkey, D. J., Sallan, S. E., Silverman, L., Hirsch, M. S., Carrasco, D. R., and Letai, A. (2011) Pretreatment mitochondrial priming correlates with clinical response to cytotoxic chemotherapy. *Science 334*, 1129−1133.
(51) Lamere, C., Santamaria, M., and Saccone, C. (2004) Comparative genomics: The evolutionary history of the Bcl-2 family. *Gene 333*, 71−79.
(52) Aouacheria, A., Rech de Laval, V., Combet, C., and Hardwick, J. M. (2013) Evolution of Bcl-2 homology motifs: Homology versus homoplasy. *Trends Cell Biol. 23*, 103−111.
(53) Zhang, L., Yu, J., Park, B. H., Kinzler, K. W., and Vogelstein, B. (2000) Role of BAX in the apoptotic response to anticancer agents. *Science 290*, 989−992.
(54) Wang, C., and Youle, R. J. (2012) Predominant requirement of Bax for apoptosis in HCT116 cells is determined by Mcl-1's inhibitory effect on Bak. *Oncogene 31*, 3177−3189.
(55) Llambi, F., Moldoveanu, T., Tait, S. W., Bouchier-Hayes, L., Temirov, J., McCormick, L. L., Dillon, C. P., and Green, D. R. (2011) A unified model of mammalian BCL-2 protein family interactions at the mitochondria. *Mol. Cell 44*, 517−531.
(56) García-Saez, A. J., Ries, J., Orzáez, M., Pérez-Paya, E., and Schwille, P. (2009) Membrane promotes tBID interaction with BCL(XL). *Nat. Struct Mol. Biol. 16*, 1178−1185.
(57) Lovell, J. F., Billen, L. P., Bindner, S., Shamas-Din, A., Fradin, C., Leber, B., and Andrews, D. W. (2008) Membrane binding by tBid initiates an ordered series of events culminating in membrane permeabilization by Bax. *Cell 135*, 1074−1084.
(58) Garg, P., Nemec, K. N., Khaled, A. R., and Tatulian, S. A. (2013) Transmembrane pore formation by the carboxyl terminus of Bax protein. *Biochim. Biophys. Acta, Biomembr. 1828*, 732−742.
(59) Ní Chonghaile, T., and Letai, A. (2008) Mimicking the BH3 domain to kill cancer cells. *Oncogene 27*, S2.
(60) Oltersdorf, T., Elmore, S. W., Shoemaker, A. R., Armstrong, R. C., Augeri, D. J., Belli, B. A., Bruncko, M., Deckwerth, T. L., Dinges, J., Hajduk, P. J., Joseph, M. K., Kitada, S., Korsmeyer, S. J., Kunzer, A. R., Letai, A., Li, C., Mitten, M. J., Nettesheim, D. G., Ng, S., Nimmer, P. M., O'Connor, J. M., Oleksijew, A., Petros, A. M., Reed, J. C., Shen, W., Tahir, S. K., Thompson, C. B., Tomaselli, K. J., Wang, B., Wendt, M. D., Zhang, H., Fesik, S. W., and Rosenberg, S. H. (2005) An inhibitor of Bcl-2 family proteins induces regression of solid tumors. *Nature 435*, 677−681.
(61) Kang, M. H., and Reynolds, C. P. (2009) Bcl-2 inhibitors: Targeting mitochondrial apoptotic pathways in cancer therapy. *Clin. Cancer Res. 15*, 1126−1132.
(62) Roy, M. J., Vom, A., Czabotar, P. E., and Lessene, G. (2013) Cell death and the mitochondria: Therapeutic targeting of the BCL-2 family-driven pathway. *Br. J. Pharmacol. 171*, 1973−87.
(63) Lee, M. J., Ye, A. S., Gardino, A. K., Heijink, A. M., Sorger, P. K., MacBeath, G., and Yaffe, M. B. (2012) Sequential application of anticancer drugs enhances cell death by rewiring apoptotic signaling networks. *Cell 149*, 780−794.
(64) Ovejero, M., Guevara, T., Sancho, M., and Perez-Paya, E. (2012) Intrinsic caspase-8 activation mediates sensitization of erlotinib-resistant tumor cells to erlotinib/cell-cycle inhibitors combination treatment. *Cell Death Dis. 3*, e435.
(65) Michels, J., Vitale, I., Senovilla, L., Enot, D. P., Garcia, P., Lissa, D., Olaussen, K. A., Brenner, C., Soria, J. C., Castedo, M., and Kroemer, G. (2013) Synergistic interaction between cisplatin and PARP inhibitors in non-small cell lung cancer. *Cell Cycle 12*, 877−883.
(66) Hessa, T., Meindl-Beinker, N. M., Bernsel, A., Kim, H., Sato, Y., Lerch-Bader, M., Nilsson, I., White, S. H., and von Heijne, G. (2007) Molecular code for transmembrane-helix recognition by the Sec61 translocon. *Nature 450*, 1026−1030.
(67) Hirst, D. J., Lee, T. H., Swann, M. J., Unabia, S., Park, Y., Hahm, K. S., and Aguilar, M. I. (2011) Effect of acyl chain structure and bilayer phase state on binding and penetration of a supported lipid bilayer by HPA3. *Eur. Biophys J. 40*, 505−514.
(68) Sila, M., Au, S., and Weiner, N. (1986) Effects of Triton X-100 concentration and incubation temperature on carboxyfluorescein release from multilamellar liposomes. *Biochim. Biophys. Acta, Biomembr. 859*, 165−170.
(69) Frezza, C., Cipolat, S., and Scorrano, L. (2007) Organelle isolation: Functional mitochondria from mouse liver, muscle, and cultured fibroblasts. *Nat. Protoc. 2*, 287−295.

Supporting Information

Peptides Derived from the Transmembrane Domain of Bcl-2 Proteins as Potential Mitochondrial Priming Tools

Vicente Andreu-Fernández[1‡], Ainhoa Genoves[1,2‡*], Tzong-Hsien Lee[3], Matthew Stellato[3], Federico Lucantoni[1], Mar Orzáez[1], Ismael Mingarro[4], Marie-Isabel Aguilar[3*] & Enrique Pérez-Payá[1,2]

*To whom correspondence should be addressed. E-mail: agenoves@cipf.es

‡These authors contributed equally to this study

This PDF file includes

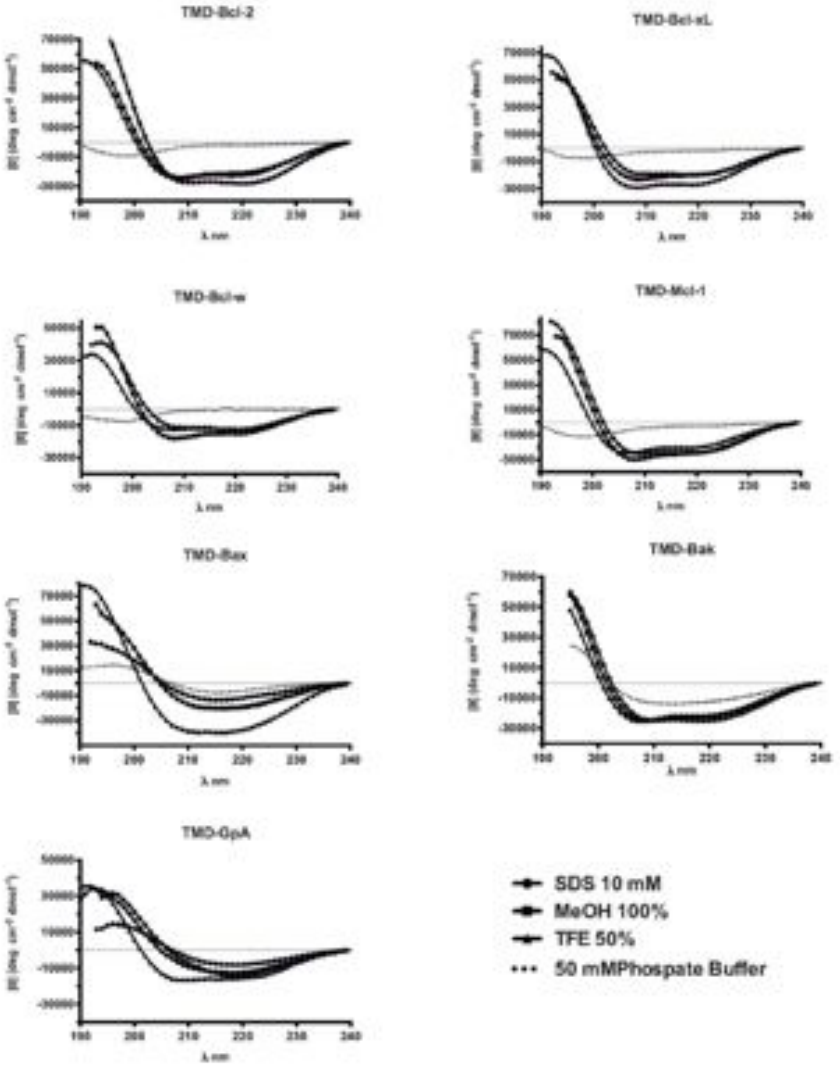

Supp. Figure S1. Circular Dichroism (CD) spectra of TMD derived peptides. CD spectra were measured between 190 and 240 nm at a temperature of 25° C using a Jasco J-810 spectropolarimeter. Each measurement was recorded using 2,2,2 – Trifluoroethanol (TFE 100%), Methanol (MeOH 100%), and Sodium dodecyl sulfate (SDS) 10 mM and Phosphate Buffer.

2

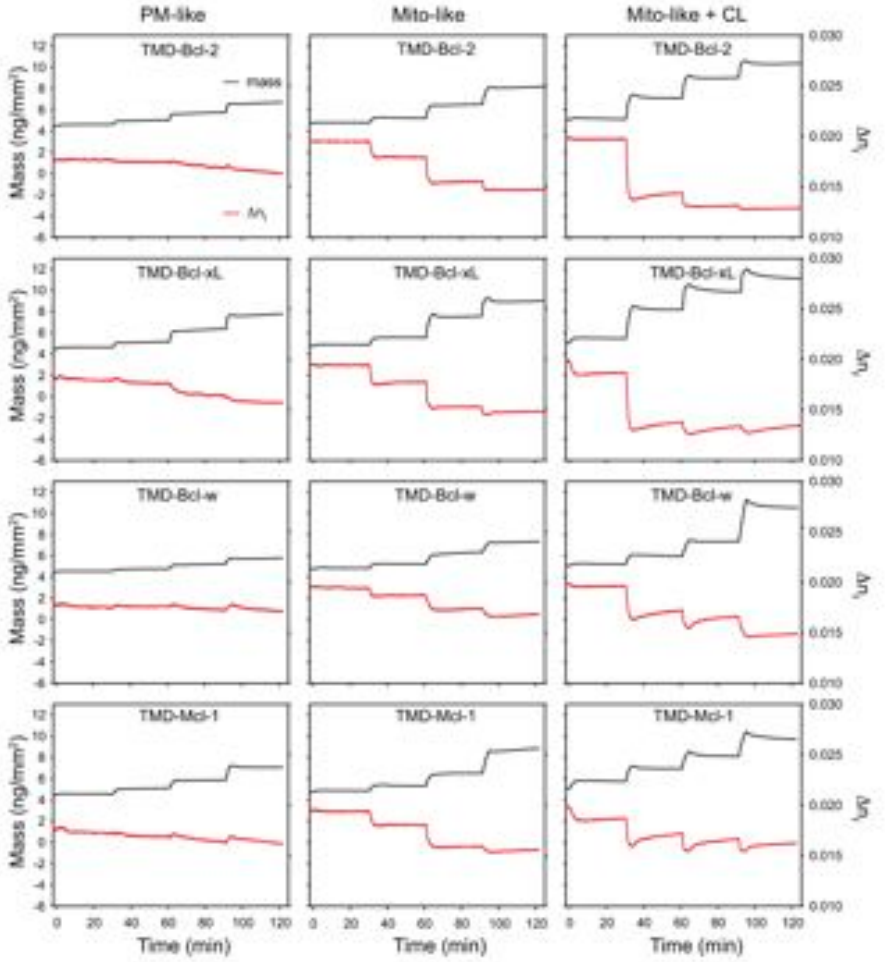

Supp. Figure S2: Dual Polarisation Interferometry. Mass (black) and birefringence (Δnf) (red) *versus* time for each TMD derived peptide on POPC (PM like) , POPC:POPE:POPS:POPI (5:3:1:1)(Mito like) and POPC:POPE:POPS:POPI:TOCL (4.8:2.8:1:1:0.4) (Mito:CL like).

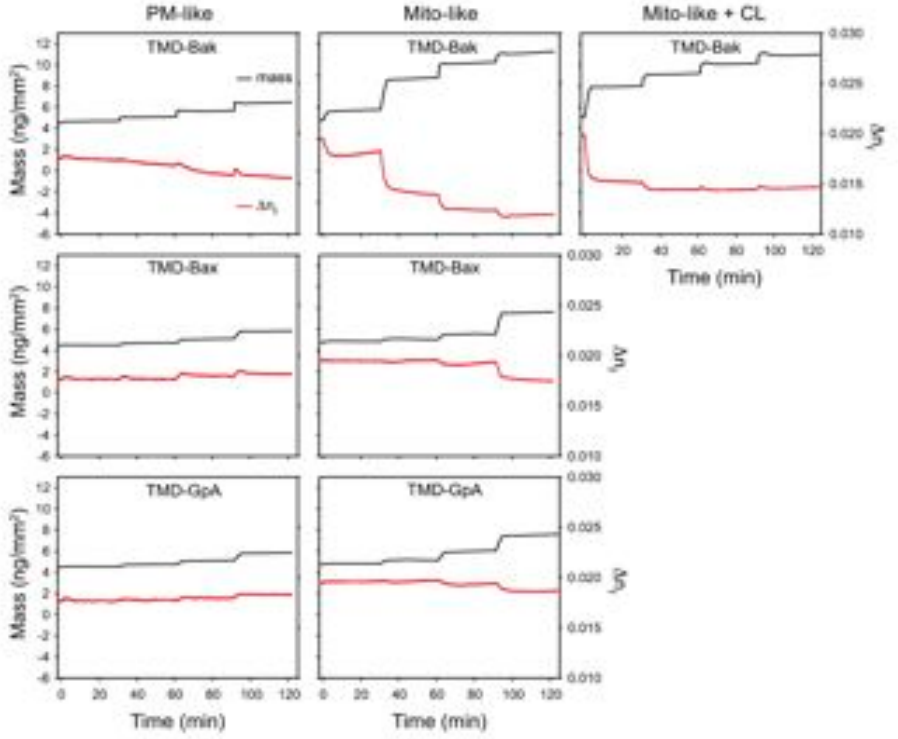

Supp. Figure S2 continued.

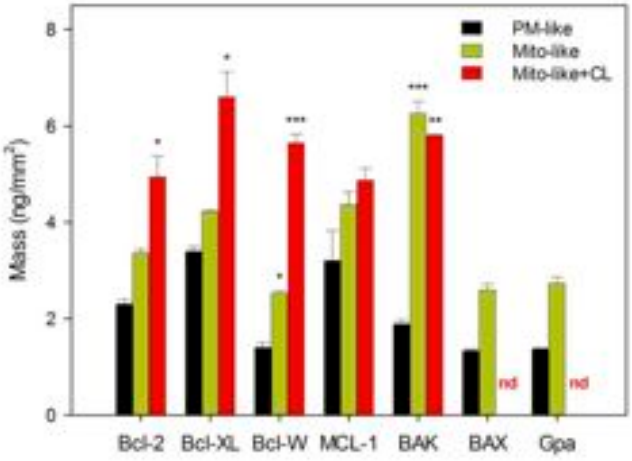

Supp. Figure S3 . TMD-pepts preferential binding to mitochondrial membrane-derived bilayers. The total mass of TMD-pepts bound to the PM-like (POPC), Mito-like (POPC /POPE/POPS/POPI = 60:30:10:10) and Mito-like+CL (POPC/POPE/POPS/POPI/TOCL = 58:28:10:10:4) obtained at the end of 20μM injection. Values indicate mean values +/- S.E.M. (*: $p < 0.02$, **: $p < 0.005$ and ***: $p < 0.001$), nd = not determined.

5

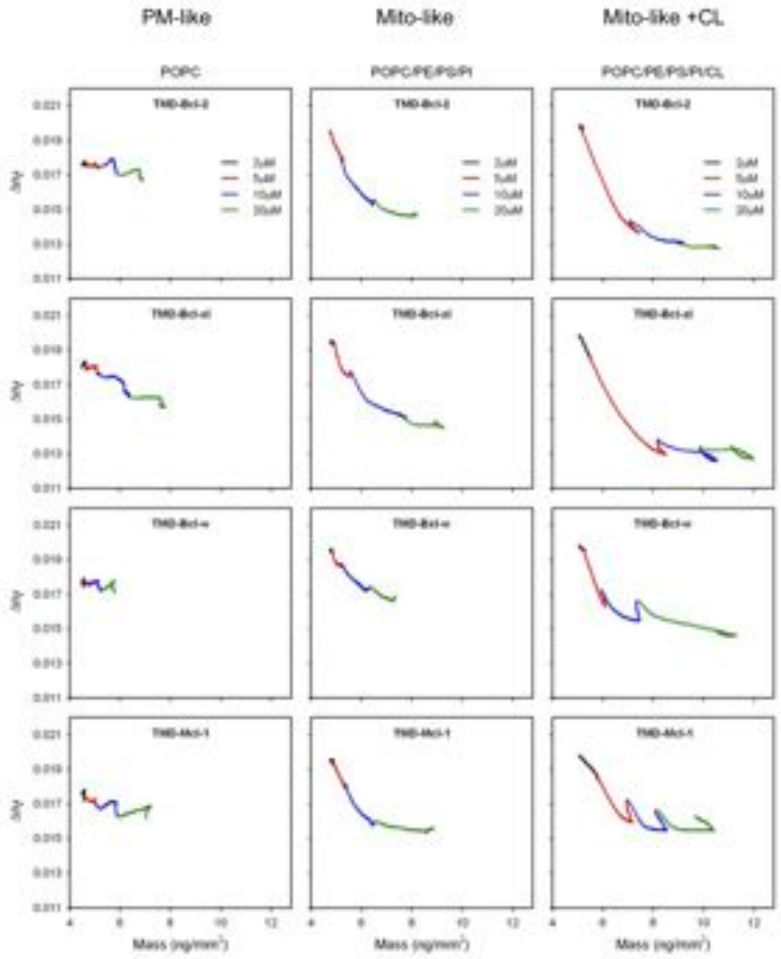

Supp. Figure S4a. Changes in bilayer order induced by TMD-pepts. Dual Polarisation Interferometry. The effect of peptides on membrane disordering is analyzed by the changes of birefringence (Δnf) as a function of membrane bound-peptide mass, in POPC (PM-like, left panels), in POPC/POPE/POPS/POPI (5:3:1:1) (MITO-like, central panels) and in POPC/POPE/POPS/POPI/TOCL (4.8:2.8:1:1:0.4) (MITO-like/CL, right panels). A decrease in birefringence corresponds to a decrease in bilayer order, while an increase in birefringence reflects an increase bilayer ordering.

6

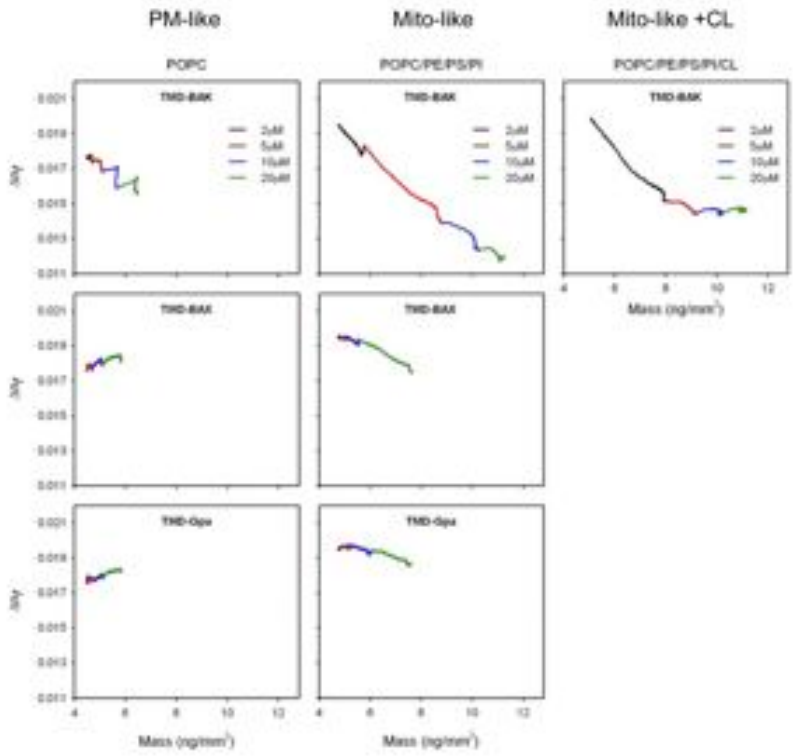

Supp. Figure S4b, continued.

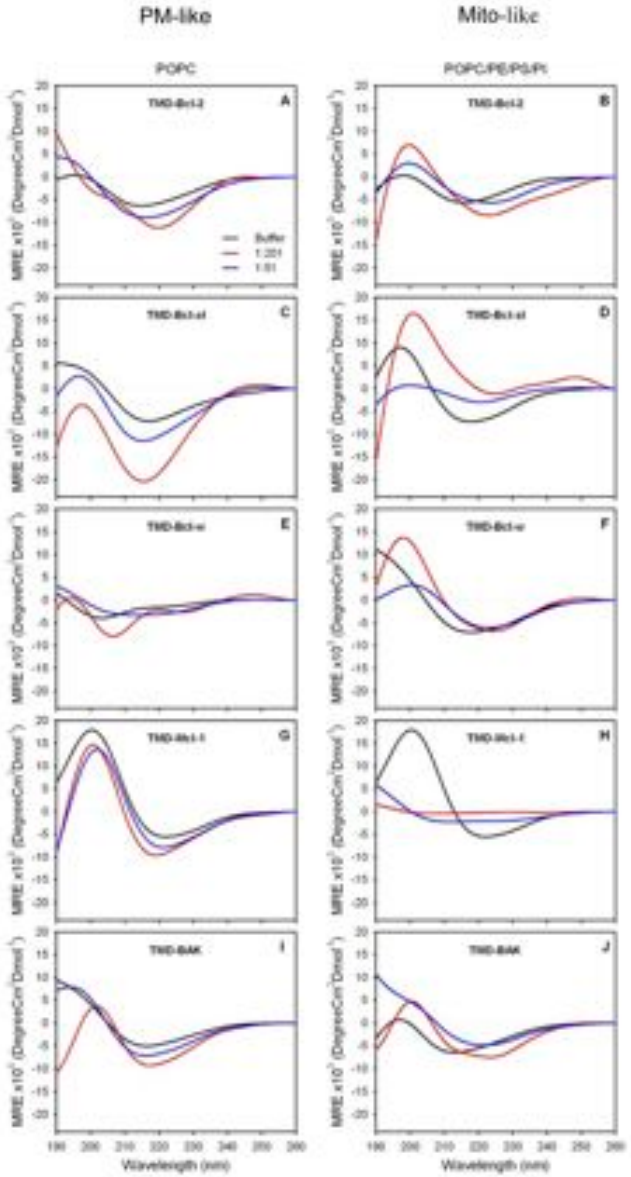

Supp.Figure S5: CD spectra of TMD-derived peptides in POPC (left panels) and POPC:POPE:POPS:POPI (5:3:1:1, right panels) at two different lipid:peptide ratios, 1:51 (blue) and 1:201 (red).

8

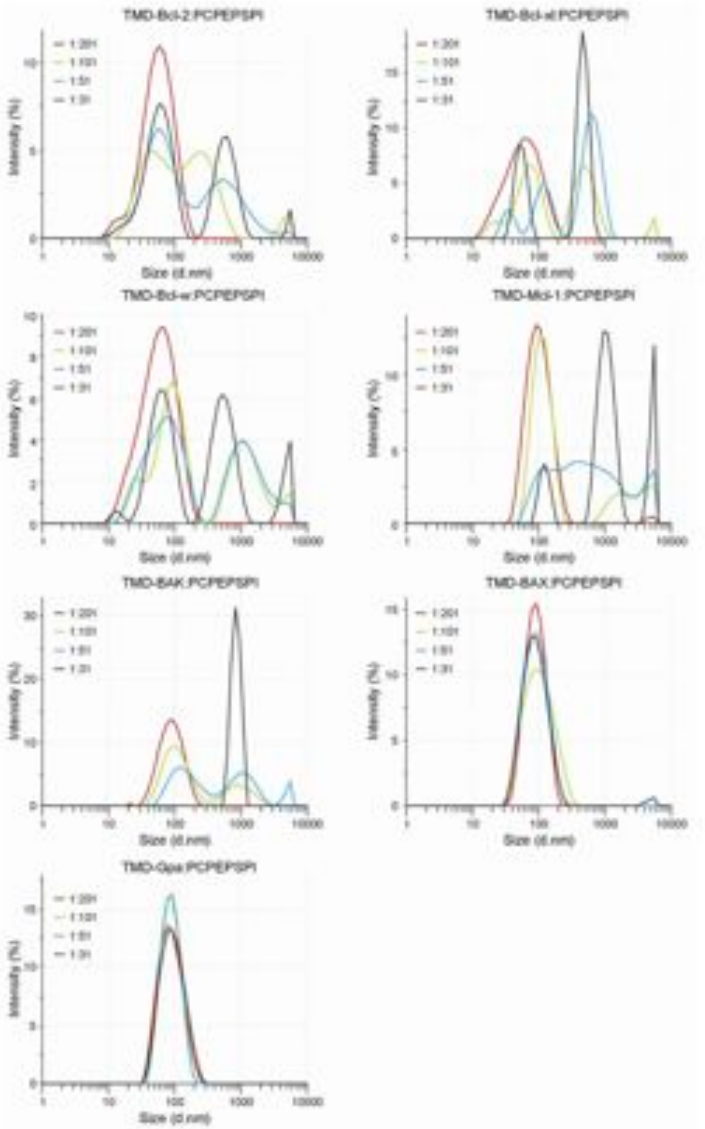

Supp. Figure S6: Analysis of the effect of TMD-derived peptides on liposome diameter in POPC and POPC:POPE:POPS:POPI (5:3:1:1), at four different lipid:peptide ratios, 1:31, 1:51, 1:101 and 1:201.

9

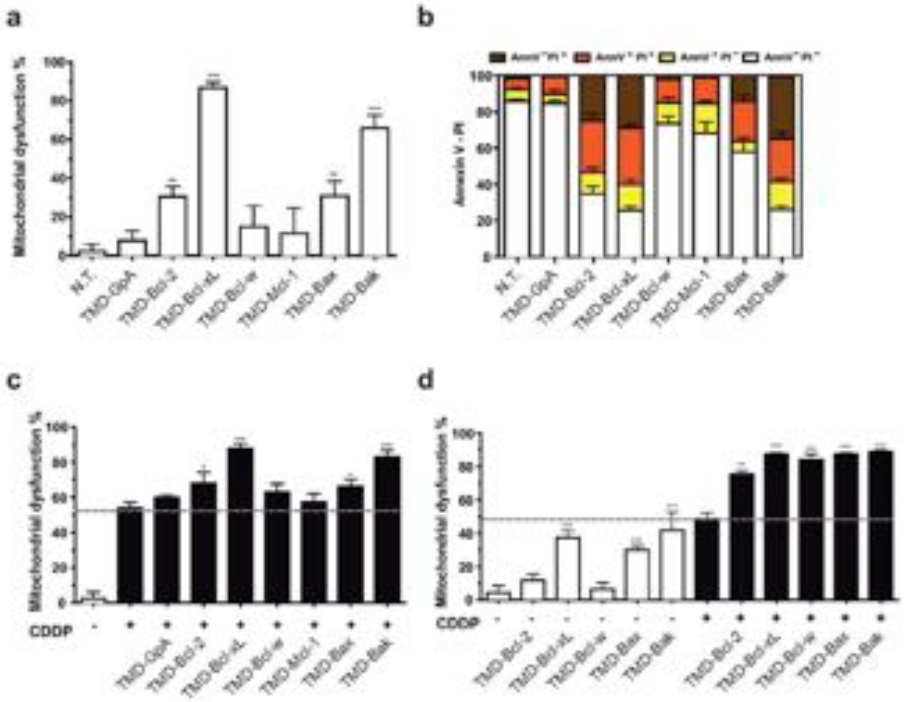

Supp. Figure S7. Mitochondrial dysfunction of HeLa cells co-treated with CDDP and Bcl-2 TM domain peptides (10 μM and 3 μM) measured by MTT. (a) Cells were treated with TM peptides at 10 μM for 24 h. (b) Apoptotic cell death promoted by the TMD-pepts at 10 μM was analyzed by flow cytometry with FITC Annexin V and PI. (c) Cells were treated with CDDP (40μM) for 12 h after transfection with TM peptides at 10 μM. (d) Cells treated with TM peptides at 3 μM for 24 h represented by white bars. Cells treated with CDDP (40μM) for 12 h after transfection with TM peptides at 3 μM represented by black bars. All bars represent the mean of three independent experiments ± s.d. (*$p < 0.1$; **$p < 0.05$, ***$p < 0.001$).

10

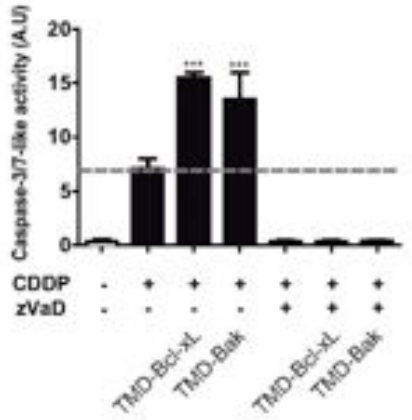

Supp. Figure S8. HeLa cells treated with TMD-Bcl-xL and TMD-Bak peptides and CDDP in presence of Caspase inhibitor zVaD. Cells were transfected with the peptides at 10 µM . zVaD (10uM) was added before CDDP (40uM) treatment, 4 h later peptide transfection (total time 24h). (a) Apoptosis activation was measured by Caspase 3-like activity measured in HeLa cells. All bars represent the mean of three independent experiments ± s.d. (ns, no significant; *$p < 0.1$).

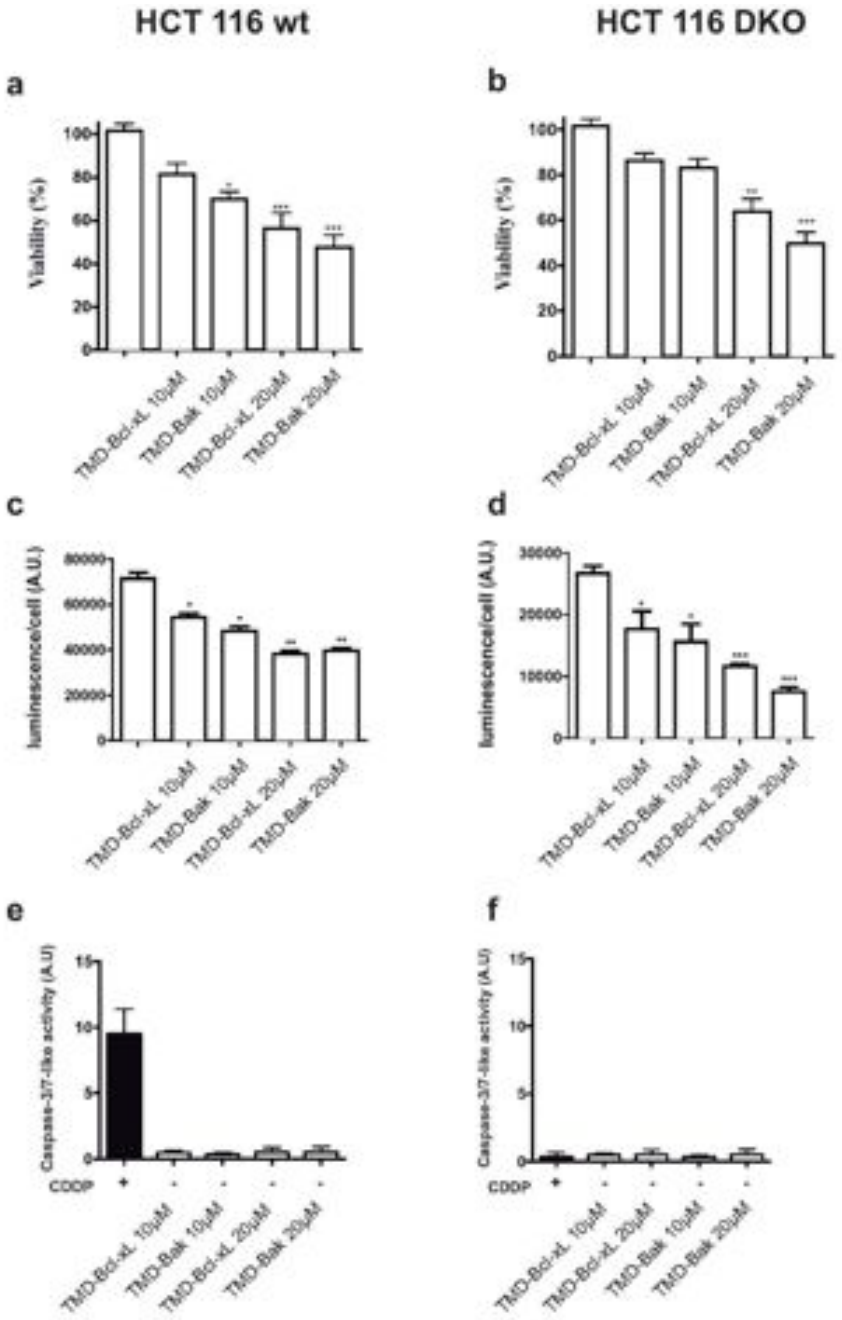
HCT 116 wt
HCT 116 DKO
a
b
c
d
e
f
Viability (%)
luminescence/cell (A.U.)
Caspase-3/7-like activity (A.U)
CDDP
TMD-Bcl-xL 10μM
TMD-Bak 10μM
TMD-Bcl-xL 20μM
TMD-Bak 20μM

12

Supp. Figure S9. HCT116 wt and DKO were treated with TMD-Bcl-xL and TMD-Bak peptides for 24h. Cells were transfected with TMD-pepts (10 and 20 μM). (a, b) Viability was measured by trypan blue assay after 24h of peptide transfection. (c, d) Measurement of intracellular ATP/cell by luminescence, bars represent the mean of three independent experiments ± s.d. (*p < 0.1; **p < 0.05; ***p < 0.001, compared with NT). (e, f) Apoptosis activation was measured by Caspase 3-like activity. Bars represent the mean of three experiments ± s.d. (*p < 0.1; **p < 0.05; ***p < 0.001 compared with NT (white bars) and CDDP (black bars)).

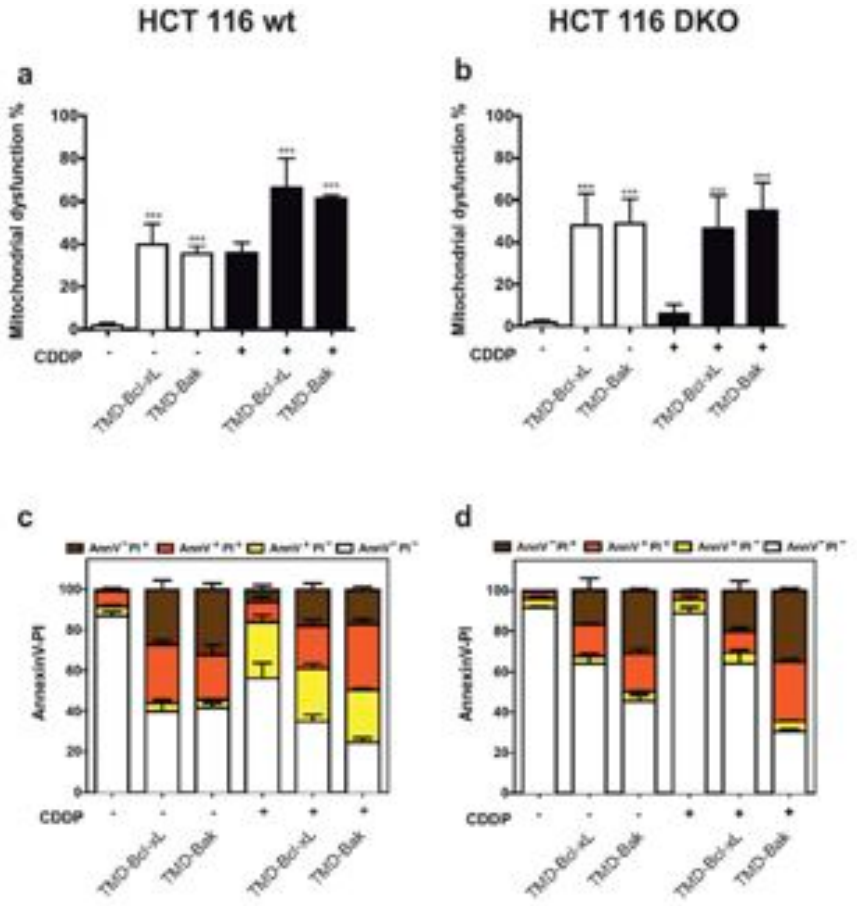

Supp. Figure S10. HCT116 wt and DKO were treated with TMD-Bcl-xL and TMD-Bak peptides for 24h. Cells were treated with TMD-pepts (20 μM) 4 hours after CDDP treatment. (a, b) Mitochondrial dysfunction was measured by MTT assay after 24h of peptide transfection.(c, d) Apoptotic cell death was analyzed by flow cytometry with FITC Annexin V and PI.

	Lipid	Thickness (nm)	Birefringence	Mass (ng/mm^2)
PM-like	POPC	4.76 ± 0.03	0.0199 ± 0.0005	4.76 ± 0.03
MITO-like	POPC/POPE/POPS/POPI (5:3:1:1)	4.48 ± 0.06	0.0176 ± 0.0005	4.47 ± 0.07
MITO-like +CL	POPC/POPE/POPS/POPI/TOCL (4.8:2.8:1:1:0.4)	4.89 ± 0.18	0.0198 ± 0.0001	4.88 ± 0.33

Supp. Table S1. Properties of the lipid bilayers formed on the planar silicon oxynitride chip surface at 20°C. (Values are averages of 12-14 repeats). Value error is one standard deviation.

Supplemental Methods

Peptide Synthesis. Peptides were prepared by Fmoc (N-(9-fluorenyl) methoxycarbonyl)-based solid phase synthesis in a 433A Applied Biosystems peptide synthesizer with a Rink Amide Resin as reported previously (64). Peptides were synthesized with 2 or 3 lysines N- and C-terminal of the sequences in order to improve solubility. Purification was performed in a C18 preparative RP-HPLC system up to 95% of peptide purity as determined by analytical RP-HPLC. Identity was confirmed by MALDI-TOF mass spectroscopy. Stock solutions of the peptides were prepared in Milli-Q water and the concentrations were determined by spectrophotometry in a NanoDrop 1000 (Thermo Scientific).

Circular Dichroism (CD) Measurements. CD spectra were recorded between 190 and 250 nm at 25 °C on a Jasco J-810 spectropolarimeter in quartz cells of 0.1-cm path length. Peptides were dissolved at 10 μM in phosphate buffer (50 mM, pH 7.0), and their ability to adopt a secondary conformation was analyzed with a 2,2,2-trifluoro-ethanol (TFE), sodium dodecyl sulfate (SDS) 1% and methanol (MeOH, 50 and 100%), respectively. Each CD spectrum was the average of 20 scans performed at 1 nm intervals. CD spectra were interpreted with the K2D software provided by Dichroweb (available on the World Wide Web). The results are expressed as mean molar residue ellipticities (degrees x cm^2 x $dmol^{-1}$). For the measurements with liposomes, 1mM of extruded liposome solution (POPC:PE:PS:PI or POPC only) prepared in 10mM Sodium Phosphate 137mM NaCl pH7.4 buffer was added to the cuvette where peptide stock (10mM HEPES 150mM NaCl pH 7.4) was titrated in to incrementally increase the peptide-liposome ratio. The ratios 1:201, 1:101, 1:51 and 1:31 were analysed to determine the effect of peptide concentration on structure. Calculation of Molar Ellipticity (θ) of the peptides and spectra smoothing was achieved using Jasco instrument software.

16

Dynamic Light Scattering. Malvern instruments Zetasizer Nano Z red (Malvern Laboratories Ltd. Malvern, UK) was utilised to determine the size of liposome particles in the presence of peptide via DLS. The relationship between particle size and Brownian motion (Stokes-Einstein relationship) is utilised by the Zetasizer to determine the average size of a population of particles in solution. 0.1mM POPC:PE:PS:PI (5:3:1:1) liposome was measured in a low volume disposable cell initially followed by incremental addition of peptide to achieve the same peptide-liposome ratios as in the CD measurements. Samples were incubated in the Zetasizer at 20°C for a total of 10 minutes prior to reading to give sufficient time for interaction between the peptide and the liposome and a consistent thermal gradient throughout the sample. Each reading consisted of 12 scans each of 10 seconds duration with parameters set to measure size in a low volume disposable sizing cell. The equilibration time was set to 60 seconds and was included in the incubation time.

APPENDIX II

- Andreu-Fernández V, Genovés A, Messeguer A, Orzáez M, Sancho M, Pérez-Payá E. "**BH3-mimetics- and cisplatin-induced cell death proceeds through different pathways depending on the availability of death-related cellular components**" *Plos One*, 2013. doi: 10.1371/journal.pone.0056881.

All the results of this publication are contained within this thesis. Vicente Andreu has performed the majority the experiments and contributed to their design and to the writing of the manuscript.

OPEN ACCESS Freely available online

PLOS ONE

BH3-Mimetics- and Cisplatin-Induced Cell Death Proceeds through Different Pathways Depending on the Availability of Death-Related Cellular Components

Vicente Andreu-Fernández[1], Ainhoa Genovés[1], Angel Messeguer[2], Mar Orzáez[1], Mónica Sancho[1], Enrique Pérez-Payá[1,3]*

1 Laboratory of Peptide and Protein Chemistry, Centro de Investigación Príncipe Felipe, Valencia, Spain, 2 Department of Chemical and Biomolecular Nanotechnology, Instituto Química Avanzada de Cataluña (CSIC), Barcelona, Spain, 3 Instituto de Biomedicina de Valencia, IBV-CSIC, Valencia, Spain

Abstract

Background: Owing to their important function in regulating cell death, pharmacological inhibition of Bcl-2 proteins by dubbed BH3-mimetics is a promising strategy for apoptosis induction or sensitization to chemotherapy. However, the role of Apaf-1, the main protein constituent of the apoptosome, in the process has yet not been analyzed. Furthermore as new chemotherapeutics develop, the possible chemotherapy-induced toxicity to rapidly dividing normal cells, especially sensitive differentiated cells, has to be considered. Such undesirable effects would probably be ameliorated by selectively and locally inhibiting apoptosis in defined sensitive cells.

Methodology and Principal Findings: Mouse embryonic fibroblasts (MEFS) from Apaf-1 knock out mouse (MEFS KO Apaf-1) and Bax/Bak double KO (MEFS KO Bax/Bak), MEFS from wild-type mouse (MEFS wt) and human cervix adenocarcinoma (HeLa) cells were used to comparatively investigate the signaling cell death-induced pathways of BH3-mimetics, like ABT737 and GX15-070, with DNA damage-inducing agent cisplatin (cis-diammineplatinum(II) dichloride, CDDP). The study was performed in the absence or presence of apoptosis inhibitors namely, caspase inhibitors or apoptosome inhibitors. BH3-mimetic ABT737 required of Apaf-1 to exert its apoptosis-inducing effect. In contrast, BH3-mimetic GX15-070 and DNA damage-inducing CDDP induced cell death in the absence of both Bax/Bak and Apaf-1. GX15-070 induced autophagy-based cell death in all the cell lines analyzed. MEFS wt cells were protected from the cytotoxic effects of ABT737 and CDDP by chemical inhibition of the apoptosome through QM31, but not by using general caspase inhibitors.

Conclusions: BH3-mimetic ABT737 not only requires Bax/Bak to exert its apoptosis-inducing effect, but also Apaf-1, while GX15-070 and CDDP induce different modalities of cell death in the absence of Bax/Bak or Apaf-1. Inclusion of specific Apaf-1 inhibitors in topical and well-localized administrations, but not in systemic ones, to avoid interferences with chemotherapeutics would be of interest to prevent chemotherapeutic-induced unwanted cell death which could improve cancer patient care.

Citation: Andreu-Fernández V, Genovés A, Messeguer A, Orzáez M, Sancho M, et al. (2013) BH3-Mimetics- and Cisplatin-Induced Cell Death Proceeds through Different Pathways Depending on the Availability of Death-Related Cellular Components. PLoS ONE 8(2): e56881. doi:10.1371/journal.pone.0056881

Editor: Shawn B Bratton, The University of Texas MD Anderson Cancer Center, United States of America

Received October 31, 2012; **Accepted** January 15, 2013; **Published** February 21, 2013

Funding: This work was supported by grants from the Spanish Ministry of Science and Innovation (MICINN - BIO2007-60066, SAF2010-15512, SAF2011-30542-C02-01 and CSD2008-00005C) and Generalitat Valenciana Prometeo 2010/005 (partially funded with ERDF). The funders had no role in study design, data collection and analysis, decision to publish, or preparation of the manuscript.

Competing Interests: Enrique Pérez-Payá currently serves as Academic Editor to PLOS ONE. This does not alter the authors' adherence to all the PLOS ONE policies on sharing data and materials.

* E-mail: eperez@cipf.es

Introduction

Current anti-tumour treatments based in inducing apoptosis target cancer cells and rapidly dividing normal cells as well as other especially sensitive differentiated cells. Therefore, these treatments do not differentiate between malignant and normal cells. Chemotherapy causes toxicity, leading to side effects like those reported for apoptosis-inducing and DNA-damaging agent cisplatin (cis-diammineplatinum(II) dichloride, CDDP), which induces ototoxicity [1] and alopecia [2]. These undesirable effects may be ameliorated by the discovery of new more specific cell death-inducing drugs [3], or by selectively and locally inhibiting apoptosis in defined sensitive cells.

The discovery of the components of the apoptosis signaling pathway is providing the basis for novel targeted therapies that can induce death in cancer cells. Then BCL-2 antagonists as the chemotherapeutical drugs called BH3-mimetics are in clinical phase II [4]. On the other hand, apoptosis inhibitors-based drugs may have the potential to locally attenuate chemotherapy-induced side effects if the effective dose of apoptosis inducer (chemotherapeutic drug) over apoptosis inhibitor is defined. Current synthetic apoptosis inhibitors include caspase inhibitors [5] and apoptosome inhibitors [6].

The proposal of developing BH3-mimetics as chemotherapeutic drugs originates from understanding the role of the Bcl-2 protein family in regulating the intrinsic apoptotic pathway by controlling

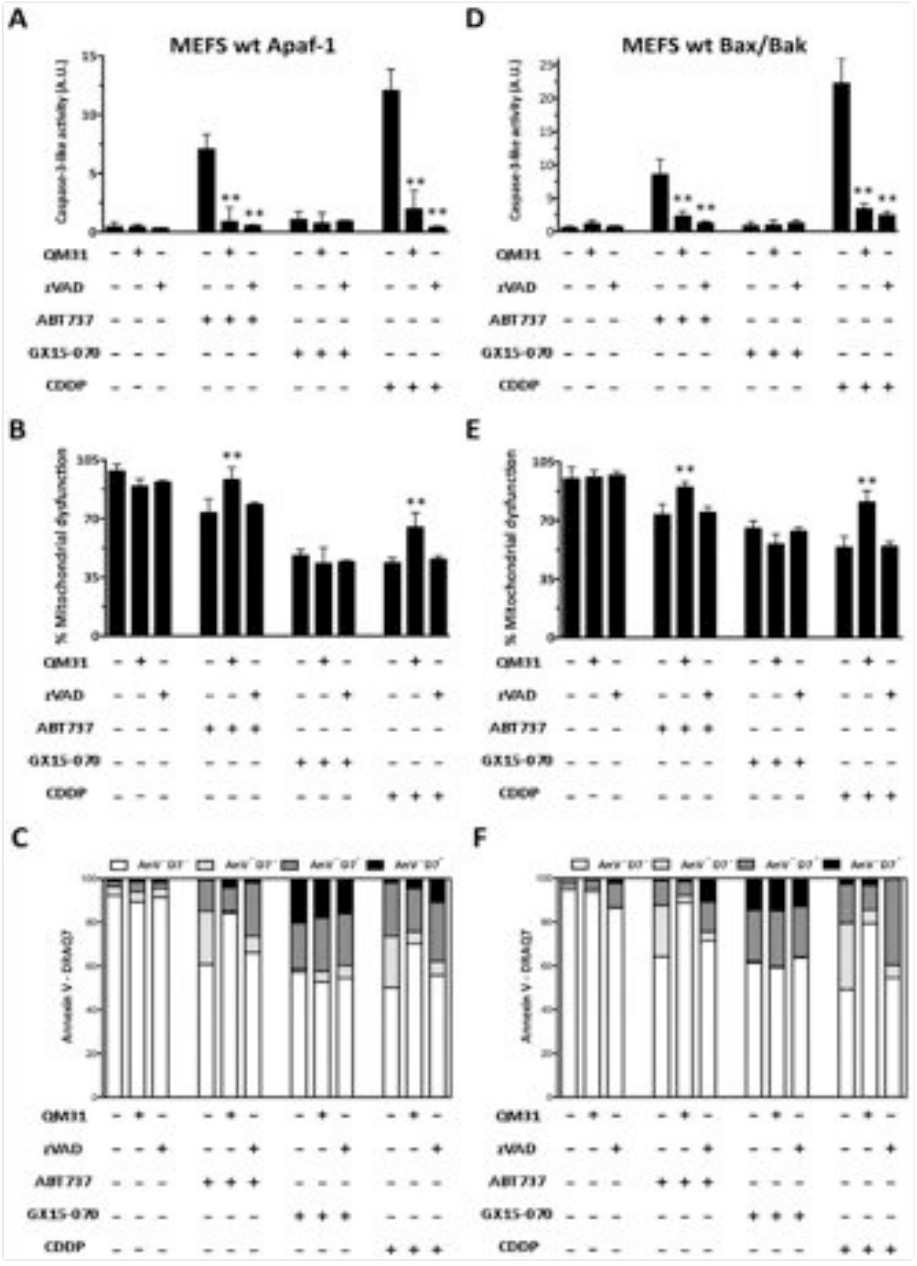
A
MEFS wt Apaf-1
Caspase-3-like activity (A.U.)
D
MEFS wt Bax/Bak
Caspase-3-like activity (A.U.)
B
% Mitochondrial dysfunction
E
% Mitochondrial dysfunction
C
Annexin V - DRAQ7
F
Annexin V - DRAQ7
QM31
zVAD
ABT737
GX15-070
CDDP

Figure 1. Apaf-1 inhibitor QM31 prevents cell death in non tumor cells treated with both ABT737 and CDDP, but not in cells treated with GX15-070. (**A and D**) Caspase 3-like activity was measured in MEFS wt Apaf-1 and MEFS wt Bax/Bak treated with ABT737 (25 μM), GX15-070 (1 μM) and CDDP (30 μM) in the presence or absence of QM31 (10 μM) and zVADfmk (5 μM). (**B and E**) Mitochondrial dysfunction was measured by an MTT assay under the same conditions described above. Bars represent the mean of three experiments ± s.d. (**p<0.05). (**C and F**) Apoptotic cell death was determined by flow cytometry with FITC Annexin V and DRAQ7. Data are representative results of three independent experiments.
doi:10.1371/journal.pone.0056881.g001

mitochondria outer membrane permeability (MOMP). The anti-apoptotic members of this family (Bcl-2, Bcl-xL, Bcl-W, Mcl-1 and A1) are characterized by the homology of four regions denominated Bcl-2 homology domains (BH1, BH2, BH3 and BH4), pro-apoptotic members, Bax, Bak and Bok, which share domains BH1-3, while the BH3-only proteins (e.g., Bad, Bid, Bim, Noxa and Puma) contain only the BH3 region [7]. BH3-only proteins promote apoptosis by suppressing anti-apoptotic proteins at the mitochondria and the endoplasmic reticulum or by directly activating Bax and Bak [8]. The anti- and pro-apoptotic balance of Bcl-2 proteins is deregulated in cancer cells [9]. Extensive work was performed to elucidate the process whereby protein-protein interactions between Bcl-2 protein family members commit cells to apoptosis. As a unified model, and under homeostatic conditions, anti-apoptotic Bcl-2 family members present a hydrophobic groove that interacts with the BH3 domain of pro-apoptotic effectors (Bax and Bak) or the BH3-only proteins to allow their sequestration, as well as the inhibition of MOMP. Apoptotic stimuli release Bax and Bak from the hydrophobic groove to induce oligomerization at the mitochondria membrane and MOMP. Therefore, cytochrome *c* (Cyt *c*) and Smac/Diablo proteins are released from the mitochondrial intermembrane space [10]. Cyt *c* binds to apoptosis protease-activating factor-1 (Apaf-1) to induce apoptosome assembling that recruits and activates initiator caspase-9, which further activates effector caspases, inducing apoptotic cell death [11].

The small molecule compounds developed as inhibitors of anti-apoptotic Bcl-2 proteins, generically named BH3-mimetics such as ABT737 (Abbott Laboratories) or obatoclax (GX15-070, Gemin X Biotechnologies), release pro-apoptotic binding partners and suffice to induce apoptosis. ABT737 binds selectivity to anti-apoptotic Bcl-2, but has a low affinity to Mcl-1 and A1 [12,13]. GX15-070 has been proposed to influence the activity of the Bak/Mcl-1 and Bim/Mcl-1 complexes [14] to induce mitochondrial-mediated apoptosis, which would imply Bax/Bak-mediated MOMP and apoptosome-mediated activation of caspases. However, in some cell lines that are relevant for disease, GX15-070-treatment has also been described to render phenotypic cell characteristics which could be associated with GX15-070 activities, including autophagy, independently of mitochondrial-mediated apoptosis. The cytotoxic activity of GX15-070 and ABT737 in Bax/Bak double knockout cells has also been reported [15,16], while the role of the apoptosome is unclear as it is still to be explored in detail. This is particularly relevant for studying the activity of BH3-mimetics in cells with low Apaf-1 contents that correlate with resistance to chemotherapeutic treatments [17,18] and for preclinically evaluating a new class of apoptosis inhibitors targeting the apoptosome [19,20], which are currently being evaluated as agents to locally prevent chemotherapy-induced secondary effects. It would then be of interest to comparatively analyze the activity of BH3-mimetics and CDDP (as a representative of established cytotoxic drugs) in cells in which Apaf-1 has been genetically deleted and to also analyze whether apoptosome inhibitors can inhibit BH3-mimetics-induced cell death.

Here we analyzed the ability of BH3-mimetics GX15-070 and ABT737 to induce cell death in mouse embryonic fibroblasts (MEFS) from Apaf-1 knockout (KO) mouse (MEFS KO Apaf-1) and in MEFS from wild-type mouse (MEFS wt) in the presence and absence of the apoptosis inhibitors Z-Val-Ala-Asp(OMe)-fluoromethylketone (zVADfmk – a general caspase inhibitor [5]) and QM31, an apoptosome inhibitor [19,20]. The results were comparatively evaluated with the effects of CDDP under the same experimental conditions and were extended to MEFS from Bax/Bak double KO mouse (MEFS KO Bax/Bak) and to human cervix adenocarcinoma (HeLa) cells.

Materials and Methods

Cell culture, treatments and chemicals

ABT737 and GX15-070 were from Abbott Laboratories and from SelleckBio, respectively; cis-diamminplatinum(II) dichloride (cisplatin, CDDP), rapamycin and 3-methyladenine (3MA) were obtained from Sigma Aldrich. QM31 is a perhydro-1,4-diazepine-2,5-dione whose general synthetic method has been recently reported [21]. The HeLa cell line was purchased from ATCC, and MEFS [22,23] were provided by Dr. Guido Kroemer (MEFS wt and KO Bax/Bak) and Dr. Francesco Cecconi (MEFS wt and KO Apaf-1). All the cell lines were grown in Dulbecco's Modified Eagle's Medium (DMEM) supplemented with 10% fetal bovine serum (FBS). Cultures were maintained at 37°C in a 5% CO_2 atmosphere. Cell media and FBS were purchased from GIBCO BRL Life Technologies. When indicated, cells were treated with 1 μM of GX50-070, 25 μM of ABT737, 30 μM of rapamycin and 30 μM of CDDP. When required, 10 mM MA, 10 μM QM31 or 5 μM zVAD were administered 30 min after treatment addition, and cells were maintained in culture for 24 h. Assays were carried out between passage 6 and 10, in all cases.

Determination of caspase activity

All cell extracts were prepared from 1.5×10^5 cells seeded in 6-well plates. After 24 h, cells were treated as indicated above and were then scrapped and washed with PBS. Pellets were resuspended in extraction buffer (50 mM PIPES, 50 mM KCl, 5 mM EDTA, 2 mM MgCl2, 2 mM DTT) supplemented with protease inhibitor cocktail (Sigma) and kept on ice for 5 min. Once pellets were frozen and thawed three times, cell lysates were centrifuged at 14000 rpm for 5 min and supernatants were collected. Quantification of the total protein concentration was performed using the BCA protein assay (Thermo Scientific). Total protein (50 μg) was mixed with 200 μL of caspase assay buffer (PBS, 10% glycerol, 0.1 mM EDTA, 2 mM DTT) containing 20 μM of the Ac-DEVD-afc (Enzo Life Sciences) caspase-3 specific substrate. Caspase activity was continuously monitored following the release of fluorescent afc at 37°C using a Wallac 1420 Workstation (λexc = 400 nm; λem = 508 nm). Caspase-3 activity was expressed as the increase of relative fluorescence units per min (A.U.).

Flow cytometry

After drug treatment, the cell culture medium was collected to retain floating cells and attached cells were dislodged using 0.5% Trypsin-EDTA (GIBCO). Floating and attached cells were combined and harvested by centrifugation. The cell pellets were suspended in 100 μl binding buffer (10 mM HEPES pH 7.4,

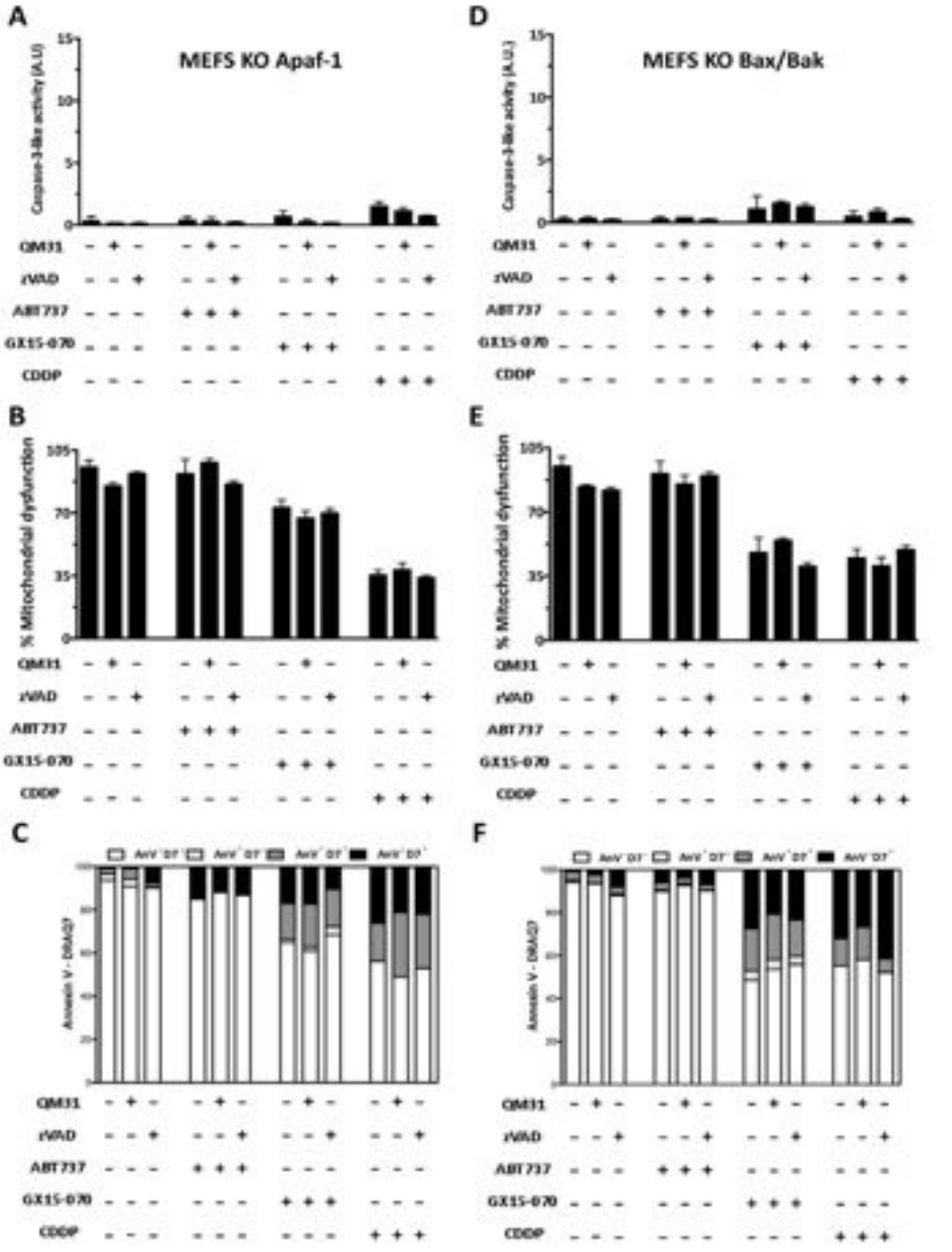
A
MEFS KO Apaf-1
Caspase-3-like activity (A.U.)
D
MEFS KO Bax/Bak
B
% Mitochondrial dysfunction
E
C
Annexin V - DRAQ7
F
QM31
zVAD
ABT737
GX15-070
CDDP

Figure 2. GX15-070 and CDDP induce caspase 3 independent cell death in Apaf-1 and Bax/Bak deficient cells. (**A and D**) Caspase 3-like activity was measured in MEFS KO Apaf-1 and MEFS KO Bax/Bak treated with ABT737 (25 μM), GX15-070 (1 μM) and CDDP (30 μM) in the presence or absence of QM31 (10 μM) and zVADfmk (5 μM). (**B and E**) Mitochondrial dysfunction was measured by an MTT assay under the same conditions described above. Bars represent the mean of three experiments ± s.d. (**C and F**) Apoptotic cell death was analyzed by flow cytometry with FITC Annexin V and DRAQ7. Data are representative results of three independent experiments.
doi:10.1371/journal.pone.0056881.g002

140 mM NaCl, 2.5 mM $CaCl_2$) and incubated with 10 μl FITC Annexin V (BD Biosciences) and 10 μl of DRAQ7 (6 μM; Biostatus) for 10 min at 37°C. Staining for Annexin V and DRAQ7 was assessed by flow cytometry on a FC500 instrument (Beckman Coulter) followed by data analysis using FlowJo software (Tree Star Inc).

MTT mitochondrial dysfunction assay

Mitochondrial functionality was measured by a 3-(4,5-dimethylthiazol-2-yl)-2,5-diphenyltetrazolium bromide (MTT) colorimetric assay. Cells were cultured in sterile 96-well microtiter plates at a seeding density of 1500 cells/well for the MEFS lines and 2000 cells/well for HeLa cells. After seeding, cells were left to adhere to the plate overnight, and then they were treated with the compounds of interest and incubated at 37°C for 24 h. MTT reagent (5 mg/ml in PBS) was added to each well and plates were further incubated for 4 h at 37°C. Finally, the medium was removed and the precipitated formazan crystals were dissolved in optical grade DMSO. Plates were read at 570 nm on a Wallac 1420 workstation.

Trypan blue exclusion assay

Cells were seeded in 6-well plates at a cellular density of 1.5×10^5 cells. After 24 h, cells were treated as described before. Cells were detached and 0.5% trypan blue dye was added in solution. Live cells possess intact cell membranes that exclude the

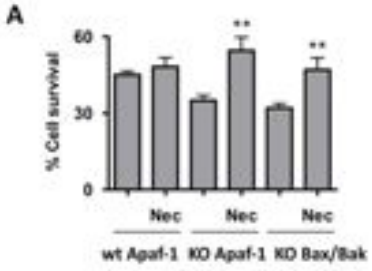

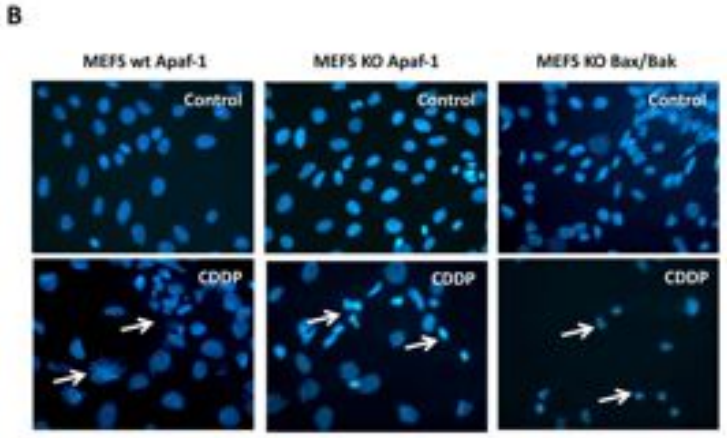

Figure 3. Non apoptotic cell death upon CDDP treatment in Apaf-1- and Bax/Bak-deficient cells. (**A**) Cell survival was measured by trypan blue exclusion upon treatment with CDDP (30 μM) in the presence or absence of necrostatin (Nec; 100 μM). Bars represent the mean of three experiments ± s.d. (**p<0.05). (**B**) MEFS wt Apaf-1, MEFS KO Apaf-1 and MEFS KO Bax/Bak were stained with DAPI upon CDDP (30 μM) treatment. Nuclei are considered to have the normal phenotype when glowing bright and homogenously. Apoptotic nuclei can be identified by the fragmented morphology of nuclear bodies. White arrows indicate dying cells.
doi:10.1371/journal.pone.0056881.g003

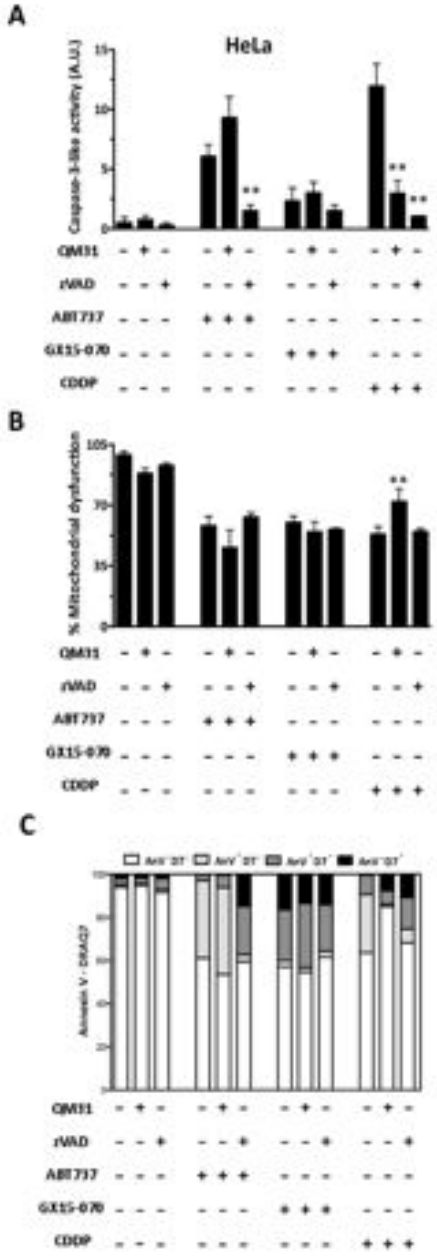

Figure 4. Apaf-1 inhibition does not protect tumor HeLa cells from death induced by ABT737 and GX15-070. (**A**) Caspase 3-like activity was measured in the HeLa cells treated with ABT737 (25 μM), GX15-070 (1 μM) and CDDP (30 μM) in the presence or absence of QM31 (10 μM) and zVADfmk (5 μM). (**B**) Mitochondrial dysfunction was measured by an MTT assay under the same conditions described above. Bars represent the mean of three experiments ± s.d. (*$p<0.1$; **$p<0.05$). (**C**) Apoptotic cell death was analyzed by flow cytometry with FITC Annexin V and DRAQ7. Data are representative results of three independent experiments.
doi:10.1371/journal.pone.0056881.g004

dye, whereas dead cells do not. Unstained (viable) and stained (non-viable) cells were counted separately in a hemacytometer and the total number of viable cells in the population was calculated.

Nuclear staining

The cells cultured on coverslips were stained with 300 nM 4′-6-diamidino-2-phenylindole (DAPI) solution. The morphology of the cells' nuclei was observed using a fluorescence microscope (Leica Vertical DM6000) at an excitation wavelength of 350 nm. Nuclei are considered to have the normal phenotype when they glow brightly and homogeneously. Apoptotic nuclei can be identified by either the condensed chromatin gathering at the periphery of the nuclear membrane or a total fragmented morphology of nuclear bodies.

Immunoblotting

Whole cell extracts were obtained by lysing cells in a buffer containing 25 mM Tris-HCl pH 7.4, 1 mM EDTA, 1 mM EGTA, 1% SDS, plus protease and phosphatase inhibitors. The protein concentration was determined by the BCA protein assay. Cell lysates were resolved by SDS-PAGE, transferred to nitrocellulose membranes, blocked with 5% non fat milk, washed with 0.1% Tween/PBS and incubated overnight with a specific primary antibody. Membranes were washed and probed with the appropriate secondary antibody conjugated to horseradish peroxidase for enhanced chemiluminescence detection (Amersham Pharmacia Biotech). The antibody against LC3 (#2775) came from Cell Signaling and α-tubulin antibody (#T8203) was from Sigma-Aldrich.

Statistical analysis

All the values represent the mean ± s.d. of at least three independent experiments. Statistical significance was determined by one-way ANOVA using the Graph Pad software, $p<0.05$ was designated as statistically significant.

Results and Discussion

Embryonic fibroblasts from wild-type mouse (MEFS wt Apaf-1 and MEFS wt Bax/Bak) [23] were treated with ABT737, GX15-070 or cisplatin (cis-diamminеplatinum(II) dichloride, CDDP), either alone or in combination with apoptosome inhibitor compound QM31 [19,20], or with broad spectrum caspase inhibitor Z-Val-Ala-Asp(OMe)-fluoromethylketone (zVADfmk). They were evaluated at 24 h post-treatment. ABT737 and CDDP treatments induced activation of caspase-3, which was inhibited by zVADfmk and by QM31. However, when cells were treated with GX15-070, only residual caspase-3 activity was observed (Fig. 1A and 1D). Cell viability was determined by MTT (Fig. 1B and 1E) to find that ABT737- and CDDP-induced death (20% and 60%, respectively) was inhibited by QM31, but not by zVADfmk, while the cell death induced by GX15-070 (around 50%) was not inhibited by either zVADfmk or QM31. Annexin V/DRAQ7 flow cytometry assays corroborate viability and apoptotic cell death

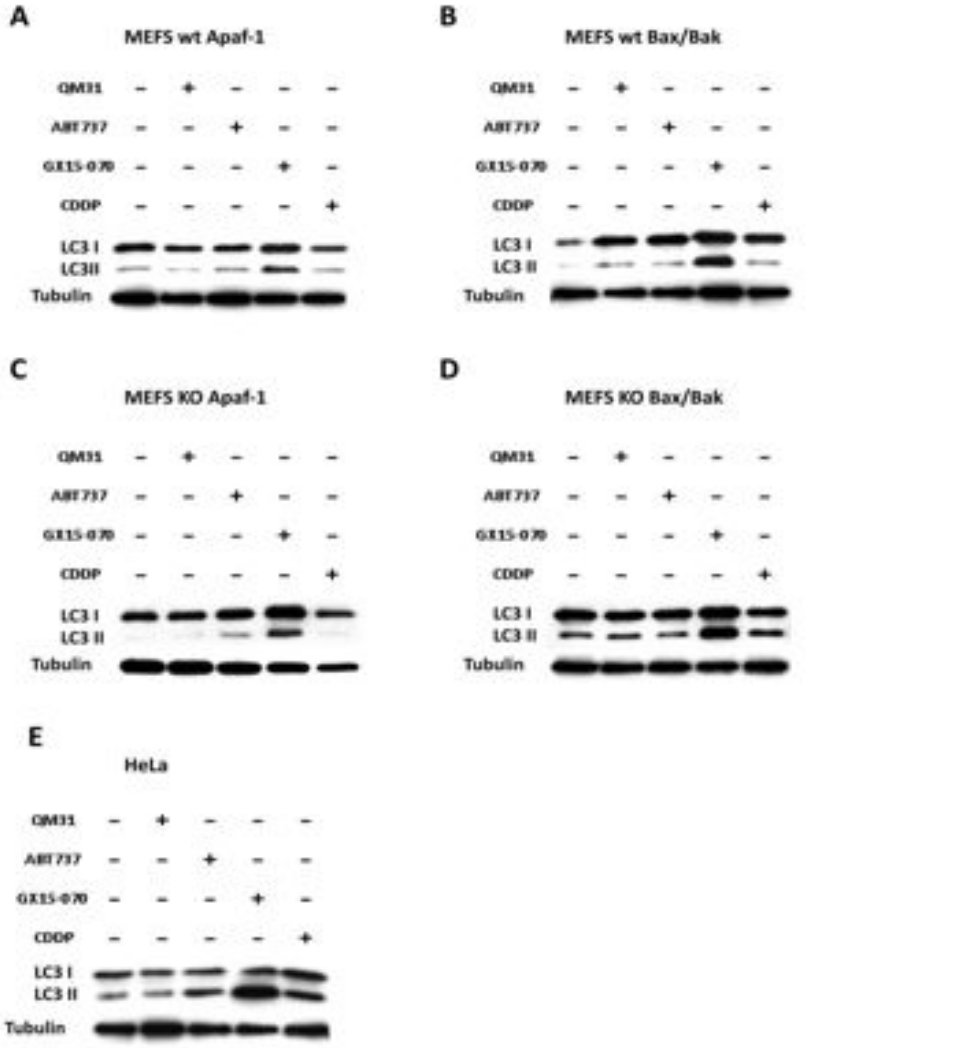

Figure 5. GX15-070 promotes the activation of the autophagic pathway via LC3 in all the cell lines. (**A–E**) LC3 detection in MEFS wt Apaf-1, MEFS wt Bax/Bak, MEFS KO Apaf-1, MEFS KO Bax/Bak and HeLa cells treated with ABT737 (25 μM), GX15-070 (1 μM), CDDP (30 μM) and QM31 (10 μM).
doi:10.1371/journal.pone.0056881.g005

results (Fig. 1C and 1F). The same experiments were conducted in Apaf-1 knockout (KO) mouse embryonic fibroblasts (MEFS KO Apaf-1) [25], in MEFS KO Bax/Bak [22] and in cervix adenocarcinoma cells (HeLa). In MEFS KO Apaf-1 (Fig. 2A) and MEFS KO Bax/Bak (Fig. 2D), none of the treatments induced caspase-3 activity, while cell viability was unaffected by the ABT737 treatment, but decreased with both GX15-070 and CDDP treatments (Fig. 2B and 2E). GX15-070- and CDDP-induced cell death in these cells was not inhibited upon apoptosome or caspase inhibition. Consequently, treatments with

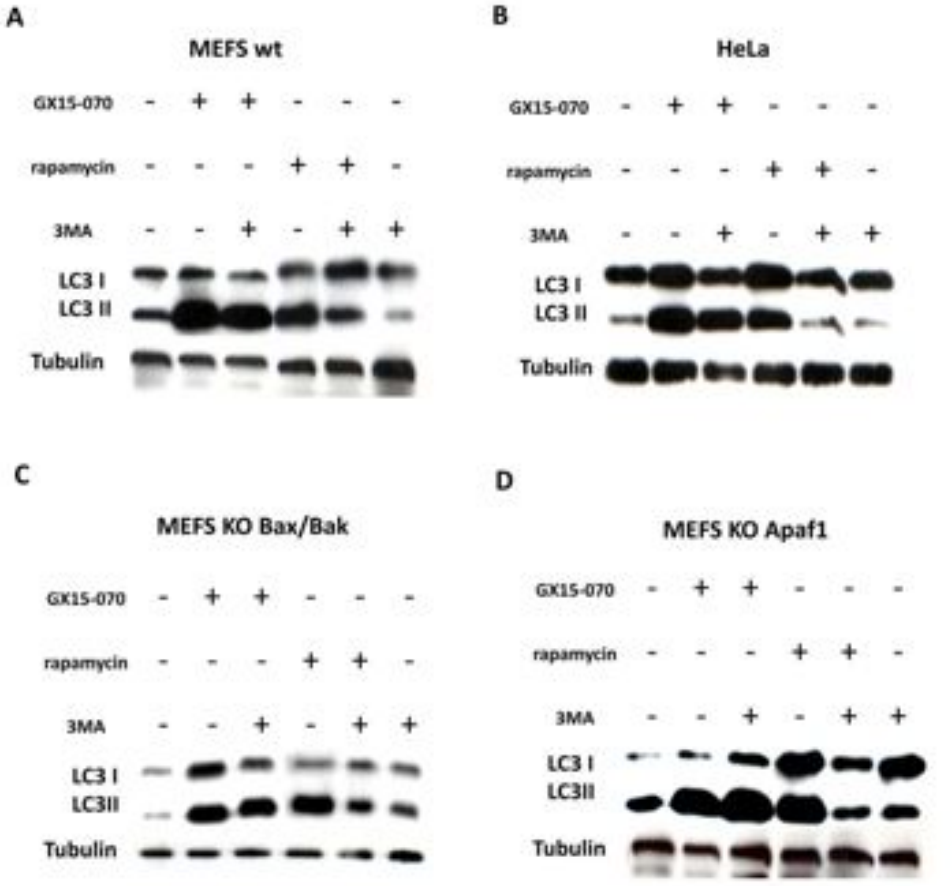

Figure 6. GX15-070 activates Beclin-1 non-dependent autophagy in all the cell lines. (**A–D**) LC3 immunoblotting in the MEFS wt Apaf-1, MEFS KO Apaf-1, MEFS KO Bax/Bak and HeLa cell lines treated with rapamycin (30 μM) and GX15-070 (1 μM) for 24 h in the presence or absence of 3MA (10 mM).
doi:10.1371/journal.pone.0056881.g006

QM31 and zVAD0mk did not significantly modify the percentage of Annexin V stained cells (Fig. 2C and 2F). These results suggest that in the absence of key death-related cellular components, such as the Bcl-2 proteins Bax and Bak and the apoptosome constituent protein Apaf-1, ABT737-triggering signaling is not fully perceived by the cell, while CDDP-depending signaling found caspase-independent cell death pathways. CDDP-induced cell death was partially recovered by necrostatin-1 (Nec), an inhibitor of RIPK1 in MEFS KO Apaf-1 and MEFS KO Bax/Bak (Fig. 3A), suggesting that necroptosis (a form of programmed necrosis that depends on activity of RIPK1) could participate in CDDP-induced death in these cells. In fact, nuclear staining upon CDDP treatment showed non apoptotic cell death in MEFS KO Apaf-1 and MEFS KO Bax/Bak cells (Fig. 3B), while treatment induced canonical apoptotic bodies in MEFS wt Apaf-1, indicating that DNA damaging agents may activate alternative cell death pathways when the intrinsic pathway of apoptosis is blocked.

In human cervix adenocarcinoma (HeLa) cells, rather than inducing caspase-3 activity, GX15-070 induced a type of cell death that was not inhibited by zVAD0mk or QM31 (Figs. 4A, 4B and 4C), which correlates with the phenotypes observed in all the MEFS cell lines. CDDP induced caspase-3 activation, which was inhibited in the presence of QM31 or zVAD0mk, and also cell death (Fig. 4A, 4B and 4C). CDDP-induced death was partially prevented by QM31, but not by zVAD0mk (Fig. 4B and 4C). Nonetheless, the zVAD0mk inhibition of ABT737-induced caspase-3 activity was unable to protect cells from dying (Fig. 4B and 4C). Interestingly, and unlike the results found in the MEFS wt,

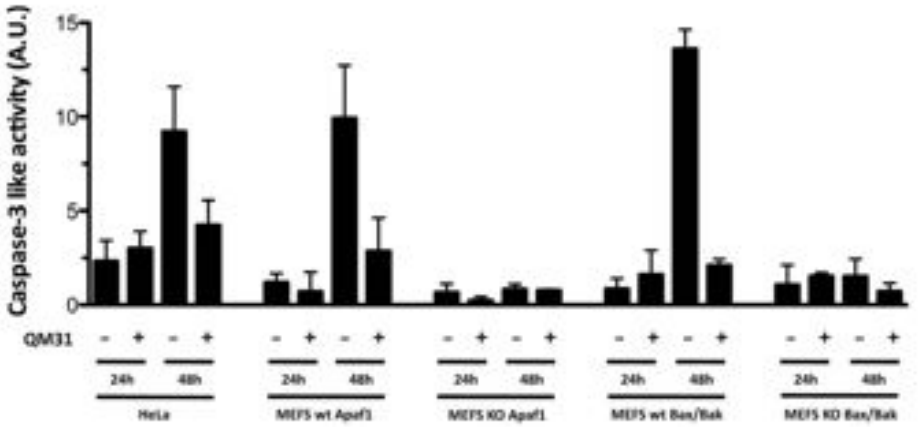

Figure 7. GX15-070 induces caspase 3-like activity after 48 h in HeLa and MEFs wt. Caspase 3-like activity was measured at 24 h and 48 h upon treatment with GX15-070 (1 μM) in the presence or absence of QM31 (10 μM) in HeLa, MEFS wt Apaf-1, MEFS KO Apaf-1, MEFS wt Bax/Bak and MEFS KO Bax/Bak.
doi:10.1371/journal.pone.0056881.g007

apoptosome inhibition by QM31 did not inhibit ABT737-induced caspase-3 and cell death (Fig. 4A and 4C).

To proceed with an initial analysis of the cell death pathway induced by GX15-070 in the MEFS wt Apaf-1, MEFS wt Bax/Bak, MEFS KO Apaf-1, MEFS KO Bax/Bak, and HeLa cells, we analyzed the expression of anti-apoptotic proteins Bcl-2, Bcl-xL and Mcl-1 and found no significant changes (data not shown). We also explored the induction of autophagy. Autophagy is a catabolic process involving the formation of autophagosomes and autolysosomes. Light chain 3 (LC3, a mammalian ortholog of yeast Atg8 - [24]) is essential for autophagosome formation and can be used as a reporter protein. When the process of autophagy proceeds, LC3-I (the cytosolic form) it is processed to the autophagosomal membrane-bound LC3-II form [24]. The LC3-II form increased considerably with GX15-070 treatment (Fig. 5A-D), suggesting that evaluated GX15-070-induced cell death was mediated by autophagy activation in all the cell lines. The activity of III phosphoinositide 3-kinase (PI3K III) is important in Beclin-1 (the human ortholog of yeast Atg-6)-induced autophagy [25], and 3-methyladenine (3MA – an inhibitor of PI3K III) is commonly used to determine the dependence of Beclin-1 in autophagy. 3MA did not modify GX15-070-induced LC3 processing (Fig. 6). Therefore, GX15-070-induced autophagy in both MEFS wt and MEFS KO Apaf-1 is independent of Beclin-1, as also reported for MEFS KO Bax/Bak and HeLa cells [15]. As an internal control, we induced autophagy by rapamycin and found that rapamycin-induced autophagy was inhibited by 3MA in all four cell lines analyzed (Fig. 6).

It has been reported that GX15-070 is able to induce apoptosis and autophagy in several cell lines [26]. Thus we performed a time-course analysis to examine whether GX15-070-treatment induces both autophagy and apoptosis. We used LC3 conversion as a marker of autophagy (Fig. 3) and caspase-3 activity as a marker of apoptosis. After 24 h we did not observe GX15-070-induced caspase-3 activation in the cell lines analyzed in the present study (Fig. 7). At 48 h however, we noted that GX15-070-induced caspase-3 activity in both MEFS wt and in HeLa cells. GX15-070-induced apoptosis at 48 h was inhibited by apoptosome inhibitor QM31. In contrast, GX15-070 did not induce apoptosis in MEFS KO Bax/Bak and in MEFS KO Apaf-1 at 48 h. These results suggest that GX15-070 can induce multiple cell death pathways, such as caspase-dependent apoptosis and autophagy. Nevertheless, GX15-070-induced apoptosis is not only dependent in Bax/Bak, as previously demonstrated [15,26], but also in Apaf-1.

In conclusion, the present study reveals that BH3-mimetic ABT737 not only requires Bax/Bak to exert its apoptosis-inducing effect, but also Apaf-1, indicating the exclusive targeting of ABT737 to Bcl-2 anti-apoptotic proteins. ABT737 upon binding to Bcl-2 and Bcl-xL removes the anti-apoptotic activity of these proteins in pro-apoptotic Bax/Bak and induces MOMP. However, MOMP-dependent signaling needs the components of the apoptotic pathway downstream of mitochondria, such as the formation of the apoptosome, to induce cell death. Hence, ABT737 treatments to cancer cells would have less side effects to differentiated cells containing low levels of Apaf-1, such as neurons and cardiomyocytes [27,28], than other treatments with lesser dependence of Apaf-1. In contrast, BH3-mimetic GX15-070 and DNA damage-inducing CDDP induce cell death in the absence of both Bax/Bak and Apaf-1. While GX15-070 induces mainly autophagy-based cell death at 24 h, a cell fraction dies by apoptosis at longer times post-treatment. On the other hand, CDDP induces necroptosis when apoptosis signaling pathway is not available. Our results extend findings by describing not only the sensitivity of different cells to the cell-inducing agents explored, but also the behavior of current apoptosis inhibitors, which could be useful in topical applications aimed to diminish unwanted cell death. Non tumor cells, as demonstrated herein with MEFS wt, could be protected from the cytotoxic effects of ABT737 and CDDP by the chemical inhibition of the apoptosome through QM31, which lowered caspase-3 activity and improved cell survival, while the use of caspase inhibitors prevented caspase activation, but did not improve survival. This scenario correlates with proposals in mammals that solely caspase inhibition,

APPENDIX III

- Sancho M, Gortat A, Herrera AE, Andreu-Fernández V, Ferraro E, Cecconi F, Orzáez M, Pérez-Payá E. **"Altered mitochondria morphology and cell metabolism in Apaf1-deficient cells"** *Plos One*, 2014. doi: 10.1371/journal.pone.0084666.

These results are part of the background of this thesis. Vicente Andreu contributed by performing the experiments required by the referees of the journal (results labeled as "Supplementary" in the publication).

OPEN ACCESS Freely available online

PLOS ONE

Altered Mitochondria Morphology and Cell Metabolism in Apaf1-Deficient Cells

Mónica Sancho[1¶], Anna Gortat[1¶], Andrés E. Herrera[1], Vicente Andreu-Fernández[1], Elisabetta Ferraro[2], Francesco Cecconi[3,4], Mar Orzáez[1*], Enrique Pérez-Payá[1,5]

1 Laboratory of Peptide and Protein Chemistry, Centro de Investigación Príncipe Felipe, Valencia, Spain, 2 Laboratory of Skeletal Muscle Development and Metabolism, IRCCS San Raffaele Pisana Institute, Rome, Italy, 3 Laboratory of Molecular Neuroembryology, IRCCS Fondazione Santa Lucia, Rome, Italy, 4 Dulbecco Telethon Institute, University of Rome "Tor Vergata", Rome, Italy, 5 Instituto de Biomedicina de Valencia, IBV-CSIC, Valencia, Spain

Abstract

Background: Apaf1 (apoptotic protease activating factor 1) is the central component of the apoptosome, a multiprotein complex that activates procaspase-9 after cytochrome *c* release from the mitochondria in the intrinsic pathway of apoptosis. Other cellular roles, including a pro-survival role, have also been described for Apaf1, while the relative contribution of each function to cell death, but also to cell homeostatic conditions, remain to be clarified.

Methodology and Principal Findings: Here we examined the response to apoptosis induction of available embryonic fibroblasts from Apaf1 knockout mice (MEFS KO Apaf1). In the absence of Apaf1, cells showed mitochondria with an altered morphology that affects cytochrome *c* release and basal metabolic status.

Conclusions: We analysed mitochondrial features and cell death response to etoposide and ABT-737 in two different Apaf1-deficient MEFS, which differ in the immortalisation protocol. Unexpectedly, MEFS KO Apaf1 immortalised with the SV40 antigen (SV40IM-MEFS Apaf1) and those which spontaneously immortalised (SIM-MEFS Apaf1) respond differently to apoptotic stimuli, but both presented relevant differences at the mitochondria when compared to MEFS WT, indicating a role for Apaf1 at the mitochondria.

Citation: Sancho M, Gortat A, Herrera AE, Andreu-Fernández V, Ferraro E, et al. (2014) Altered Mitochondria Morphology and Cell Metabolism in Apaf1-Deficient Cells. PLoS ONE 9(1): e84666. doi:10.1371/journal.pone.0084666

Editor: Dhyan Chandra, Roswell Park Cancer Institute, United States of America

Received April 19, 2013; **Accepted** November 18, 2013; **Published** January 9, 2014

Funding: This work has been supported by grants from the Spanish Ministry of Science and Innovation (MICINN-BIO2007-60066, -SAF2010-15512, and CSD2008-00005C), and by the Generalitat Valenciana (GV) Prometeo 2010/005 (funded in part with ERDF) to EPP. The funders had no role in study design, data collection and analysis, decision to publish, or preparation of the manuscript.

Competing Interests: The authors have declared that no competing interests exist.

* E-mail: morzaez@cipf.es

¶ These authors contributed equally to this work.

Introduction

Apoptosis is an essential process of programmed cell death for normal development, cell homeostasis, and also as a defence mechanism to eliminate harmful cells, such as tumour cells or cells infected by viruses. It is characterised by specific morphological changes, such as shrinkage of cell and chromatin condensation. Apoptosis can be triggered by extrinsic (death receptor-mediated [1]) or intrinsic (mitochondrial) pathways. The intrinsic pathway can be initiated by many stresses [2], and both pathways can provoke mitochondrial outer membrane permeabilisation (MOMP) mediated by proteins of the Bcl-2 family (Bcl-2s). Cytochrome *c* (Cyt *c*) is then released into the cytosol and induces the formation of the apoptosome complex. The apoptosome is a holoenzyme complex formed by Cyt *c*-activated Apaf1, dATP and procaspase-9 [3,4]. Apoptosome-bound procaspase-9 is activated, and subsequently proteolyses and activates downstream effector caspases, leading to the progression of cell death. Apaf1 is a 135 kDa protein that is known for its apoptotic role. However, recent studies have suggested additional non-apoptotic functions for Apaf1, including a pro-survival role [5–10]. How these, in principle, opposite functions of the protein operate in cells remains a controversial matter, and there are still important questions to answer about the Apaf1 biological function, not only when cells die, but also under homeostatic conditions.

Although the cells deriving from Apaf1 knockout (KO) animals are expected to be resistant to the majority of apoptotic insults, different laboratories have presented evidence that some, but not all, immortalised Apaf1-deficient cell types can switch between apoptotic and necrotic cell death [11–14]. These differences might be related to an influence of the immortalisation process on the availability of cell death signalling components [15,16] or to a more complex role of Apaf1 in the cell than expected. In addition, the relationship between the extent of Cyt *c* release from the mitochondria and the completeness of downstream apoptotic signalling is still controversial. Studies at the single cell level have provided clear evidence for a single-step release mechanism of Cyt *c* and of other mitochondrial proteins, such as Smac/DIABLO, even in Apaf1-deficient cells [17,18]. Moreover in cells of different origins lacking Apaf1, it has been reported that Cyt *c*-release is either inhibited [12] or, in contrast, it increases [9]. Furthermore, the pharmacological inhibition of Apaf1 has been reported to

induce a reduction in the total amount of Cyt *c* released from a cell population [7].

Here we report a profound characterisation of available embryonic fibroblasts from Apaf1 KO mouse (MEFS KO Apaf1). We found that distinct MEFS KO Apaf1 cells behave differently in response to apoptotic insults. We analysed the apoptotic response to such insults, as well as the mitochondrial and metabolic status in MEFS KO Apaf1, which were spontaneously immortalised (SIM) or immortalised by the transfection of the SV40 antigen (SV40IM). In the absence of Apaf1, cells present mitochondria with an altered morphology which affects Cyt *c* release and basal metabolic status.

Materials and Methods

Cell culture, treatments and chemicals

All the cell lines were grown in Dulbecco's Modified Eagle's Medium (DMEM) supplemented with 10% foetal bovine serum (FBS). Cultures were maintained at 37°C in a 5% CO_2 atmosphere. Cell media and FBS were purchased from GIBCO BRL Life Technologies. When indicated, cells were treated with 5 μM of etoposide (E), acquired from Sigma Aldrich. When required, 100 μM necrostatin (Nec; Enzo Life Sciences), 10 μM SVT016426 (SVT) or 5 μM Z-Val-Ala-Asp(OMe)-fluoromethylketone (zVAD; Tocris) were administered 1 h prior to treatment addition, and cells were maintained in culture for 24 h. MEFS cell lines were previously established in the referenced publications [4,9]. For the MEFS cells established by spontaneous immortalisation (SIM), two clones of each cell line (WT and KO Apaf1) were tested. No intrinsic variability was observed between them. Lipofectamine™ 2000 (Invitrogen) was used according to the manufacturer's instructions to transfect HeLa cells with a control random siRNA (Rsi) and Apaf1 siRNA (Asi), obtained from Cell Signaling.

Caspase activity determination

Cell extracts were prepared from 2.0×10^5 cells seeded in 6-well plates. After 24 h, cells were treated as indicated above, and were scraped and washed with PBS. Pellets were lysed in extraction buffer (50 mM PIPES, 50 mM KCl, 5 mM EDTA, 2 mM $MgCl_2$, 2 mM DTT, supplemented with protease inhibitors). Having frozen and thawed three times, cell lysates were centrifuged at 14,000 rpm for 5 min and supernatants were collected. Quantification of the total protein concentration was performed by the BCA protein assay (Thermo Scientific). Total protein (50 μg) was mixed with 200 μL of caspase assay buffer (PBS, 10% glycerol, 0.1 mM EDTA, 2 mM DTT) containing 20 μM Ac-DEVD-afc (Enzo Life Sciences) of the caspase-3 substrate. Caspase activity was continuously monitored following the release of fluorescent afc at 37°C with a Wallac 1420 Workstation (λ_{exc} = 400 nm; λ_{em} = 508 nm). Caspase-3-like activity was expressed as the increase of relative fluorescence units per min (A.U.).

Trypan blue exclusion assay

Cells were seeded in 6-well plates at a cellular density of 2.0×10^5 cells/well. After 24 h, cells were treated as described before to be then detached, and 0.05% trypan blue dye was added in solution. Live cells possess intact cell membranes that exclude the dye, whereas dead cells do not. Unstained (viable) and stained (non-viable) cells were counted separately in a haemacytometer and the total number of viable cells in the population was calculated.

Nuclear staining

The cells cultured on coverslips were stained with 300 nM 4'-6-diamidino-2-phenylindole (DAPI) solution. The morphology of cells' nuclei was observed under a fluorescence microscope (Leica Vertical DM6000) at the 350 nm excitation wavelength. Nuclei are considered to have the normal phenotype when they glow brightly and homogeneously. Apoptotic nuclei can be identified by either a condensed chromatin gathering at the periphery of the nuclear membrane or a total fragmented morphology of nuclear bodies.

Immunoblotting

Whole cell extracts were obtained by lysing cells in a buffer containing 25 mM Tris-HCl pH7.4, 1 mM EDTA, 1 mM EGTA, 1% SDS, plus protease and phosphatase inhibitors. Protein concentration was determined by the BCA protein assay. Cell lysates were resolved by SDS-PAGE, transferred to nitrocellulose membranes, blocked with 5% non-fat milk, washed with 0.1% Tween/PBS and incubated overnight with a specific primary antibody. Membranes were washed and probed with the appropriate secondary antibody conjugated with horseradish peroxidase for enhanced chemiluminescence detection (Amersham Pharmacia Biotech). The antibody against Apaf1 (#611365) was acquired from BD Biosciences, Bcl-X_L (#2764) and Bcl-2 (#2870) came from Cell Signaling, and β-tubulin antibody (#T8203) was purchased from Sigma-Aldrich.

DiOC staining

Cells were incubated with 50 nM 3,3'-Diethyloxacarbocyanine iodide ($DiOC_2(3)$) at 37°C, 5% CO_2, for 15 minutes in 500 μL of PBS. Then, samples were analysed in a Cytomics FC 500 (Beckman Coulter) flow cytometer with 488 nm excitation using the appropriate emission filters for Alexa Fluor ® 488 dye.

Cytochrome *c* release assay

MEFS cells were grown in 6-well plates under the same conditions described above. After 24 h of etoposide treatment, mitochondrial Cyt *c* was followed using the InnocyteTM Flow Cytometric Cytochrome *c* Release kit (Calbiochem). Cells were analysed in a Cytomics FC 500 (Beckman Coulter) flow cytometer.

Immunofluorescence

Cells were fixed with 4% paraformaldehyde, permeabilised with 0.1% Triton X-100, and blocked in 2% gelatin in PBS. Then they were labelled with a primary antibody against Cyt *c* (SC13561; Santa Cruz), followed by anti-mouse IgG conjugated with FITC (Jackson ImmunoResearch). Images were obtained under a Leica DM 6000 microscope (Leica DC500 camera) with a 20× objective. Two hundred cells were counted and classified according to the localisation of Cyt *c* in the mitochondria (tubular morphology) or cytosol (diffuse pattern).

Transmission electron microscopy

MEFS cells were seeded at 3×10^5 cells per chamber on Lab-Tek chamber slides of 4 wells (Nalge Nunc International). Then, cells were fixed for 1 h in 3.5% glutaraldehyde at 37°C and postfixed for 1 h in 2% OsO_4 at room temperature. Cellular staining was performed at 4°C for 2 h in 2% uranyl acetate in the dark. Finally, cells were rinsed in sodium phosphate buffer (0.1 M, pH 7.2), dehydrated in ethanol and infiltrated overnight in Araldite (Durcupan, Fluka, Buchs SG, Switzerland). Following polymerisation, embedded cultures were detached from the chamber slide and glued to Araldite blocks. Serial semi-thin

(1.5 µm) sections were cut with an Ultracut UC-6 (Leica, Leica, Heidelberg, Germany), mounted onto slides and stained with 1% toluidine blue. The selected semi-thin sections were glued (Super Glue, Loctite) to araldite blocks and detached from the glass slide by repeated freezing (in liquid nitrogen) and thawing. Ultrathin (0.07 µm) sections were prepared with the Ultracut UC-6 and stained with lead citrate. Finally, photomicrographs were obtained under a transmission electron microscope (FEI Tecnai Spirit G2) using a digital camera (Morada, Soft Imaging System, Olympus). Then, mitochondrial width was quantified by using the ImageJ Java-based image processing software (NIH).

ATP, lactate and pyruvate measurements

HeLa cells were seeded at a density of 5×10^5 cells/mL. An ATP measurement was taken in duplicate by employing the Luminescence ATP Detection Assay System (Perkin Elmer) according to the manufacturer's instructions. The KO MEFs results were normalised to their respective WT controls. Lactate was measured with the Lactate Assay Kit II (BioVision) following the manufacturer's instructions. Pyruvate was measured using the Pyruvate Assay Kit (BioVision) according to the manufacturer's instructions. The KO MEFs results were normalised to their respective WT controls.

Results and Discussion

The embryonic fibroblast cell lines from wild-type (MEFS WT) and from Apaf1 KO mouse (MEFS KO Apaf1) [4] were previously established by spontaneous immortalisation (SIM) or by infection with SV40 antigen T (SV40IM) [9]. The cell lines were analysed to study the relevance of Apaf1 in the homeostasis of the cell and their behaviour upon apoptotic stimuli. As an apoptotic insult, we used etoposide, a DNA damage-inducing drug that is well-characterised as an intrinsic apoptosis inducer [19]. SV40IM-MEFS KO Apaf1 cells were more sensitive to etoposide than SV40IM-MEFS WT as manifested by lower counts of cell survival determined by trypan blue exclusion (Fig. 1A). In contrast, and as initially expected [4], SIM-MEFS KO Apaf1 cells were resistant to etoposide (Fig. 1A), while SIM-MEFS WT cells showed a similar percentage of death to SV40IM-MEFS WT cells. SIM-MEFS WT and SV40IM-MEFS WT death concurred with caspase activation, while etoposide-induced death in SV40IM-MEFS KO Apaf1 proceeded without caspase activation (Fig. 1B). In etoposide-induced SV40IM-MEFS WT, caspase-3 activity diminished in the presence of the irreversible caspase inhibitor Z-Val-Ala-Asp(OMe)-fluoromethylketone (zVAD) and in the presence of the Apaf1 inhibitor SVT016426 (SVT) (not shown), while cell viability increased only in the presence of SVT016426 (Fig. 1C). Neither RIPK1 inhibitor necrostatin (Nec) nor zVAD had any effect on cell viability in these cells. In contrast in SV40IM-MEFS KO Apaf1 cells, neither zVAD nor SVT016426 influenced cell death, while Nec increased cell survival, suggesting that these cells can engage alternative death pathways as necroptosis in the absence of Apaf1. In fact nuclear morphology studies by DAPI staining showed that when cells were treated with etoposide, SV40IM-MEFS KO Apaf1 cells did not present apoptotic nuclear bodies as SV40IM-MEFS WT cells did (white arrows; Fig. 1D). Instead dead KO Apaf-1 cells showed smaller and brighter nuclei (Fig. 1D). In order to clarify which of the two cell line systems was physiologically more relevant, Apaf1 was depleted transiently by siRNA in HeLa cells (due to the difficulty of transfecting MEFS cells) and was treated with etoposide. When the HeLa cells transfected with a control random siRNA were treated with etoposide, caspase-3-like activity (Figure 1E) was observed and cell death came close to 60% (figure 1F). However in the Apaf1 siRNA-based knockdown cells, caspase-3-like activity diminished with a slight decrease in cell death of the cell population (Figure 1E and F), which might be explained by the fact that, in the absence of Apaf1, etoposide induced caspase-independent cell death in these cells, as described previously elsewhere ([11,20] These results indicate that the SV40 immortalised and the siRNA Apaf-1 transient depleted cells behave similarly. Thus the SV40 immortalisation procedure better reflects the punctual elimination of Apaf-1 from the cell than the SIM immortalisation procedure, which probably reproduces the adaptation and selection process produced by the permanent absence of Apaf-1 in the cell. From the pharmacological point of view, both models could probably be relevant depending on the chronic or acute nature of the treatment with Apaf-1 inhibitors required for disease resolution.

Next we evaluated the mitochondrial membrane potential ($\Delta\Psi m$). It is well-accepted that DNA-damaging agents, such as etoposide, induce signalling processes that convey into the mitochondria by inducing Cyt *c* release and a subsequent decrease in $\Delta\Psi m$ [17]. With etoposide-treated SV40IM-MEFS KO Apaf1, the population of cells with low $\Delta\Psi m$ increased when compared to the SV40IM-MEFS WT cells (Fig. 2A). As expected from the previous cell death susceptibility results (Fig. 1A), the resistant SIM-MEFS KO Apaf1 cells showed less cells with low $\Delta\Psi m$ than SIM-MEFS WT (Fig. 2A). Then we examined the release of Cyt *c* from the mitochondria after the etoposide treatment in both cell line types by flow cytometry. SV40IM-MEFS KO Apaf1 released more Cyt *c* to the cytosol than the equivalent SV40IM-MEFS WT. However, SIM-MEFS KO Apaf1 released less Cyt *c* than the control SIM-MEFS WT (Fig. 2B). These results correlate well with previous death sensitivity findings (Fig. 1A, B and C) and mitochondrial membrane potential (Fig. 2A). The immunocytochemistry experiments in the SV40IM-MEFS cell lines confirmed that Cyt *c* was located mainly in the mitochondria in the absence of a cell death inducer (Fig. 2C). Nevertheless, etoposide induced Cyt *c* release from the mitochondria to the cytosol in about 30% of SV40IM-MEFS WT cells and in around 70% of SV40IM-MEFS KO Apaf1 (Fig. 2C). All these results suggest that upon etoposide induction, Cyt *c* release is enhanced in the SV40IM-MEFS KO Apaf1 cells, which is in agreement with early kinetic observations [9]. Yet due to the absence of Apaf1, the death signalling wave probably proceeds through a necroptosis-like pathway. Thus, the immortalisation process may affect the genetic background and might be responsible for the differences between both MEFS KO Apaf1 cellular models. ABT-737 treatment induced activation of caspase-3 and death in SV40IM-MEFS WT. However in SV40IM-MEFS KO Apaf-1 and SIM-MEFS, both parameters remain unaffected (Fig. S1). These results suggest that ABT737-triggering signalling is not fully perceived by the cell, while DNA damaging agents may activate alternative cell death pathways when the intrinsic pathway of apoptosis is blocked. These results indicate that the differences between both KO cell lines probably lie at the mitochondrial level and not necessarily in the nuclear signalling events responsible for apoptosis induction.

Next we performed a series of analyses for the characterisation of both SV40IM- and SIM-MEFS KO Apaf1. The proteins of the Bcl-2 family have been described to participate in MOMP regulation [21]. It has been reported that SV40IM-MEFS KO Apaf1 exhibits a lower expression of anti-apoptotic proteins Bcl-2 and Bcl-X_L [9], which might be related to the differences observed in Cyt *c* release. We found that not only SV40IM-MEFS KO Apaf1, but also SIM-MEFS KO Apaf1 show low levels of Bcl-2 and Bcl-X_L (Fig. 3A). In addition, SV40IM- and SIM-MEFS KO

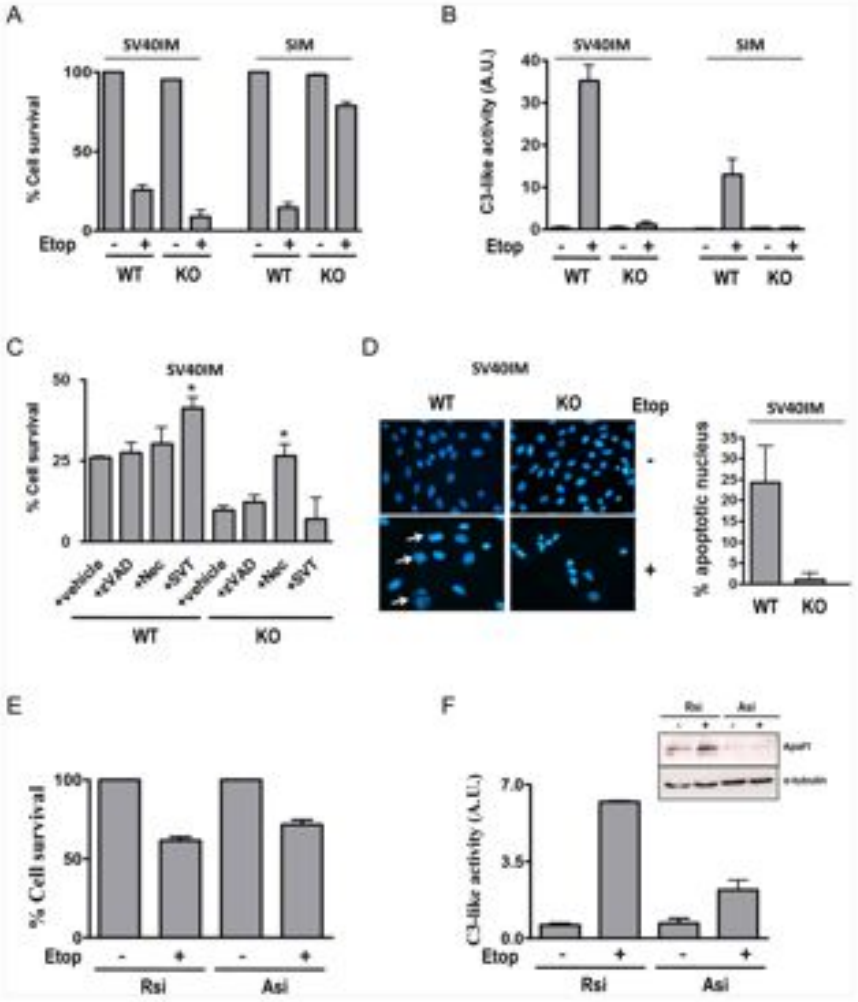

Figure 1. Caspase-independent cell death in SV40IM Apaf1 KO cells. (A) Cell survival was measured by the trypan blue exclusion assay in SV40IM and SIM MEFS, WT and Apaf1-depleted cells in the presence of etoposide (5 μM) for 24 h. (B) Caspase-3-like activity was measured under the same etoposide treatment conditions (+; 5 μM) described above. In all cases, bars represent the mean of three experiments ± s.d. (C) Cell survival was measured in the SV40IM cell lines treated with etoposide (5 μM) in the presence or the absence of z-VAD (5 μM), necrostatin (Nec; 100 μM) or SVT016426 (10 μM). (mean ± s.d, n = 3, *p≤0.05). (D) DAPI staining to analyse the apoptotic features between WT and Apaf1 KO cells in the presence of etoposide (5 μM). In all, 500 nuclei were counted and classified according to apoptotic nuclear bodies (white arrows). Quantification is shown in the right panel. (E) Cell survival was measured by the trypan blue exclusion assay in the HeLa cells transfected with random siRNA (Rsi) or Apaf1 siRNA (Asi) for 24 h and treated with etoposide (+; 5 μM) for another 24-hour period. (F) Caspase-3-like activity was measured under the same conditions described above. Bars represent the mean of three experiments ± s.d. The immunoblotting of the Apaf1 silencer is shown in the right panel.
doi:10.1371/journal.pone.0084666.g001

Apaf1 present a fragmented mitochondrial network (Fig. 3B), which correlates well with recently reported data and suggests that in SV40IM-MEFS KO Apaf1, the fission protein Drp1 localises in the mitochondria to a greater extent than in MEFS WT, thus favouring a fragmented mitochondrial network [9]. Next, we examined the ultra-structure of mitochondria by transmission

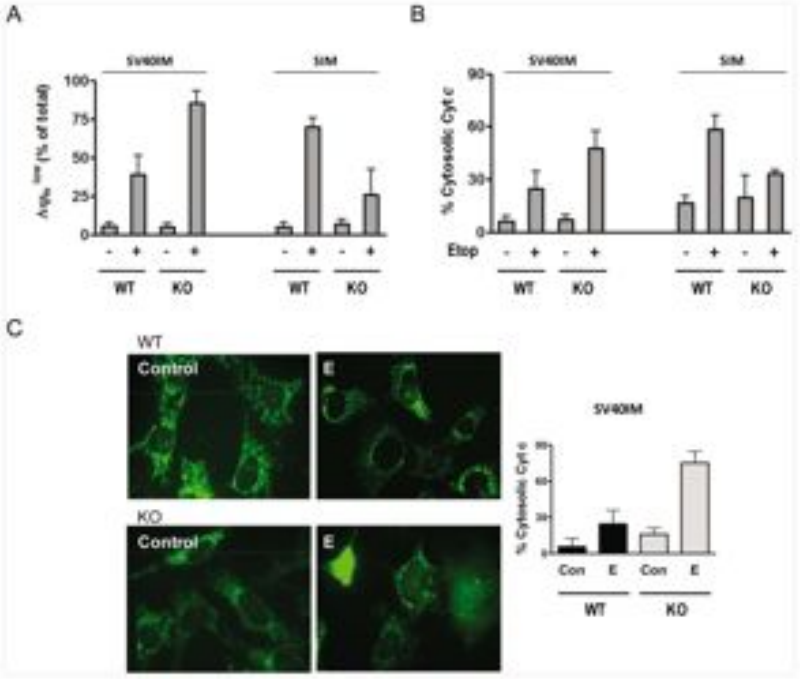

Figure 2. SV40IM Apaf1 KO cells showed faster Cyt *c* release. (A) Membrane potential study through $DIOC_2(3)$ staining in all the cell types upon etoposide treatment (+; 5 μM). (B) Percentage of cells with mitochondrial Cyt *c* measured by the cytometry analysis after incubation with etoposide (+; 5 μM) (mean ± s.d., n = 3). (C) Immunofluorescence against Cyt *c* in SV40IM WT and Apaf1 KO MEFS in the absence (Control) or presence of etoposide (E, 5 μM). In all, 200 cells were counted and classified according to mitochondrial or cytosolic Cyt *c* staining (white arrows). Quantification is shown on the right as the percentage of cells with cytosolic Cyt *c* staining (mean ± s.d., n = 3).
doi:10.1371/journal.pone.0084666.g002

electron microscopy (TEM). The mitochondria in the control MEFS WT cells were rounded with well visible cristae (Fig. 3C - black arrows in the WT-labelled panels). However, the mitochondria in the Apaf1-deficient cells (in both SV40IM- and SIM-MEFS KO Apaf1) were rather elongated and thinner (Fig. 3C - black arrows in the KO-labelled panels). Mitochondrial morphology changes have been linked to alterations of the cell's metabolic status [22]. These observations have been confirmed by the quantification of mitochondrial dimensions. Since samples were cut in the preparation process (see Methods), we assessed only mitochondrial width. In SV40IM-MEFS KO Apaf1, mitochondrial width decreased by an average 33% when compared to SV40M-MEFS WT (Fig. 3C, right panel), while a 52% reduction in width was obtained in SIM-MEFS KO Apaf1 when compared to SIM-MEFS WT (Fig. 3C, right panel). It was also interesting to notice that the mitochondria in the MEFS WT control cells were mostly in the 'orthodox' state [23], whereas they were in a 'condensed' state, with greater electron density in the matrix, in MEFS KO Apaf1. These two different mitochondria 'states' have been previously characterised. In fact, 'mitochondria states' are related to mitochondrial status, and mitochondria populate one 'state' or the other depending on ADP availability. Mitochondria display 'condensed' conformation when ADP is in excess, but they revert to the 'orthodox' state when ADP is limiting [24,25]. Then the TEM analysis suggests that in both SV40IM-MEFS KO Apaf1 and SIM-MEFS KO Apaf1, mitochondria are more active than in the control MEFS WT cells. In fact, we analysed the levels of intracellular ATP in SV40IM- and in SIM-MEFS KO Apaf1 to find that the two cell lines showed a significantly higher ATP content when compared to SV40IM- and SIM-MEFS WT (Fig. 4A). In SV40M MEFS KO Apaf1, ATP almost doubled the content of the control cells (from 100.0±0.0 in SV40IM-MEFS WT to 196.6±25.42), while a 60% increase was observed in SIM-MEFS KO Apaf1 (from 100.0±0.0 in SIM MEFS WT to 161.8±3.740).

ATP production can vary to match energy demands [26]. ATP is produced from carbon fuels through glycolysis in the cytosol and via oxidative phosphorylation (OxPhos) in mitochondria. Glycolysis produces pyruvate for OxPhos under non-stressful conditions to generate 2 moles of ATP from 1 mole of glucose. However under stress due to a sudden drop in intracellular ATP, cells accelerate glycolysis through which the ATP generation rate becomes almost 100 times faster than that of OxPhos, be it with poor ATP production efficiency. Consequently, it leads to

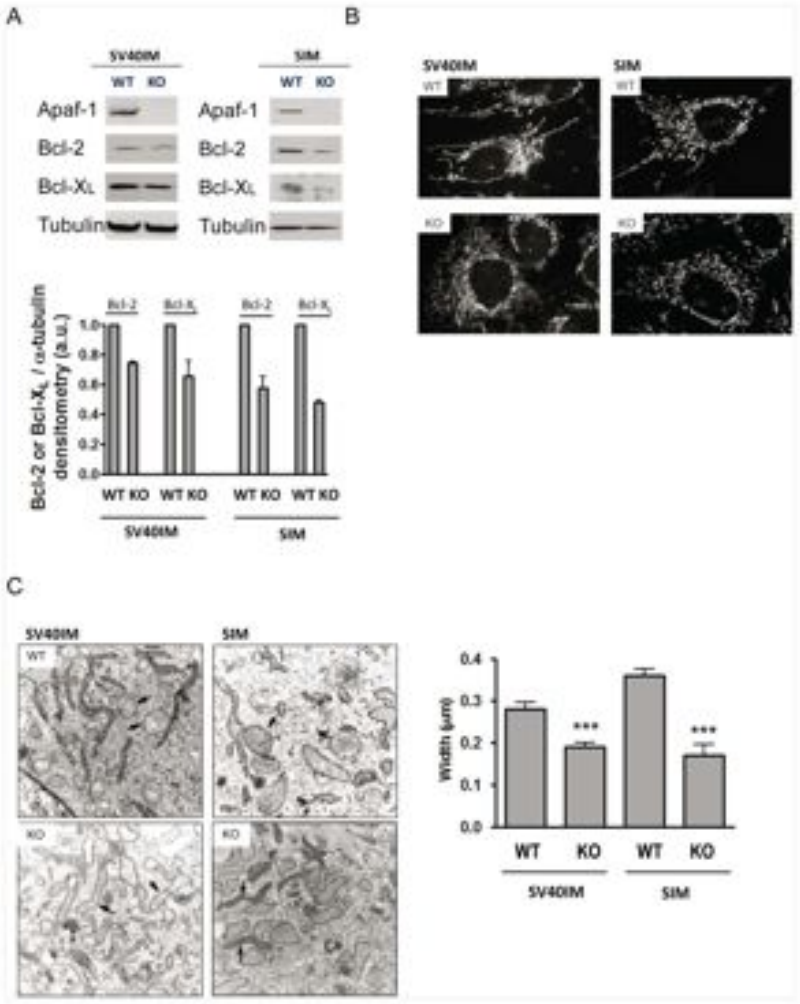

Figure 3. Mitochondrial network in Apaf1-deficient cells is affected. (A) Bcl-2 and Bcl-X_L protein levels in the SV40IM and SIM cell lines by immunoblotting. α-tubulin was also assayed as a loading control. Densitometric analyses were performed using the Image J software, normalised for α-tubulin and reported as arbitrary units (a.u). Values are means ± s.d. of three independent immunoblots. (B) The mitochondrial network in the untreated SV40IM and SIM MEF cell lines was visualised using an anti-Cyt *c* antibody. (C) Transmission electron photomicrographs of the mitochondria in MEFs. Ultrathin (0.07 μm) sections of the MEF cell lines were prepared as described in sMaterials and Method. Black arrows indicate the representative mitochondria of each sample. Scale bars indicate 1 μm. The Image J Java-based image processing software was used to quantify the width of approximately 70 different mitochondria from each cell type using the images obtained by TEM. Two-tailed Student's *t*-tests were performed (***p≤0.001). SV40IM-MEFS WT Apaf1 is of 0.2939±0.01501 μm and SV40IM-MEFS KO Apaf1 is of 0.1980±0.009215 μm. SIM-MEFS WT Apaf1 is of 0.3539±0.01625 μm and SIM-MEFS KO Apaf1 is of 0.1697±0.02228 μm.
doi:10.1371/journal.pone.0084666.g003

increased lactate production from pyruvate [27]. Then if the structural differences found in the mitochondria in MEFS KO Apaf1 can affect OxPhos, we should find increased lactate/pyruvate (L/P) ratios in these cells. In fact, it has been formerly reported that upon apoptotic treatment, the cell metabolism in the apoptosome-deficient cells is maintained by glycolysis [28]. We

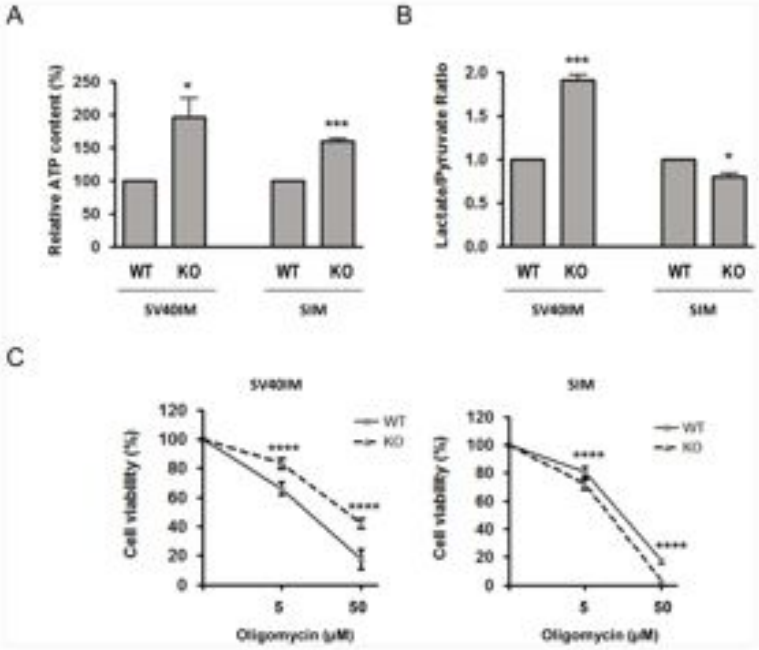

Figure 4. Metabolic status in Apaf1-deficient cells. (A) Absolute level of intracellular ATP in Apaf1-deficient MEFs is greater than in WT cells. ATP content was measured using the commercially available Luminescence ATP Detection Assay System (Perkin Elmer) following the manufacturer's instructions. The results obtained from each Apaf1-deficient cell line were normalised to their respective WT controls and were submitted to the two-tailed Student's t-test (*p≤0.05; ***p≤0.001)). The ATP in SV40IM-MEFS WT Apaf1 is of 100.0±0.0 and of 196.6±28.42 in SV40IM-MEFS KO Apaf1. The ATP in SIM-MEFS WT Apaf1 is of 100.0±0.0 and of 161.8±3.740 in SIM-MEFS KO Apaf1. (B) Lack of Apaf1 in MEFs affects its lactate to pyruvate (L/P) ratio. Lactate and pyruvate contents were measured using the commercially available Lactate Assay Kit II (BioVision) and the Pyruvate Assay Kit (BioVision) following the manufacturer's instructions. The results obtained from each Apaf1-deficient cell line were normalised to their respective WT controls and submitted to the two-tailed Student's t-test (*p≤0.05; ***p≤0.001). The L/P ratio in SV40IM-MEFS KO Apaf1 represents 188.9% of SV40IM-MEFS WT Apaf1 and SIM-MEFS KO Apaf1 represent 76.39% of SIM-MEFS WT Apaf1. (C) Apaf1-deficient MEFs were able to obtain ATP from both OxPhos and glycolysis. Cells from each cell line were treated with 0, 5 or 50 μM oligomycin for 24 h to block mitochondrial ATP synthase and were submitted to the MTT cell proliferation assay. The obtained results were normalised in relation to the 0 μM oligomycin control for each cell line and were submitted to the two-tailed Student's t- test (****p≤0.0001). The cell viability of SV40IM-MEFS WT as compared with SV40IM-MEFS KO Apaf1 changed from 81.32±1.06% to 72.23±3.08% at 5 μM oligomycin and from 17.72±0.62% to 5.96±0.2% at 50 μM oligomycin. The cell viability of SIM-MEFS WT Apaf1 as compared with SIM-MEFS KO Apaf1 changed from 84.13±1.89% to 72.23±2.52% at 5 μM oligomycin and from 43.01±2.67% to 17.89±6.86% at 50 μM oligomycin.
doi:10.1371/journal.pone.0084666.g004

found that this was indeed the case in SV40IM-MEFS KO Apaf1 (Fig. 4B), suggesting that the main ATP source for these cells should be based on an increased glycolytic rate [29]. Conversely in the SIM-MEFS KO Apaf1 cells, we found that the L/P ratio was slightly lower as compared to the SIM-MEFS WT cells, suggesting the major relevance of OxPhos in ATP production in these cells. Next we reasoned as follows: if SIM-MEFS KO Apaf1 cells depend on OxPhos for ATP production, while SV40IM-MEFS KO Apaf1 cells rely on the glycolytic rate, then SIM-MEFS KO Apaf1 cells should be more sensitive to oligomycin (an inhibitor of mitochondrial ATP synthase) than the SV40IM-MEFS KO Apaf1 cells. Therefore, both KO Apaf1 cells were treated with oligomycin, while mitochondrial activity was evaluated by MTT. Dependence on ATP synthase can be clearly seen when comparing the results with the respective MEFS WT cells. The SV40-MEFS KO Apaf1 cells were more resistant to oligomycin than the control SV40-MEFS WT (Fig. 4C). However, SIM-MEFS KO Apaf1 cells were slightly more sensitive to the drug than the SIM-MEFS WT control cells (Fig. 4C).

In conclusion, we analysed mitochondrial features and cell death response to etoposide in two different Apaf1-deficient MEFS that differ in the immortalisation protocol. Unexpectedly, both, MEFS KO Apaf1 immortalised with the SV40 antigen (SV40IM-MEFS Apaf1) and those that spontaneously immortalised (SIM-MEFS Apaf1), presented relevant structural differences at the mitochondria when compared to MEFS WT, indicating a role for Apaf1 at the mitochondria. In fact when Apaf1 was absent, the mitochondria appeared more fragmented, elongated and thinner when compared to the MEFS WT mitochondria from animals with the same genetic background (SV40IM-MEFS WT and SIM-

MEFS WT). These irregular mitochondria were predominantly found in a 'condensed' state and contained higher ATP levels than the counterpart mitochondria in MEFS WT. However, the origin of this ATP accumulation in the mitochondria was not clearly revealed, provided that the SV40IM-MEFS KO Apaf1 cells showed a more marked dependence on ATP production with high glycolytic rates, while SIM-MEFS KO Apaf1 were more dependent on OxPhos. Furthermore, etoposide-treated SV40IM-MEFS KO Apaf1 released more Cyt *c* and showed more cells with low $\Delta\Psi m$ than the counterpart cells from the WT animals. These cells died by caspase-independent processes, which were partially inhibited by Nec. In contrast, the SIM-MEFS KO Apaf1 cells were resistant to etoposide treatments as they maintained $\Delta\Psi m$ and showed minimal Cyt *c* release.

Hence the genetic background and immortalisation protocol might influence cells' response to death signals. Genetic ablation of Apaf1 dampens mitochondria which, depending on the genetic background, make cells more or less sensitive to DNA-inducing agents such as etoposide which, in sensitive cells, probably induces necroptosis when the canonical apoptosis components are not available. These studies, together with previous reports [6,9,11], illustrate not only the complex role that Apaf1 might play in cells, but also the importance of unravelling the network of signalling pathways that converges in the key proteins controlling apoptosis in probably not only cell death, but also in cell homeostasis. Through direct binding or accessory proteins, the results indicate a role for Apaf1 in the structural (and functional) arrangement of homeostatic mitochondria. It would be interesting to perform a thorough identification of the molecular mechanism as to how Apaf1 affects the mitochondria given their relevance and central position in cell fate decisions.

Supporting Information

Figure S1 ABT737 treatment induces cell death in SV40IM WT MEFS but not SV40IM KO MEFS and SIM MEFS. (A) Percentage of cell survival measured by the trypan blue exclusion assay in SV40IM and SIM MEFS, WT and Apaf1 depleted, in the presence or absence of ABT737 (20 μM) for 24 h. (B) Caspase-3 like activity was measured under the same conditions described above. (C) Cells with Cyt c released measured by the flow cytometry analysis after incubation with ABT737 (20 μM) for 24 h. In all cases, bars represent the mean of three experiments ± s.d.
(TIF)

Acknowledgments

This paper is dedicated to the memory of Professor Enrique Pérez-Payá. We thank all the members of our laboratories for discussions.

Author Contributions

Conceived and designed the experiments: EPP MS FC. Performed the experiments: MS AG AEH MO VAF. Analyzed the data: MS MO EPP. Contributed reagents/materials/analysis tools: EF FC. Wrote the paper: MS EPP.

References

1. Peter ME, Krammer PH (2003) The CD95(APO-1/Fas) DISC and beyond. Cell Death Differ 10: 26–35.
2. Tait SW, Green DR (2010) Mitochondria and cell death: outer membrane permeabilization and beyond. Nat Rev Mol Cell Biol 11: 621–632.
3. Zou H, Li Y, Liu X, Wang X (1999) An APAF-1.cytochrome *c* multimeric complex is a functional apoptosome that activates procaspase-9. J Biol Chem 274: 11549–11556.
4. Cecconi F, Alvarez-Bolado G, Meyer BI, Roth KA, Gruss P (1998) Apaf1 (CED-4 homolog) regulates programmed cell death in mammalian development. Cell 94: 727–737.
5. Mouhamad S, Galluzzi L, Zermati Y, Castedo M, Kroemer G (2007) Apaf-1 Deficiency Causes Chromosomal Instability. Cell Cycle 6: 3103–3107.
6. Zermati Y, Mouhamad S, Stergiou L, Besse B, Galluzzi L, et al. (2007) Nonapoptotic role for Apaf-1 in the DNA damage checkpoint. Mol Cell 28: 624–637.
7. Mondragon L, Galluzzi L, Mouhamad S, Ovejero M, Vicencio JM, et al. (2009) A chemical inhibitor of Apaf-1 exerts mitochondrion-protective functions and interferes with the intra-S-phase DNA damage checkpoint. Apoptosis 14: 192–196.
8. Ohsawa S, Hamada S, Kuida K, Yoshida H, Igaki T, et al. (2010) Maturation of the olfactory sensory neurons by Apaf-1/caspase-9-mediated caspase activity. Proc Natl Acad Sci U S A 107: 13366–13371.
9. Ferraro E, Pesaresi MG, De Zio D, Cecconi ME, Gortat A, et al. (2011) Apaf1 plays a pro-survival role by regulating centrosome morphology and function. J Cell Sci 124: 3450–3463.
10. Pinan-Lucarre B, Gabel CV, Reina CP, Hulme SE, Shevkoplyas SS, et al. (2012) The core apoptotic executioner proteins CED-3 and CED-4 promote initiation of neuronal regeneration in *Caenorhabditis elegans*. PLoS Biol 10: e1001331.
11. Miyazaki K, Yoshida H, Sasaki M, Hara H, Kimura G, et al. (2008) Caspase-independent cell death and mitochondrial disruptions observed in the Apaf1-deficient cells. J Biochem 129: 965–969.
12. Franklin EE, Robertson JD (2007) Requirement of Apaf-1 for mitochondrial events and the cleavage or activation of all procaspases during genotoxic stress-induced apoptosis. Biochem J 403: 113–122.
13. Ashraf QM, Mishra OP, Delivoria-Papadopoulos M (2007) Mechanisms of expression of apoptotic protease activating factor-1 (Apaf-1) in nuclear, mitochondrial and cytosolic fractions of the cerebral cortex of newborn piglets. Neurosci Lett 415: 253–258.
14. Shiraishi H, Okamoto H, Hara H, Yoshida H (2010) Alternative cell death of Apaf1-deficient neural progenitor cells induced by withdrawal of EGF or insulin. Biochim Biophys Acta 1800: 405–413.
15. Almaja D, Saenz-Robles MT, Pipas JM (2005) SV40 large T antigen targets multiple cellular pathways to elicit cellular transformation. Oncogene 24: 7729–7745.
16. Rodriguez-Enfedaque A, Delteau E, Guillaume A, Gaumez S, Mignotte B, et al. (2012) cVAD-fmk upregulates caspase-9 cleavage and activity in etoposide-induced cell death of mouse embryonic fibroblasts. Biochim Biophys Acta 1023: 1343–1352.
17. Goldstein JC, Munoz-Pinedo C, Ricci JE, Adams SR, Kelekar A, et al. (2005) Cytochrome *c* is released in a single step during apoptosis. Cell Death Differ 12: 453–462.
18. Rehm M, Dussmann H, Prehn JH (2003) Real-time single cell analysis of Smac/DIABLO release during apoptosis. J Cell Biol 162: 1031–1043.
19. Lassenante MA, Possanzo E, Dussmann H, Rauen JA, Wurstle ML, et al. (2011) Proteasome inhibition can induce an autophagy-dependent apical activation of caspase-9. Cell Death Differ 18: 1384–1397.
20. Andreu-Fernandez V, Genovesi A, Mesaeger A, Ovejero M, Sancho M, et al. (2013) BH3-Mimetics and Cisplatin-Induced Cell Death Proceeds through Different Pathways Depending on the Availability of Death-Related Cellular Components. PLoS One 8: e56202.
21. Daniel NN, Korsmeyer SJ (2004) Cell death: critical control points. Cell 116: 205–219.
22. Gomes LC, Di Benedetto G, Scorrano L (2011) During autophagy mitochondria elongate, are spared from degradation and sustain cell viability. Nat Cell Biol 13: 589–598.
23. Hackenbrock CR (1968) Chemical and physical fixation of isolated mitochondria in low-energy and high-energy states. Proc Natl Acad Sci U S A 61: 598–605.
24. Mannella CA (2006) Structure and dynamics of the mitochondrial inner membrane cristae. Biochim Biophys Acta 1763: 542–548.
25. Mannella CA (2006) The relevance of mitochondrial membrane topology to mitochondrial function. Biochim Biophys Acta 1762: 140–147.
26. Nogueira V, Rigoulet M, Piquet MA, Devin A, Fontaine E, et al. (2001) Mitochondrial respiratory chain adjustment to cellular energy demand. J Biol Chem 276: 46304–46310.
27. De Feo P, Di Loreto C, Lucidi P, Murdolo G, Parlanti N, et al. (2003) Metabolic response to exercise. J Endocrinol Invest 26: 851–854.
28. Ferraro E, Pulicati A, Cencioni MT, Cozzolino M, Navoni F, et al. (2008) Apoptosome-deficient cells lose cytochrome *c* through proteasomal degradation but survive by autophagy-dependent glycolysis. Mol Biol Cell 19: 5136–5148.
29. Finley LW, Carracedo A, Lee J, Souza A, Egia A, et al. (2012) SIRT3 opposes reprogramming of cancer cell metabolism through HIF1alpha destabilization. Cancer Cell 19: 416–428.

Supplemental Information

Supporting Figure 1

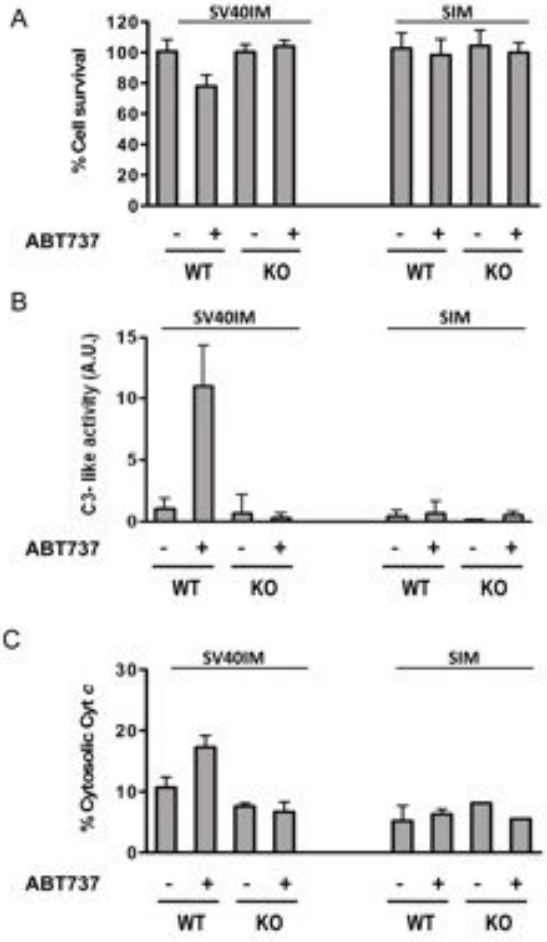

Figure S1. ABT737 treatment induces cell death in SV40IM WT MEFS but not SV40IM KO MEFS and SIM MEFS. (A) Percentage of cell survival measured by the trypan blue exclusion assay in SV40IM and SIM MEFS, WT and Apaf1 depleted, in the presence or absence of ABT737 (20 μM) for 24 h. (B) Caspase-3 like activity was measured under the same conditions described above. (C) Cells with Cyt c released measured by the flow cytometry analysis after incubation with ABT737 (20 μM) for 24 h. In all cases, bars represent the mean of three experiments ± s.d.